T Cell Kinetics in HIV Infected Children

DELALI KORSIWOR SEFE

Thesis submitted to **University College London** for the degree of **Doctor of Philosophy**

Infectious Disease & Microbiology Unit

Institute of Child Health

University College London

2011

I, Delali Korsiwor Sefe, confirm that the work presented in this thesis is my own. Where information has been derived from other sources, I confirm that this has been indicated in the thesis.

ABSTRACT

Infection with Human Immunodeficiency Virus, type 1 (HIV-1) is associated with a gradual progressive decline in the number of $CD4^+$ T lymphocytes. Effective treatment suppresses viral replication and is accompanied by a concomitant increase in the number of $CD4^+$ T cells. Immune reconstitution of $CD4^+$ T cells in children following treatment is characterised by a sustained increase of naïve cells, a pattern that differs from that seen in adults. The aim of this thesis was to explore how these changes occur. $CD4^+$ T cells in blood samples from HIV-1 infected children were identified, divided into sub-populations and analysed for apoptosis, proliferation, activation and differentiation by flow cytometry. Four $CD4^+$ T cell sub-populations, with varying contributions to the total $CD4^+$ T cell pool were thus identified: (i) recent thymic emigrants (RTEs) made up the largest population yet maintained very low levels of proliferation despite increased viral replication and cellular activation, and were consistently greater in children with undetectable viraemia; (ii) central naïve cells, which were fairly constant in HIV-1 infected children of all ages regardless of CD4 count; (iii) $CD31^-$ memory cells that increased as CD4 count fell and (iv) $CD31^+$ memory cells that despite their high level of activation and proliferation remained a small population across age, viral load and CD4 count. Treatment interruption and the resulting increased viraemia and decreased CD4 count were associated with only transient changes to the percentage contribution of each subset, which supports the existence of a setpoint for each subpopulation. This thesis infers the importance of thymic output in maintaining the CD4 count and hence the potential for using RTEs in monitoring response to treatment and sheds light on the role and origin of $CD31^+$ memory cells as a small but highly activated population that may be important in disease pathogenesis.

LIST OF ABBREVIATIONS

AIDS	Acquired immune deficiency syndrome
APC	Antigen presenting cell
BALT	Bronchus-associated lymphoid tissue
BSA	Bovine serum albumin
CDC	Centres for Disease Control and Prevention
cPPPT	central polypurine tract
CPZ	Chimpanzee
CRF	Circulating recombinant form
DC	Dendritic cell
DN	Double negative
DP	Double positive
EDTA	Ethylenediaminetetraacetic acid
Env	Envelope
FCS	Foetal calf serum
FLICA	Fluorescent inhibitor of caspases
FSC	Forward scatter
Gag	Group-specific antigen
GALT	Gut-associated lymphoid tissue
Gp	Glycoprotein
HEV	High endothelial vessel
HIV	Human immunodeficiency virus
HR	Heptad repeat
HSC	Haematopoietic stem cell
HTLV	Human T-lymphotropic virus
IL	Interleukin
IN	Integrase
IQR	Interquartile range
IRIS	Immune reconstitution inflammatory syndrome
LN	Lymph node
LTR	Long terminal repeat
MALT	Mucosa-associated lymphoid tissue

MFI	Median fluorescence intensity
MHC	major histocompatibility complex
mRNA	Messenger RNA
Nef	Negative regulatory factor
NKT	Natural killer T
ORF	Open reading frame
Pbs	Primer binding site
PBS	Phosphate buffered saline
PFA	Paraformaldehyde
PIC	Pre-integration complex
Pol	Polymerase
PPT	Polypurine tract
Rev	regulator of virion expression
RNase	Ribonuclease
Rpm	Revolutions per minute
RPMI	Roswell Park Memorial Institute
RT	Reverse transcriptase
SIV	Simian immunodeficiency virus
SMM	sooty mangabey monkeys
SSC	Side scatter
Tat	Transactivator of transcription
TCR	T cell receptor
TE	Tris EDTA
Tfh	T follicular helper
TGF	Transforming growth factor
tRNA	Transfer RNA
UCHL1	ubiquitin carboxyl-terminal esterase L1
UNAIDS	Joint United Nations Programme on HIV/AIDS
Vif	virion infectivity factor
Vpr	Viral protein R
Vpu	Viral protein U

CONTENTS

TABLE OF FIGURES

LIST OF TABLES

ACKNOWLEDGEMENTS

First, I would like to thank my primary supervisor Nigel Klein for offering me the unique opportunity of working on such an exciting project and providing guidance and direction. Thank you as well to Deenan Pillay for conceiving and directing the virology component of this PhD.

I am truly grateful to the virology department at the Windeyer, especially Jeremy Garson, one of the most inspiring people I've ever met, for his endless patience in supervising me in the lab and teaching me so much about qPCR. I also thank Paul Grant for allowing me space in his lab, for the kind gift of aliquots of 8E5 cell line DNA extract and for other materials.

This PhD would not have been possible without the help of our collaborators on PENTA11, Di Gibbs, Hannah Castro and Anita De Rossi and her lab. Thank you all for letting me join the project, for assistance with the statistics and for allowing me to include the Italian cohort data in my thesis.

Throughout my thesis I had the benefit of amazing support, assistance and advice from an amazing group of fellow PhD students and postdoctoral fellows. Thank you so much to Iren Bains, Hannah Jones, Marianne Jacobsen, Vania de Toledo and everyone else for sharing in the joys and frustrations over the years.

I completed my PhD as part of an MBPhD degree so I'd like to thank Gordon Stewart for giving me this amazing opportunity and for all his kind advice, help and guidance over the years. Thank you so much to my fellow MBPhD students and close friends Marieke Bokhoven, Nicola Wilson, Shao Ong, Abhishek Das and everyone else who journeyed with me.

Finally and most importantly I would like to thank my family especially my father, Francis Sefe, to whom this thesis is dedicated and without whom none of this would have been possible. For inculcating in me a desire for knowledge and understanding, for their countless sacrifices and their constant support and encouragement all the way I am forever grateful. Thank you.

CHAPTER 1

GENERAL INTRODUCTION

1.1 THE HIV EPIDEMIC

The human immunodeficiency virus (HIV) was identified in 1983 and is the causative agent of acquired immunodeficiency syndrome (AIDS) (Chermann et al. 1983). AIDS was first described in 1981 when the U.S. Centers for Disease Control and Prevention (CDC) reported a cluster of *Pneumocystis carinii* (now *Pneumocystis jiroveci*) pneumonia in homosexual men. (CDC 1981) but HIV/AIDS has since become a global epidemic affecting all areas of society and is now the 6th leading cause of death worldwide (WHO 2009).

Since its discovery the prevalence of HIV has increased massively and the joint United Nations programme on HIV/AIDS (UNAIDS) now estimates that there are 33 million (30 million-36 million) people living with HIV infection worldwide. Though the distribution of HIV is global, by far the worst afflicted region is sub-Saharan Africa with over 20 million infected individuals. This region, which is home to only 10% of the world's population, accounts for 67% of the world disease burden. An even higher proportion of the total AIDS deaths reported annually come from this region, 72% of the two million who died from AIDS in 2007 were in sub-Saharan Africa (UNAIDS 2008). The global prevalence is shown in Figure 1.1.

Though HIV was initially described in homosexual men most infections are transmitted by heterosexual intercourse; contaminated needles and blood products; and from mother to child, during birth, in utero or via breast milk (Hansasuta and Rowland-Jones 2001). Indeed globally, women now account for half of all people living with HIV and in sub-Saharan Africa HIV infected women exceed HIV infected men, making up 60% of the HIV infected population.

Due mostly to perinatal transmission, HIV is also a significant infection in children. The 2008 'Report on the global AIDS epidemic' produced by UNAIDS reported an estimated 2 million (1.9-2.3 million) children, under the age of 15, living with HIV

worldwide (UNAIDS 2008) with almost 90% living in sub-Saharan Africa. However with the advent of effective antenatal screening to identify HIV infected pregnant women, and the use of antiretroviral prophylaxis before birth, caesarean section deliveries and formula feeding, the rate of new infections in children appears to have peaked in 2000-2002 (UNAIDS 2008).

Tremendous progress has been made in the study of HIV infection, ranging from the discovery of the simian origins of the HIV virus, transmission and prevention, entry into the $CD4^+$ T cell host and replication therein, pathogenesis, through to treatment and vaccine development; yet HIV infection remains arguably among the worst pandemics of the modern world.

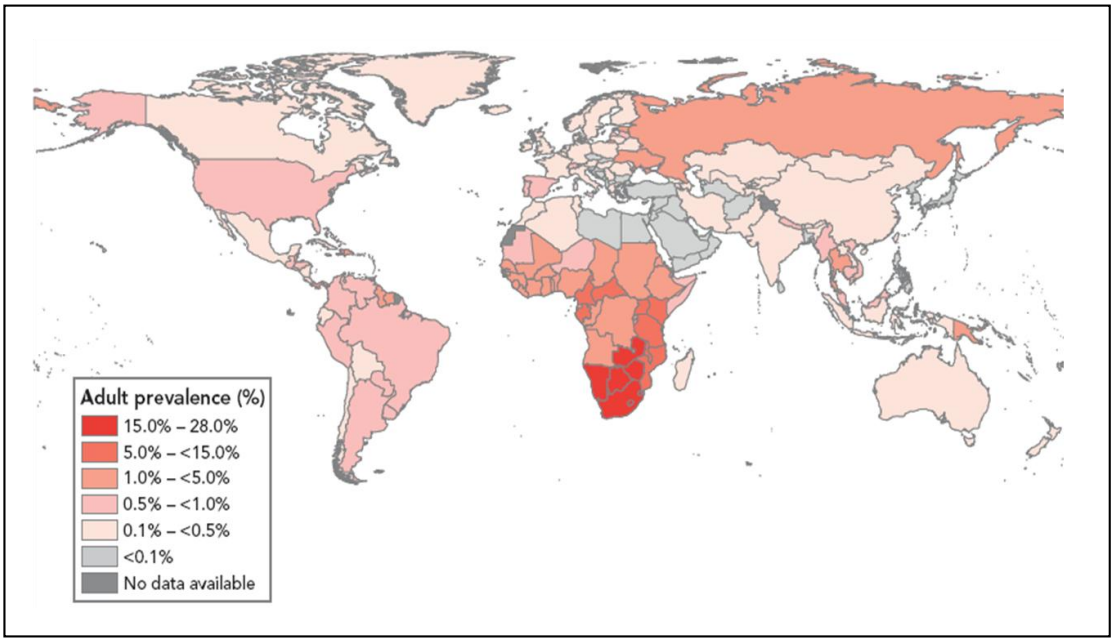

Figure 1.1 A global view of HIV infection, 2007

The prevalence of HIV infection amongst adults is shown for each country in the world. The darker the shade of red, the higher is the prevalence in that country. The highest prevalences occur in sub-Saharan Africa, specifically Southern Africa and outside of Africa in Russia. Reproduced from UNAIDS Global Report on HIV (UNAIDS 2008)

1.2 $CD4^+$ T CELL IMMUNOLOGY

An understanding of CD4 lymphocyte immunology is important in the study of HIV pathogenesis because $CD4^+$ T cells are the major target for HIV and disturbance to their normal homeostasis is central to disease pathogenesis.

1.2.1 Generation of $CD4^+$ T cells

$CD4^+$ T cells are a sub-class of lymphocytes, which also include B cells and other types of T cells. They are derived from haematopoietic stem cells (HSC), which possess long-term self-renewal capability. Antenatally, lymphocytes are generated from these stem cells in the foetal liver, whereas post-natally, the bone marrow is the major source of haematopoiesis (Abbey and O'Neill 2008), (Kawamoto and Katsura 2009). Some of these HSC possess the capacity to emigrate to the thymus based on their expression of the chemokine receptors 7 and 9 (CCR7 and CCR9) (Krueger et al. 2010), in addition to the stem and progenitor cell markers: KIT (CD117), stem cell antigen 1 (SCA1) and the growth factor receptor tyrosine kinase FLT3 (Rothenberg, Moore, & Yui 2008). The unique microenvironment of the thymus allows the HSC to progress through multiple developmental pathways to develop into a T-cell.

Once in the thymus, the T cell progenitors, characterized as double negative (DN) cells that lack expression of CD4, CD8, and CD3, progress through four main stages, DN1-DN4, although in recent years these stages have been further subdivided. The cells begin by proliferating extensively and switching off genes that would allow differentiation into non-T-cell lineages (Rothenberg, Moore, & Yui 2008). At the DN1-DN2 stage of development, Notch receptors on the thymocyte cell surface interact with their ligands present on stromal cells of the thymus and the ensuing signalling inhibits non-T cell differentiation, which in combination with interleukin-7 (IL-7) driven proliferation commits thymocytes to the T cell lineage (Garcia-Peydro, de Yebenes, & Toribio 2006).

Somatic rearrangement of the genes encoding the T cell receptor (TCR) β, γ and δ chains, which is essential for TCR expression, begins in DN2 cells and is mainly completed during the DN3 stage, committing thymocytes to either the αβ or γδ T-cell lineages. During the DN3 to DN4 transition, αβ T cells undergo selection of their β chain via signalling of the pre-TCR complex, which consists of the TCRβ chain, the pre-Tα chain, CD3ε, CD3γ, and TCRζ. These signals induce allelic exclusion of the β chain and promote the survival, proliferation, and differentiation of DN thymocytes to the double positive (DP) stage of development, where thymocytes express both CD4 and CD8 coreceptors and unique αβ TCRs (Hayday and Pennington 2007), (Taghon and Rothenberg 2008).

Conventional αβ T cells develop from αβ thymocytes, which begin to express both TCR co-receptor proteins, CD4 and CD8 thus are referred to as double positive (DP) thymocytes. DP thymocytes undergo positive and negative selection depending on how strongly they recognise self antigen. Within the thymic cortex thymocytes showing moderate recognition of self peptide-major histocompatibility complex (MHC) complexes are positively selected via TCR signalling that results in RAG gene repression, long-term survival and progression to the thymic medulla for negative selection. Negative selection in the medulla is determined by how strongly or weakly thymocytes recognise self peptide-MHC complexes. Those thymocytes bearing TCRs with no affinity for self peptide-MHC complexes do not receive TCR signalling and die from neglect. Thymocytes with strong affinity for the self peptide-MHC complex are potentially harmful; therefore these undergo programmed cell death, known as apoptosis. Finally thymocytes that recognise self antigen-peptide weakly receive appropriate TCR signalling and continue to differentiate (Starr, Jameson, & Hogquist 2003), (Wagner 2006).

Conventional T cells, which express αβ TCRs, are characterised by a polyclonal repertoire and constitute the majority of T cells. More recently, unconventional subsets of T cells called innate T cells have been described (Sigal 2005). They are generally characterised by a more restricted TCR repertoire. Examples of innate T cells include γδ T cells and natural killer T (NKT) cells. Other characteristics that distinguish

conventional versus innate T cells include differential expression of surface markers, effector functions, and signalling pathway requirements during development (Prince et al. 2009). Innate T cells do not require differentiation and can exert their effector functions immediately (de Vries, Cornain, & Rumke 1974). In contrast conventional αβ T cells exhibit a naïve phenotype and require antigen-mediated activation and differentiation to exert their effector functions.

TCR signals generated by interactions with class II MHC-peptide complexes are required for the CD4 αβ T-cell fate, whereas those generated by class I MHC-peptide complexes are necessary for the CD8 αβ T-cell fate. Accordingly, interaction of DP cells with MHC class I results in loss of CD4 expression and their maturation into CD8 T-cells, while interaction of DP cells with MHC class II results in loss of CD8 expression and their maturation into CD4 T-cells. Differences in strength, duration, and/or the number of TCR signals integrated over time are critical factors in determining the CD4/CD8 T-cell fate decision. A quantitative model for CD4/CD8 lineage commitment, with stronger/longer TCR signals favouring the CD4 lineage and weaker/shorter signals favouring the CD8 lineage is widely accepted (Singer, Adoro, & Park 2008). The difference in TCR signalling strength results in differential expression of transcriptional regulators, which determine CD4/CD8-lineage choice. Accordingly cells can be forced to change from one lineage to the other by artificially blocking or lowering lineage specific transcription factors (Rothenberg 2009). The process of T cell differentiation in the thymus to produce a $CD4^+$ T cell is shown in Figure 1.2.

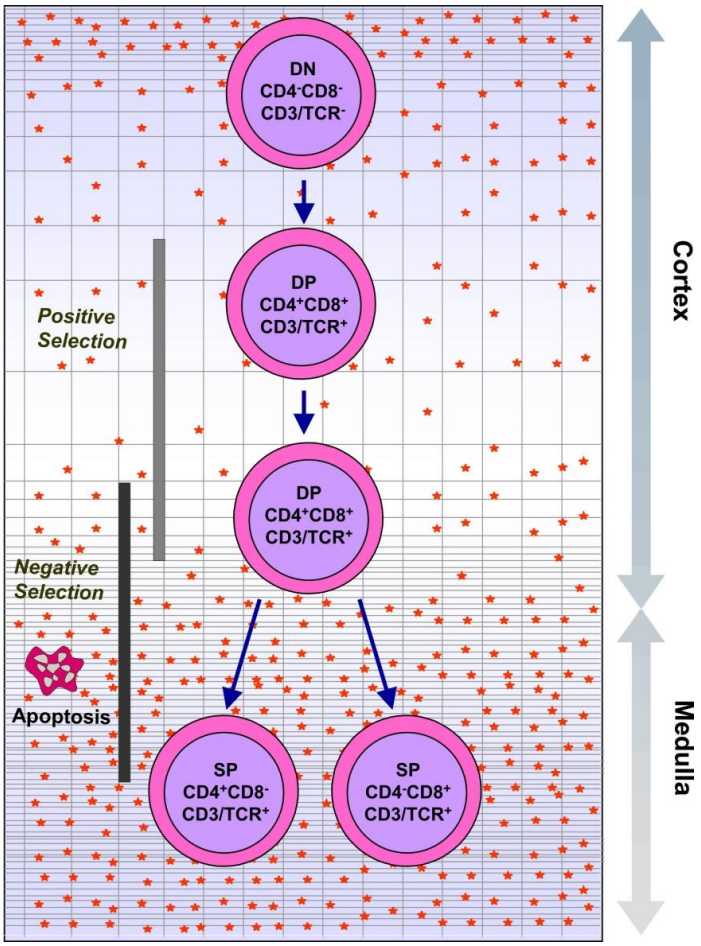

Figure 1.2 Intra-thymic T cell differentiation

The diagram shows development of a CD4$^+$ T cell from a double negative (DN) cell in the cortex, through the processes of positive selection, where thymocytes in the cortex showing moderate recognition of self peptide-MHC complexes are positively selected via TCR signalling and then progress to the medulla for negative selection, where those thymocytes bearing TCRs with no affinity for self peptide-MHC complexes do not receive TCR signalling and undergo apoptosis. Reproduced from (Savino 2006).

1.2.2 CD4$^+$ T cell circulation

The CD4$^+$ T cells that survive selection leave the thymus into the peripheral circulation. They are referred to as naïve cells, as they have not encountered their specific antigen. Naïve T cells continuously recirculate, trafficking from blood into secondary lymphoid organs and then back into the circulation.

T cell generation and development occur in primary lymphoid organs: bone marrow and thymus whereas immune responses are initiated in the secondary lymphoid organs, which include the lymph nodes (LN), spleen and mucosal associated lymphoid tissue (MALT). MALT comprises bronchial associated lymphoid tissue (BALT) and gut associated lymphoid tissue (GALT). All secondary lymphoid organs share a similar basic structure, and are organised to trap antigen from sites of infection, facilitate antigen presentation and provide the optimum microenvironment for lymphocyte maturation (Keogan, Wallace, & O'Leary 2006).

Naïve T cells enter secondary lymphoid organs through high endothelial vessels (HEVs) (Mackay, Marston, & Dudler 1990). To move from the HEV into the lymphoid organs a naïve cell undergoes a series of adhesion steps mediated by interactions between proteins on the naïve cell surface and their respective ligands expressed on the endothelial cell surface.

Within the HEV, naïve cells are subject to vascular shear flow pushing them through the vessel, however interactions between the selectin CD62 ligand (CD62L) expressed on the lymphocyte cell surface and peripheral node addressin (PNAd) on HEVs results in weak tethering that allows the cells to "roll" along the endothelial surface (Denucci, Mitchell, & Shimizu 2009).

The rolling cells come to a stop when CCR7, expressed by naïve cells interacts with its ligands, CCL19 and CCL20. The resulting signalling mediates activation of integrins and firm adhesion to the vascular endothelium. The integrin that is activated depends on the lymphoid organ. For example in peripheral LN leukocyte function-associated antigen-1 (LFA-1), also called α1β2 integrin or CD11a/CD18, is important for adhesion to endothelial intercellular adhesion molecule-1 (ICAM-1) whereas within the Peyer's patches, α4β4 integrin is activated and becomes firmly adherent to mucosal addressin cell adhesion molecule-1 (MAdCAM-1), which is preferentially expressed in this tissue (Denucci, Mitchell, & Shimizu 2009).

The final step is extravasation or transendothelial migration whereby the naïve cell passes either between, paracellular, or directly through the endothelial cells, transcellular, into the lymphoid tissue. This process is thought to be mediated by β1 and β2 integrins, which interact with endothelial junction integrin ligands such as junctional adhesion molecules-B and -A (JAM-B and JAM-A), respectively (Denucci, Mitchell, & Shimizu 2009). Once within the lymphoid tissue naïve cells home to T cell areas. They spend 12 to 24 hours in T cell areas but typically spend less than a half hour in the circulation before homing to another lymphoid organ (von Andrian and Mempel 2003), (Ebert, Schaerli, & Moser 2005).

T cells leave the lymphoid organs and return to the blood stream either in lymph via efferent lymphatic vessels from lymph nodes and Peyer's patches, which ultimately merge into the blood stream; or directly back into the blood stream from the spleen. Naïve lymphocytes can live for several months by circulating continuously, receiving survival signals through low affinity TCR engagement by self peptide-MHC and through IL-7 receptor (Cyster 2003).

1.2.3 $CD4^+$ T cell function

$CD4^+$ T cells are stimulated to differentiate upon activation by antigen. This occurs when the peptide specific for the TCR is presented by MHC class II molecules on antigen presenting cells (APC). Naïve cells by continually trafficking through T cell areas in lymphoid organs have access to the highest concentration of MHC II molecules, present on dendritic cells (Weiss and Samelson 2003).

When a T cell recognises foreign antigen bound to MHC II it forms a tight synapse with the APC at the point of the interaction. Formation of the synapse is associated with rapid clustering of more TCR molecules binding to antigen-MHC II on the APC and the accumulation of intracellular signalling molecules within the immunological synapse. The TCRs form complexes with CD3 molecules. TCR/CD3 triggering is aided by

numerous co-stimulatory molecules that bind to complementary molecules present on the APC. Triggering culminates in an intracellular signalling cascade that results in differential gene expression and naïve cell proliferation (Weiss and Samelson 2003).

The differentiation pathway that a naive $CD4^+$ T cell embarks on is determined by the strength of TCR signalling. Strength of signalling is affected by the following: the length of contact between the TCR and the MHC bound antigen; the number of TCRs engaged and therefore the antigen density; the frequency of specific antigen presenting cells and the presence of co-stimulatory molecules such as CD27 and CD28 which act to lower the signalling threshold. They form part of the TCR complex and are involved in signalling. Upon TCR ligation, co-stimulatory molecules are upregulated and act to enhance cell expansion. In the absence of co-stimulatory molecules, T cells that have received low level TCR input do not survive. Loss of co-stimulatory molecules is irreversible and indicates T cell terminal effector differentiation. Depending on the strength of the signalling, TCR triggering can produce three actions. Weak signalling results in anergic cells that undergo apoptosis. Intermediate signalling produces long lived memory cells. Strong signalling produces short lived effector cells (Hendriks et al. 2000), (Sallusto, Geginat, & Lanzavecchia 2004), (Lanzavecchia and Sallusto 2005).

Effector $CD4^+$ T cells lack CCR7, which is required for lymph node homing and CD27, which is involved in T cell activation, and instead express a diverse range of homing molecules that allow them to migrate to the site of the antigen, such as the gut or skin. Once the antigen has been eliminated most of the effector cells undergo apoptosis and die but a small fraction remain as long lived memory cells (Sprent and Surh 2002).

APCs induce naïve $CD4^+$ T cells to differentiate into effector cells, where the effector subtype is determined by which cytokines are released by the APCs. Similarly, the effector subtypes are defined by their pattern of cytokine production, which determines their specific functional capabilities. In general $CD4^+$ effector cells, and their cytokine products, are involved in regulating other cells of the immune system. The effector subtypes that are currently recognised, Th1, Th2, TReg and Th17, the cytokines that

induce their production, their specific functions and their characteristic effector molecule profiles are briefly described in (Table 1.1). In addition to these effectors, transforming growth factor beta (TGF-β)-producing Th3 cells, IL-10-producing TR1 cells, IL-9-producing Th9 cells and T follicular helper (Tfh) cells have also been proposed as separate lineages. However, they do not have distinct cytokine release profiles because Tregs also produce TGF-β, and all Th cells are capable of producing IL-10 under certain circumstances, whereas IL-9 was originally described as a Th2 cytokine, and Th9 cells are developmentally related to Th2 cells (Zhu, Yamane, & Paul 2010).

Subtype	Inducers	Function	Effectors
Th1	IL-12 and IFN-γ	mediate cellular immune response to intracellular pathogens (enhancing microbicidal activity by macrophages and cytotoxic cells) and induce delayed-type hypersensitivity responses	IL-2, IFN-γ, TNF-α and TNF–β (lymphotoxin)
Th2	IL-2 and IL-4	mediate humoral immunity against helminths and other extracellular pathogens; play a role in allergic reactions, help B cells to develop into antibody producing cells and recruit neutrophils, eosinophils, and basophils to sites of infection and inflammation	IL-4, IL-5, IL-9 and IL-13
Th17	TGF-β, IL-6, IL-21 and IL-23	induction of tissue inflammation and immune responses against extracellular bacteria and fungi	IL-17
TReg	IL-10	maintain self antigen tolerance by down-regulating immune response to self and non-self antigens by controlling activation and function of $CD4^+$ T cells, $CD8^+$ T cells and APCs	TGF–β

Table 1.1 $CD4^+$ T cell effector subtypes

The effector lineages known to be derived from naïve $CD4^+$ T cells in the periphery are listed in their table with the cytokines required to induce their production, their functions and the characteristic cytokine profiles that define them.

Immunological memory refers to the ability of clones of differentiated antigen-specific $CD4^+$ T cells to persist for considerable time after their specific antigen is no longer present. Memory cells differ from naïve cells by undergoing expansion faster than naïve cells in response to specific antigen. Their time to division is faster and therefore they are able to rapidly produce a much larger response of effector cells.

Memory cells can be distinguished from naïve cells in a number of ways. They are usually larger, more sensitive to antigenic stimulation and less dependent on co-stimulation. CD4 memory and naïve cells also have differential expression of several surface proteins including CD45RA and CD45RO. CD45RA and CD45RO are the high and low molecular weight isoforms respectively of the leukocyte common antigen, CD45. CD45 is a protein tyrosine phosphatase, essential for TCR signal transduction (Hermiston, Xu, & Weiss 2003). CD45RA is expressed on naïve cells and CD45RO on memory cells, therefore their expression is mostly reciprocal (Terry, Brown, & Beverley 1988) though there is frequently a tiny fraction of antigen primed cells, less than 1% of $CD4^+$ T cells, that co-express CD45RA and CD45RO (Hamann et al. 1996).

Two functional subsets of memory cells are recognised, central memory cells (T_{CM}) and effector memory cells (T_{EM}) (Sallusto et al. 2000). Central memory cells are a pre-effector cell type. They constitute most of the memory T cells present in peripheral blood. When they encounter their cognate antigen, the interaction causes them to upregulate certain chemokine receptors including CCR7, which enables them to home to T cell areas in secondary lymphoid organs. Based on their dominant chemokine profile of either CXCR3 or CCR4 they can be divided into preTh1 and preTh2 respectively. Within the lymphoid organ preTh1 proliferate and differentiate into Th1 effector memory cells, and preTh2 differentiate into Th2 effector memory cells.

Effector memory cells tend to express activation markers and therefore in this respect closely resemble effector cells. Like effector cells, they are short lived and do not express CCR7, migrating instead preferentially from blood to peripheral tissues to provide a rapid response to pathogens at their point of entry. There they exhibit

cytolytic activity or secrete Th1 or Th2 type cytokines. They have short telomeres and don't express telomerase so have reduced capacity to divide. The differentiation pathway undertaken by naïve cells to produce effector and memory cells is summarised in Figure 1.3.

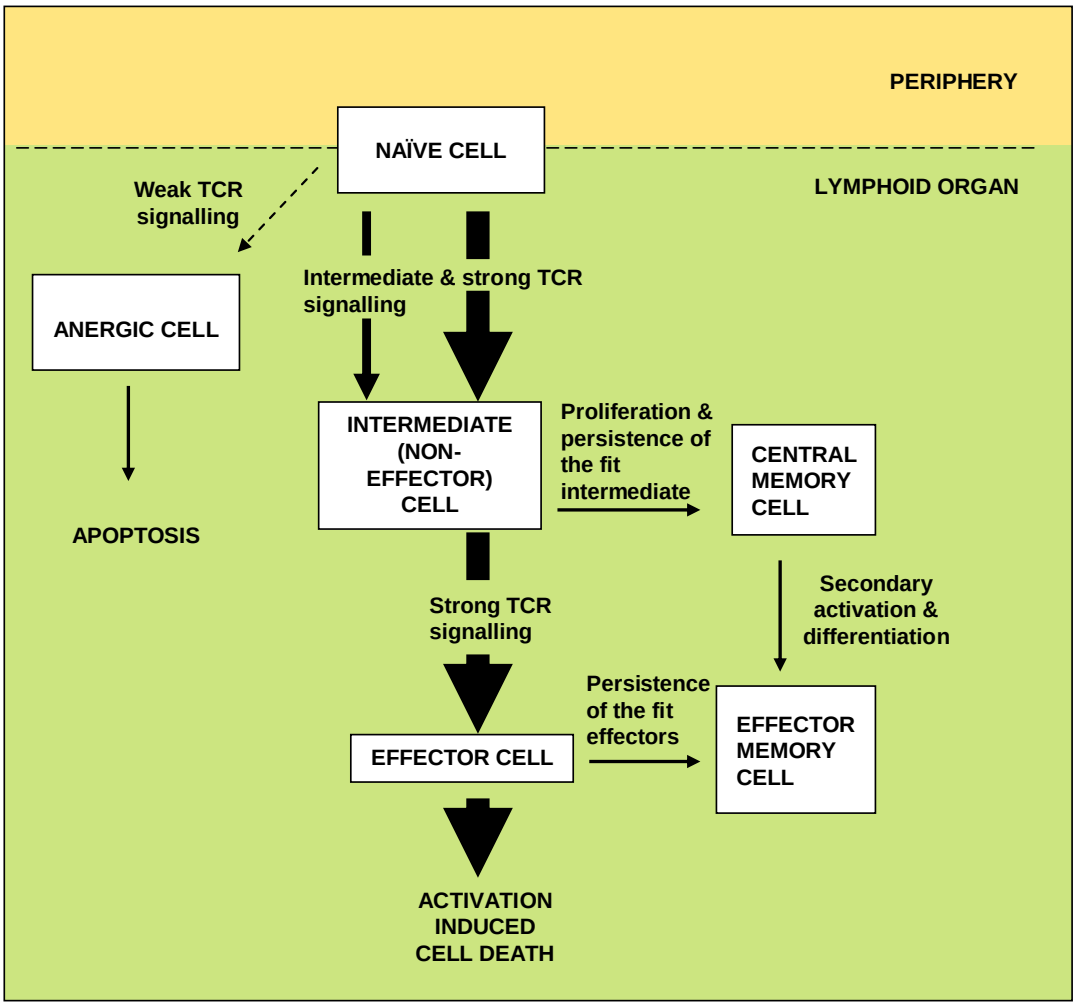

Figure 1.3 Differentiation pathway of $CD4^+$ T cells

The diagram shows how the strength of TCR signalling determines the differentiation of T cells. Adapted from (Sallusto, Geginat, & Lanzavecchia 2004).

1.2.4 Numbers of $CD4^+$ T cells during aging

Throughout aging the proportion of $CD4^+$ T cells in the lymphocyte pool remains more or less the same. In healthy children (0-18 years) $CD4^+$ T cells make up around 30%-60% of the total lymphocyte count (Shearer et al. 2003) and in healthy adults 32%-61%

of lymphocytes are $CD4^+$ cells. In adults this translates to a median absolute count of 885 cells/µl of blood (493 - 1666) (95% reference range in parenthesis) (Santagostino 1999). However in children the normal range for absolute cell counts decreases with age. Up to 2 years of age the median CD4 count is around 2000 cells/µl and from 12-18 years it is around 800 cells/µl (Shearer et al 2003). Body size increases with age and so does the total circulating blood volume. Therefore even though the concentration of $CD4^+$ T cells decreases the total body number of $CD4^+$ T cells increases for the first 5 years and then remains fairly constant at around 3×10^{11} cells (Hazenberg et al. 2004).

The composition of the $CD4^+$ T cell pool also changes with aging. At birth over 90% of $CD4^+$ T cells in cord blood express CD45RA, which is expressed by naïve cells (Persaud et al. 2000). With increasing age, and therefore greater exposure to antigen, more naïve cells differentiate into effector and memory $CD4^+$ cell types. Thus the concentration of naïve cells drops steeply within the first 8-12 years of life (Shearer et al 2003). However, the total body number of naïve cells has been demonstrated to increase for the first five years (Hazenberg et al 2004). Measurement of CD45RO expression has shown that though the proportion of memory cells varies greatly amongst individuals, by age 18 years it has increased from less than 5% at birth to around 40% (Shearer et al 2003). From age 18 onwards, the proportion of memory $CD4^+$ T cells increases slightly with age but this increase is only statistically significant after age 70 years (Naylor et al. 2005). A regression model of the absolute counts and relative frequencies of $CD4^+$ T cells and $CD45RA^+$ and $CD45RO^-$ subsets is shown in Figure 1.4.

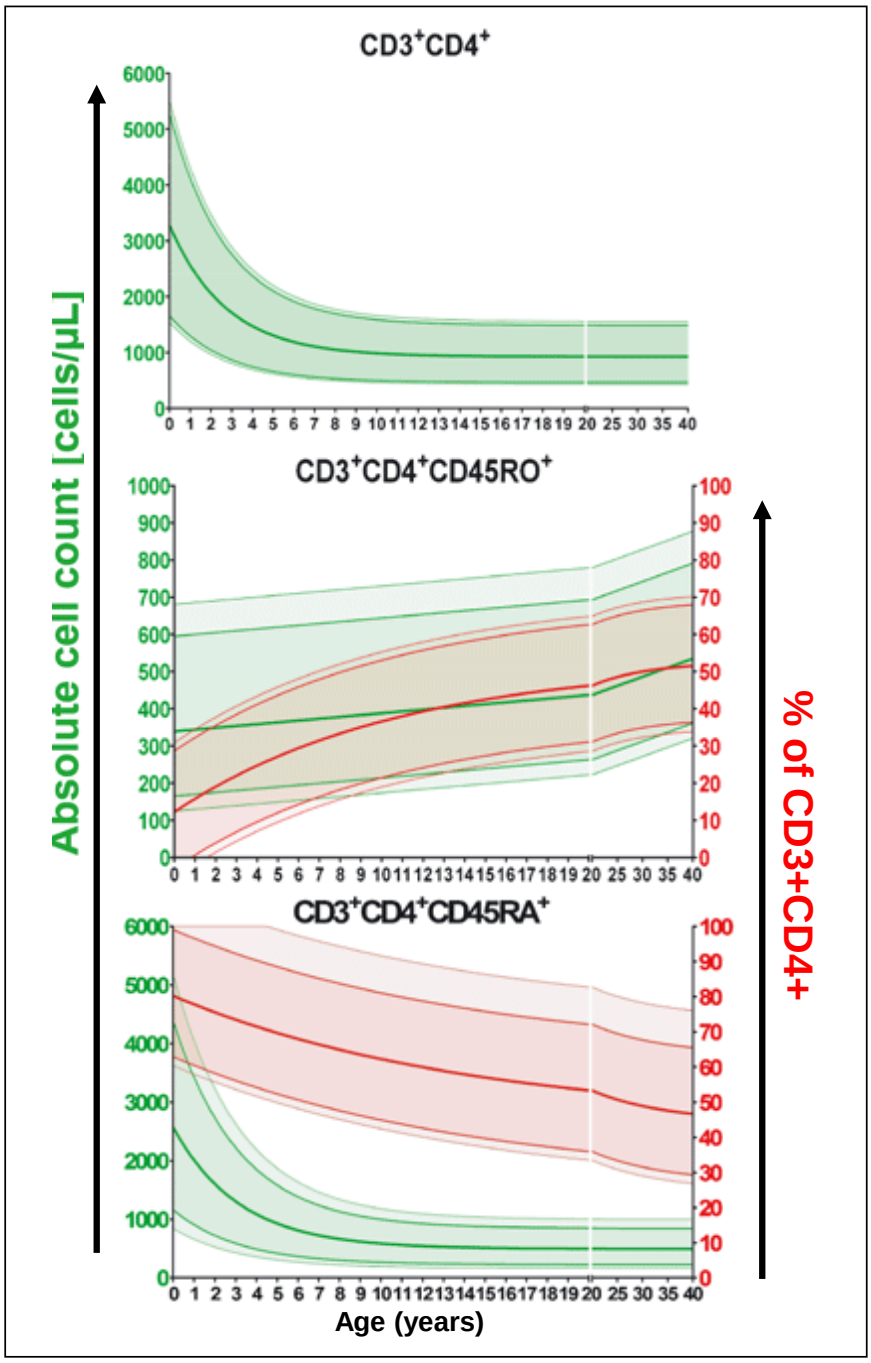

Figure 1.4 Age associated changes to $CD4^+$ T cell population and naive and memory subsets
The graphs show a continuous exponential regression model of absolute size of the $CD4^+$ T cell pool as well as relative frequencies of the memory ($CD3^+CD4^+CD45RO^+$) and naïve subset ($CD3^+CD4^+CD45RA^+$). The left y-axis shows the absolute cell count [cells/µL] of the considered population (green) and the right y-axis shows the relative frequencies, as a % of $CD4^+$ T cells (red). The thickest curve indicates the predicted value, the middle width curve indicates the upper and lower limit of a 90% confidence level of the predicted value and the thin curve a 95% confidence interval. Reproduced from (Huenecke, Behl, & Zimmerman 2008).

1.2.5 Maintenance of the $CD4^+$ T cell pool

Turnover reflects the rate at which cells within a population are replaced. T cell turnover is a function of cell production, which is a combination of thymic export and peripheral proliferation, and cell loss, through death or change of phenotype. Turnover is dynamic so both input and loss occur simultaneously. If the rate of input and output are equal, the size of the population remains constant. This is referred to as steady-state replacement. As mentioned previously the total body number of $CD4^+$ T cells increases for the first 5 years of life and thereafter is relatively constant. This would suggest that initially processes of input exceed output but after 5 years of age, input and output from the total T cell pool are balanced. If the rates of input and loss to the system are high a slight increase or decrease in either produces an exaggerated effect on the population size.

The rates of proliferation and disappearance have been estimated *in vivo* using isotope labelling techniques to measure DNA synthesis and loss (Macallan et al. 1998), (Neese et al. 2001). Briefly, subjects are either given an intravenous infusion of deuterated glucose ([6,6-$^2H_2$]glucose) or an oral dose of deuterated water (^2H_2O). Therefore DNA synthesised during the labelling period will incorporate deuterium, which is heavier than the common hydrogen isotope because its nucleus contains a neutron. Blood is sampled during and after the labelling period, then the cell population of interest is isolated, the genomic DNA is extracted and further processed to isolate the deoxyribonucleosides. The deoxyribonucleosides are subjected to gas chromatography-mass spectrometry to measure the heavy isotope enrichment. The ratio of the heavy to common isotype provides the fraction of newly synthesised DNA and therefore new cells during the period. Thus the rate of accumulation and subsequent decay of the label from a sample of DNA from the cell population of interest can be used to calculate proliferation and disappearance from the population. Measurements have been made in healthy young adults for naïve and memory T cells (Macallan et al. 2003), for T cell memory subsets (Macallan et al. 2004), in the elderly for naïve and memory T cells (Wallace et al. 2004) and also in HIV infected adults (Hellerstein et al. 1999). Unfortunately it has not been possible to similarly determine rates of turnover in young children.

From eight healthy adults the average rates of proliferation and disappearance for naïve ($CD45RA^+$) and memory ($CD45RO^+$) $CD4^+$ T cells were estimated to be 0.6%/day and 7.3%/day, and 2.7%/day and 7.4%/day, respectively (Macallan et al 2003). In healthy adults there is no net change in the $CD4^+$ T cell population size with time, yet for both naïve and memory cells, the rate of disappearance from the population exceeds the rate of proliferation. At present there are two key explanations for this discrepancy. Mohri argued that this reflects the presence of a significant input from the thymus (Mohri et al. 1998). However, the large discrepancy in rates implies that thymic production must contribute 10 times more cells than peripheral proliferation. This does not appear to be compatible with studies showing that the contribution of peripheral proliferation is increasingly important with age and exceeds the contribution of thymic production in the maintenance of the naïve $CD4^+$ T cell pool, even in young children (Kohler et al. 2005), (Berzins, Boyd, & Miller 1998), (Hazenberg et al 2004), (Bains et al. 2009). In terms of absolute numbers, this argument requires the export of some 10^{10} cells per day by the thymus. Thymic export is difficult to measure explicitly, however, current estimates are of the order of 10^8 T cells per day (Haynes et al. 2000). A second explanation is to recognise that the interpretation of *in vivo* labelling studies is confounded by heterogeneity within the T cell population (Asquith et al. 2002). Label is made available to the entire population of cells, thus it is possible to estimate an average rate of proliferation for the entire population. However, only the rate of disappearance of labelled cells is measured hence the estimate is biased towards the rate of loss of rapidly proliferating cells. It is expected that recent proliferation would correlate with a higher probability of death therefore rates of proliferation, rather than disappearance, may likely give a better estimate of average population turnover (Bains et al 2009).

The mechanisms governing T cell homeostasis are poorly understood but it is observed that under steady state conditions both the naïve and memory $CD4^+$ T cell compartments slowly turnover, in a seemingly antigen independent manner (Macallan et al 2004). Interestingly, the rates of turnover do not appear to be changed from early adulthood (mean age 26) to old age (mean age 76) (Wallace, 2004). Naïve $CD4^+$ T cells have an inter-division time of approximately 1 year, which is significantly longer than

the shorter-lived memory population; the inter-division time is identified as 15 and 48 days for T_{EM} memory $CD4^+$ T cells, $CD45RO^+CCR7^-$, and T_{CM} memory $CD4^+$ T cells, respectively. The rate of turnover of T_{EM} is more than double that of T_{CM} which would suggest that T_{EM} cells are short-lived and require a higher rate of replacement to maintain their numbers.

However, the rate of $CD4^+$ T cell turnover appears to change during HIV infection. Stable isotope studies in HIV-1 infected and uninfected adults have shown that the half-life of $CD4^+$ T cells in HIV infection is one-third as long as in uninfected controls and is not compensated for by increased production. The HIV-1 infected subjects commencing HAART was associated with an increased rate of production of $CD4^+$ T cells but not a longer half-life of circulating cells. These results suggest that HIV associated $CD4^+$ lymphopenia may be due to shortened survival time and failure to increase the production of circulating $CD4^+$ T cells.

The heterogeneity in the average rate of replacement of cells within the sub-populations of $CD4^+$ T cells likely reflects the different mechanisms that maintain naïve T cell diversity and are responsible for the long-term survival of T cell memory. It has been shown that survival of the naïve T cell compartment is dependent upon contact with IL-7 (Tan et al. 2001) as well as low affinity recognition of self-peptide MHC molecules (Takeda et al. 1996) (Tanchot et al. 1997), whereas, $CD4^+$ memory is largely maintained by a combination of IL-7 and IL-15 and does not appear to require IL-2, TCR signalling or co-stimulatory molecules such as CD28. Adoptive transfer of naive cells into T cell deficient hosts have been useful for studying the process of homeostatic division and investigating the importance of the size of the T cell niche and space available. However, the dividing cells rapidly convert to memory phenotype and it is therefore thought that this is a better model of lymphopenia-induced proliferation than the homeostatic mechanisms that drive division during steady-state (Min et al. 2003) (Surh and Sprent 2008). The processes that maintain the number of $CD4^+$ T cells are summarised in Figure 1.5.

Cells being lost from the naïve pool are an additional source of input to the memory population by undergoing immune activation and differentiating into memory cells, thus the rate of activation within this naïve pool will in part determine the rate of appearance of new cells into the memory pool.

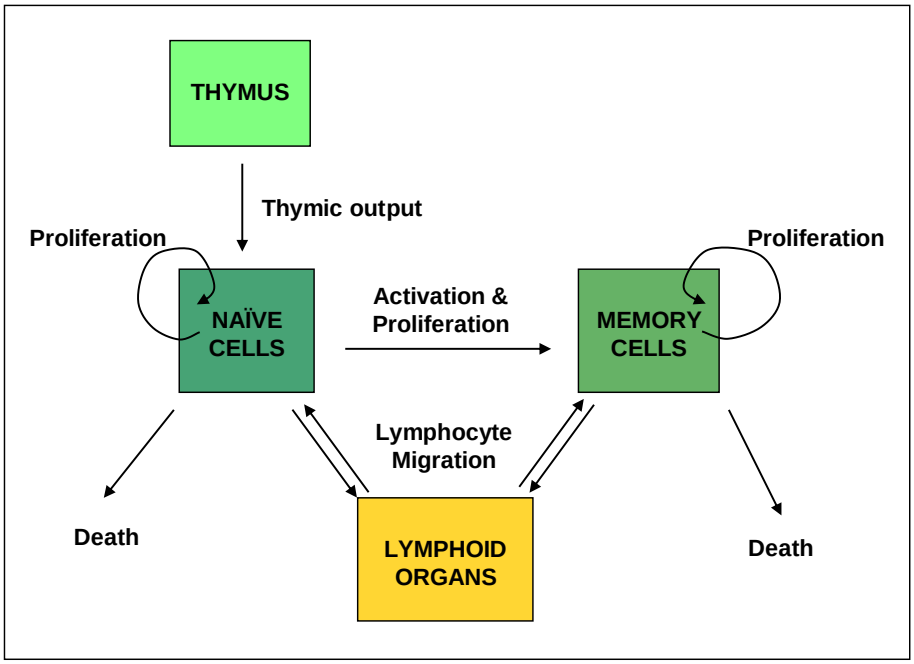

Figure 1.5 Maintenance of the number of $CD4^+$ T cells
Processes that contribute to maintenance of the $CD4^+$ T cell concentration are shown.

1.3 HIV VIROLOGY

1.3.1 Classification of HIV

HIV belongs to the retrovirus family, a group of viruses with a plus sense RNA genome, which replicate through a DNA intermediate with the help of a viral RNA-dependent DNA polymerase. The earliest retroviruses studied were isolated from birds and were associated with tumours in the host animal. The first human retrovirus, human T cell Lymphotropic virus (HTLV), was discovered in 1980 by Gallo *et al.* (Poiesz et al. 1980). There are currently 5 known human retroviruses, HTLV-I, HTLV-II, HTLV-V, HIV-1, and HIV-2. Both HIV type 1 (HIV-1) and HIV type 2 (HIV-2) cause AIDS.

However HIV-1, on which this work is focussed, is the more virulent type and accounts for 90% of the entire global disease burden.

Initially retroviruses were divided into three genera based on their pathogenesis: oncoviruses, spumaviruses and lentiviruses (Buchschacher 2001). Oncoviruses are associated with tumourigenesis in both animals and humans. The human retroviruses, HTLV-I, HTLV-II and HTLV-V, are oncoviruses associated with adult T cell leukaemia. Although other oncogenic viruses, such as Epstein-Barr Virus (EBV), which can cause Hodgkin's disease, Burkitt's lymphoma and nasopharyngeal carcinomas are known, they differ from oncoviruses in that they cause cancer indirectly via immunosuppression whereas oncoviruses cause cancer directly by inserting viral oncogenes into the host genome or enhancing oncogenes already present in the host genome (Butel 2000).

Spumaviruses, also called foamy viruses because they produce a foamy appearance in cultured cells, are highly cytopathic *in vitro*. However there is currently no evidence of pathogenesis in humans or animals though infections are common in both (Switzer et al. 2005).

The last retrovirus genus, ‘lentivirus’, literally means ‘slow virus’; and these viruses were so called because the course of infection was characterized by a long interval between initial infection and the onset of serious symptoms. HIV is the only human member of lentivirus group. Other members are the animal immunodeficiency viruses such as the simian immunodeficiency viruses (SIV), which infect monkeys and chimpanzees.

Based on phylogenetic analysis of the nucleotide sequence of the *env* gene HIV-1 strains have been divided into three groups: M, N and O. M is the most prevalent, globally it accounts for over 95% of HIV-1 isolates. Currently Group M is further subdivided into nine clades A, B, C, D, F, G, H, J and K (including the sub-subtypes

A1, A2, A3, A4, F1 and F2). The most prevalent are clades B (found predominantly in North America and Europe), A and D (found mainly in Africa), and C (found mainly in Africa and Asia) Recombination between and within the clades produces recombinant strains called circulating recombinant forms (CRFs). 18% of the global HIV burden is due to CRFs most of which are recombinations with clade A viruses (Taylor et al. 2008).

1.3.2 Origin of HIV

Disputes about the origins of HIV were finally settled at the turn of this century and it is now generally agreed that HIV arose from its close Lentivirus relative, Simian Immunodeficiency Virus (SIV), by cross species transmission (zoonotic transmission) (Sharp et al. 2001). In nature, SIV infection is common in many catarrhini, old world monkeys and apes, such as the African green monkey, sooty mangabeys and chimpanzees though some catarrhini simians such as macaques are not natural reservoirs. In contrast new world monkeys, platyrrhini, do not seem to be natural reservoirs of SIV. Within their natural hosts, SIV viruses are generally not pathogenic but have been shown to be pathogenic in other species. When macaques are inoculated with SIV from sooty mangabey monkeys a pathogenic infection is observed (Lewis et al. 1992). Isolates of SIV have been shown to infect human $CD4^+$ T cells, monocytes and macrophages, as does HIV itself (Grimm et al. 2003).

HIV-1 and HIV-2 probably arose from different SIV lineages since each is more closely related to a particular SIV than to each other. Thus it is believed that SIV from chimpanzees (SIV_{CPZ}) in southern Cameroon and SIV from sooty mangabey monkeys (SIV_{SMM}) in west-central Africa were responsible for the introduction of HIV-1 and HIV-2 respectively, into the human population. The differing simian origins of HIV-1 and HIV-2 were elucidated by reconstructing the phylogenetic relationships among the many strains of HIV-1 and HIV-2, as well as related SIV strains. A simplified phylogenetic relationship trees for primate lentiviruses (derived from *pol* sequences), which place the two HIV types in different SIV lineages is shown in Figure 1.6.

There was some controversy in the 1990s that SIV was introduced from its primate host into the human population in east-central Africa during the 1950s by an oral polio vaccine that was contaminated with SIV_{CPZ}. This was mostly discredited because molecular clock analysis, which uses models of HIV-1 sequence evolution, place the HIV-1 group M ancestor earlier than 1940 with 95% certainty. It is more widely accepted that SIV entered the human population from the practice of hunting and eating monkeys as bushmeat in central Africa. In this region primate species including chimpanzees and sooty mangabey monkeys are routinely killed for food. It is thus very plausible that during the butchering or perhaps eating of poorly cooked bush meat people were exposed to blood or other primate secretions (Sharp et al 2001).

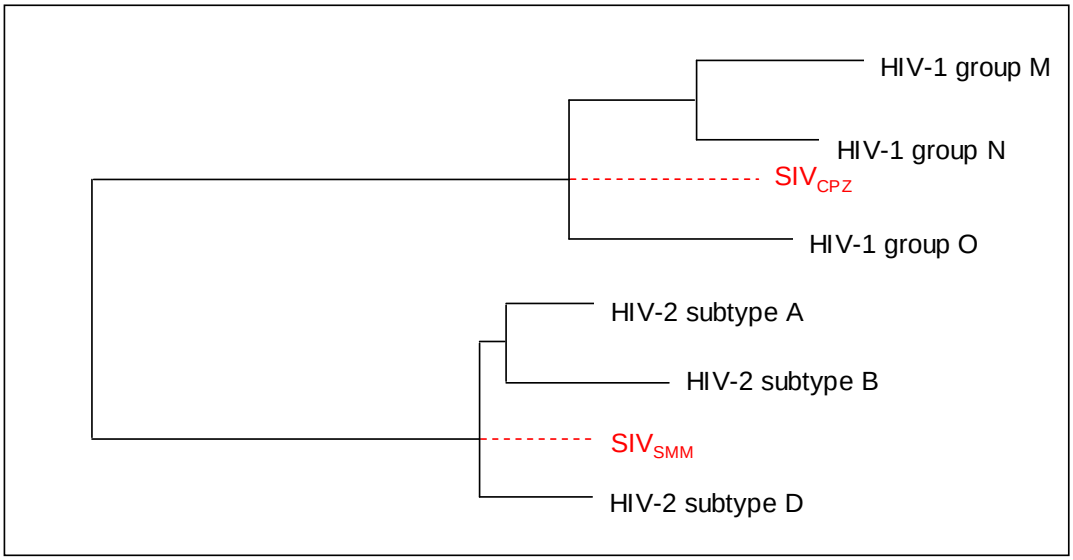

Figure 1.6 Phylogenetic relationship tree of primate lentiviruses
Diagram shows interspersion of the HIV-1 and HIV-2 groups around SIV_{CPZ}. Horizontal distances indicate genetic separation between strains. CPZ= chimpanzee, SMM= sooty mangabey monkey. Adapted from (Sharp et al 2001).

1.3.3 Structure of HIV

The structure of the HIV virus (Turner and Summers 1999) consists of a nucleic acid core, encapsulated by a capsid consisting of 2,000 copies of the viral protein, p24 as shown in Figure 1.7 . Enclosed within the capsid are the enzymes integrase and reverse transcriptase and other viral proteins. Around the capsid is another protein casing called

the matrix. The viral enzyme protease is present within the matrix. Around the matrix is an envelope derived from the host cell plasma membrane, acquired when the virus buds through the cell membrane. Embedded in the envelope are the viral glycoproteins, gp120 and gp41. The core contains two copies of the single stranded RNA genome, arranged as a dimer.

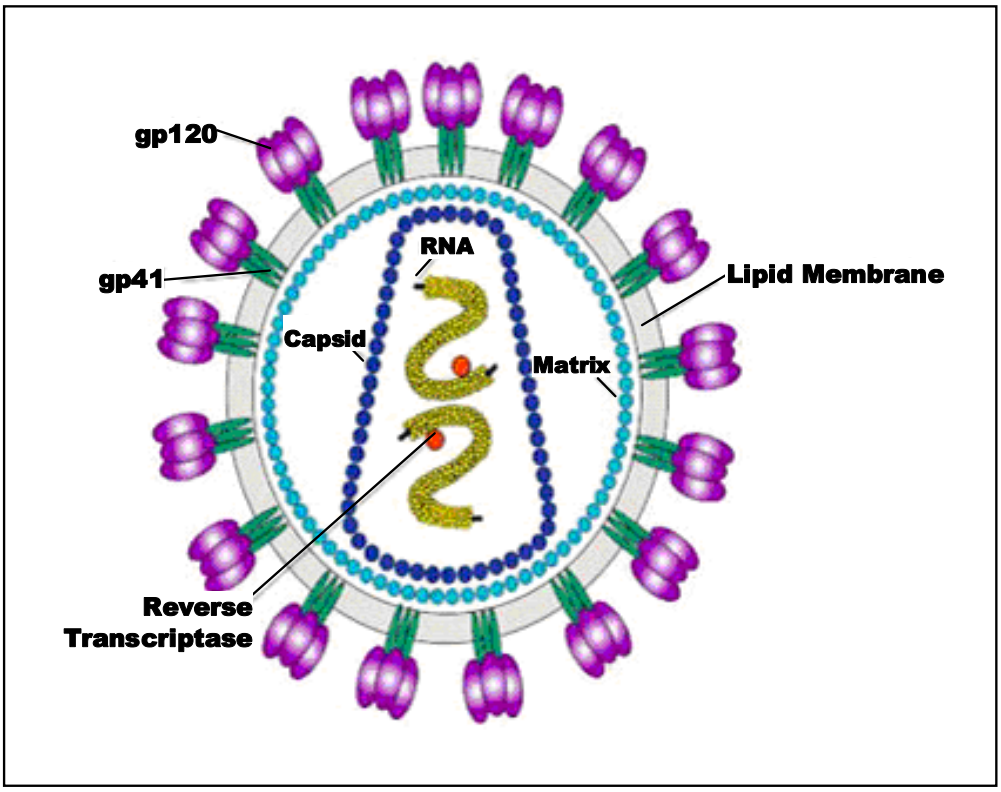

Figure 1.7 Structure of an HIV virion

The diagram shows the organisation of the HIV virion The lipid membrane, also known as the envelope, is derived from the host cell plasma membrane. Reproduced from (CDC 2008)

Compared to other viruses the HIV-1 genome is relatively small. Shown schematically in Figure 1.8 it is approximately 9 kilobases (kb) and contains only 3 open reading frames (ORFs), which are common to all retroviruses: *gag*, *pol* and *env*. These ORFs are flanked by long terminal repeats (LTRs), sequences of repeated nucleotides generated during reverse transcription and found at the ends of viral DNA (the provirus). They regulate synthesis of viral RNA.

Gag (group specific antigen) encodes the precursor protein, gag, which is cleaved to give the internal major structural proteins of the virus: matrix, capsid, nucleocapsid and p6 proteins. *Pol* (polymerase) encodes the viral enzymes protease, reverse transcriptase and integrase. *Env* (envelope) encodes the precursor (gp160) of the viral envelope proteins gp41, also called transmembrane protein, and gp120, also called surface protein 14.

In addition to these, HIV also expresses the regulatory genes *tat* and *rev* that are essential for viral replication, and the accessory genes *vif*, *vpr*, *vpu* and *nef*. The accessory genes function to make the host biology promote the virus life cycle and are important in determining the virulence of the virus (Nielsen, Pedersen, & Kjems 2005).

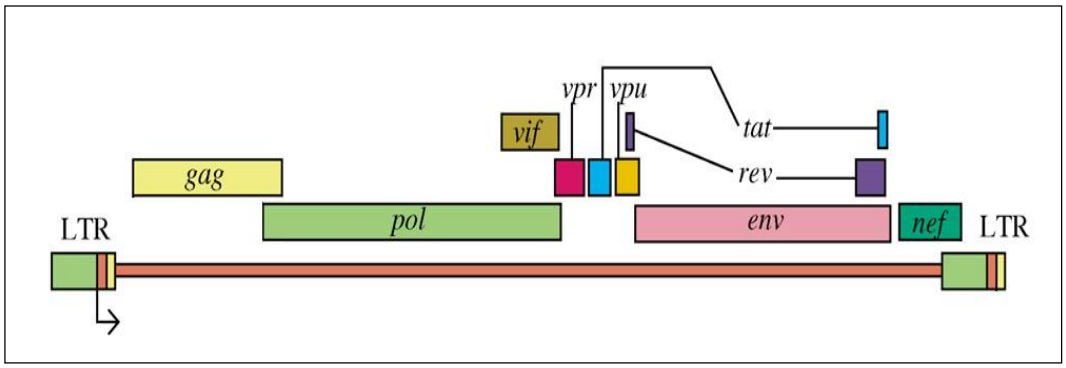

Figure 1.8 Schematic representation of the HIV-1 genome

Schematic representation of the HIV-1 provirus. Gag, group specific antigen; Gag-Pol, group specific antigen-polymerase; Env, envelope; Tat, trans-activator of transcription; Rev, regulator of expression of virion proteins; Nef, negative effector; Vif, virion infectivity factor; Vpr, viral protein r; Vpu, viral protein u; LTR, long terminal repeat. Reproduced from (Nielsen, Pedersen, & Kjems 2005).

1.3.4 HIV life cycle

First, HIV must enter the body. This can occur in infected sexual secretions at epithelial surfaces lining the genital tracts or it can be introduced directly into the bloodstream by

blood transfusions, contaminated needles and during childbirth. Infection is far more likely if HIV is introduced directly into the blood stream than from exposure of epithelial surfaces to infected sexual secretions. Either way the virus can be carried as free virions in blood or lymph or bound to dendritic cells until it reaches a target cell, where the complex HIV replication cycle then occurs.

1.3.4.1 Viral entry and uncoating

Entry into target cell is via binding of the viral glycoprotein gp120 to CD4 on the host cell surface (Dalgleish et al. 1984), (Klatzmann et al. 1984). As was shown in Figure 1.7, gp120 is the surface subunit and is bound to the transmembrane protein gp41 in a trimeric arrangement, 3 pairs of gp120-gp41 structures together. Gp41 contains two amphipathic helical domains, heptad repeat-1 and heptad repeat-2 (HR1 and HR2), and a fusion peptide. Binding to CD4 causes a conformational change in the structure of gp120, which exposes the co-receptor binding sites. Co-receptor binding results in a conformational change to gp41 allowing HR2 and HR1 to interact with each other to form a stable six helix bundle structure. This produces a fusion pore and HIV enters the cytoplasm leaving the viral envelope at the cell surface behind (Jones, Korte, & Blumenthal 1998).

Evidence that CD4 alone is not sufficient for viral fusion came from attempts to infect murine cells expressing human CD4; although HIV was bound the cells did not become infected (Ashorn, Berger, & Moss 1990). Additionally HIV isolates derived from T cells could not infect monocytes or macrophages and vice versa, suggesting the existence of multiple co-factors that must be cell type specific (Gartner et al. 1986). The first co-receptor identified was CCR5, previously known as fusin, which is used preferentially by T cell line-tropic HIV isolates (Feng et al. 1996). Subsequently the co-receptor used by macrophage-tropic isolates was found to be C-X-C motif chemokine receptor four (CXCR4), previously known as CCKR5 (Alkhatib et al. 1996). The chemokine receptor used as a co-receptor by a virus is determined by the V3 loop of its gp120 but most commonly, CCR5 and CXCR4 are used (Markovic and Clouse 2004). CCR5 is the co-receptor used by primary isolates at the beginning of HIV-1 infection and individuals with a 32-base pair deletion in the CCR5 gene (Δ32) have been shown

to be highly resistant to infection by primary HIV-1 isolates (Kostrikis et al. 1999). During later stages of HIV infection mutations by viral isolates allow them to use CXCR4 as a co-receptor (Bahbouhi, Landay, & Al-Harthi 2004).

The requirement for CD4 and a co-receptor limits the tropism of HIV to thymocytes, $CD4^+$ T lymphocytes, macrophages, $CCR5^+$ dendritic cells and glial cells of the nervous system (Poveda et al. 2006). For successful entry, multiple receptors and co-receptors must be recruited therefore $CD4^+$ T cells are the main target cells for HIV because they are more abundant and have a higher surface density of CD4 and chemokine co-receptors. Amongst $CD4^+$ T cells more memory than naïve cells are infected (Spina, Prince, & Richman 1997). This may be partly explained by their differential co-receptor expressions. Expression of CCR5, which is used by most virus isolates, is largely restricted to memory cells. CXCR4, which is used by viral isolates in advanced infection, is expressed on both naive and memory cells but more so on naive cells (Mo et al. 1998).

Retroviruses show a cell cycle restriction to infection (Yamashita and Emerman 2006). Most can only infect dividing cells and those that can infect non-dividing cells, cells in G_0, usually do so with reduced efficiency. HIV and the other lentiviruses show the least restriction. Cells in G_0 are in a distinct quiescent phase outside of the cell cycle. They are neither dividing nor preparing to divide and cell cycle machinery is removed. HIV can infect with equal efficiency into dividing cells and terminally differentiated non-dividing cells. Naïve unactivated quiescent cells in the periphery can also be infected but at lower efficiency. This may also explain why more memory than naïve cells are infected and also allows the establishment of major viral reservoirs such as non-activated $CD4^+$ T cells and terminally differentiated macrophages. For infection to be productive, resulting in the generation of new virions, the host cell needs to be activated because viral production has been shown to require the same cytokine signalling that is elicited from the IL-2 receptor following TCR triggering (Oswald-Richter et al. 2004).

Successful interaction between the virus and a suitable cell allows the virus to enter the cell, disassemble the capsid, referred to as uncoating, thereby exposing viral RNA and enzymes. Although, uncoating is the least understood part of the HIV replication cycle, it is known to occur in activated cells but not resting cells because lysate from activated cells can trigger uncoating but lysate from resting cells cannot. This also suggests the involvement of host cellular factors in the uncoating process. A cellular kinase, peptidyl-prolyl isomerase Pin1, that specifically recognizes a capsid protein motif and phosphorylates its' serine residue has been shown to be required for the disassembly of the HIV-1 capsid (Misumi et al. 2010).

1.3.4.2 Reverse transcription

After uncoating the RNA genome, HIV is reverse transcribed by viral reverse transcriptase (RT) (Freed and Mouland 2006) (Castro et al. 2006). RT is a holoenzyme consisting of 2 protein subunits, DNA polymerase and RNase H. The DNA polymerase subunit is an RNA dependent DNA polymerase that catalyses the addition of deoxynucleotides complementary to the RNA strand to form the nascent DNA strand. RNase H is a ribonuclease that catalyses the hydrolytic cleavage of the 3'-O-P-bond of RNA in a DNA/RNA duplex. As mentioned in section 1.3.3 each HIV virion contains 2 complementary RNA molecules, the plus strand and the minus strand, also called the positive sense strand and the negative sense strand respectively. The plus strand is the coding strand, which means it is identical to viral messenger RNA (mRNA) and can be directly translated into protein. The minus strand is non-coding.

RT, like all DNA polymerases, requires a primer with a free 3'-hydroxyl to initiate DNA synthesis. On the plus strand, where reverse transcription begins, the primer is a host cell transfer-RNA (tRNA) molecule, added to the virus during assembly of the viral particle The tRNA molecule anneals to an 18 nucleotide sequence close to the 5' end of the plus strand, called the primer binding site (pbs). The DNA polymerase subunit of RT catalyses the addition of a deoxynucleotide to the 3' end of the tRNA primer and from here synthesis of a complementary DNA strand proceeds to the 5' end of the plus strand RNA (Litvak et al. 1994). The RNase H subunit then catalyses the degradation of the RNA strand where it was hybridised to the nascent DNA strand. The

short DNA strand produced, called the minus-strand strong stop DNA, then moves from the 5’ to the 3’ end of the plus strand, a step referred to as the first strand transfer. Here its 3’end acts as the primer for the synthesis of the complete minus DNA strand. The tRNA primer is then removed by RNase H (Freed and Mouland 2006).

During DNA minus strand synthesis when the RNA plus strand was hydrolysed by RNAse H action small fragments remained. These small fragments of plus strand RNA are used as primers for the synthesis of the DNA plus strand. They anneal to purine rich sequences on the RNA minus strand, the polypurine tract (PPT) and the central PPT (cPPT). Removal of the tRNA allows RT to move to the minus strand where it adds deoxynucleotides to the 3’ end of the RNA primers (Freed 2001). The template switching, where RT moves from one RNA strand to the other is one of the mechanisms that generate genetic diversity in HIV viruses (Basu et al. 2008). If the two RNA molecules in a virion are not identical then template switching results in a novel recombinant DNA genome made of sequences from both RNAs. The process of reverse transcription is summarised in Figure 1.9.

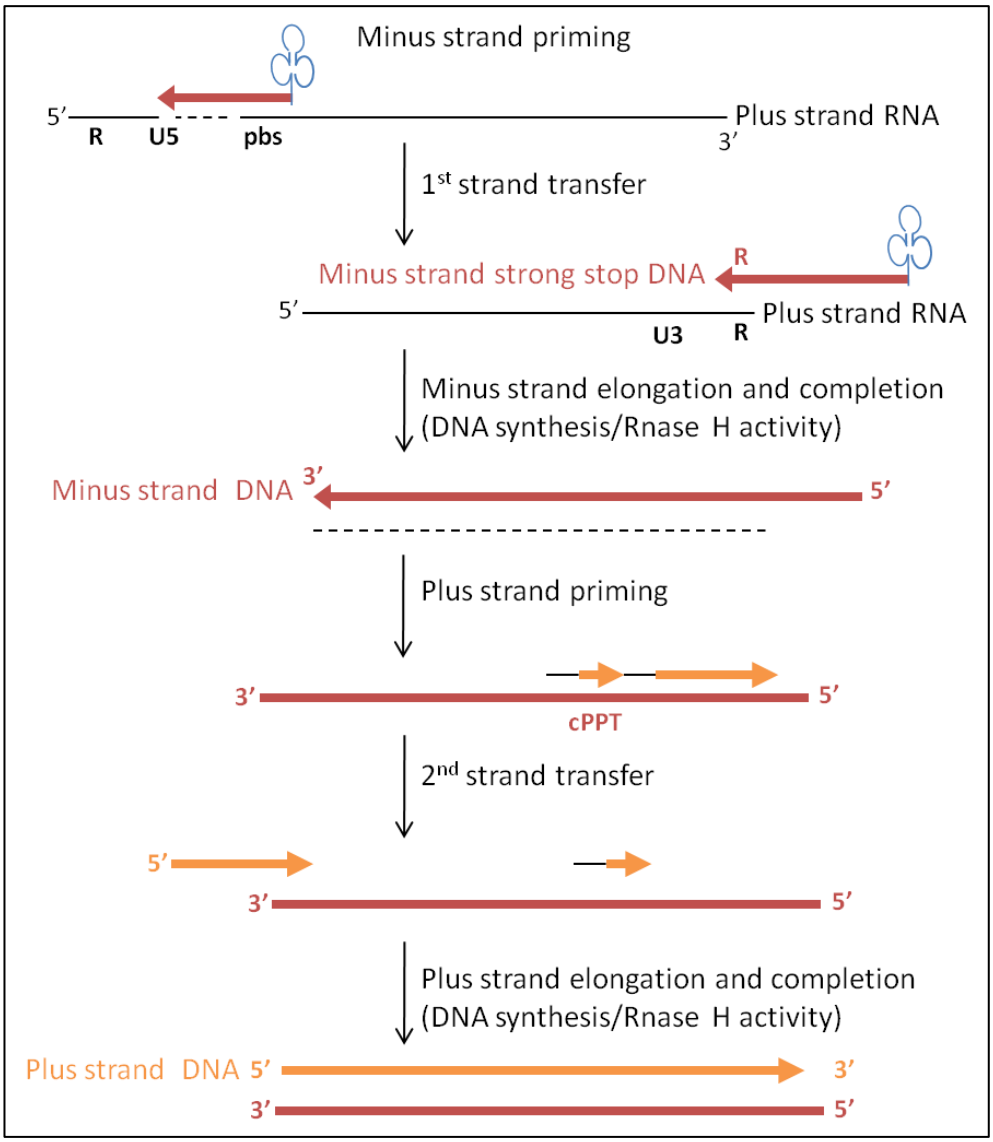

Figure 1.9 Process of reverse transcription

Synthesis of the first DNA strand, the minus strand, is initiated from the primer binding site (PBS) on the RNA plus strand, utilising a tRNA as a primer. Synthesis of the second DNA strand, the plus strand, is initiated from the central polypurine tract (cPPT) using RNA fragments generated from hydrolysis of the RNA plus strand during DNA minus strand synthesis. Adapted from (Freed 2001).

1.3.4.3 Proviral integration and transcription

The new viral DNA, known as the provirus, is then imported into the nucleus as part of the pre-integration complex (PIC). The PIC consists of viral and cellular proteins required for integration. The integration of the provirus into the host genome is mediated by the viral enzyme integrase (IN) (Delelis et al. 2008). First IN cleaves off nucleotides from the 3' ends of both strands of the provirus. Then at the integration site

IN cleaves the host DNA in a staggered manner and the 3' ends of the provirus join to the cleaved ends of the host DNA. Host cell repair enzymes then fill in the gaps between the viral DNA and the host DNA.

The provirus can lie latent and the infected cell continues to function, or in the presence of certain transcription factors including NF-$_K$B, the virus can become active and replicate. In the latter case, replication begins with transcription of viral DNA, which starts at the long terminal repeat (LTR) with the binding of the viral protein, Tat, to an RNA element, the transactivation response region, and results in the production of over 30 viral RNAs (Wu and Marsh 2003). They are divided into unspliced, partially spliced and small multi-spliced RNAs. The unspliced full-length viral RNA is exported from the nucleus under the direction of the viral protein, Rev, which binds to the Rev responsive element in the viral RNA and is destined to be packaged into progeny virions as genomic RNA. The spliced RNAs are translated in the cytoplasm. Translation of the partially spliced RNAs results in the synthesis of the structural proteins, the Gag polyprotein precursor, the Gag-Pol polyprotein precursor, the Env glycoprotein precursor, gp160. Translation of the small multispliced RNAs results in the synthesis of tat and rev as well as the accessory proteins Nef Vif, Vpr and Vpu.

1.3.4.4 Virion assembly and budding

The next two steps, assembly of the viral particle and budding from the cell membrane, occur simultaneously beginning with the transportation of viral proteins and viral genomic RNA via the golgi apparatus, to the plasma membrane. Within the golgi apparatus the Env glycoprotein precursor, gp160, is cleaved into gp120 and gp41 by a host protease. At the cytoplasmic side of the plasma membrane assembly is directed by Gag. The Gag protein is divided into functional domains, each with an associated activity that is required for efficient generation of immature viral particles. The N-terminal matrix domain, directs Gag to the plasma membrane, the central capsid domain determines particle morphology, the nucleocapsid domain binds RNA, enabling the packaging of the viral genome, and the C-terminal domain, p6, is required for the separation of the viral envelope from the host cell membrane, releasing new virions into the extracellular space (Bieniasz 2009). Maturation of the viral particles requires the

action of viral protease, which catalyses a series of cleavage reactions in gag resulting in morphological and structural changes that render the virions infectious. A pictorial representation of the steps of the HIV replication cycle and their cellular locations are shown in Figure 1.10.

1.3.4.5 Innate restriction factors against HIV

The HIV replication cycle is subject to the effects of innate restriction factors, proteins produced by host cells that target intracellular HIV-1 replication, which may be important in the development of novel therapeutic agents against HIV infection. The restriction factors, which operate at different stages of the HIV-1 life cycle, include Apolipoprotein B mRNA-editing enzyme 3G (APOBEC3G), which inhibits reverse transcription by catalysing the deamination of viral minus strand cytidines to uracil, bone marrow stromal cell antigen 2 (BST-2), which limits the release of viral particles possibly by tethering them to the cell membrane and tripartite motif protein 5 alpha (Trim5α), which blocks reverse transcription and nuclear import of the HIV provirus possibly by binding to incoming virion cores and prematurely uncoating them. Restriction factors, however, do not operate unopposed because HIV encodes proteins, Vif, Vpu and Tat, which counteract their effects (Strebel, Luban, & Jeang 2009).

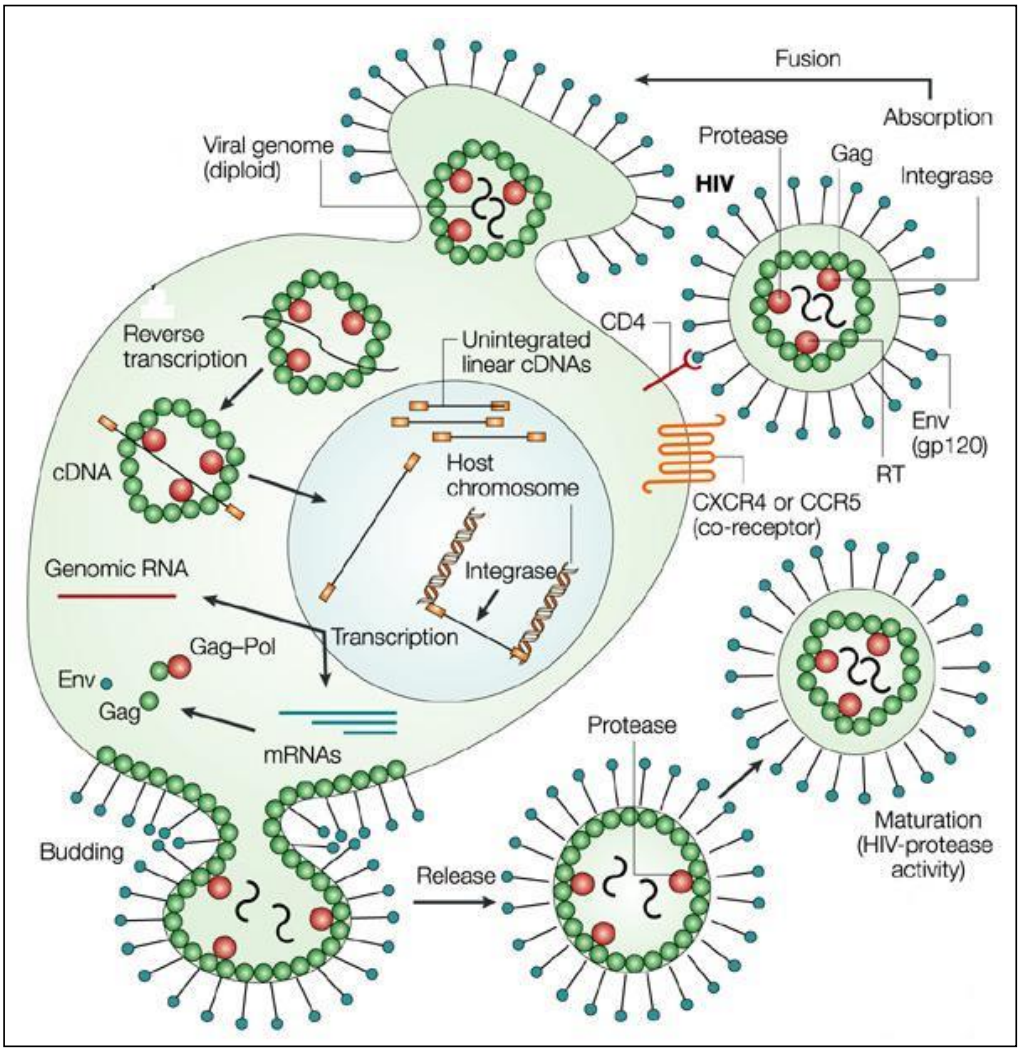

Figure 1.10 Replication cycle of HIV

The diagram shows the steps in the replication of an HIV virion from cell entry through to release of the new virions. Reproduced from (Monini et al. 2004)

1.4 PATHOGENESIS OF HIV INFECTION

1.4.1 The clinical course of HIV-1 infection

HIV infection is a chronic viral infection, characterised by a decline in the CD4 count and other immune dysregulation. The immunodeficiency allows for the opportunistic infections and neoplastic changes that ultimately result in death. The course of HIV infection and the associated changes in plasma viraemia and CD4 count are summarised in Figure 1.11.

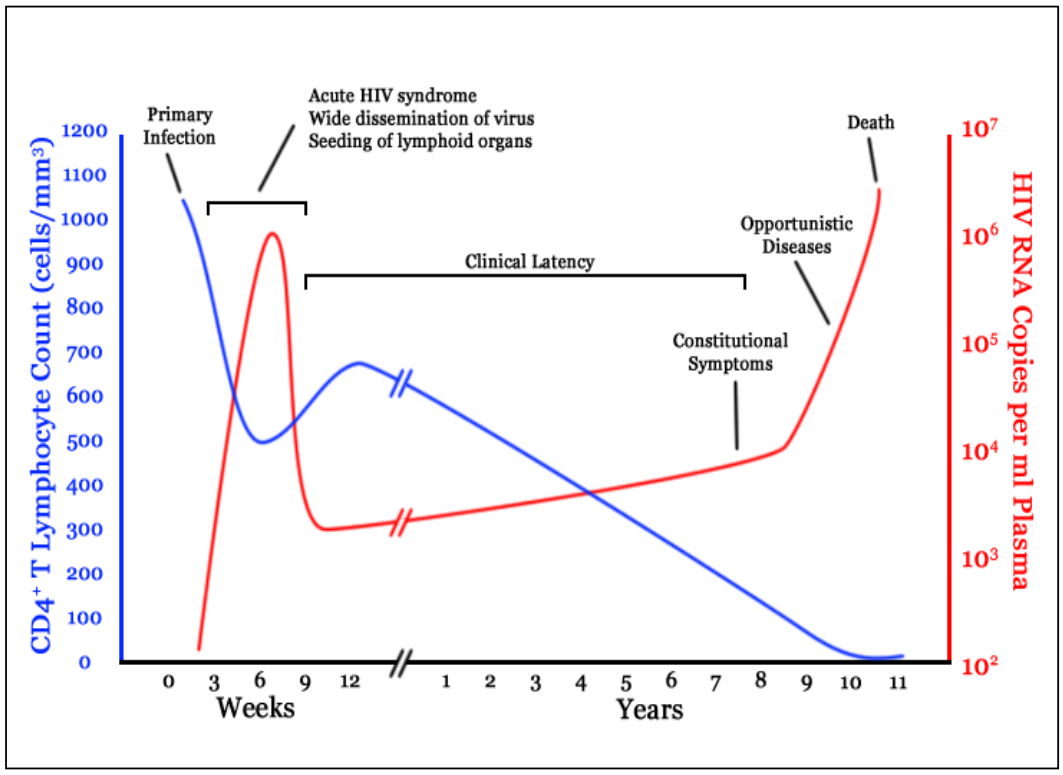

Figure 1.11 Generalised course of untreated HIV-1 infection

The changes to CD4 count (blue line) and plasma viral load (red line) during the different phases of HIV-1 infection are shown. The length of each phase, especially clinical latency vary greatly between individuals. Reproduced from *Wikipedia*, originally published as *Figure 1* in (Pantaleo, Graziosi, & Fauci 1993).

HIV infection in most individuals begins with an acute phase of high-level viraemia within 2 months of infection. During this period viral replication is rampant resulting in the dissemination and seeding of virus in all peripheral lymphoid organs as well as in mucosal-associated lymphoid tissue. The rampant viral replication is reflected by a high viral load that can reach millions of copies of virus per millilitre of plasma. Therefore the acute phase is the most infectious phase. The acute phase ends as the viral load decreases and plateaus to a set point, as the immune system mounts an anti-viral response. This set point is very important because high viral set points are associated with rapid disease progression to AIDS (Sterling et al. 2001), even though there is no standard method for calculating the viral load set point The viral load set point is determined by host factors such as gender, age, race, other diseases, and human genetic variation as well as viral factors such as co-infection with multiple HIV subtypes, which

is associated with an increased set point (Streeck and Nixon 2010). During the acute phase there is also a marked drop in the numbers of circulating $CD4^+$ T cells but they rebound, though still below normal values, as the viral load declines. Most patients experience cold and flu-like symptoms such as fever, lymphadenopathy, fatigue, malaise and myalgia during this period (Vergis and Mellors 2000), (Hicks, Gay, & Ferrari 2007).

The immune response is characterised by a rapid increase in the concentration of $CD8^+$ T cells and the release of antibodies against HIV-1 into the bloodstream. Activated HIV-1 specific $CD8^+$ T cells kill HIV-1 infected cells but are unable to entirely contain viral replication and eradicate HIV. The decline in viral load down to the set point is associated with a decline in CTL number and activity, which may partly explain why HIV is not eradicated (Miedema et al. 1994). In addition HIV continually mutates to generate virus that escapes from control by HIV-1 specific $CD8^+$ T cells. Anti-HIV-1 antibodies appear to have little impact on viral replication but their presence in the plasma is utilised for diagnosis. Enzyme linked immunosorbent assays (ELISA) specific for HIV-1 antibodies are used to diagnose HIV-1 infection after seroconversion (Morris 2002).

The second phase of infection, clinical latency, is an asymptomatic chronic phase, which without treatment is associated with a gradual decrease in CD4 count, and little change in viral load from the set point established during primary infection. This phase is of extremely variable length, some individuals remain asymptomatic for over 10 years without treatment and others progress rapidly to full blown AIDS within a few years (Vergis and Mellors 2000), (Jaffar et al. 2004). Though little decrease in CD4 count is seen during this phase the rate of CD4 attrition is actually high but is adequately compensated by rapid replacement of the cells. Kinetic measurements with deuterated glucose have shown that in HIV infected individuals over 50% of the new cells produced/day were short lived compared to 30% in HIV negative subjects (Hellerstein et al 1999).

The last phase of infection, AIDS, is associated with a steep increase of the viral load and rapid decline in CD4 count. During this final phase of infection, the immune system fails and the body becomes progressively more susceptible to opportunistic infections and neoplasms, which ultimately result in death. Typical AIDS defining opportunistic infections include *candida, mycobacterium* species and *Pneumocystis carinii.* The most common cancers seen in HIV-1 infected individuals include Kaposi's sarcoma and B cell lymphomas (Libman 1992), (Vergis and Mellors 2000).

The pathogenesis of HIV-1 is complex and determined by both viral and host factors. Multiple modes of pathogenesis have been proposed and studied. Pathogenesis is more complicated than CD4 depletion resulting in compromised immunity because non $CD4^+$ T cell populations are also depleted. B cell function and numbers have been shown to be compromised in HIV infection independently of $CD4^+$ T cell impairment (Moir and Fauci 2008). Additionally virally induced CD4 depletion by SIV in the natural host monkey has been observed without progression to AIDS (Milush et al. 2007). This thesis however is confined to $CD4^+$ T cell depletion and recovery, and the next sections describe possible causes of the CD4 depletion observed in HIV infection, focussing on the dynamic between $CD4^+$ T cells and HIV.

1.4.2 Direct elimination of HIV-1 infected cells by HIV and CTLs

In the 1980s several groups demonstrated the cytopathic effect of HIV replication on $CD4^+$ T cells in culture, when productively infected cells were lysed (Fenyo, Albert, & Asjo 1989), (De Rossi et al. 1986), (Fisher et al. 1985). The amino terminal end of the viral protein gp41 on its' own can lyse up to 40% of cells in culture (Mobley et al. 1992). *In vivo* only infection of activated cells is cytopathic whereas infection of quiescent cells by HIV results in a non-replicated latent infection (Briant et al. 1996). However latently infected cells present viral antigens on their cell surface so can be killed by CTLs (Riviere et al. 1989), (Grant, Smaill, & Rosenthal 1993) and complement and antibody mediated lysis (Gregersen et al. 1990).

1.4.3 Indirect elimination of HIV uninfected $CD4^+$ T cells via apoptosis

Direct killing of $CD4^+$ T cells by HIV lytic infection and CTLs may mostly explain the initial loss of $CD4^+$ T cells during the acute phase of HIV infection. However, by the chronic phase the number of HIV-1 specific CTLs is markedly reduced and neither lytic infection nor CTLs can account for the depletion of uninfected cells in HIV-1 infection. Then crosslinking of gp120 on the surface of $CD4^+$ T cells was demonstrated to induce their death by apoptosis (Banda et al. 1992). Additionally apoptosis was shown to occur predominantly not in infected $CD4^+$ T cells but in the bystander uninfected $CD4^+$ T cells hence the term the 'bystander effect' (Finkel et al. 1995). Other studies also reported increased apoptosis in HIV infected people compared to uninfected controls (Laurent-Crawford et al. 1991), (Patki, Georges, & Lederman 1997). It has been demonstrated *in vitro* that PBMCs from HIV-1 infected patients are more likely to undergo spontaneous apoptosis than similarly treated peripheral blood mononuclear cells (PBMCs) from uninfected adult controls. In both the controls and the infected individuals cells in synthesis phase (S phase), the phase of the cell cycle when DNA is replicated, were more likely to undergo apoptosis than other cells (in G_0-G_1) but the CD4 cells from infected individuals were more likely to enter S phase (Patki et al. 2000).

Increased apoptosis has been found to be associated with disease progression (Gougeon et al. 1996). Individuals with the lowest CD4 counts (0-99 cells/µl) have higher levels of apoptosis in PBMCs than individuals with higher CD4 counts (Patki, Georges, & Lederman 1997). Children who are long term non progressors (LTNPs), those who have survived with HIV for over 5 years, without significant anti-retroviral therapy (ART), were shown to have characteristically low frequencies of apoptotic CD4 and CD8 cells and less mitochondrial membrane disruption (Moretti et al. 2000). Expression of CD95, a death receptor on the surface of cells that leads to programmed cell death (apoptosis), has been shown to be strongly increased in both $CD45RO^+$ and $CD45RA^+$ T cells of HIV-1-infected children (Baumler et al. 1996). Similar apoptotic changes, increased activation of the cyclin B complex are found in HIV and pathogenic SIV infection (Paiardini et al. 2006).

1.4.4 Increased activation induced cell death during HIV infection

In 1991 Jean Claude Ameisen and André Capron proposed that the increased apoptosis in HIV-1 infection might be mediated by activation on the basis that thymocytes undergo apoptosis in response to activation during selection in the thymus (Ameisen and Capron 1991). They showed that only $CD4^+$ T cells from HIV infected individuals underwent apoptosis after mitogen stimulation *in vitro* compared to $CD4^+$ T cells from uninfected controls (Groux et al. 1992). Studies by other groups also found that apoptosis of $CD4^+$ T cells *in vitro* was increased by activation with IL-12 (Meyaard et al. 1992), (Estaquier et al. 1995). These findings were echoed in a murine (Saha, Yuen, & Wong 1994) and a primate model of HIV infection (Wallace et al. 1999).

Numerous studies using different markers of activation such as CD25, CD38 and HLA-DR have demonstrated that in both adult and paediatric HIV infections, the proportion of activated cells within the CD4 pool is increased (Lees et al. 1993), (Mahalingam et al. 1993), (Plaeger-Marshall et al. 1994). Immune activation has been shown to correlate with CD4 count (Sousa et al. 2002) and disease progression (Carbone et al. 2000).

Increased activation is a plausible cause of CD4 depletion via apoptosis. As explained in section 1.2.3 activation of the TCR, depending on signal strength, can lead to anergy and therefore cell death, or differentiation from long lived cells into short lived effectors that are prone to activation induced cell death. Additionally activated cells are at greater risk of productive HIV infection (Williams and Greene 2007). All of these would deplete $CD4^+$ T cells, however HIV viral antigens would only be recognised by the TCRs of HIV-1 specific $CD4^+$ T cell and they make up a small fraction of the T cell repertoire. Therefore if HIV antigen recognition by HIV specific $CD4^+$ T cells alone was the cause of $CD4^+$ T cell activation it would be insufficient to cause the massive T cell loss.

HIV has however been shown to increase expression of co-stimulatory molecules and as explained previously co-stimulatory molecules lower the threshold required for immune activation. A mechanism by which chronic expression of co-stimulatory molecules

might cause CD4 depletion has been shown in mice that constitutively express CD70. CD70 is the ligand for the co-stimulatory molecule CD27 and is present on B cells (Tesselaar et al. 2003). In these mice all TCR stimulation was accompanied by co-stimulatory CD27-CD70 signalling and they showed a progressive fall in naïve T cells with a concomitant increase in effector-memory cells. This ultimately resulted in the depletion of naïve cells from the lymph nodes and spleen with the mice succumbing to the opportunistic infection *Pneumocystis carinii*. Correspondingly in humans, expression of proliferation markers, markers of terminal differentiation and effector memory cells has been shown to be higher in HIV-1 infected individuals than in healthy controls; whereas the proportion of naïve cells is reduced compared to healthy controls (Jordan et al. 2006).

Initially it was assumed that HIV replication and antigens were inducing non-specific activation but studies showing no relationship between CD4 depletion and viral load would imply that this was unlikely (Albuquerque et al. 2007). A significant proportion of individuals on HAART achieve suppression of viral replication yet still have low CD4 counts (Albuquerque et al 2007). HIV infected children with a low CD4 count (less than 15% of total lymphocyte count) have been shown to have a greater proportion of memory $CD4^+$ cells than uninfected controls, and this result was independent of viral load. In addition the proportion of naïve cells ($CD45RA^{hi+}CD62L^+$) was much lower regardless of viral load. For those children with good CD4 counts (more than 25%) they showed a proportion of CD4 memory cells similar to healthy controls regardless of their viral load. This was also true for the proportion of $CD45RA^{hi+}CD62L^+$ cells. The proportion of activated cells increased as CD4 percentage fell regardless of each viral load (Resino et al. 2006).

A similar observation has been made in adults. When symptomatic HIV-1 infected adults were compared to asymptomatic long term non-progressors with equally high viral loads, the asymptomatic long term non progressors had significantly lower levels of $CD4^+$ T cell activation and proliferation, as measured by HLA-DR and Ki67 expression respectively (Choudhary et al. 2007).

In SIV infection within the natural host there is usually persistently high viral load and viral replication but little cell activation or cell depletion (Kornfeld et al. 2005). This would suggest that viral replication does not directly cause immune activation. However if a foreign host is infected, for example Asian rhesus macaques infected with SIV_{SM}, increased immune activation is detected. This model shows a very similar pathogenesis to human AIDS. Both have an initial acute period of high viraemia which is then partly controlled by $CD8^+$ cells followed by a longer asymptomatic phase characterised by persistent viral replication and slow but gradual CD4 depletion. In this pathogenic model as in HIV there was an increase in immune activation. In these monkeys, as in HIV infected individuals, lower levels of viraemia are associated with a slower disease course.

These data in children, adults and monkeys would suggest that some other antigens, not HIV, are acting to lower the required threshold for cell activation and thus triggering non-specific wide spread immune activation.

1.4.5 $CD4^+$ T cell depletion in the gut

As mentioned earlier CCR5 using viruses predominate during the early stages of HIV infection and CCR5 expression is restricted to memory cells yet Zaunders *et al* were able to demonstrate that it was the decrease in the concentration of $CCR5^-$ cells, not $CCR5^+$ cells, whose concentration remained unchanged, that accounted for the decline in $CD4^+$ T cell count during the primary phase of infection and also that it is was the concentration of circulating $CCR5^-$ cells that increased after treatment with antiretroviral therapy. They noted that after initiation of antiretroviral therapy during primary phase infection the concentration of non-proliferating ($Ki67^-$) $CCR5^-$ cells increased which would suggest that the increase in cell number was due to the release of cells previously sequestered within lymphoid tissue. They also noted that the proportion of $CCR5^+$ cells that expressed Ki67, and therefore were proliferating, was increased yet there was no significant increase in the number of $CCR5^+$ cells (Zaunders et al. 2001), which begs the questions, what is the fate of newly produced $CCR5^+$ cells in the circulation?

Previously $CD4^+$ T cells in GALT, which have a predominantly memory phenotype, had been shown to be depleted during primary HIV infection compared to uninfected individuals (Lim et al. 1993) and it had been established that SIV infection of rhesus macaques resulted in profound and selective depletion of $CD4^+$ T cells in the intestines within days of infection (Veazey et al. 1998). $\alpha_4\beta_7$ is the integrin required for gut homing and Krzysiek *et al* have shown that the concentration of $\alpha_4\beta_7^+CCR5^+$ cells is much lower in HIV infection than in healthy controls. Additionally they found that the low concentration of $\alpha_4\beta_7^+CCR5^+$ cells was not improved after initiating anti-retroviral therapy (Krzysiek et al. 2001). Taken together these data might suggest that $CCR5^+$ cells proliferate and migrate to the gut to replace $CCR5^+$ cells being lost here.

Indeed more recently, Brenchley *et al* demonstrated that the first $CD4^+$ T cell subset depleted from the gut in HIV infection are $CCR5^+$ memory cells in the GI tract mucosa. Comparing $CD4^+$ T cell depletion in peripheral blood, mesenteric lymph nodes, inguinal lymph nodes, and the jejunum, within 17 days after SIV infection of macaques, Brenchley *et al* observed that the percentage of $CD4^+$ T cells within gut mucosa dropped from over 40% down to less than 1%. In 50 HIV infected persons flow cytometric analysis of gut biopsies showed much lower percentages of $CCR5^+$ $CD4^+$ T cells compared to healthy controls (Brenchley et al. 2004).

In SIV infected rhesus macaques gut memory cells were subsequently shown to be productively infected during the acute phase of high viral replication and viraemia by Li *et al.* and therefore likely depleted by direct killing (lytic infection) despite their predominant resting state ($Ki67^-$). As discussed previously the viral replication peaks during the acute phase and declines in part due to elimination of infected cells in the periphery by virus-specific CTLs. However CTL responses in the colon are minimal and Li *et al* propose that the $CD4^+$ T-cell depletion markedly reduces the size of the population of susceptible cells available for infection and hence peak viraemia declines. They also show that productive infection alone would be unlikely to explain the massive depletion of $CD4^+$ T cells from the gut because at the peak of viral production only 7%

of cells were actually infected. By demonstrating increased levels of caspase 3, Fas and Fas ligand, Li *et al* provide evidence for the depletion of uninfected memory cells from the colon by bystander apoptosis (Li et al. 2005).

1.4.6 Bacterial translocation and activation of circulating $CD4^+$ T cells

The gut is a unique immune environment; only a thin epithelium separates GALT immune cells within the lamina propria from high numbers of bacteria and microbial products within the gut lumen. Gut lymphocytes need to be able to respond swiftly against pathogenic bacteria and ignore innocuous food allergens and commensal organisms. Inappropriate responses to commensal organisms in the gut result in atrophy of the gut mucosa as seen in inflammatory bowel disease (Scharl and Rogler 2010). TRegs may be important in limiting the activation of GALT T cells by harmless organisms and their products. Additionally gut cells are predominantly resting and proliferate poorly in response to activating cytokines (Zeitz et al. 1994). Depletion of $CD4^+$ T cells from the gut may enable microbial translocation, the passage of microbes and microbial products into the body and systemic circulation. Bacterial translocation occurs in many other conditions including inflammatory bowel disease, where it is associated with systemic immune activation. Therefore it has been hypothesised that the profound depletion of $CD4^+$ T cells from the gut in HIV infection causes a breakdown of the mucosal barrier thus increasing susceptibility to microbial translocation from the GI tract to the systemic circulation (Douek 2007).

The endotoxins, lipopolysaccharide (LPS) and lipooligosaccharide (LOS), found within the outer membrane of gram negative bacteria, are potent inducers of inflammation and immune activation (Heumann and Roger 2002). Detection of LPS within the plasma indicates bacteraemia hence measuring plasma LPS can be used as a measure of bacterial translocation. Plasma LPS levels were measured in people without HIV and people at various stages of HIV infection, acute, chronic and advanced disease. Plasma LPS was significantly higher in HIV-1 infected individuals in the chronic and AIDS phases of infection than in uninfected controls and individuals with acute phase HIV infection. The median plasma LPS level in patients with chronic or advanced disease

was 75 pg/ml (Brenchley et al. 2006). 14 pg/ml is sufficient to produce systemic immune activation therefore the level of LPS measured in HIV infection could account for the increased immune activation characteristic of HIV infection (Douek 2007).

Plasma LPS levels in monkeys with pathogenic SIV can be dramatically reduced by administering antibiotics that target microbes in the GI tract (Brenchley et al 2006). This finding supports the gut as the likely source of LPS in HIV infection. However this was associated with only a modest decrease in the measures of LPS-mediated *in vivo* monocyte stimulation. SIV infection in macaques is pathogenic and plasma LPS levels in infected macaques are significantly higher than in uninfected macaques. However there is no difference in plasma LPS levels between SIV infected and uninfected sooty mangabeys, the natural host (Brenchley et al 2006).

LPS triggered immune activation is transduced via surface CD14 and soluble CD14 (sCD14) therefore sCD14 increases when monocytes are stimulated by LPS (Heumann and Roger 2002). HIV infected individuals at all stages of infection show significantly higher levels of sCD14 compared to uninfected controls. In HIV infected individuals starting HAART, after 48 weeks plasma LPS was inversely correlated to $CD4^+$ T cell count (Brenchley et al 2006). This suggests that one of the mechanisms underlying the increase in CD4 count observed in HAART could be decreased bacterial translocation. However this requires further substantiation, for example, by determining whether HIV infected individuals, not receiving HAART, experience increased CD4 counts when bacterial translocation is blocked or reduced, perhaps by administering antibiotics that target gut microbes.

More recently depletion of $CD4^+$ T cells has been shown to occur in non-pathogenic SIV infection in sooty mangabey and African green monkeys but is not associated with increased mucosal or systemic immune activation. There was also no significant difference in depletion kinetics between non-pathogenic infection is sooty managabeys and pathogenic infection in Rhesus macaques. Though non-pathogenic SIV infection in sooty mangabey is not associated with increased systemic immune activation, a

transient increase in activated proliferating PBMCs has been shown to occur early in infection. In 2 out of 5 monkeys followed up there was also a transient increase in plasma LPS levels (Gordon et al. 2007). These results suggest that CD4 depletion on its own may not be enough to compromise the mucosal barrier thus permitting microbial translocation or that sooty managabeys may be able to adjust to the depletion of $CD4^+$ T cells from gut mucosa and re-establish the barrier against microbial translocation with decreased number of cells.

As discussed previously $CCR5^+$ $CD4^+$ T cells are depleted from the gut in HIV infection however within peripheral blood Brenchley *et al* found no difference between the percentages of circulating $CCR5^+$ $CD4^+$ T cells in HIV infected and uninfected individuals and that the concentration of HIV-1 infected $CCR5^+$ memory cells in the gut was over a 100 fold greater than the concentration of HIV-1 infected $CCR5^+$ memory cells in peripheral blood (Brenchley et al 2004). This difference between the rates of infection, and the possible resulting difference in death rates, could partly explain why depletion of $CCR5^+$ $CD4^+$ T cells appears to be restricted to the gut. Compared to the gut where they account for 40-80% of all $CD4^+$ T cells, only 10-30% of circulating $CD4^+$ T cells were found to express CCR5. Memory $CD4^+$ T cells in GALT are quite distinct from other populations of memory cells. As has mentioned previously they are predominantly resting ($Ki67^-$) and additionally it has demonstrated in non-human primates that they do not undergo proliferation in response to antigen (Zeitz et al 1994).

As mentioned in previous sections, apart from proliferation of existing memory cells, naïve cell activation and differentiation into memory cells contributes to the number of memory cells. As gut memory cells poorly proliferate and low frequencies of naïve cells are present in the gut, homeostatic mechanisms available to attempt to compensate for the dramatic depletion of memory cells from the gut could hypothetically be limited to immigration of peripheral blood memory cells that express $\alpha_4\beta_7$ and therefore have gut homing potential. This could be another potential mechanism contributing to $CD4^+$ T cell depletion from peripheral blood. The question remains though, why administration of antiretroviral therapy is associated with an increase of $CD4^+$ T cells in the periphery but not in the gut?

Additionally the loss of memory cells from peripheral blood could be offset by increased activation driven differentiation of naïve cells into memory cells because in adults the composition of the $CD4^+$ T cell pool in peripheral blood is 70-90% naïve and 10-30% memory cells as compared to 20-60% naïve and 40-80% memory in the gut (Centlivre et al. 2007). Thus in the gut, activation driven differentiation of a small naïve cell population would be unable to keep up with the rapid depletion of memory cells.

1.4.7 Role of $CD4^+$ T regulatory cells in HIV pathogenesis

As described previously immune activation is usually controlled by Tregs. Tregs could have either or both of two opposing roles in HIV infection. They could be deleterious by inhibiting antiviral T cell responses which could lead to viral persistence and more rapid disease progression. Tregs could be advantageous by suppressing non-specific immune activation and thus slowing down disease progression by limiting viral replication and activation-associated immunopathology (Hartigan-O'Connor, Abel, & McCune 2007). However the role of Tregs in HIV infection is poorly understood in part due to different research groups producing conflicting results, which are affected by the poor consensus in identifying Tregs.

There is a general consensus that Tregs are increased in tissues of HIV infected individuals and pathogenic SIV infected monkeys and that Treg tissue numbers are proportional to viral load. However there is conflicting data about the numbers of circulating Tregs (Chougnet and Shearer 2007). The role of Tregs in HIV remains elusive.

1.5 HIV INFECTION IN CHILDREN

There are significant differences between adult and paediatric HIV infection in part due to differences between the immature immune systems in children and the more mature

systems in adults. There are also separate distinct difficulties in diagnosis and management that are specific to children.

1.5.1 Transmission

It is estimated that 90% of paediatric HIV infection occurs by vertical transmission from mother to child (UNAIDS 2002). HIV infection can occur in utero during foetal development. HIV has been detected in both foetal tissue and amniotic fluid indicating passage of infected cells or virus across the placenta (Sprecher et al. 1986). The next time point for infection is the intrapartum period, during birth. Then after birth in the postpartum period the child can be infected by exposure to virus or infected cells during breast-feeding (Sprecher et al 1986). Most neonates (65%) are infected in the peripartum period during and after delivery (Sprecher et al 1986)

1.5.2 Diagnosis

HIV is more difficult to diagnose in children than in adults. ELISAs specific for anti-HIV-1 IgG antibodies are commonly used for diagnosing infection in adults. However they are not suitable for diagnosing HIV-1 infection in infants as maternally derived antibodies continue to circulate for up to 12 or 18 months after birth. PCR detection of HIV DNA can detect 25-30% of infected newborns and the rest can be dected by 1 month of age (Read 2007). Testing infants born to HIV infected mothers should therefore begin within 48 hours of birth, repeated at 1 to 2 weeks and then at 1, 2, and 6 months, although guidelines vary amongst hospitals. Additionally infants with a single positive PCR test results should have it confirmed by follow-up PCR and viral isolation. Vertically transmitted HIV-1 infection can only be excluded in those infants with PCR test results that remain negative through 6 months of age (Luzuriaga and Sullivan 1998).

1.5.3 Clinical course of paediatric HIV-1 infection and pathogenesis

HIV infection is more aggressive and rapid in vertically infected children. As a result the death rate in HIV-infected children is higher than in HIV-infected adults. Before the

advent of HAART an estimated 23% of infected children developed AIDS before the age of 1 year, and nearly 40% by 4 years. 10% died before age 1 year and 28% before age 5 years (European Collaborative Study 1994).

From birth, viral load increases rapidly and peaks at 1-2 months (median values at 1 and 2 months, 318,000 and 256,000 copies/ ml respectively) then slowly declines to a median of 34,000 copies/ ml at 24 months (Shearer et al. 1997). This is a higher peak and a slower decline than seen in adults. Prognostic indicators of disease progression such as viral load and CD4 count are less reliable in children; in the first several months of life viral load cannot be used to distinguish infants with rapid disease progression from those with slower disease progression (Luzuriaga and Sullivan 1998). This is because in children, the high plasma viraemia observed in the primary infection phase usually continues for much longer than in adults yet during this time they can sometimes maintain a CD4 count within normal levels for their age groups. During this time the turnover of $CD4^+$ T cells is very high with the thymus generating $CD4^+$ cells to replace the high numbers being lost (Krogstad et al. 1999). This feeds viral replication as the emergence of new cells presents a greater number of potential targets to the virus.

Deficiencies in the immature immune system may account for the high viral loads and progression seen in children. Mature cellular and humoral responses, especially functional cytotoxic T lymphocytes (CTLs) are mostly lacking in the young infant (Buseyne and Riviere 1993) (Luzuriaga et al. 1993). $CD4^+$ T cells responses are also poorer in infants. They are characterized by lower frequencies of antigen-specific T cells and a reduced magnitude of the response i.e. smaller clonal expansion compared to adults. Antigen presentation in infants is also poorer. In contrast to adult DCs, infant DCs express lower levels of MHC and adhesion molecules, their ability to produce IL-12, which is required to stimulate naïve $CD4^+$ T cell differentiation, is lower. Therefore the adaptive immune response in infants is compromised and may in part explain the high viraemia in this age group.

In some aspects the rapid disease progression in paediatric HIV infection is surprising. As previously discussed, the early events in HIV infection include a profound loss of activated memory cells from GALT. However children, especially infants, are less antigen-experienced than adults and have lower frequencies of memory cells in lymph nodes and peripheral blood, as discussed previously, and thus have fewer suitable targets for HIV infection. Studies of neonatal macaques infected with SIV have shed light on this paradox. In common with human neonates, peripheral blood and lymphoid T cells in macaques neonates are mainly naïve however examination of intestinal lamina propria from macaque neonates, even on the day of birth, revealed that most, 40-90% of the $CD4^+$ T cells were activated memory cells (defined by CD45RO and CD95 expression in macaques) and within 21 days of infection with SIV the vast majority of were found to have been selectively eliminated by direct viral infection (Wang et al. 2007) (Veazey et al. 2003). This result is in contrast to the adult gut where the majority of directly infected and eliminated memory cells were in the resting state.

1.6 TREATING HIV INFECTION

There is currently no cure or vaccine for HIV. Treatment mainly consists of antiretroviral drugs that delay the progression to full-blown AIDS.

1.6.1 Anti-retroviral drugs

The first anti-retroviral (ARV) zidovudine, formerly azidothymidine (AZT), became available over 20 years ago. AZT is a nucleoside reverse transcriptase inhibitor (NRTI) based on the structure of deoxythymidine. During reverse transcription, the reverse transcriptase enzyme incorporates nucleotides, which are phosphorylated nucleosides, at the 3’ hydroxyl (OH) end of the primer being used to synthesise the viral DNA. In human cells, DNA polymerase normally removes misincorporated bases. However, reverse transcriptase does not show proofreading nuclease activity so cannot remove misincorporated bases, which allows nucleoside analogues like AZT to function. Unlike deoxythymidine, AZT lacks the 3’ OH required for DNA strand elongation. Like a

normal nucleoside, AZT is phosphorylated by host cellular kinases to produce the nucleotide, deoxythymidine triphosphate, and then incorporated by reverse transcriptase. Chain elongation is terminated because there is no 3' OH and RT cannot remove the AZT base (Furman and Barry 1988). Many other drugs which were analogues of other nucleosides such as lamivudine and didanosine were produced.

The next class of drug discovered were non-nucleoside reverse transcriptase inhibitors (NNRTIs). NNRTIs are a group of structurally diverse compounds that prevent viral replication by allosteric inhibition of the reverse transcriptase enzyme. The allosteric inhibition is mediated by the NNRTI interacting with a hydrophobic binding pocket near to but distinct from the enzyme's active site, which is where nucleotide analogues bind. This may lead to conformational changes in the active site and inhibit the enzyme's flexibility and consequently its activity (Wainberg 2003)

Protease inhibitors were discovered in 1996. They block the action of viral protease (PR). PR is responsible for cleaving precursor molecules to produce structural proteins of the mature virion core therefore protease inhibitors are an effective form of anti viral therapy because new virions synthesised do not mature and are not infective. PR inhibitors like saquinavir mimic the enzyme's peptide substrate (Flexner 1998).

The 3 classes of anti-retrovirals described thus far interfere with viral replication and production. Only one class of drugs, fusion inhibitors, prevent viral entry into the cell. As described previously in section 1.3.4 during entry HIV attaches to the host cell membrane via the gp120-CD4 interaction which is mediated by gp41. The helices, HR1 and HR2, of gp41 pack together to form a fusion pore. Fusion inhibitors mimic the helical domains, and inhibit fusion by interacting with their complementary domain on gp41. Enfuvirtide (T20), the only approved fusion, is an analogue of HR2. It competes with HR2 for binding with HR1 thus preventing formation of the fusion pore (Lazzarin 2005)

The newest class of ARVs, integrase inhibitors has only one approved member. Raltegravir, approved by the FDA in October 2007, is the first commercially available drug in this class. The drug interferes with integration of the provirus into the host cell genome by inhibiting the strand-transfer step of integration by blocking the active site of integrase, inhibiting the action of the viral enzyme, integrase (Cocohoba and Dong 2008).

1.6.2 Non-antiretroviral agents

Given in combination with antiretroviral drugs, other agents have a small role in the management of HIV infection by acting upon host factors rather than the HIV virus. The most prominent of these is maraviroc, a CCR5 inhibitor. It works by binding to a hydrophobic pocket in the transmembrane helices of CCR5, separate from the site of gp120 binding, thus altering the conformation of the extracellular loops bound to by gp120 (Tilton and Doms 2009).

The association between immune activation and rapid disease progression led to the supposition that agents that suppress inflammation and immune activation could be beneficial against HIV infection. Use of cyclooxygenase type 2 inhibitors has been associated with decreased expression of markers of immune activation, particularly in patients with viraemia (Kvale et al. 2006). Use of corticosteroids as an adjunct to HAART have shown no added advantage over HAART alone (Wallis et al. 2003). Additionally long term use of corticosteroids is associated with significant toxicities specifically bone necrosis and Cushing's disease.

Other drugs have been given to boost $CD4^+$ T cell division. Treatment with IL-7, which is required for T cell development and naïve cell survival, can enhance $CD4^+$ T cell numbers therefore IL-7 was considered as a possible adjunct to anti-retroviral drugs. However IL-7 stimulates HIV replication *in vitro* as demonstrated in thymic organ cultures, enhances HIV entry into cells through CXCR4 and chronically elevated levels of IL-7 up-regulate Fas (or CD95) expression (Capitini, Chisti, & Mackall 2009). Treatment with intermittent cycles of IL-2 leads to significant and sustained increases in

CD4 T cell counts by increasing the survival but not proliferation of $CD4^+$ T cells. However the effect is limited to central memory and naïve cells that express the IL-2R (CD25). These cells have high levels of FoxP3 (Read et al. 2008). Though only weak suppressive effects have been detected the wisdom of selectively expanding what is potentially a population of Tregs is questionable. It could be associated with decreased non-specific immune activation and/or decreased HIV-specific responses.

1.6.3 Highly Active Anti-retroviral Therapy

Used in isolation ARVs are effective at reducing viral replication. However this does not last long as HIV rapidly develops resistance to all anti-retroviral agents, highly active anti-retroviral therapy (HAART) circumvents this problem. HAART is the description given to the most effective anti-retroviral drug regime. It consists of at least 3 drugs belonging to at least 2 of the ARV classes. A typical regimen would be two NRTIs plus either a protease inhibitor or an NNRTI.

Within 2 weeks of instituting HAART viral loads drops in the vast majority of individuals and a slower increase in CD4 count is seen. This is sustained during further treatment. The increase in the CD4 count is associated with the alleviation of clinical symptoms. HAART does not cure HIV but if strictly adhered to it keeps the plasma viral load below the limit of detection by conventional PCR, 50 copies/ml, and the CD4 count remains close to normal. If it is stopped the viral load soon rebounds.

Most individuals on HAART regimens have to take several pills multiple times a day without end. The regimes are further complicated by meal restrictions and other issues. Also ARVs are associated with hepatotoxicity, renal toxicity and many unpleasant side effects like lipodystrophy, dyslipidaemia, insulin resistance and increased risk of cardiovascular disease. Therefore it is not surprising adherence is a significant problem especially amongst children, drug users, individuals with psychiatric disease and inadequate social support. Poor adherence results in the emergence of drug resistant HIV mutant strains. Then the regimen is no longer effective and must be changed.

However there is a very limited number of ARVs available thus there are few options available for patients who have failed multiple regimes.

If HAART is commenced in a severely immunosuppressed individual immune reconstitution inflammatory syndrome (IRIS) can occur. IRIS occurrs when anti-retroviral therapy restores immune responses in an individual who are currently or recently infected with a pathogen. It usually results in inflammation of tissues infected with the pathogen. As IRIS is characterised by increased numbers of circulating IFNγ producing T cells it is considered to be the result of a protective but excessive immune response that is inadequately regulated. The major risk factor for IRIS is initiating antiretroviral treatment when the $CD4^+$ T cell count is very low (<100 cells/µl) (French 2009).

Since the introduction of HAART, countries where it is widely available, have seen a decline in the incidence of HIV related morbidity and mortality.

1.7 RESPONSE OF HIV INFECTION TO THERAPY

1.7.1 Response in adults

In adults effective treatment with HAART produces an initial quick rise in $CD45RO^+$ memory cells in the first few months followed by a slower second phase increase in $CD45RA^+$ cells (Pakker et al. 1998), (Notermans et al. 1999). These findings are, however, dependent upon the stage of HIV infection when treatment was initiated. If HAART is initiated very early after seroconversion or before, the rate and size of recovery of naïve cells appears the same as memory cells. This rapid phase, both for memory and for naïve cells, is believed to be due to release of sequestered cells. However, for both early and late treated people, after at least 3-6 months on therapy, the rates of their naïve cell recovery become almost parallel. So by this time the method of CD4 replacement may be similar.

1.7.2 Response in Children

Initially treating children was very difficult as available antiretroviral medicines were initially developed for adults, and most standard fixed-dose combinations were inappropriate for children. This challenge, however was overcome as a result of increased availability of paediatric regimens (Bowen, Palasanthiran, & Sohn 2008).

One of the first studies of HAART in children, 2-16 months of age reported that the drugs were well tolerated without clinically important adverse events and reported marked reductions, up to 2.5 logs compared with baseline levels, in plasma HIV-1 RNA levels during the first 14 to 28 days of therapy (Luzuriaga et al. 1997). However rates of viral suppression below the limit of detection among children have tended to be lower than among adults (Pavia 2008).

Numerous studies have reported increases in absolute CD4 count and percentage and other changes in CD4 subsets in children receiving HAART (Gibb et al. 2000), (van Rossum et al. 2001), (Hainaut et al. 2003), (Rosenblatt et al. 2005), (Newell et al. 2006), (Zanchetta et al. 2006). The study by Hainault et al looked at the effect of age on immune reconstitution (Hainaut et al 2003). Over the 12 months of their study they recorded a progressive increase in $CD4^+$ cells (as a percentage of all lymphocytes). They observed also an increase in memory cells $CD4^+$ cells (as a percentage of all lymphocytes) for the first 3 months and an increase in naïve cells (as a percentage of all lymphocytes) that continued for the whole 12 months of the study. Similar findings over a longer period, 48 months, were made by Zanchetta *et al* (Zanchetta et al 2006). Figure 1.12 from Gibb *et al* illustrates these changes (Gibb et al 2000). Significantly higher recovery rates of naive, memory and total $CD4^+$ T cells were observed in children below the age of 3 years as compared with older children and were 10-40 fold higher than reported in adults (Cohen Stuart et al. 1998).

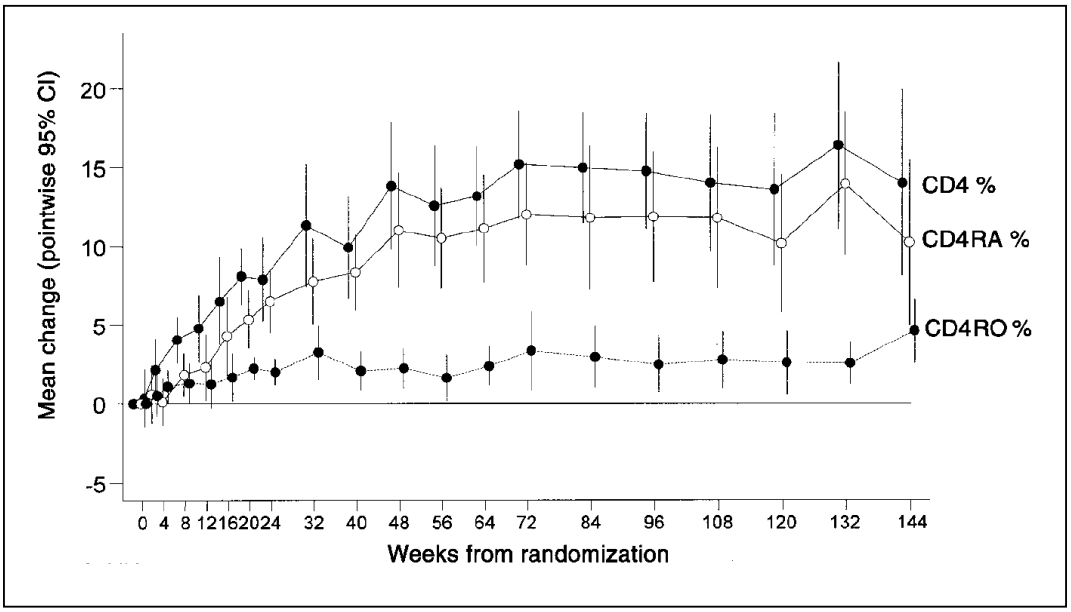

Figure 1.12 Changes to percentage of $CD4^+$ T cells and subsets in children receiving HAART
The graph reproduced from (de Rossi A. et al. 2002) shows the rise in the percentage of $CD4^+$ T cells and CD45RA $CD4^+$ T cells in children with time after initiating HAART. There was also a small initial increase in CD45RO $CD4^+$ T cells.

A significant question in the management of paediatric HIV infection has been when to start treatment. Children who are younger at the start of treatment have been found to achieve a close to normal naïve cell count faster than older children but by the end of the study the older children had achieved the same immune recovery (Zanchetta et al 2006). This finding is echoed in work by van Rossum *et al* (van Rossum et al 2001) and in Newell *et al* (Newell et al 2006) where there was no statistically significant difference in the likelihood of attaining a 20% increase in CD4 count by children who initiated therapy below 5 months compared to those who initiated after 5 years of age. These results would suggest that efficacy of HAART in children is not affected by age at initiation of treatment. However it does not indicate whether children who start treatment at an older age are immunologically disadvantaged in the long term. Additionally any immunological advantage conferred by early treatment must be weighed against the associated risks of long term toxicities including lipid, glucose and bone metabolism, the known difficulties of maintaining suppression in children, the risk of resistance mutations and the possibility of running out of effective agents before the child reaches adulthood (Pavia 2008). A recent study in adults followed people starting

HAART over 9 years and assessed the effect on survival of early initiation of HAART (CD4 count≥500 cells/mm3) versus late initation (CD4 count<500 cells/mm3). The authors found there was an increased in the risk of death of 94% in the late treatment group (Kitahata et al. 2009). In a similar study, infants 6-12 weeks old were assigned to start HAART immediately or to start after the $CD4^+$ T cell percentage fell below 20% (or 25% if the child was younger than 1 year), most of this group initiated treatment after 40 weeks follow up. Reductions in infant mortality and HIV progression of 76% and 75% respectively were demonstrated in the early start group over the deferred start group (Violari et al. 2008).

In conclusion HIV is a devastating infection with a complicated pathogenesis involving depletion of $CD4^+$ T cells, especially memory cells initially from the gut which compromises the mucosal barrier against bacterial translocation. The ensuing bacterial translocation into the circulation, results in increased non-specific activation of circulating CD4 cells, especially memory cells. The activated cells differentiate into shorter lived cells, which are more susceptible to apoptosis. However the process of HIV infection in children may differ from adults because initially they have a much smaller proportion of memory cells and greater thymic potential. This thesis sought to further elucidate the processes of $CD4^+$ T cell depletion and recovery in HIV-1 infected children by achieving the following aims:

- Investigate the changes to $CD4^+$ T cell sub-populations during paediatric HIV-1 infection and the role played by cellular activation, differentiation, proliferation and apoptosis and viral replication in these changes.
- Investigate the effect of planned treatment interruption on $CD4^+$ T cell sub-populations and the cellular processing controlling their numbers compared to continuous treatment with anti-retrovirals
- investigate the effect of planned treatment interruption on HIV latency and replication

CHAPTER 2

MATERIALS & METHODS

2.1 MATERIALS

2.1.1 Chemicals and solvents

All chemicals and solvents were obtained from *Sigma Aldrich (Dorset, UK),* except where otherwise stated, and were of analytical grade or above. All water used for buffer preparation was purified and deionised using a Millipore water purification system (Millipore R010, followed by Milli-Q Plus) (*Millipore Ltd., Watford, UK*) to ultrapure (Grade I).

2.1.2 Tissue culture materials (including plastics)

Sterile foetal calf serum (FCS) and Roswell Park Memorial Institute (RPMI) cell culture medium were purchased from *Invitrogen* (*Paisley, UK*). FCS was heat inactivated for 1 min at 60 °C in a waterbath. Sterile tissue culture flasks and plates were obtained from *Nunc* (*Roskilde, Denmark*). Polypropylene centrifuge tubes were obtained from *Corning*, (*Amsterdam, Holland*), and disposable serological pipettes from *VWR International (Leicestershire, UK).*

2.1.3 qPCR reagents

Nuclease free water and Magnesium chloride were obtained from Sigma Aldrich (Dorset, UK). Two Taq enzyme systems were used, the Brilliant II QPCR mastermix (Stratagene, Cedar Creek, Texas) and the Quantitect QPCR mastermix (Qiagen Inc., Hiden, Germany). Human placental DNA and tRNA carrier were obtained from Sigma Aldrich (Dorset, UK). The 8e5 cell line DNA extract was a kind gift of Dr Paul Grant (UCH Diagnostic Virology Services).

2.1.4 qPCR probes and primers

All probes and primers were obtained from *Eurofins MWG Operon, Ebersberg, Germany*. The nucleotide sequences are provided in Table 2.1. The *PDH* nucleotide sequences were kindly provided by UCH Diagnostic Virology Services, who use *PDH,*

the housekeeping gene in their in-house semi-quantitative HIV DNA assay. The Gag nucleotide sequences were as described in (Douek et al. 2002).

OLIGONUCLEOTIDE	SEQUENCE
LTR forward primer	5'-GCC TCA ATA AAG CTT GCC TTG A-3'
LTR reverse primer	5'-GGC GCC ACT GCT AGA GAT TTT-3'
LTR probe	5'-FAM TGT GAC TCT GGT AAC TAG AGA TCC CTC AGA C TAMRA-3'
Pol forward primer	5'-GCC TCA ATA AAG CTT GCC TTG A-3'
Pol reverse primer	5'-GGGCGCCACTGCTAGAGA-3'
Pol probe	5'-FAM CCAGAGTCACACAACAGACGGG CACA TAMRA-3'.
Gag forward primer	5'-GGT GCG AGA GCG TCA GTA TTA AG-3'
Gag reverse primer	5'-AGC TCC CTG CTT GCC CAT A-3'
Gag probe	5'-FAM AAA ATT CGG TTA AGG CCA GGG GGA AAG AA TAMRA-3'
PDH forward primer	5'-TGA AAG TTA TAC AAA ATT GAG GTC ACT GTT-3'
PDH reverse primer	5'-TCC ACA GCC CTC GAC TAA CC-3'
PDH probe	5'-JOE CCC CCA GAT ACA CTT AAG GGA TCA ACT CTT AAT TGT TAMRA-3'

Table 2.1 nucleotide sequences of probes and primers

2.1.5 Antibodies

The monoclonal antibodies specific to the protein of interest used for flow cytometry are shown in Table 2.2. Each antibody was conjugated to one of the fluorochromes fluorescein isothiocyanate (FITC), phycoerythrin (PE) peridinin chlorophyll protein (PerCP), tandem dye phycoerythrin:cyanine (Pe-Cy5) or allophycocyanin (APC).

HUMAN TARGET MOLECULE	MOUSE ISOTYPE	CONJUGATE	SOURCE	DILUTION
CCR7	IgG2a	PE	R&D	1/50
CD31	IgG1	PE	Insight Biotechnology	1/100
CD38	IgG1	FITC	Insight Biotechnology	1/100
CD4	IgG1κ	PE	Insight Biotechnology	1/200
CD4	IgG1κ	PE-Cy5	Insight Biotechnology	1/100
CD4	IgG1	PerCP	Becton Dickinson	1/25
CD45RA	IgG2b	APC	Caltag	1/200
CD45RA	IgG1κ	FITC	Insight Biotechnology	1/100
CD45RA	IgG1	PE-Cy5	Insight Biotechnology	1/100
CD69	IgG1	FITC	Insight Biotechnology	1/100
HLA-DR	IgG1	FITC	Caltag	1/100
HLA-DR	IgG1	PE	Insight Biotechnology	1/100
CD45RO	IgG1	FITC	Insight Biotechnology	1/100
CD3	IgG1	PE	Becton Dickinson	1/50
Ki67	IgG1	FITC	Becton Dickinson	1/25

Table 2.2 Antibodies used in flow cytometric analysis

The source, isotype, fluorochrome conjugation and the dilution utilised are shown for each antibody.

2.1.6 Patient samples

2.1.6.1 UK samples

Whole blood samples were collected from HIV-1 infected children attending Great Ormond Street Hospital (GOSH), according to GOSH/UCL local research ethics council (LREC) standards and with parental consent before collection. 900 µl was collected from these children, and larger volumes (4-10ml) from healthy adult volunteers recruited within ICH. Venepuncture was performed either by myself or another appropriately trained person using a butterfly needle and syringe. The blood was collected into ethylenediaminetetraacetic acid (EDTA) to prevent coagulation.

2.1.6.2 PENTA 11 trial

6 ml whole blood in EDTA from HIV-1 infected children in London and Italy recruited to the PENTA 11 trial according to the EU Directive on Clinical Trials 2001/20.

Samples were then stored at room temperature, before being processed within 24 hrs after collection except samples for apoptosis investigation which were processed immediately unless otherwise stated.

2.1.7 Buffer preparation

Buffers and solutions used were prepared as described in Table 2.3.

Buffer	Composition
FACS Buffer	0.2% bovine serum albumin (BSA), 0.02% sodium azide in phosphate buffered saline (PBS)
Perm Buffer	1% FCS, 0.1% sodium azide, 0.1% saponin in PBS
MACS Buffer	0.5% BSA, 2mM EDTA, 0.09% sodium azide in PBS. Passed through a 0.22µm filter membrane (Nalgene)
4% paraformaldehyde PFA	4% (PFA) in PBS dissolved by heating at 65°C for 45 min

Table 2.3 Composition of buffers used

The table describes the composition and preparation conditions of buffers used in the study.

2.2 METHODS

2.2.1 PBMCs

2.2.1.1 PBMC isolation

Lymphoprep centrifugation gradient medium purchased from *Axis-Shield (Dundee, UK)* was used to separate PBMCs according to manufacturer's instructions. Briefly, blood was diluted with an equal volume of PBS then carefully layered over an equal volume of lymphoprep before being centrifuged in a Sorvall legend RT for 20 min at 800 xg without brake. The buffy coat containing the PBMCs was removed by pipette to a polypropylene centrifguge tube. The cells were then washed twice in RPMI at 300 xg for 5 minutes. The RPMI was then removed, and the cell pellet either used immediately or stored for future use, as described below.

2.2.1.2 PBMC storage

PBMCs intended for future use were cryopreserved, by resuspending the pellet in a solution of 90% (v/v) fetal calf serum and 10% (v/v) dimethyl sulfoxide. The suspension was aliquoted into volumes of 1ml into cryotubes and stored at -80°C.

2.2.1.3 PBMC preparation for experiments

Both fresh and frozen PBMCs were used. Frozen PBMCs were prepared for use by quick thawing in a water bath at 37°C. Each aliquot was shaken in the water bath until almost no ice remained. The tube was then transferred to a sterile flow cabinet. Initially, approximately 1ml FCS was slowly added drop by drop until no ice remained. The cell suspension was transferred to a polypropylene centrifuge tube and washed by adding 10ml warmed RPMI, before centrifugation at 300 xg for 10 minutes at room temperature. The supernatant was removed, taking care not to disturb the pellet, then this wash step was repeated with a further 10ml RPMI. Cells were then resuspended in FACS buffer (Table 2.3.). Cell pellets that could not be resuspended were assumed to be dead and excluded from further experimentation. Successfully resuspended cell pellets were further evaluated for cell death by a trypan blue exclusion assay.

2.2.1.4 Cell counting and trypan blue exclusion assay

Trypan blue was added to a small aliquot of the cell suspension to a final concentration of 0.02% then 10 µl of the cell suspension applied to an improved Neubauer haemocytometer (Hawksley, Sussex). The principle of the trypan blue exclusion assay is that viable cells, which have an intact cell membrane, are impermeable to the negatively charged blue dye. Therefore, the cells which are dyed by the trypan blue are counted as non-viable. The haemocytometer was viewed under the 10X objective of a microscope and appeared as shown in Figure 2.1. Using a hand tally counter, the total number of cells and the number of blue cells in the 5 areas, marked by red squares in Figure 2.1, are counted.

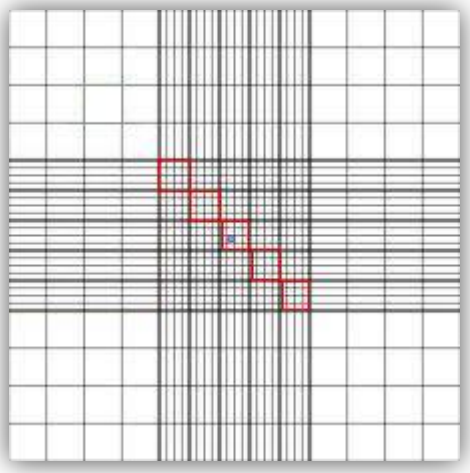

Figure 2.1 Improved Neubauer haemocytometer

The improved Neubauer haemocytometer as viewed under a microscope 10X field is shown. The 5 counting chambers used to determine the average number of cells per chamber are marked in red.

To obtain the concentration of the cell suspension the total count from the 5 squares is divided by 5 to yield the average number of cells per counting chamber, which is multiplied by 2 to adjust for the 1:1 dilution in trypan blue. The volume of the counting chamber is 0.0001 ml therefore the product multiplied by 10^4 is the concentration of the cell suspension. Combining these elements together produces the equation for determining cell concentration shown in Figure 2.2.

$$\text{Cell concentration (cells/ml)} = \frac{\text{Total count}}{5} \times 2 \times 10^4$$

Figure 2.2 Cell concentration equation

Then using the total cell count and the number of cells stained blue in the 5 counting chambers, the percentage viability was determined using the equation shown in Figure 2.3 (Fernandez-Botran and Vetvicka 2001).

$$\%\ \text{viable cells} = \frac{\text{number of viable cells (unstained)}}{\text{total number of cells}} \times 100$$

Figure 2.3 Cell viability equation

If the viability was less than 95% the sample was rejected and discarded because the median viability using this method of PMBC separation, freezing and thawing has been shown to have a median viability of 95% when samples are thawed after up to 12 years of storage (Kleeberger et al. 1999) additionally $CD4^+$ T cell function has been shown to be deteriorate below a PBMC viability of 90% as measured by IFNγ response to varicella zoster virus challenge (Smith et al. 2007).

2.2.1.5 Red blood cell lysis

In order to retrieve PBMCs from the whole blood samples, the red blood cell lysis method was used, as the sample volumes were too small to perform density gradient PBMC separation. Unless otherwise stated FACS lysing solution (Becton Dickinson, Oxford UK), which is a hypotonic solution of diethylene glycol, heparin, citrate buffer and formaldehyde, pH 7.2, was used as the lysis reagent. Hypotonic lysis of RBCs relies on osmosis thus when RBCs are placed in a hypotonic solution there is a net influx of water into the cells and the resulting osmotic pressure is sufficient to lyse the cells (Bird

1972). White blood cells are not lysed because their cell membranes remain constant during volume changes (Schmid-Schonbein, Shih, & Chien 1980).

FACS Lysing solution was diluted 10-fold with distilled water, warmed to room temperature and 1 ml added per every 100 µl whole blood. The solution was mixed and incubated at room temperature for 20 min. Then the lysed red blood cells were removed by washing twice with 1 ml of FACS Buffer at 300 xg for 5 min and discarding the supernatant each time. The cell pellet was then resuspended in 100 µl of 4% PFA (Table 2.3)

2.2.2 Immunofluorescence methods

2.2.2.1 Antibody titration

To maximise the ratio of specific to non-specific binding all antibodies were titrated alongside a mouse immunoglobulin of the same isotype as the antibody and conjugated to the same fluorochrome. This served as a negative controls for nonspecific binding. A 2-fold dilution series of the antibody was prepared using FACS buffer, starting at the concentration recommended by the manufacturer. Then 2µl of each concentration was added to 100,000 PBMCs suspended in 100 µl of FACS buffer. At each concentration of antibody the mean fluorescence intensity (MFI) of the negative and positive cell populations on a histogram were noted. The ideal concentration chosen was a concentration where the maximum difference in MFI between the positive and negative populations was achieved. (McCarthy 2007) and the MFI of the negative population exceeds the MFI of the isotype control. The titrations of three antibodies were repeated on whole blood samples to ensure that titration results between PBMCs and whole blood were the same. As an example the titration curve for CD4-PECy5 is shown (Figure 2.4) where the optimal concentration was 2%.

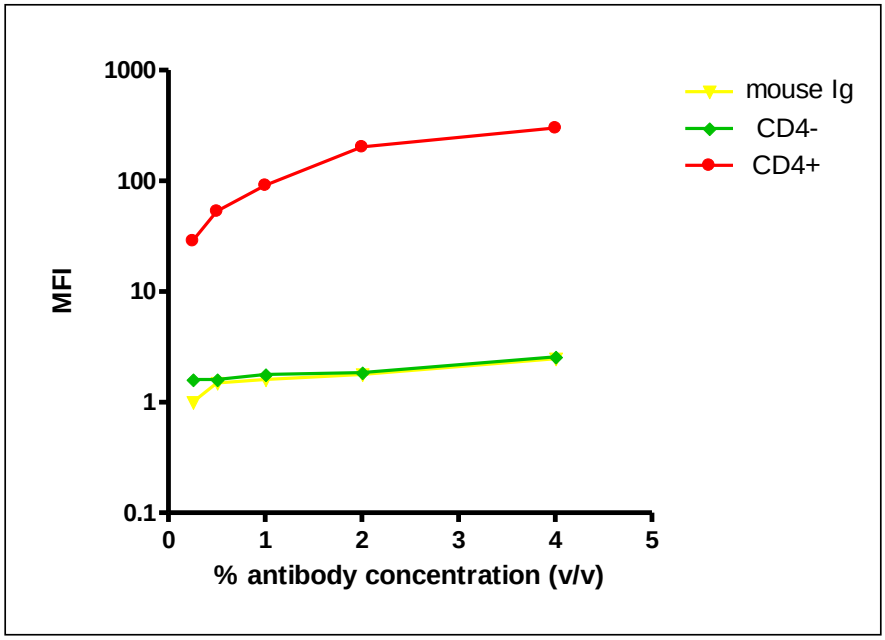

Figure 2.4 CD4-PECy5 antibody titration

The CD4-PECy5 antibody and isotype control were titrated over a 2-fold dilution series from 4% to 0.25% (v/v). The MFI at each concentration were plotted on a graph.

2.2.2.2 Extracellular immunostaining

Extracellular staining for targets on the cell surface was carried out as previously described (Milson et al. 1986) but briefly 100 µl of whole blood or 10^5 PBMCs suspended in 100µl FACS Buffer from each patient, as available, was incubated for 30 min, either at room temperature for whole blood or at 4 °C for PBMCs, with a combination of 3-4 antibodies added as described in Table 2.2. Two washes were then performed with FACS Buffer to remove unbound antibody as well as lysed red blood cells in the case of whole blood immunostaining. After decanting the supernatant, cell pellets were fixed by resuspending in 100 µl of 4% paraformaldehyde.

2.2.2.3 Intracellular immunostaining

Intracellular staining for the nuclear target Ki67 was carried out as previously described (Jacob, Favre, & Bensa 1991). Briefly following extracellular staining cells were permeabilized with Perm buffer then incubated with the anti-Ki67 antibody for 30 minutes. Perm Buffer contains saponin therefore it was chosen as it does not destroy the cell or affect membrane expression of surface antigens. The excess antibody was

removed by washing with Perm buffer then FACS buffer both at 300 xg for 5 min. Finally cells were fixed with 4% paraformaldehyde

2.2.2.4 Flow cytometry

All flow cytometry was carried out on a Facs Calibre (Becton Dickinson) or Cyan (Dako). The electronic standardisation of the instrument was performed similarly to methods described previously (Loken, Green, & Wells 2000). First a suspension of unstained PBMCs were run on the flow cytometer whilst observing the forward scatter (FSC) and side scatter (SSC) dot plot. The gain setting on the FSC amplifier and the voltage on the SSC were adjusted in order to visualise a clearly define lymphocyte population on the FSC/SSC dot plot (see chapter 3, Figure 3.3).

With the unstained cells still flowing through the flow cytometer an electronic gate was drawn around the lymphocyte population and applied to histograms of FL1, FL2, FL3 and also FL4 if 4 fluorescent channels were to be used. Then the voltage for each fluorescent channel was adjusted such that almost all the signal from the unstained cells appeared in the first decade of fluorescence (again see chapter 3, Figure 3.3).

Compensating for the overlap of emission spectra for different fluorescent dyes is a very important part of flow cytometric analysis because without correction cells labelled with only one fluorochrome, for example, FITC may be detected by both the FL1 (FITC) and the FL2 (PE) detector. To perform spectral compensation cells labelled with only antibody-fluorescent conjugate are acquired on the cytometer for each antibody to be used. Then taking each antibody one at a time the compensation network is set such that when singly stained cells are viewed in another fluorescent channel they record the same fluorescence as unlabelled cells. For example cells labelled with CD4-PE should appear in the first decade on a histogram of FITC expression. When compensation is correctly applied the MFI of the FITC fluorescence of $CD4^-$ and $CD4^+$ cells are equal. Post-acquisition compensation and analysis were performed with Summit v. 4.3 (Dako).

Although running unstained cells is an appropriate control that provides a measure of non-specific binding when determining the threshold of unstained and stained cells for an antibody, isotype controls can be also be useful when using antibodies that yield a more continuous rather than discrete populations. Therefore in addition to the unstained cells appropriate isotype controls were also acquired.

After mixing, all test samples were run on the flow cytometer and a minimum of 10, 000 lymphocytes were acquired and saved for each sample. Data files were then analysed using Summit v. 4.3 (Dako) software.

During analysis the hyperviscosity of plasma from HIV infected individuals combined with the high prevalence of nucleated red blood cells mean that it was sometimes difficult to identify a lymphocyte population based on light scatter because of the contamination of PBMCs by nucleated red blood cells, which failed to lyse. Where this occurred back-gating on CD4 was used to identify the position of lymphocytes.

Antibody expression by each population of interest was expressed as percentage of population positive for the antibody except for CD38 where in addition to percentage positive, to indicate the intensity of CD38 staining, the shift in mean fluorescence intensity (ΔMFI) was calculated compared to cells stained with the isotype control.

Flow cytometric data was shown on histograms and colour density dot plots.

2.2.3 Cell stimulation assay

Phorbol myristate acetate (PMA) in combination with ionomycin has been shown to induce cellular proliferation. PMA activates the serine and threonine-specific intracellular enzyme, protein kinase C, and ionomycin, a divalent cation ionophore draws calcium into the cell to initate replication (Balk, Morisi, & Gunther 1984). Therefore to stimulate lymphocytes, fresh whole blood was divided between 2 wells in

a sterile tissue culture plates within a sterile flow cabinet. To one aliquot PMA and ionomycin were added to a final concentration of 25 ng/ml and1 µg/ml respectively. Both aliquots were then thoroughly mixed and incubated in a Heraeus HERAcell incubator (Thermo Fisher Scientific, Loughborough, UK) programmed to 37 °C and 5% CO_2 for 4 hours.

2.2.4 Apoptotic cell detection

2.2.4.1 Selection of assay method

Several factors had to be taken into consideration when selecting an appropriate method for detecting apoptotic cells in this study. A flow cytometric method was required due to the small volume of blood available. Additionally the agent would need to be specific for apoptotic cells and exclude cells dying by necrosis. Activation of the caspase pathway is specific to apoptosis and does not occur in death by necrosis. HIV is a dangerous pathogen thus all samples must be fixed before acquired on flow cytometers thus the assay chosen had to be amenable to fixing. This precluded the use of annexin V, 7AAD and propidium iodide. Therefore apoptosis was measured by flow cytometry using the Vybrant FAM poly caspase kit (Invitrogen). The active agent is a green fluorescent inhibitor of caspases (FLICA), which binds irreversibly to the cysteine group on active caspases.

2.2.4.2 Optimisation of protocol

The protocol supplied by the manufacturer was designed for cultured cells therefore had to be adapted for this study. A 150X stock solution of FLICA reagent was prepared according to manufacturer's instruction by adding 50 µl of DMSO (supplied in the kit) to the lyophilized FLICA reagent and mixing. The stock solution was divided in 5 aliquots of 10 µl and then stored at -20 °C. To prepare the 30X FLICA reagent working solution, after thawing at room temperature 40 µl of PBS was added to an aliquot of 150X FLICA and mixed. 30X FLICA solution was added to aliquots of whole blood to produce the following dilutions 1/30 (recommended by manufacturer) 1/50, or 1/100. After mixing, the blood was incubated for 60 min at room temperature. The red cells were then lysed as described in section 2.2.1. Using 2 ml of the apoptosis wash buffer

supplied with the kit, lysed red cells were removed by washing at 300 xg for 5 min then the remaining PBMCs were fixed using 60 µl of the formaldehyde solution provided with the kit.

To generate a positive control, camptothecin, a potent inhibitor of topoisomerase I, which is required for DNA synthesis was used to induce apoptosis. Fresh whole blood was aliquoted into two wells of a tissue culture plate. Camptothecin was added to one well to give a final concentration of 10 µM. The blood was placed in an incubator for 4 hours at 37 °C, 5% CO_2. The non-induced and camptothecin blood were then divided into 4 aliquots. Each aliquot was incubated for a further hour with no FLICA or with FLICA at one of the following dilutions, 1/30, 1/50 and 1/100.

Use of FACS Lyse solution was associated with non-specific binding of FLICA therefore a hypotonic ammonium chloride lysis buffer without fixative, Pharm Lyse (Becton Dickinson, Oxford, UK) was used according to manufacturer's instructions. As before 30X FLICA was added to 100 µl whole blood at a concentration of 1/50 (v/v) and incubated for 1 hour at room temperature. Then 1 ml of Pharm Lyse was added, the sample vortexed and incubated at room temperature for 15 min. The sample was washed with 2 ml of apoptosis wash buffer at 200 xg for 5 min and the supernatant carefully pipetted off. The wash step was repeated and then the remaining cells fixed. However this method of red blood cell lysis was not robust especially when used on HIV infected blood samples. Incomplete lysis frequently occurred. Thus it was decided not to remove the red blood cells but instead to titrate the volume of FLICA reagent for whole blood unlysed.

2 µl of 30X FLICA reagent was added to 100 µl of whole blood and incubated at room temperature for 1 hour. The wash buffer and fixative supplied with the kit were used to wash off the excess FLICA, which diffuses out of the cell, and to fix the cells as described previously. The stained cells were then suspended in 500 µl PBS and passed through a 40 µm cell strainer to avoid clogging the flow cytometer. The flow cytometers used only allowed parameters to be saved for 10 million cells, which included only

1000-5000 $CD4^+$ cells. Thus to allow for at least 10,000 $CD4^+$ T cells to be acquired the threshold was changed from FSC to CD4 expression thus only $CD4^+$ cells would be considered as an event/cell.

2.2.5 Isolation of naïve and memory $CD4^+$ T cells

$CD4^+$ T cells were isolated from PBMCs using the Miltenyi $CD4^+$ T Cell Isolation Kit II (Miltenyi Biotech, Bergisch Gladbach, Germany) according to manufacturer's instructions except that PBMCs were incubated with antibody cocktail for 60 min instead of 30 min.

PBMCs were thawed as described in 2.2.1.3 then centrifuged at 300 x *g* for10 min at 4 °C. The supernatant was completely removed. The pellet was resuspended in 40 µl MACS Buffer and 12 µl of biotin-antibody cocktail was added. The solution was mixed well and incubated for 30 min at 4 °C. After adding 30 µl MACS Buffer and 23 µl anti-biotin microbeads and mixing, cells were washed with another 600 µl buffer at 300 x *g* for 10 min. The supernatant was completely removed and the pellet resuspended in 500 µl buffer.

An MS column (Miltenyi Biotech, Bergisch Gladbach, Germany) was rinsed with 500 µl buffer and placed within the magnetic field of a MACS separator (Miltenyi Biotech, Bergisch Gladbach, Germany). Then the PBMC cell suspension was applied to the column. The effluent that dripped through the column, which contains the purified $CD4^+$ T cells was collected in a propylene centrifuge tube. The column was then washed three times with 500 ul buffer and the entire effluent collected in the same tube.

Following this naïve and memory $CD4^+$ T cells were isolated using the Miltenyi CD45RO microbeads (Miltenyi Biotech) according to manufacturer's instructions. The $CD4^+$ cell suspension obtained previously was centrifuged at 300 x *g* for 10 min. The supernantant was completely removed and the $CD4^+$ cell pellet resuspended in 80 µl MACS Buffer. 20 µl CD45RO microbeads were added. The cell suspension was mixed

and incubated for 30 min at 4 °C. The cells were washed with 2 ml buffer at 300 x *g* for 10 min. The supernatant was completely removed and the pellet resuspended in 500 µl buffer.

MS column (Miltenyi Biotech, Bergisch Gladbach, Germany) was rinsed with 500 µl buffer and placed within the magnetic field of a MACS separator (Miltenyi Biotech, Bergisch Gladbach, Germany). Then the $CD4^+$ T cell suspension was applied to the column. The effluent that dripped through the column, which contains the purified $CD45RO^-CD4^+$ T cells was collected in a propylene centrifuge tube. The column was then washed three times with 500 µl buffer and the entire effluent collected in the same tube. The column was then removed from the magnet and bound cells, $CD45RO^+CD4^+$, flushed out with 1 ml buffer into a polypropylene tube.

2.2.6 DNA extraction

Cells were spun down for 10 min at 1400 rotations per minute (rpm). The supernatant was decanted and the cells resuspended in 200 µl of supernatant and brought up to room temperature. Whole genomic DNA was then extracted using the QIAamp DNA blood minikit (Qiagen, Hiden, Germany) according to manufacturer's instructions. The kit makes use of the broad spectrum serine protease, proteinase K, to break down the cells exposing nucleic acid and to denature nucleases which would otherwise degrade the nucleic acid. Buffers then stabilise nucleic acids and enhance selective DNA adsorption to the QIAamp membrane. RNA does not adhere to the membrane.

DNA purity was assessed using a Nanodrop 2000 spectrophotometer.

2.2.7 Real-time PCR conditions

Two different enzyme formulations were available, QuantiTect (Qiagen) and Brilliant II QPCR Mastermix (Stratagene). The thermal cycling conditions for each are shown in

Table 2.4. All amplifications were conducted with a Mx3000P spectrofluorometric thermal cycler (Stratagene) using a two temperature cycling regime.

QPCR MASTERMIX	**QuantiTect**	**Brilliant II**
PHASE	**CONDITIONS**	
Activation	95°C, 10 min	95°C, 10 min
	50 cycles of:	
Denaturation	95°C, 10 s	95°C, 15 s
Annealing and elongation	65°C, 1 min	60°C, 1 min

Table 2.4 qPCR reaction conditions

The thermal cycling conditions used for the QuantiTect and Brialliant II enzyme formulations.

The final HIV DNA qPCR assay for quantifiying HIV DNA in DNA extracted from samples of naïve and memory $CD4^+$ T cells was as follows. qPCR reactions were performed in a total reaction volume of 25 µl, containing 12.5 µl 2X Qiagen Quantitect QPCR Mastermix (no-ROX) (Qiagen Inc., Hiden, Germany), 0.5 µl distilled water, 9 µl template, 0.5 µl *gag* probe and 0.5 µl *PDH* probe at 10 pmol/µl (equivalent to effective concentration of 200 nM), 0.5 µl *gag* primers at 20 pmol/µl (equivalent to effective concentration of 400 nM) and the *PDH* primers at 3 pmol/µl (equivalent to effective concentration of 120 nM).

The templates were test DNA samples, Tris EDTA (TE) (Qiagen Inc., Hiden, Germany) for the non-template controls and 8E5 DNA extract diluted in transfer RNA carrier (Sigma–Aldrich,Dorset, UK) for the standards used for calibration of copy and cell number. The 8E5 DNA standards were prepared using 30 ng/µl transfer RNA carrier to produce a 3-fold dilution series of 8E5 DNA extract from 3000 copies/µl down to 4.1 copies/µl. Thermal cycling conditions are shown in Table 2.4.

2.2.8 Statistical analysis

Statistical analyses were performed using GraphPad InStat software (version 3.06; GraphPad). All tests for statistical significance were two-tailed and *p* values <0.05 were considered significant. Where *p* values and coefficients required rounding they were rounded off to the nearest 2 significant figures. The population characteristics of both cohorts are described by their medians and interquartile ranges (IQR) as data was non-parametric. The difference in the distribution of a parameter such as percentage of a subset between 2 groups such as HIV-1 infected children and uninfected adults was tested for statistical significance using the Mann-Whitney test (or Kruskal-Wallis if more than 2 groups were compared) as data was non-parametric. Associations between 2 continuous variables were tested for statistical significance using the Spearman's rank correlation test. To visualise the association, the variables were plotted against each other and GraphPad set to fit the appropriate regression line (and its associated 95% confidence interval).

CHAPTER 3

CHARACTERISING $CD4^+$ T CELLS FROM CHILDREN WITH HIV

3.1 INTRODUCTION

3.1.1 Identifying $CD4^+$ T cells by flow cytometry

As discussed in chapter one, HIV infection and treatment with HAART are associated with changes to the balance of $CD4^+$ T cell subsets. Since the conception of flow cytometry most laboratories in the developed world and increasingly in the developing world use flow cytometry to quickly and accurately study and quantify these sub-populations in large numbers of samples, while requiring only very small sample volumes. To accurately assess these sub-populations, red blood cells are excluded either through red cell lysis leaving all the populations of peripheral blood leukocytes (PBLs) or by density gradient centrifugation which removes red blood cells (RBCs) and frequently polymorphonuclear cells thus only the peripheral blood mononuclear cells (PBMCs) composed of lymphocytes and monocytes remain (Patel, Ford, & Rickwood 1998), (McCarthy 2001).

Flow cytometry identifies cell populations through differentiation of their size, granularity and antigenic expression (Carter and Ormerod 2000). Lymphocytes, of which $CD4^+$ T cells are a subset, can be distinguished from other leukocytes by their smaller size and lack of granularity. $CD4^+$ T cells express a wide range of extracellular, cytoplasmic and nuclear proteins, which can be used to differentiate them from other lymphocytes. Expression of CD3, an integral part of the T cell receptor distinguishes T cells from B cells and natural killer cells. Use of antibodies specific for CD4 and CD8 enables discrimination between $CD4^+$ T cells and $CD8^+$ T cells. Monocytes and macrophages also express CD4 but the density of CD4 molecules on the cell surface is so much lower on these cells than on $CD4^+$ T cells that they can be distinguished from one another (Stewart, Fujimoto, & Levy 1986).

3.1.2 Distinguishing between naïve and memory $CD4^+$ T cells

$CD4^+$ T cells can be divided into numerous functional subsets with differing expression of surface and intracellular proteins. A commonly used functional division of $CD4^+$ T

cells is into naïve and memory cells which can themselves be further subdivided into several populations.

As mentioned in chapter one, different isoforms of the leucocyte common antigen, CD45, can be used to identify different subsets of $CD4^+$ T cells. CD45 is a high molecular weight glycoprotein expressed on leucocytes and immature RBCs. CD45 has a cytoplasmic tail and an extracellular domain. The cytoplasmic region is extremely conserved among mammals, showing 95% homology in the species analyzed. In contrast, the expression of the extracellular domain is highly variable, showing only 35% homology. The variation in the extracellular domain means that CD45 exists as various isoforms with molecular weight ranging from 180 kDa to 240 kDa. Variation in the extracellular domain is produced by alternative splicing of exons 4, 5, and 6, also called A, B and C, which can generate at least eight different isoforms, protein expression of five of these have been detected in humans (Hermiston, Xu, & Weiss 2003). The structure of the highest, CD45RABC, and lowest, CD45RO, molecular weight isoforms are shown in Figure 3.1.

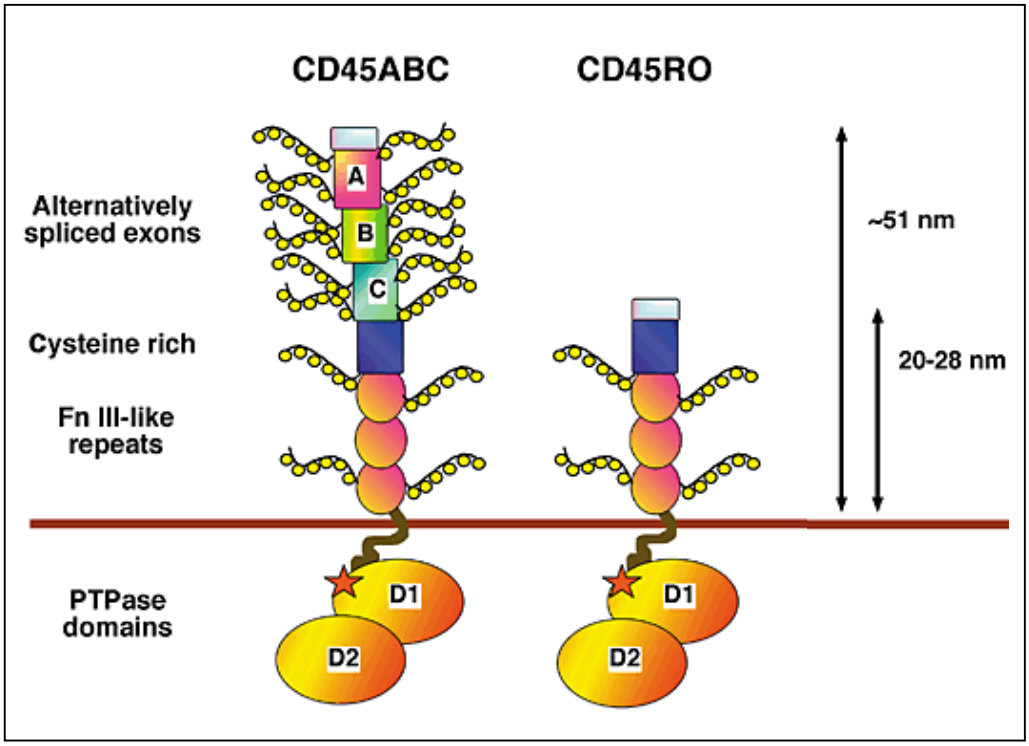

Figure 3.1 Illustration of the structure of CD45

The high (CD45RABC) and low (CD45RO) molecular weight isoforms of CD45 are shown on the left and right respectively. CD45RABC contains exons 4/A, 5/B and 6/C and CD45RO lacks all 3 consisting of just the cysteine−rich domain followed by three fibronectin type III (Fn III)−like repeats, a single transmembrane region and a long intracellular tail containing two tandemly duplicated PTPase homology domains, D1 and D2. Reproduced from (Penninger et al. 2001).

Peripheral blood T cells express four isoforms of CD45 with the following molecular weights, 180, 190, 200 and 220 kDa. The monoclonal antibody CD45RA binds to the high molecular weight isoforms and the monoclonal antibody CD45RO binds to the low, 180 kDa molecular weight isoform (Terry, Brown, & Beverley 1988), (Rogers et al. 1992). Akbar et al demonstrated that upon activation of T cells expressing the high molecular weight isoforms ($CD45RO^-$, ubiquitin carboxyl-terminal esterase $L1^-$ ($UCHL1^-$)), up to 40% of the cells co-express both high ($CD45RA^+$) and low ($CD45RO^+$, $UCHL1^+$) molecular weight isoforms of CD45 by day 3, and by day 7 $CD45RA^+$ $UCHLl^-$ cells fell from 90 to less than 21 % whereas $CD45RA^-UCHLl^+$ cells rose from 2 to 93%. This change was unidirectional as stimulated $CD45RA^-UCHLl^+$ cells remain $CD45RA^-UCHLl^+$ during 7 days in culture (Akbar et al. 1988).

When $CD45RA^+$ T cells were challenged with alloantigen by culturing with allogeneic non-T cells in a mixed lymphocyte reaction, two populations were found: a population of small un-activated lymphocytes that remained $CD45RA^+$ $UCHL1^-$ and a population of large activated blast cells, the majority of which expressed UCHL1. When these two populations were separated and re-challenged with the same alloantigen, $UCHL1^+$ T cells showed 7 to 20-fold more proliferation than the $CD45R^+$ population as determined by [^{3}H] thymidine incorporation (Akbar et al 1988).

Taken together these results suggest that on T cells the high molecular weight form of CD45, CD45RA is expressed on naïve cells, that activation of naïve cells results in the acquisition of a memory phenotype, which is characterised by acquisition of the low molecular weight form of CD45, UCHL1, now known as CD45RO, and loss of CD45RA expression and that memory cells do not regain expression of CD45RA. However Rothstein *et al*. subsequently demonstrated that cyclic re-stimulation of polyclonal $CD45RA^+$ cell lines derived from peripheral blood $CD4^+CD45RA^+$ cells could produce $CD45RO^+$ cells that regained CD45RA expression after re-stimulation, whilst still retaining CD45RO expression (Rothstein et al. 1991). This was also demonstrated in T cells and NK cells in culture (Warren and Skipsey 1991). Arlettaz et al also showed in bone marrow transplant recipients that reacquisition of CD45RA expression by $CD45RA^-CD45RO^+$ cells occurs without loss of CD45RO expression (Arlettaz et al. 1999). In a similar study a population of $CD4^+$ $CD45RA^+$ cells from patients who had received haematopoietic cell transplants were shown to display effector function and phenotype, and the authors suggested that the CD45RA antigen should not be used alone to define naïve $CD4^+$ T cells when monitoring T cell reconstitution (Fallen et al. 2003). However it has been shown that when $CD45RA^+$ and $CD45RO^+$ $CD4^+$ T cells are sorted from the peripheral blood of both individuals allergic and non-allergic to house dust mite, in all the individuals tested, the larger polyclonal response was seen in the $CD45RO^+$ population (Richards et al. 1997).

3.1.3 Sub-populations of memory $CD4^+$ T cells

Although $CD4^+$ T cells are very heterogeneous, in terms of their phenotype and functional capabilities, two memory cell subsets are commonly recognised, central memory and effector memory cells (Sallusto et al 2000). Central memory cells, which

are longer lived are important in HIV infection because long lived resting memory cells are the major stable reservoir of latent HIV virus (Chun et al. 1997), (Chomont et al. 2009). Central and effector memory cells were originally thought to be distinguishable by differential expression of the lymphoid homing cysteine chemokine receptor, CCR7, which is restricted to central memory cells (Sallusto et al. 1999), however, there is contrasting evidence that most cytokine-secreting T cells, which have an effector phenotype, are $CCR7^+$ and may be capable of lymphoid homing (Kim et al. 2001).

Other phenotypic markers that may distinguish between central and effector memory cells have been proposed including CD27. CD27 is a lymphocyte specific member of the TNF receptor family that regulates T cell survival through interaction with its ligand CD70. CD27 can be constitutively expressed on T cells but its expression is upregulated following T cell activation. It is preferentially expressed on $CD45RA^+$ $CD4^+$ T cells (Sugita et al. 1992), (Croft 2009). Upon TCR ligation, CD27 expression is transiently increased and then irreversibly lost after repeated antigenic stimulation. $CD27^-$ memory cell populations contain a high frequency of differentiated T-helper cells that secrete considerable amounts of cytokines (Hintzen et al. 1994), (Hamann et al. 1999). Thus central memory cells are believed to express CD27, whilst effector memory cells lack CD27 expression (Sallusto et al 1999).

Another co-stimulatory molecule that has been proposed to divide memory cells into functionally different populations is CD28. As mentioned in chapter one, co-stimulatory molecules act to reduce the threshold for TCR activation thus when CD28 is present $CD4^+$ T cells respond more rapidly to lower levels of TCR occupancy. Upon engagement of CD28, membrane and intracellular kinase-rich raft microdomains cluster at the sites of TCR ligation (Viola et al. 1999). CD28 is not absolutely essential for $CD4^+$ effector/memory T-cell development, as these cells can be generated in reduced numbers in $CD28^{-/-}$ mice (Dooms and Abbas 2006). Memory cells display differential expression of CD28 and those lacking CD28 expression have been shown to be terminally differentiated with shorter telomeres (Appay et al. 2002), (Appay 2004).

Analysing $CD4^+$ T cells using a combination of the phenotypic markers thus far described including, CD45RA, CCR7, CD27 and CD28 yields several populations. $CD45RA^+$ cells are fairly homogenous in that the majority (>90%) are $CCR7^+CD27^+CD28^+$. Central memory cells are also $CCR7^+CD27^+CD28^+$ Based on these markers three populations of effector memory cells are defined, $CCR7^-CD27^+CD28^+$, $CCR7^-CD27^-CD28^+$ and $CCR7^-CD27^-CD28^-$, of which the latter are the most terminally differentiated (Okada et al. 2008).

3.1.4 Recent thymic emigrants

An increase in naïve cell numbers has been observed in children receiving ART (Hainaut et al 2003), (Gibb et al 2000), which could be due to increased thymic output, increased division of existing naïve cells in the periphery and/or decreased loss of naïve cells from the periphery. Therefore it is important in understanding HAART associated naïve cell increases to be able to quantify thymic output or identify naïve cells that have newly emerged from the thymus, denoted as recent thymic emigrants (RTEs).

Initially thymic output was estimated by real-time PCR quantification of TCR excision circles (TRECs). T cells in the thymus undergo a rearrangement of V, D and J gene segments to produce a large variety of TCRs. In the process, the intervening chromosomal DNA is excised resulting in the formation of small circular episomes, called TRECs. As TRECs are generated during thymic T cell gene rearrangement, and as episomal DNA is not replicated during cell division, TRECs were previously considered as a surrogate measurement for thymic activity and the entry of newly formed T cells into the T cell pool (Kong et al. 1999). However, this was confounded by the discovery that altered rates of proliferation within the naïve pool will affect the TREC count (Hazenberg et al. 2000) because a decrease in TREC count could be accounted for both either decreased thymic output or the diluting effect of increased $CD4^+$ T cell proliferation.

Until recently it did not appear to be possible to distinguish phenotypically between RTEs and long-lived naive cells in the periphery. However a seminal study using the

platelet endothelial cell adhesion molecule-1 (PECAM-1), also known as CD31, identified two populations of $CD45RA^+$ $CD4^+$ T cells with disparate TREC content. TRECs were found to be highly enriched in the $CD31^+$ population and barely present in the $CD31^-$ population. Furthermore, the $CD45RA^+CD31^+$ cell population was shown to diminish with increasing age. In addition the low production of effector cytokines by $CD45RA^+CD31^+$ cells indicates the suitability of using co-expression of CD31 and CD45RA as a marker of RTEs (Kimmig et al. 2002).

Kimmig et al. put forward a model of naïve $CD4^+$ T cell homeostasis based on an *in vitro* study that showed loss of CD31 after TCR triggering. They suggested that naïve cells can be divided into two groups: RTEs that express CD31 and central naïve cells that do not express CD31. In this model, activation of either of these groups within the periphery by foreign antigen leads to their differentiation into $CD45RO^+$ (memory) $CD4^+$ T cells. However RTEs when presented with self antigen undergo homeostatic proliferation and lose CD31 expression and differentiate into central naïve cells. Although this work was concerned only with naïve cells, a subsequent study added to this evidence by demonstrating the progressive loss of CD31 and gain of CD45RO expression by $CD31^+$ cells, by showing that telomere length was longest in $CD45RO^-$ $CD31^+$, then $CD45RO^-CD31^-$, $CD45RO^+CD31^+$ and least in $CD45RO^+CD31^-$ cells. They also showed telomerase activity was much higher in $CD45RO^-CD31^+$ than $CD45RO^-CD31^-$ cells (Junge et al. 2007).

3.1.5 Activated $CD4^+$ T cells

Activation, proliferation and apoptosis were discussed in chapter one as important processes maintaining and regulating the number of $CD4^+$ T cells. The expression of numerous proteins have been characterised as evidence of these processes occurring.

Activation of $CD4^+$ T cells results in a wide variety of cellular changes including the induction of specific gene expressions. The change in expression levels of these gene products can be used to identify changes in the activation state of a $CD4^+$ T cell. One of the earliest molecules to be expressed is CD69, also known as activation inducer

molecule, very early activation antigen, MLR-3 and Leu-23. CD69, which is a glycoprotein that serves as a co-stimulatory molecule for T cell proliferation, can be found on the cell surface within 2 hours of activation and can persist for at least 3 days CD69 expression can be induced by activating T cells through the CD3/TCR complex, CD2 or CD28 and also by stimulation with phytohaemagglutinin (PHA) or phorbol myristate acetate (PMA) (Ziegler, Ramsdell, & Alderson 1994), (Marzio, Mauel, & Betz-Corradin 1999). Conversion from a naïve ($CD45RA^+$) to a memory phenotype ($CD45RO^+$) has been shown to be associated with activation, as determined by increased CD69 expression, and proliferation, as determined by bromodeoxyuridine incorporation (Johannisson and Festin 1995). When naïve cells are activated by interferon-alpha (INF-α) they do not undergo division but express CD69, therefore CD69 is most likely an activation specific not a proliferation specific protein (Tough et al. 1999). In patients with rheumatoid arthritis and chronic inflammatory disease unstimulated peripheral blood T lymphocytes do not express CD69 but high percentages of $CD69^+$ T cells have been found in unstimulated synovial fluid from rheumatoid arthritis patients and in the liver of patients with chronic inflammatory liver diseases (Marzio, Mauel, & Betz-Corradin 1999).

Another commonly used marker of T cell activation is nicotinamide adenine dinucleotide glycohydrolases/adenosine diphosphate ribosyl cyclase (NADase/ADPRC) enzyme, CD38. CD38 is a transmembrane glycoprotein within the extracellular domain, and is expressed by T cells, B cells, dendritic cells and granulocytes. CD38 exerts its functions in T cells by cell surface association with the TCR/CD3 complex and can produce cell activation and proliferation, transcription of cytokine genes, apoptosis and tyrosine phosphorylation of intracellular proteins. Although resting T cells express CD38, the density of their expression is increased after activation (Malavasi et al. 2006).

Expression of HLA-DR has been detected on activated T cells (Schendel and Johnson 1985). HLA-DR is an MHC class II cell surface receptor encoded by the human leukocyte antigen (HLA) complex on chromosome 6 (Kaufman et al. 1984). The heterodimeric HLA-DR molecule and the specific peptide dimerise to act as a ligand for

TCRs on T cells specific for both the MHC and the antigen. As the primary function of HLA-DR is to present antigen to $CD4^+$ T cells it is typically found on APCs such as macrophages, B cells and dendritic cells (Murphy, Travers, & Walport 2008). It is not expressed on resting T cells but has been shown to be expressed on T cells activated by alloantigen in a mixed leukocyte reaction (Evans et al. 1978), (Fu et al. 1978). It has been suggested that the functional role of HLA-DR molecules expressed on activated $CD4^+$ T cells may be to deliver intracellular signals to opposing $CD4^+$ T cells (Altomonte, Pucillo, & Maio 1999).

3.1.6 Proliferating $CD4^+$ T cells

Numerous methods to quantify cellular proliferation or the growth fraction of a population have been described. In chapter one the results of *in vivo* isotope labelling studies which provided a measure of the rate of cell division were discussed. However studies utilising the two most commonly used methods, heavy water and deuterated glucose (Macallan et al 1998), (Neese et al 2001) have produced conflicting results. The lack of consensus likely reflects the inability of these assays to distinguish between mature cells dividing in the periphery and thymocytes that divided and were exported during the labeling period (Bains et al 2009). Additionally such methods require the use of large volumes of blood incompatible with paediatric studies such as those described in this thesis.

In vitro methods based on various principles are available. Cell division requires the synthesis of cellular DNA during S-phase therefore assays have been developed that measure DNA synthesis. Most commonly cells are cultured in media containing labelled nucleoside analogues such as tritiated thymidine (^{3}H-thymidine) and bromodeoxyuridine (BrdU), which are then incorporated into the DNA of dividing cells. Such methods provide a measure of the DNA synthesis taking place during the period of exposure to the label but not prior to this when the majority of proliferation may have taken place (Lyons and Parish 1994). Therefore quantifying ^{3}H-thymidine may well underestimate the growth fraction.

The quantity of an intracellular protein will halve when a cell divides therefore detecting the dilution of an intracellular protein that has been labelled with fluorescent dye can be used to measure the rate of cell division over time. Carboxyfluorescein diacetate succinimidyl ester (CFSE) represents an improvement on this method. CFSE is an intracellular fluorescent label that is divided equally between daughter cells upon cell division. Compared to assays utilizing nucleotide analogues, CFSE allows the division history of different populations in culture to be quantified and compared.

The proliferation assays thus far discussed are *in vitro* techniques, in that the cells are cultured and therefore no longer represent normal physiology. *Ex vivo* detection assays allow the quantification of the proportion of cells proliferating during the physiological condition by detecting metabolites or cell cycle proteins, such as Ki67, that are associated with cellular proliferation.

The Ki67 protein was characterised in 1983 (Gerdes et al. 1983). Gerdes *et al* found that a monoclonal antibody generated by immunising mice with nuclei of a Hodgkin lymphoma cell line was specific for a nuclear structure present exclusively in proliferating cells. Ki67 was present in the nuclei of cells in the G1, S, and G2 phases of the cell division cycle as well as in mitosis but cells in the G0 phase (quiescent or resting cells) did not express Ki67 (Scholzen and Gerdes 2000). Therefore unlike other methods which require cells to be in S phase at the time of processing, Ki67 assays can identify cells at all stages of proliferation. However, there are limitations to the Ki67 assay, such as the incorrect identification of quiescent cells which have undergone S phase, as actively proliferating. Furthermore, Ki67-based assays can only estimate the growth fraction but not the intermitotic time or rate of cell proliferation which would also be relevant to any study of cell population kinetics. Additionally the functional role of Ki67 within the cell cycle, if indeed it does perform a role in cell cycle regulation or progression, remains unknown.

3.1.7 Apoptosis

In chapter one, apoptosis, programmed cell death, was described as a means of T cell loss, thus investigating changes to the proportion of cells undergoing apoptosis is important to understanding and characterising CD4 depletion and restoration during HIV infection. Many methods to investigate apoptosis have been developed, however the major limitation is the insensitivity of some assays to distinguish between apoptosis and necrosis. Necrosis, which is cell death due to severe damage, differs significantly from apoptosis; it is characterised by osmotic dysregulation, cell swelling and lysis unlike apoptosis, which is characterised by chromatin condensation and internucleosomal DNA fragmentation, together with cell shrinkage and membrane blebbing (Hotchkiss et al. 2009). A third type of cell death, autophagy, which is an energy generating process by which a cell digests its own organelles and macromolecules, is recognised but is restricted to starving cells (Loos and Engelbrecht 2009). Assays based on the detection of steps common to apoptosis and necrosis will not distinguish between the two pathways for example DNA fragmentation, detected by TUNEL and comet assays, is common to both processes (Grasl-Kraupp et al. 1995), (Collins et al. 2008). Although necrosis is an important process in disease no significant increase is seen in HIV infection *in vivo* (Echaniz, de, & Cuadrado 1995).

Two major apoptosis pathways are recognised, one mediated by death receptors and the other mitochondrially mediated (Figure 3.2). However they both include the activation of the enzyme caspase 3 therefore this can be used to detect apoptosis taking place via either pathway (Hotchkiss et al 2009).

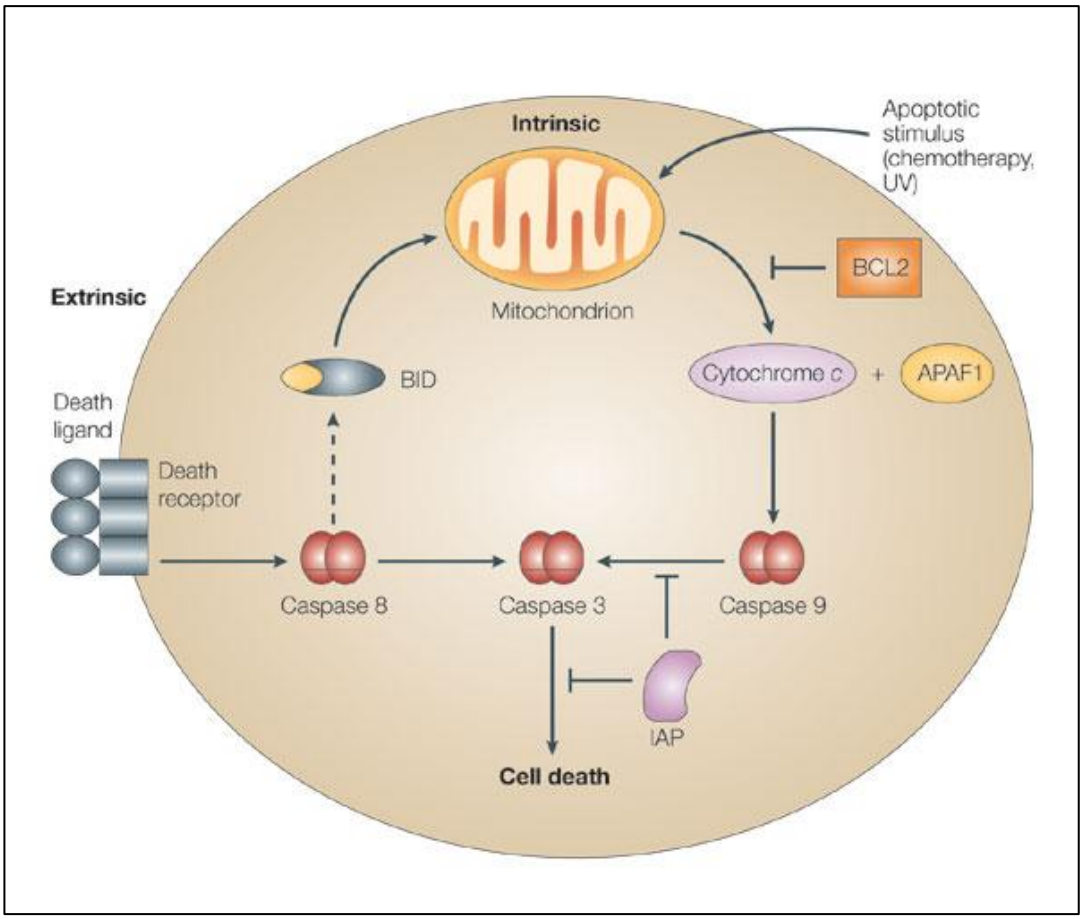

Figure 3.2 Apoptosis pathways

The two major pathways of apoptosis, the extrinsic, death receptor mediated, and the intrinsic, B-cell lymphoma protein 2 (BCL2)-regulated mitochondrial pathway, are shown simplified. Activation of both pathways culminates in caspase 3 activation. Pathway regulators are shown, inhibitors of apoptosis protein (IAPs) apoptosis-activating factor 1 (APAF1) and the BCL2 family death agonist. Reproduced from (Andersen, Becker, & Straten 2005).

The studies described in this chapter aimed to identify methods to enumerate $CD4^+$ T cell sub-populations and characterise activation, proliferation and apoptosis, within them by flow cytometry to enable the study of $CD4^+$ T cell kinetics in children infected with HIV. The methods used had to take into account the large number of samples to be processed, the small sample volumes available and the difficulty of concentrating leucocytes in HIV infected blood samples. Additionally the methods used had to be compatible and reliable with both fresh whole blood and cryopreserved PBMCs because this study utilized both small volumes of fresh whole blood from the GOSH cohort (described fully in chapter 4) and larger samples of cryopreserved PBMCs from the PENTA 11 cohort (described fully in chapter 5 and 6). Methods were first identified in

blood samples from uninfected adult donors and then verified in blood samples from HIV-1 infected children because cell separation and flow cytometry procedures to identify sub-populations of cells in blood from HIV-1 infected donors can often produce poorer or less distinct populations.

3.2 METHODS

3.2.1 Blood collection

As described in chapter 2, whole blood was obtained from healthy adults and HIV-1 infected children by venesection and anticoagulated by collection into tubes prepared with EDTA.

3.2.2 Lymphocyte enrichment

Where lymphocyte enrichment was required this was achieved either by lysis of RBCs or density gradient centrifugation as described in chapter 2.

3.2.3 Flow cytometry

A full list of the antibodies and reagents used to stain cells for flow cytometry is provided in chapter 2 with corresponding fluorochromes along with the methods used. Three-colour flow cytometry was performed on a FACSCalibur (BD) and four-colour on a Cyan (Dako). All analysis was performed with Summit v4 (Dako).

3.3 RESULTS

3.3.1 Identifying $CD4^+$ T lymphocytes: density gradient centrifugation

PBMCs were isolated from fresh whole blood from healthy adult donors. An aliquot from each donor was cryopreserved and the remainder incubated with antibodies against CD4 and CD3 then analysed by flow cytometry. Two populations were identified that expressed CD4, one population that expressed high levels of CD4 ($CD4^{high}$) and another that expressed low levels ($CD4^{low}$) (Figure 3.3A). The $CD4^{high}$ and $CD4^{low}$ populations were found to have distinctly different FSC and SSC profiles. $CD4^{high}$ was represented by a smaller and less granular population (Figure 3.3B). Additionally the CD3 expression was found to be restricted to the $CD4^{high}$ population.

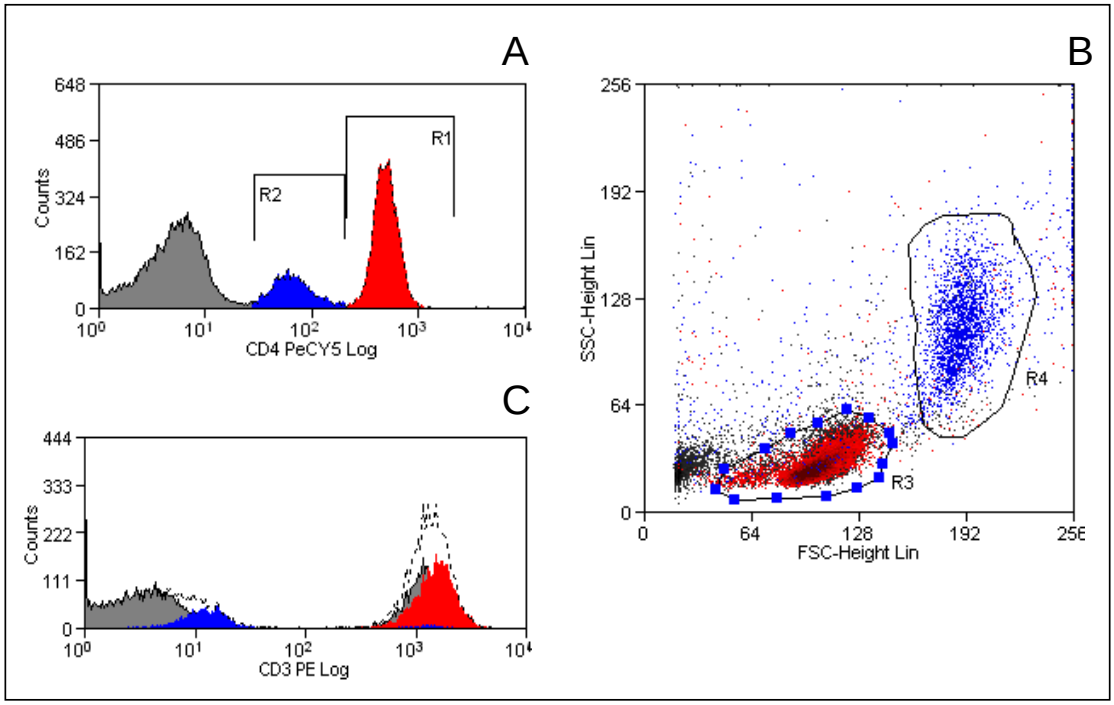

Figure 3.3. CD3 and CD4 expression in PBMCs from a healthy adult donor

A) A $CD4^{high}$ (red peak, R1) and $CD4^{low}$ (blue peak, R2) population are marked on the histogram and applied to the FSC versus SSC dot plot, B). The $CD4^{high}$ cells are almost exclusively located in R3, a region of low FSC and SSC and the $CD4^{low}$ cells are mostly located in R4, a region of high FSC and SSC. C) The $CD4^{high}$ (red peak, R1) and $CD4^{low}$ (blue peak, R2) populations are then applied to a histogram of CD3 expression.

The cryopreserved PBMC aliquots were thawed 24 hours later and similarly processed by incubating with antibodies against CD3 and CD4. As described with the fresh samples, two CD4 populations were identified, a $CD4^{high}$ population of small non-granular cells and a $CD4^{low}$ population of larger more granular cells where CD3 expression was restricted to the $CD4^{high}$ population.

Fresh and cryopreserved PBMCs from HIV-1 infected children were incubated with antibodies against CD3 and CD4 and analysed by flow cytometry. As with the PBMCs from the healthy adult donors, two distinct CD4 populations separated by size and granularity with visible were CD3 expression was restricted to the $CD4^{high}$ population. (Figure 8.1).

3.3.2 Identifying $CD4^+$ T lymphocytes: red cell lysis

Density gradient separation was not feasible on blood samples from the GOSH cohort as theses were a great number of samples of low volume, less than 1 ml. In these samples leukocytes would be concentrated by lysis of red cells. Therefore fresh whole blood from healthy adult donors was incubated with antibodies against CD3 and CD4. After red cell lysis and fixation cells were analysed by flow cytometry. As with PBMCs, analysis revealed two distinct CD4 populations, $CD4^{high}$ and $CD4^{low}$, separated by size and granularity (Figure 3.4). Incomplete red cell lysis was occasionally observed but as the red cells and cell fragments were very small relative to the leukocytes and did not stain for CD3 or CD4 they were easily excluded.

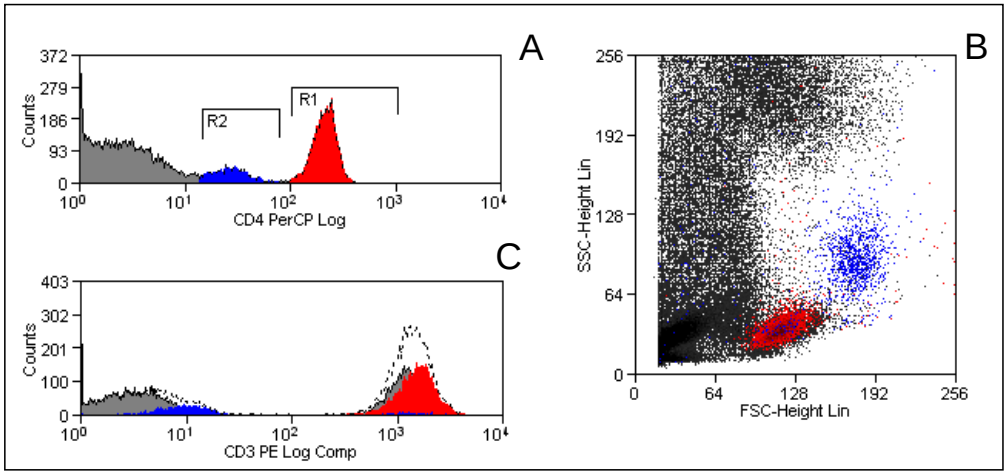

Figure 3.4 CD3 and CD4 expression in red cell lysed whole blood from a healthy adult donor
A) A $CD4^{high}$ (red peak, R1) and $CD4^{low}$ (blue peak, R2) population are marked on the histogram and applied to the FSC versus SSC dot plot, B). The $CD4^{high}$ cells are almost exclusively located in R3, a region of low FSC and SSC and the $CD4^{low}$ cells are mostly located in R4, a region of high FSC and SSC. C)The $CD4^{high}$ (red peak, R1) and $CD4^{low}$ (blue peak, R2) populations are then applied to a histogram of CD3 expression.

Similarly fresh whole blood from HIV-1 infected children was incubated with antibodies directed against CD4 and analysed by flow cytometry following red cell lysis. Similarly to whole blood from healthy adult donors distinct $CD4^{high}$ and $CD4^{low}$ populations with greater incomplete lysis were seen (Figure 8.2).

3.3.3 Defining $CD4^+$ T lymphocytes as naïve and memory populations by expression of CD45RA and CD45RO

As discussed in chapter 1, $CD4^+$ T cells can be divided into naïve and memory populations. It has been established in $CD4^+$ T cells that differentiation from a naïve to memory phenotype is associated with decreased expression of the RA isoform of CD45 and increased expression of the RO isoform (Akbar et al 1988). Therefore naïve cells and memory cells can be distinguished by either CD45RA or CD45RO expression. However small populations of primed $CD4^+$ T cells that express both CD45RA and CD45RO have been described (Hamann et al 1996).

The proportion of $CD4^+CD45RA^+$ cells that also expressed CD45RO was investigated in both uninfected adult donors and in HIV-1 infected children by incubating blood with antibodies against CD4, CD45RA and CD45RO and analysed by flow cytometry (Figure 3.5). There was little overlap between CD45RA and CD45RO expression in both the uninfected adults and HIV-1 infected children tested. From 6 adults and 11 children the mean proportion of $CD45RA^+$ cells that co-expressed CD45RO was 2.4% and 2.8% respectively, which were not significantly different (Mann-Whitney test p=0.72). Interestingly gating on $CD45RA^-$ $CD4^+$ lymphocytes in the 6 adults and 14 children found that CD45RO expression was not universal, a mean proportion of 88.2% and 91.0% expressed CD45RO, which was not significantly different (Mann-Whitney test, p=0.27) (Figure 3.6).

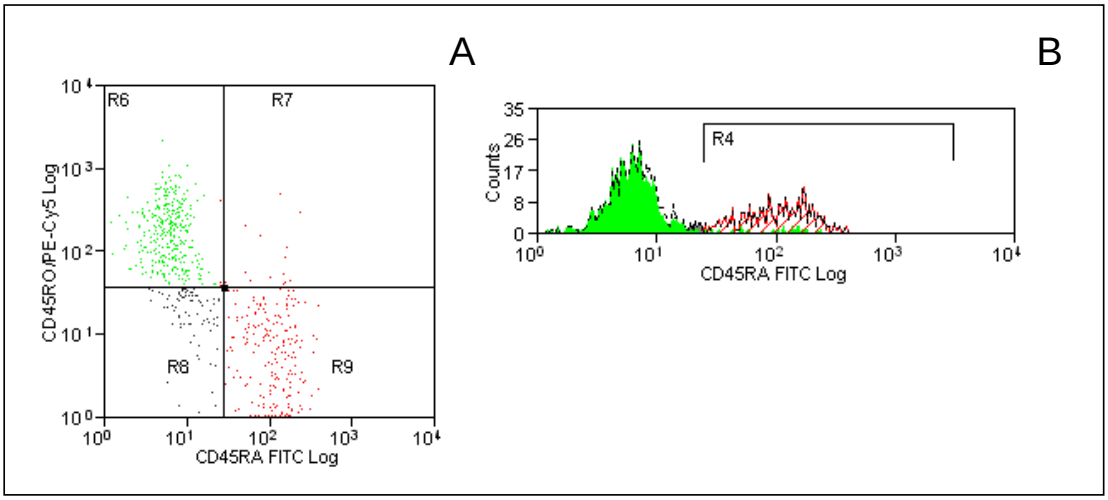

Figure 3.5. Representative dot plot and histogram of CD45RA and CD45RO expression
A) dot plot of CD45RA and CD45RO expression by $CD4^+$ T cells from one individual. (B) Histogram of CD45RA expression (red) with CD45RO expression overlayed (green).

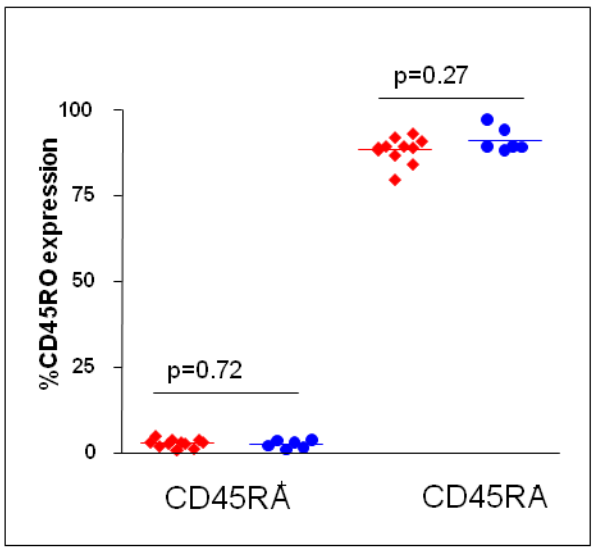

Figure 3.6 CD45RO expression by CD45RA$^+$ CD4$^+$ cells in HIV-1 infected children and uninfected adults

CD45RO expression by CD45RA$^+$ CD4$^+$ T cells from 11 HIV-1 infected children (red) was compared to 6 uninfected adults (blue). Similarly CD45RO expression by CD45RA$^-$ CD4$^+$ T cells was compared between the two groups. Statistical differences between the adults and children are shown.

3.3.4 CCR7 and CD27 expression by CD45RA CD4$^+$ T cells

As mentioned previously naïve CD4$^+$ T cells have been described as having fairly homogenous expression of CD27 (Croft 2009;Sugita et al 1992) and CCR7 (Okada et al 2008). Therefore the expression of CD27 and CCR7 by CD45RA$^+$ T cells was investigated in 10 HIV-1 infected children and 6 uninfected adults. Peripheral blood was incubated with CD4, CD45RA and either CCR7 or CD27. In the 10 children sampled it was found that CD4$^+$CD45RA$^+$ have almost universal expression of CD27 (mean=99.43%) and CCR7 (mean=99.59%) (Figure 3.7). Similarly amongst the 6 adults mean CD27 and CCR7 expression were 99.53% and 99.60%. Additionally a Wilcoxon matched pairs test showed no statistical difference between the level of CCR7 and CD27 expression (p=0.23 and p=0.34) for the children and adults respectively.

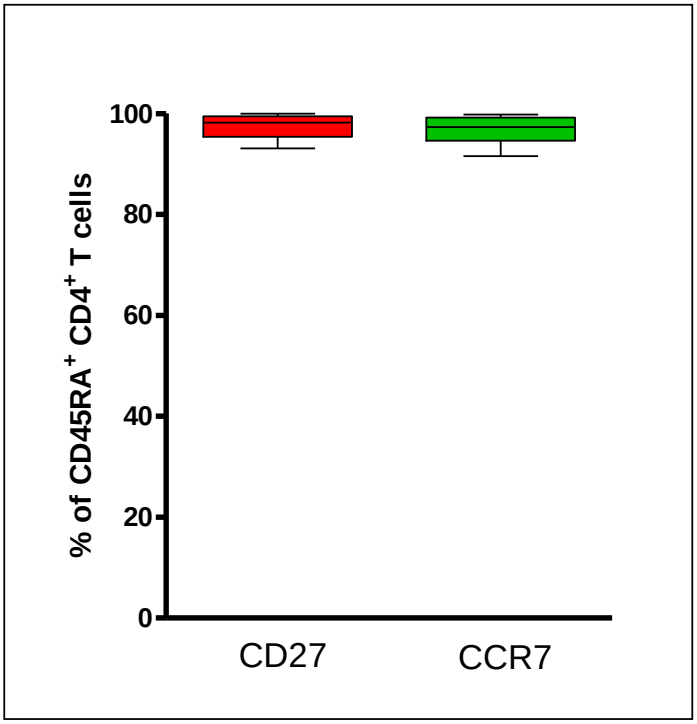

Figure 3.7. Comparison of CD27 and CCR7 expression by CD45RA$^+$ T cells
CD27 and CCR7 are expressed by almost all CD45RA$^+$ T cells in HIV-1 infected children. There was no statistical difference between the level of CD27 and CCR7 expression for each child.

3.3.5 Defining memory CD4$^+$ T cells by CD27 versus CCR7 expression

CD27 and CCR7 expression by memory cells is more variable than for naïve cells. Co-staining with CD45RA and CD27 or CD45RA and CCR7 allows CD4$^+$ memory (CD45RA$^-$) cells to be subdivided into 2 functionally distinct group characterised by expression or lack of expression of CD27 or CCR7 (Sallusto et al 1999). This was carried out on blood samples from ten children and six uninfected adults. The difference between the percentage of CD4$^+$ cells that were CD45RA$^-$CD27$^+$ and the percentage of CD4$^+$ cells that were CD45RA$^-$CCR7$^+$ was tested by Wilcoxon matched pairs test and found to be non significant in children and adults (p=0.35 and p=0.46 respectively). Representative dot plots from 1 child are shown (Figure 3.8).

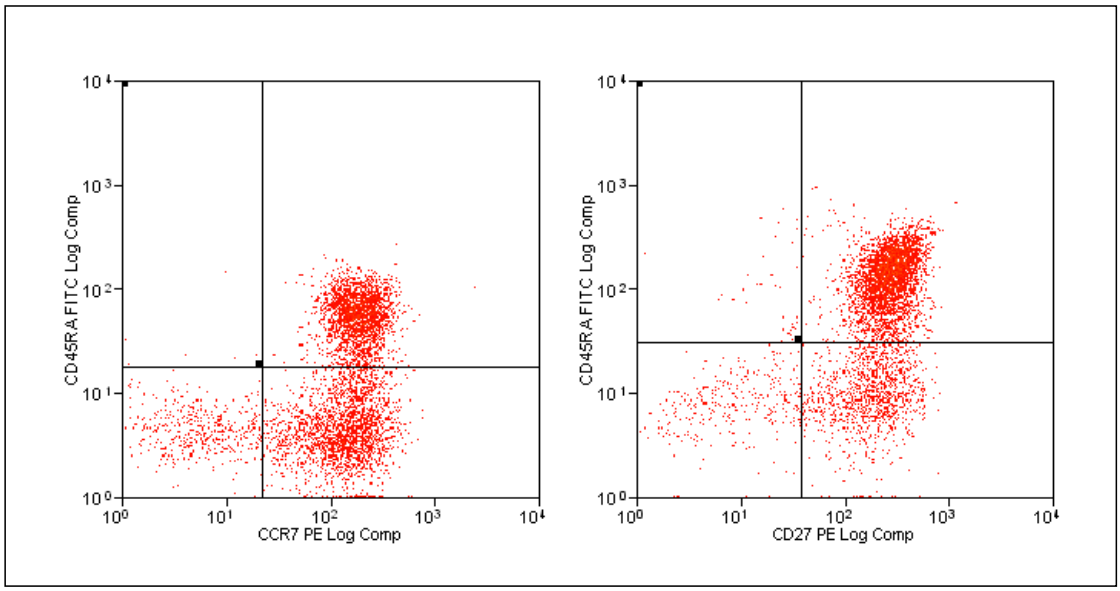

Figure 3.8 CCR7 and CD27 both divide CD45RA$^-$ CD4$^+$ T cells into two populations.
Representative dot plots from one child showing that CD27 and CCR7 divide CD45RA$^-$ CD4$^+$ T cells into two populations. The percentage of CCR7$^+$ cells is not significantly different from the percentage of CD27$^+$ CD45RA$^-$ CD4$^+$ T cells in each child (p=0.348).

3.3.6 Defining CD4$^+$ T cell subsets by expression of CD45RA and CD31

Co-staining with CD45RA and CD31 allows CD4$^+$ naive (CD45RA$^+$) cells to be subdivided into 2 functionally distinct group characterised by expression or lack of expression of CD31 (Kimmig et al 2002). Similarly the CD4$^+$ memory (CD45RA$^-$) cells are also divided. The significance, however, of CD31 expression or lack of expression by CD4$^+$ memory cells has not been investigated. Whole blood from 11 HIV-1 infected children and 5 uninfected adult donors was incubated with antibodies against CD4, CD45RA and CD31 and following red cell lysis were analysed by flow cytometry. In both the adults and the children 4 distinct CD4$^+$ T cell subpopulations were produced. A representative dot plot of CD31 and CD45RA expression on CD4$^+$ T cells from one child is shown (Figure 3.9). However the proportions of the populations differed significantly between the two sample groups. The percentage of CD45RA$^+$CD31$^+$ was significantly higher amongst the HIV-1 infected children than amongst the uninfected adults (p=0.0007) whereas the percentage of CD45RA$^-$CD31$^-$ and CD45RA$^+$CD31$^-$ cells were significantly lower (p=0.008 and p=0.0047 respectively). There was no significant different between the percentage of CD45RA$^-$CD31$^+$ cells between the two groups (Figure 3.10).

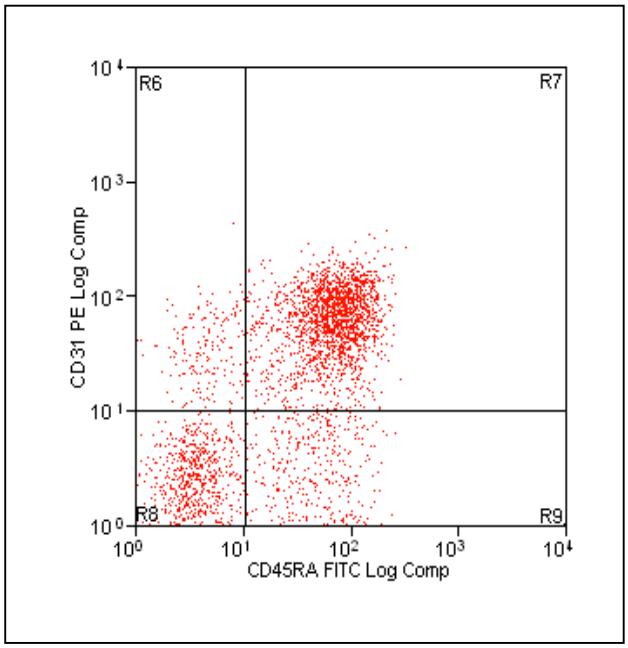

Figure 3.9 . Co-expression of CD45RA and CD31 by $CD4^+$ T cells

Whole blood was incubated with anti-CD4, CD45RA and CD31 fluorochrome conjugated antibodies. The immunostained cells were analysed by flow cytometry. A lymphocyte (FSC versus SSC) and CD4 expression gate was applied and the enclosed $CD4^+$ T cells were evaluated for their expression of CD45RA and CD31.

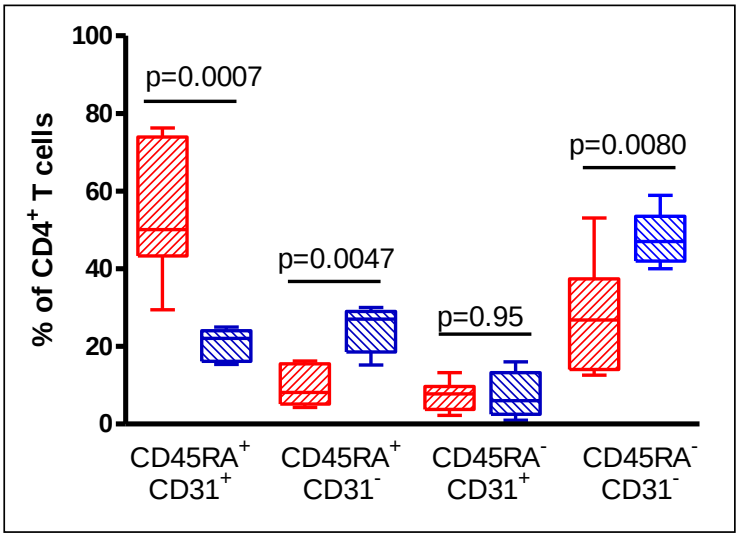

Figure 3.10 CD45RA and CD31 defined $CD4^+$T cells in HIV-1 infected children and uninfected adults

The proportions of CD45RA and CD31 defined $CD4^+$ T cells were compared between 10 HIV-1 infected children (red) and 5 uninfected adults (blue) and tested for statistical significance by Mann-Whitney test. The resulting values are indicated for each subpopulation.

3.3.7 Characterising activated $CD4^+$ T helper cells

In response to specific antigen or non-specific co-factors $CD4^+$ T cells can become activated. Activation results in a change in global gene expression and therefore usually results in the cell undergoing apoptosis, differentiation or division. Activation, as discussed in chapter one section four, has been implicated in the pathogenesis of HIV and thus should be investigated. The most common markers of $CD4^+$ T cell activation investigated by flow cytometry are CD38, CD69 and HLA-DR. Therefore to investigate activation of CD4 subpopulations whole blood from 9 HIV-1 infected children and 7 uninfected adults was incubated with antibodies against CD4, CD45RA, and either CD69, HLA-DR or CD38. $CD4^+$ T cells were gated on and the expression of each marker by the $CD4^+$ T cell sub-populations, $CD45RA^+$ and $CD45RA^-$ was determined because HIV infection is associated with higher levels of activation and activation has been demonstrated to be higher in memory cells than in naïve cells as discussed in chapter one. The results for one child are provided (Figure 3.11), where the histograms show the relative sizes of the CD69, CD38 and HLA-DR positive and negative fractions in the $CD4^+$ T cell pool and the dot plots compare the distribution of CD69, CD38 and HLA-DR in the $CD45RA^+$ and $CD45RA^-$ $CD4^+$ T cells.

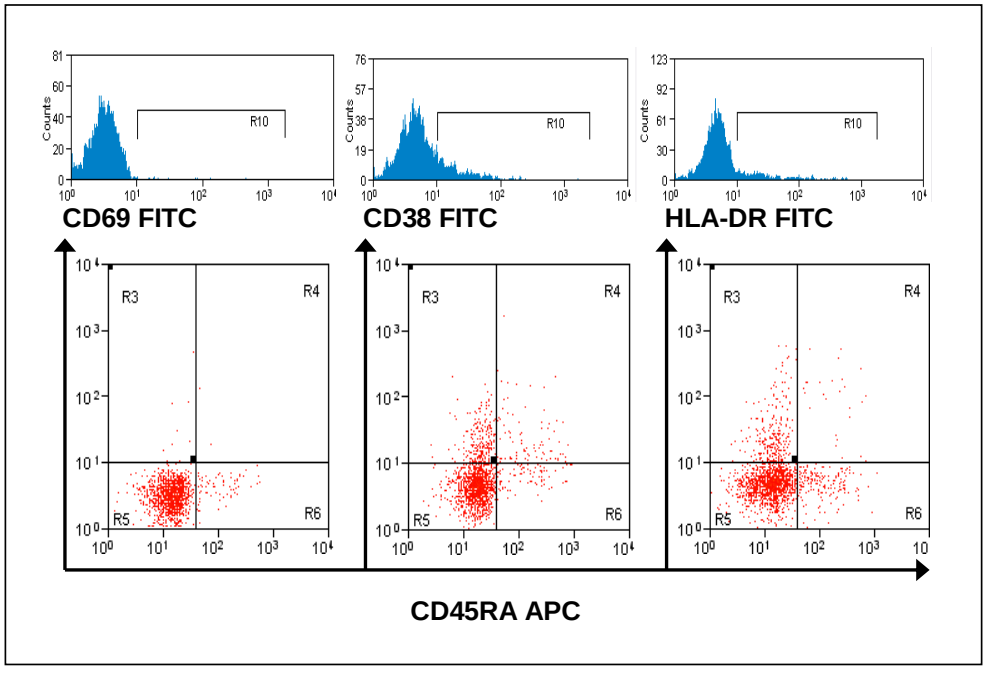

Figure 3.11. CD38, HLA-DR and CD69 expression on $CD4^+$ T cells

Representative staining from one child. The histograms show the relative sizes of the CD69, CD38 and HLA-DR positive and negative fractions in the $CD4^+$ T cell pool. The dot plots compare the distribution of CD69, CD38 and HLA-DR in the $CD45RA^+$ and $CD45RA^-$ $CD4^+$ T cells.

The difference in expression of these proteins was tested between the sample groups and the $CD4^+$ T cell sub-populations (Figure 3.12). Expression of CD38 and HLA-DR was significantly greater in HIV-1 infected children compared to uninfected adults but CD69 expression did not differ significantly between the two groups. Within each sample group protein expression was significantly greater by the $CD45RA^-$ population than, $CD45RA^+$ population. Comparing CD38, CD69 and HLA-DR, CD38 expression was the highest and CD69 expression was the lowest in both samples and both $CD4^+$ T cell sub-populations.

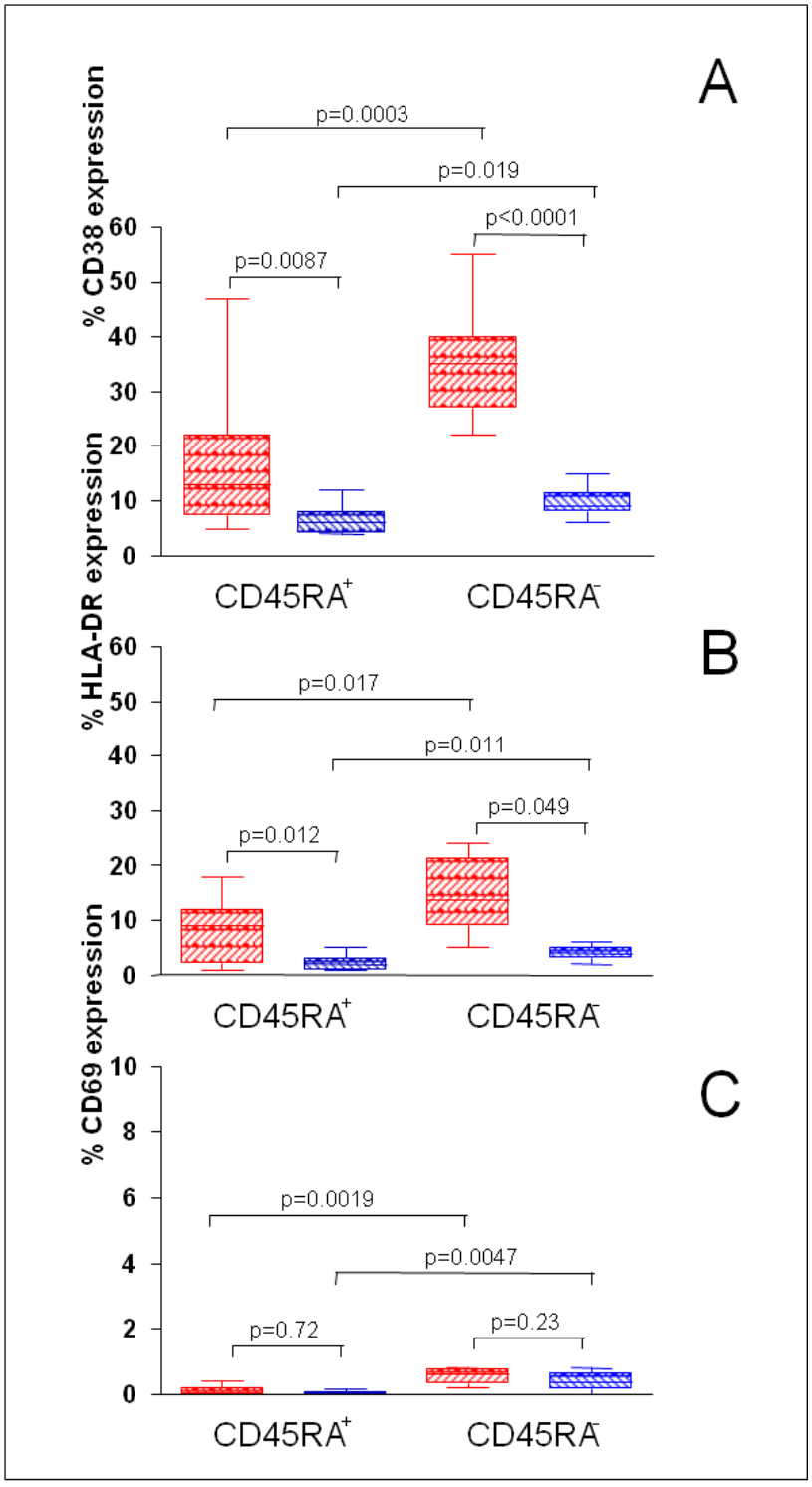

Figure 3.12. Expression of CD38, HLA-DR and CD69 on $CD4^+$ T cell s in children and adults

The box-whisker plots (A), (B) and (C) show the percentage expression of CD38, HLA-DR and CD69 respectively by $CD45RA^+$ and $CD45RA^-$ $CD4^+$ T cell sub-populations in a group of HIV-1 infected children (red boxes) and uninfected adults (blue boxes). The line through each box indicates the median. The statistical significance of the differences, produced by Mann-Whitney test, between adults and children and between $CD45RA^+$ and $CD45RA^-$ sub-populations are shown.

The paucity of CD69 expression could have been due to the CD69 antibody failing to bind or being used at too low a concentration. Thus to ensure this was not the case the expression of CD69 by stimulated and non-stimulated cells was compared. Fresh whole blood from three uninfected adult donors was divided into 2 aliquots. To one aliquot from each donor PMA and ionomycin were added to a final concentration of 25 ng/ml and 1 µg/ml respectively. Both aliquots were then incubated in an incubator for 4 hours at 37 °C and 5% CO2. The blood was then incubated with anti-CD69 antibody and processed and analysed as previously described. CD69 expression was greater in the stimulated cells (Figure 3.13).

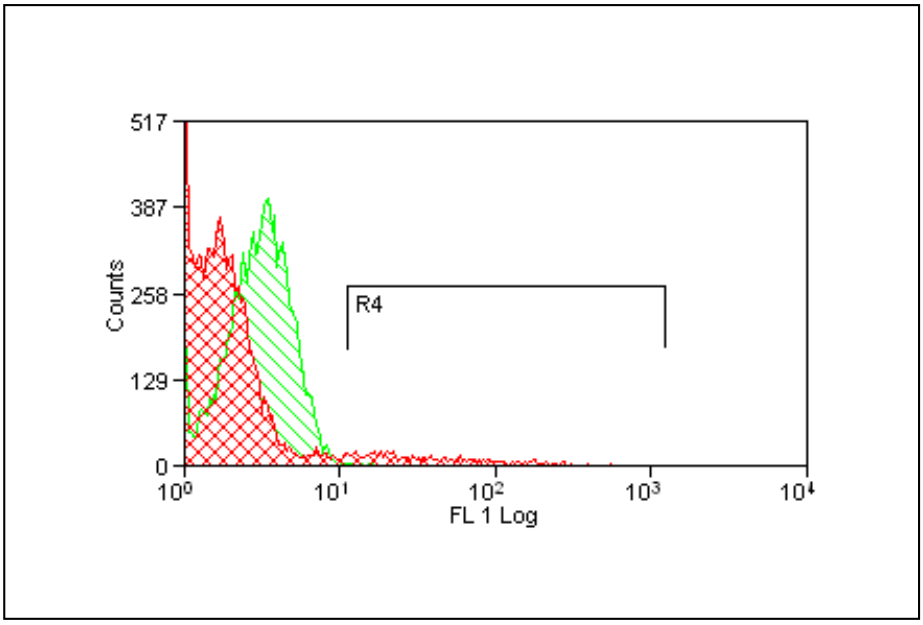

Figure 3.13 CD69 expression by stimulated and non-stimulated PBLs

Fresh whole blood from uninfected adult donors was incubated with and without PMA and ionomycin and CD69 expression determined. Stimulated and non-stimulated cells are in red and green respectively. The mean CD69 expression (R4) for the stimulated and non-stimulated PBLs were 0.27% and 7.41% respectively

CD38 is constitutively expressed by naïve cells therefore it is problematic to divide cells into a group that do not express and a group that do express CD38 (Malavasi et al 2006). So additionally, the relative fluorescent intensity was calculated (Figure 3.14).

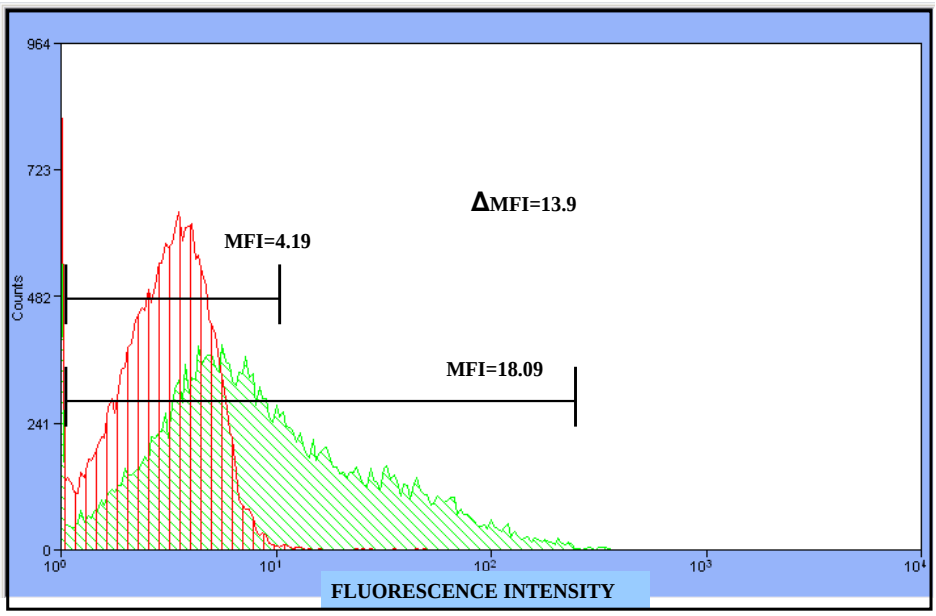

Figure 3.14. Relative mean fluorescent intensity (MFI) of CD38 on CD45RA$^+$ CD4$^+$ T cells
CD4$^+$ CD45RA$^+$ T cells were evaluated for their expression of CD38. The CD38 MFI was calculated by subtracting the MFI of a FITC conjugated IgG isotype (red peak) from the MFI of the FITC conjugated CD38 antibody (green peak)

3.3.8 Investigating Ki67 expression by CD4 subsets

Proliferation is likely an important process in the CD4$^+$ T cell decline and recovery associated with HIV infection and HAART respectively because, as discussed in chapter one, section two, it contributes to cell turnover. In this study an intracellular antibody against the nuclear cell cycle protein, Ki67, was used to determine proliferation. Ki67 has been shown to be expressed during the cell cycle but not in quiescent cells, cells in G_0. Ki67 expression was investigated in HIV-1 infected children and uninfected adults and in CD45RA$^+$ and CD45RA$^-$ CD4$^+$ T cell sub-populations. A representative dot plot of the relative Ki67 expression of CD45RA$^+$ and CD45RA$^-$ CD4$^+$ T cells for one child is shown (Figure 3.15).

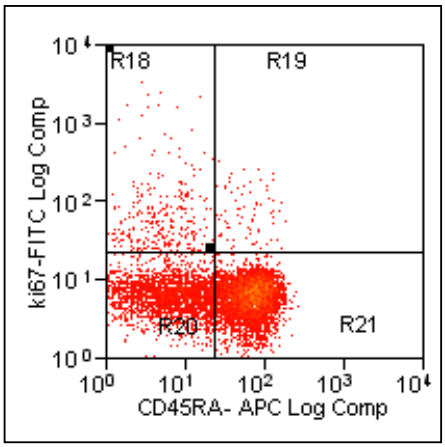

Figure 3.15. Ki67 expression by CD4$^+$ T cells

The figure shows Ki67 expression of CD45RA$^+$ and CD45RA$^-$ CD4$^+$ T cells for HIV-1 infected child.

The difference in Ki67 expression was compared between the HIV-1 infected and uninfected sample groups and the CD4$^+$ T cell sub-populations (Figure 3.16). Ki67 expression was significantly greater in HIV-1 infected children compared to uninfected adults and within both sample groups Ki67 expression was significantly greater in the CD45RA$^-$ population than the CD45RA$^+$ population.

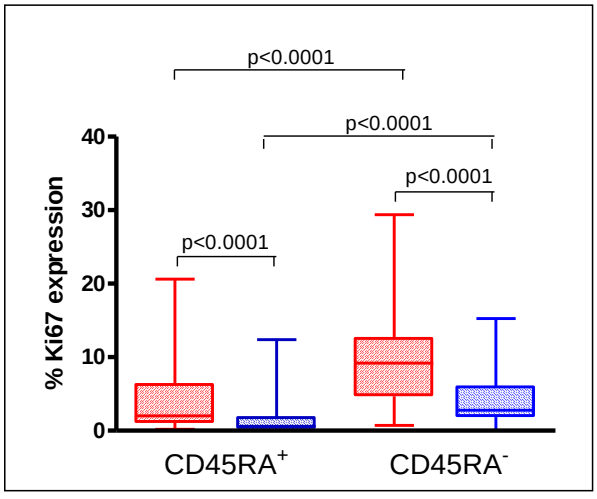

Figure 3.16 Differential Ki67 expression by CD4$^+$ T cell sub-populations in children and adults

Ki67 expression by CD45RA$^+$ and CD45RA$^-$ CD4$^+$ T cell sub-populations is displayed as a box-whisker plots in red and blue for HIV-1 infected children and uninfected adults respectively where horizontal bands indicate means and the significance of the differences, produced by Mann-Whitney test, between adults and children and between CD45RA$^+$ and CD45RA$^-$ sub-populations are shown.

3.3.9 Characterisation of CD31$^+$ and CD31$^-$ CD4$^+$ memory cells

As mentioned previously CD31 expression by CD45RA$^+$ cells has in recent years been used as an indication of recent thymic origin but the significance of CD31 expression by CD4$^+$ memory cells is not known. To investigate functional differences between CD31$^+$ and CD31$^-$ CD4$^+$ memory cells whole blood samples from 10 HIV-1 infected children were stained with a combination of anti-CD4, anti-CD45RA, anti-CD31 and one of the functional markers CD27, HLA-DR or Ki67 (Figure 3.17). The difference in the mean expression of each of these markers between CD31$^+$ and CD31$^-$ CD4$^+$ memory cells was analysed for statistical significance. There was a statistically significantly higher expression of Ki67 in the CD31$^+$ cells.

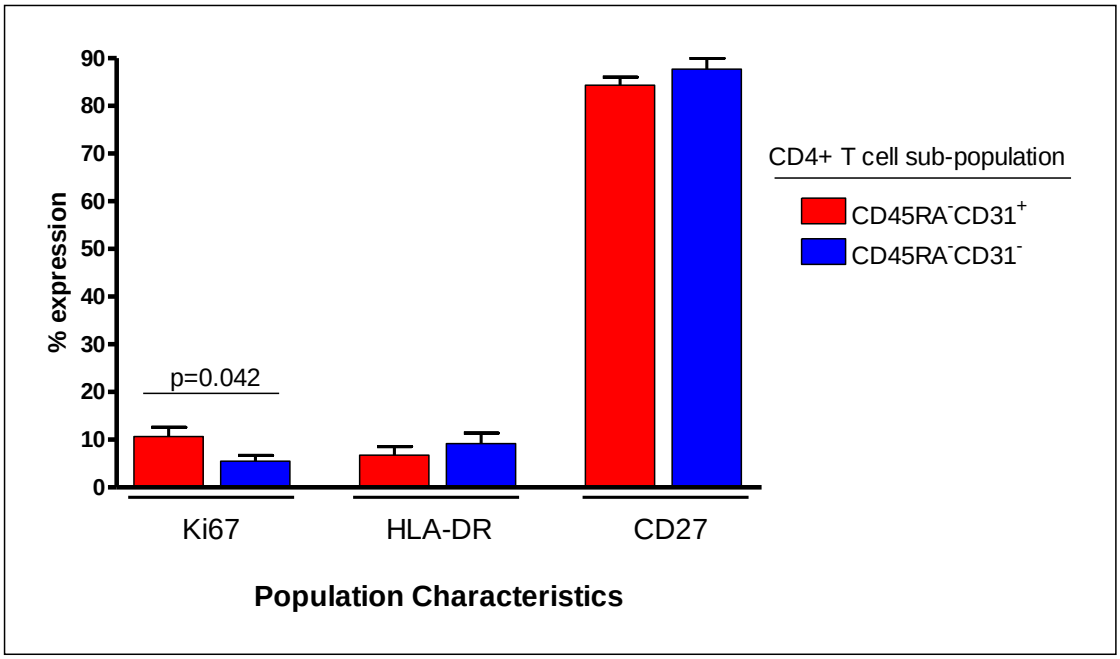

Figure 3.17. Characteristics of CD45RA$^-$CD31$^+$ versus CD45RA$^-$CD31$^-$ CD4$^+$ T cell sub-populations
The expression of the markers Ki67, HLA-DR and CD27 by CD45RA$^-$CD31$^+$ and CD45RA$^-$CD31$^-$ CD4$^+$ T cell sub-populations were compared for n=10 children.

3.3.10 Flow cytometric detection of apoptotic CD4$^+$ T cells ex vivo and at 24 hours

Apoptosis is believed to be the principle mechanism of death of CD4$^+$ T cells in HIV infection hence a flow cytometric method of detecting and measuring apoptotic cells was developed using FLICA, which binds to a caspase specific amino acid sequence. As described in chapter 2 the FLICA reagent was obtained as part of the Vybrant FAM Poly Caspases Assay Kit (Invitrogen, Molecular Probes, Paisley). To verify the volume

of FLICA required freshly drawn whole blood from three healthy donors was divided into 3 aliquots of 100 µl. To each aliquot of blood, 30X FLICA solution was added to produce the following dilutions 1/30 (recommended by manufacturer) 1/50, or 1/100. The red cells were lysed, washed off and the remaining PBMCs fixed as described in chapter 2. The percentage FLICA expressions at the 3 concentrations were compared by flow cytometry using a lymphocyte gate (Figure 3.18). Each histogram is an overlay of the FLICA expression of unlabelled lymphocytes (grey peak) and the FLICA expression of labelled lymphocytes at that concentration of FLICA (red peak). All FLICA concentrations produced similar population distributions on the histograms. Without an isotype control for FLICA the unlabelled cells were used as a negative control. This implied that all cells (red peak) expressed FLICA and were therefore apoptotic. It is, however, unlikely that freshly drawn PBMCs would exhibit such high levels of apoptosis. It is more likely that either, in each histogram the red peak, R2, was the FLICA negative fraction, approximately 99%, and R3, a FLICA positive fraction, less than 1% or that the FLICA was bound non-specifically and therefore expressed by all cells.

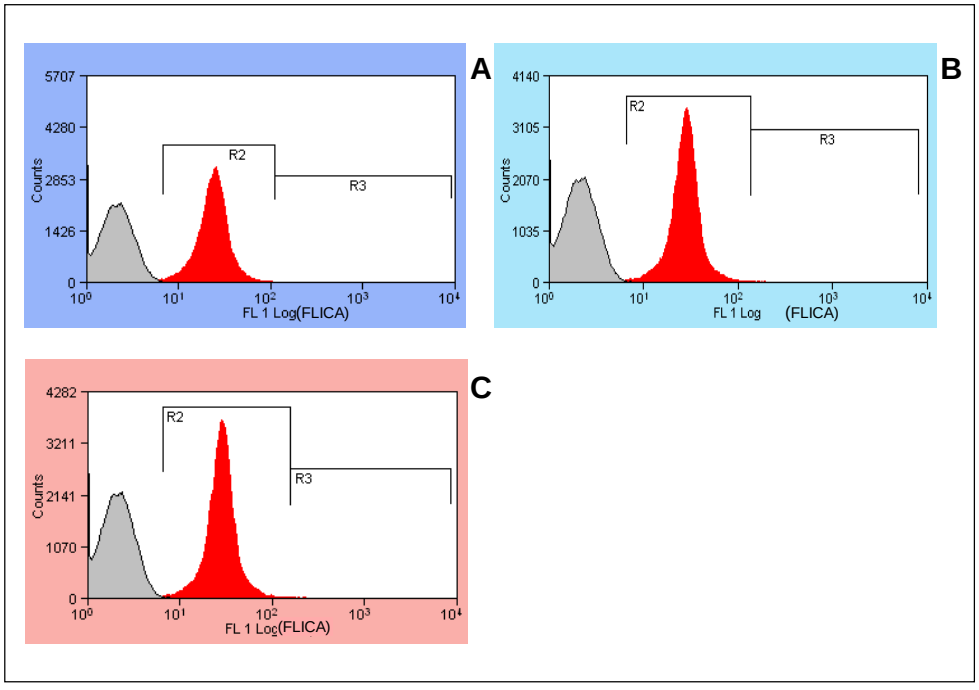

Figure 3.18 FLICA expression by lymphocytes from freshly drawn blood

Freshly drawn whole blood was incubated with 30X FLICA reagent at the following dilutions 1/100 (A), 1/50 (B) and 1/30 (C). A FSC versus SSC lymphocyte gate was applied and the FLICA expression (red) overlayed with the FL1 distribution of unlabelled cells. For (A), (B) and (C) FLICA R3 was 0.43, 0.49 and 0.59% respectively.

Investigating the specificity of FLICA binding without an appropriate negative control required a positive control, a population of cells where the level of apoptosis would be expected to be higher than in freshly drawn blood. The time taken to FLICA staining post venesection was therefore used as a positive control, on the premise that the level of apoptosis would have increased after 24 hours. The blood used in Figure 3.18 was incubated for 24 hours at room temperature and processed as before using FLICA solution at a 1/50 dilution. The sample was analysed as before, with unlabelled cells overlayed and used as a negative control, grey peak (Figure 3.19). The blue peak of FLICA expression showed the same distribution as Figure 3.18 and the region R4 made up 1.06% of the histogram.

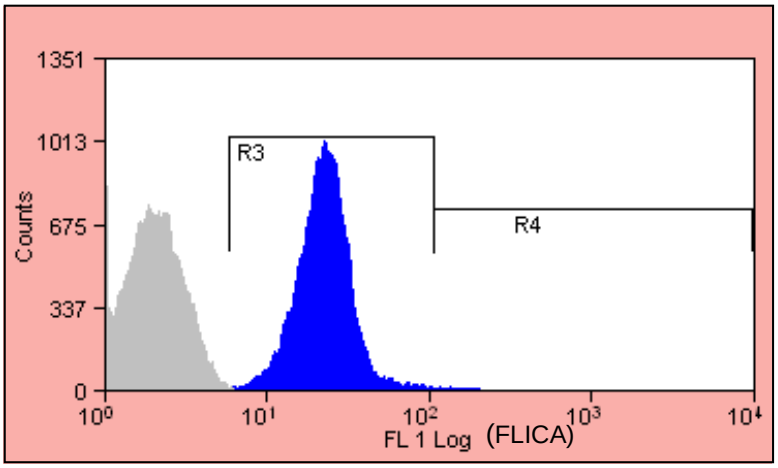

Figure 3.19. FLICA expression by lymphocytes in 24 hour old blood
Freshly drawn whole blood was incubated for 24 hours at room temperature and stained with 7 µl of 30X FLICA reagent. A FSC versus SSC lymphocyte gate was applied and the FLICA expression (blue) overlayed with the FL1 distribution of unlabelled cells. R4 was 1.06%.

The comparison of FLICA expression in fresh versus whole blood was not conclusive as it appeared that after 24 hours the expression of FLICA had only increased from 0.49% to 1.06%, which would have been unlikely. As the fresh and old samples were acquired on different days though on the same flow cytometer, this small and insignificant increase could have been due to analysing the samples on different days.

Therefore a second method to investigate the specificity of FLICA binding was attempted. To generate a positive control, camptothecin, a potent inhibitor of topoisomerase I, which is required for DNA synthesis was used to induce apoptosis. Fresh whole blood was aliquoted into two wells of a tissue culture plate. Camptothecin was added to one well to give a final concentration of 10 µM. The blood was placed in an incubator for 4 hours at 37 °C, 5% CO_2. The non-induced and camptothecin blood were then divided into 4 aliquots. Each aliquot was incubated for a further hour with no FLICA or with FLICA at one of the following dilutions, 1/30, 1/50 and 1/100. The samples were processed as previously described and overlay histograms of the results were generated (Figure 3.20). For each volume of FLICA used the FLICA expression of camptothecin incubated cells, apoptosis induced (red peak) was overlayed onto the FLICA expression of cells incubated without camptothecin (green peak). To these were added the FLICA expression profiles of unlabelled cells incubated with and without camptothecin, black and grey peaks respectively.

At each FLICA dilution the FLICA distribution for camptothecin incubated and non-camptothecin incubated cells were the same except where FLICA was used at a 1/50 dilution. Here the FLICA staining of the cells incubated without camptothecin had a higher MFI than the cells incubated with camptothecin. If FLICA staining was specific for apoptotic cells the red and green peaks on each histogram would have represented the FLICA negative fraction and R3 (and R5 in Figure 3.20C) would represent the FLICA positive fraction. Therefore if FLICA expression was specific R3 would have been greater for the camptothecin incubated cells. Instead, however, R3 was identical for camptothecin incubated cells and for cells incubated without camptothecin. At 10 µl and 3 µl of FLICA R3 was 0.6% and 0.5% respectively. At the 1/50 FLICA dilution the cells incubated with and without camptothecin showed different distributions therefore on the histogram for the FLICA concentration R3 represents the FLICA positive fraction of cells incubated with camptothecin and R5 represents the FLICA positive fraction of cells incubated without camptothecin. R3 and R5 were, however the same size, 0.2%.

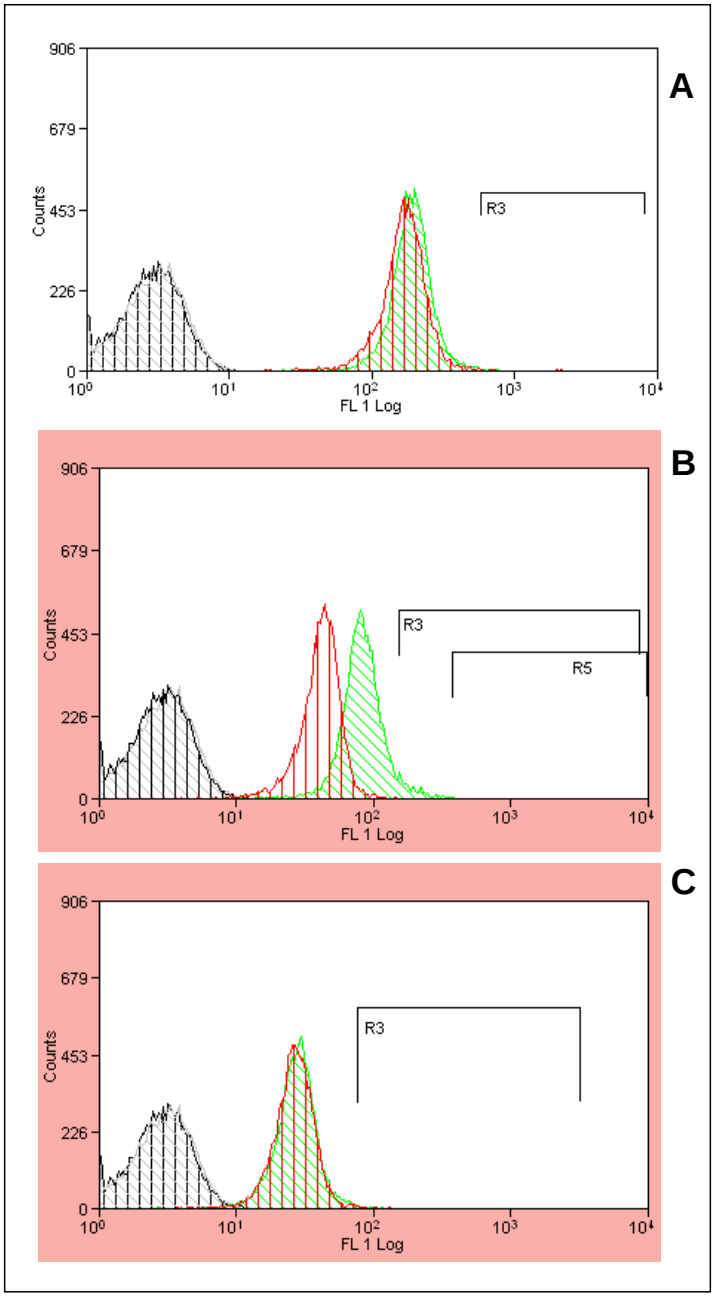

Figure 3.20 Comparison of FLICA expression after incubation with or without camptothecin. Whole blood was either incubated with camptothecin and then with FLICA (red peaks) or without FLICA (black peak) or without camptothecin and then with FLICA (green peak) or without FLICA (grey peak). FLICA was used at the following dilutions 1/30, 1/50 and 1/100 for A, B, and C respectively. For each concentration the FLICA expression of unlabelled cells (black and grey peaks) was overlayed on the FLICA expression of FLICA labelled cells (green and red peaks).

Incubating fresh versus old blood and camptothecin incubated versus blood incubated without camptothecin produced identical population distributions. If FLICA bound specifically incubation time and camptothecin use would have resulted in a greater

proportion of cells expressing FLICA. This was not the case therefore either FLICA failed to bind at all or bound non-specifically to all cells. FLICA staining produced populations with an MFI higher than unstained cells therefore it is improbable that FLICA failed to bind to cells and instead FLICA must have bound non-specifically to all cells.

In flow cytometry and immunohistochemistry adding excessive quantities of an antibody to cells can produce non-specific binding but in such a case the extent of the non-specific binding is dose-dependent therefore the percentage of cells expressing the antibody would decrease when the antibody is applied at lower concentrations. FLICA was tested at a range of concentrations yet the expression of FLICA staining was unchanged. Additionally the FLICA reagent is not an antibody but a small moiety that passes into the cell. The unbound reagent should diffuse out of the cell and be washed away. In the protocol used before unbound FLICA was washed off, erythrocytes were removed with Facs Lysing solution (BD) as described in chapter 2. FACS Lysing solution contains diethylene glycol for red cell lysis and formaldehyde to fix the remaining PBMCs. The oxygen atoms of formaldehyde, chemical formula, CH_2O, form hydrogen bonds with the amine functional groups of certain amino acids thus cross linking proteins (Schander and Kenneth 2003). The FLICA reagent consists of a fluoromethyl ketone attached to the amino acid recognition sequence valine-alanine-aspartic acid. The green fluorescence comes from the carboxyfluorescein (FAM) attached as a reporter. Excess FLICA might therefore become cross linked to proteins within the cell, proteins that would not be removed from the cell by washing with phosphate buffered saline.

Isotonic ammonium chloride can also be used to lyse erythrocytes. Fresh whole blood from a healthy donor was incubated with the FLICA reagent and the red cells lysed with an isotonic solution of ammonium chloride (Figure 3.21). The ammonium chloride was found to effectively remove erythrocytes from the blood sample. In the absence of formaldehyde the non-specific FLICA binding was abrogated. The first cytogram of FSC versus SSC showed clear and distinct populations of lymphocytes (R1) and granulocytes (R4). The second cytogram was back gated for FLICA expression to show

the location of FLICA positive cells. The FLICA histograms, C and D, are gated on the regions R1 and R4 respectively to show the FLICA expression by lymphocytes and granulocytes, 3.9% and 87.9% respectively. Removing red blood cells from HIV infected samples is notoriously problematic regardless of the method used and unfortunately ammonium chloride yielded insufficient red cell lysis when used on blood drawn from HIV infected children (data not shown) and therefore could not be used for this study.

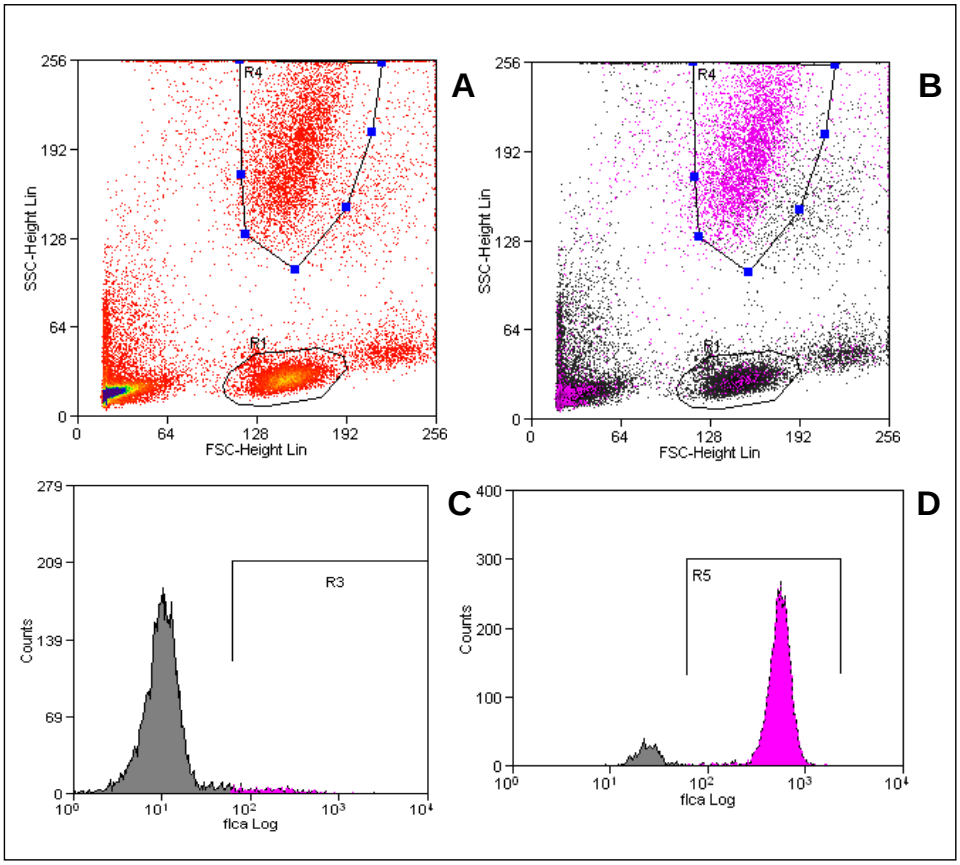

Figure 3.21 FLICA expression of PBLs after ammonium chloride red cell lysis
Whole blood was incubated with FLICA and red cells removed by addition of ammonium chloride. The PBL populations that remained are shown in the FSC versus SSC cytogram (A) and colour gated for FLICA expression (B). The PBL sub-populations R1, lymphocytes, and R4, granulocytes were gated on and the FLICA expression determined for each determined. The FLICA expression of the lymphocytes (C) and the granulocytes (D) was 3.9% and 87.9% respectively.

Given the small blood samples available from each child, less than 1 ml, a ficoll density gradient centrifugation separation to separate the PBMCs from the erythrocytes was not

feasible. Additionally given the fragility of apoptotic cells red cell lysis and ficoll protocols would likely have meant the loss of some of the apoptotic cells. It was therefore decided not to separate the PBMCs but instead to subject the entire whole blood fraction to flow cytometry.

Whole blood was incubated with anti- CD4 and CD45RA fluorochrome labelled antibodies and FLICA, then washed and fixed. The samples were re-suspended in PBS and passed through a cell strainer to avoid clogging the flow cytometer and then evaluated by flow cytometry without red cell lysis. Events were acquired up to the 10 million event limit of the flow cytometer. This yielded a small number of $CD4^+$ T cells, typically 4000 cells. Their FSC/SSC location was verified and their FLICA expression determined and found to be 3.4% (Figure 3.22).

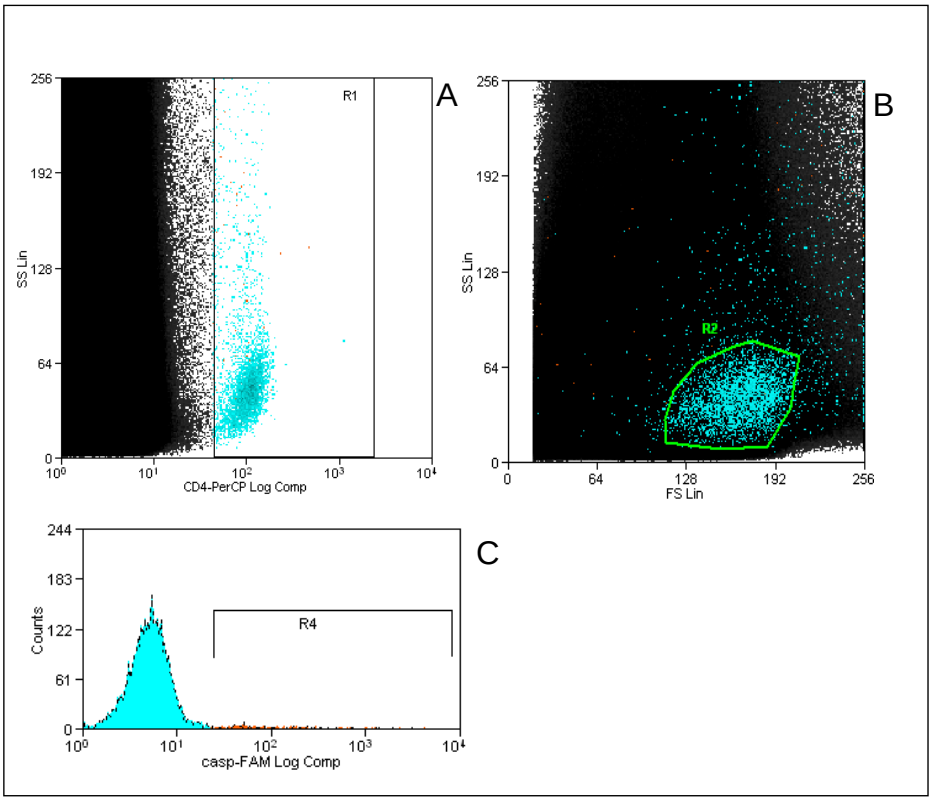

Figure 3.22 FLICA expression by $CD4^+$ T cells in whole blood without erythrocyte lysis
Whole blood was incubated with FLICA and anti-CD4 antibody and analysed by flow cytometry without red cell lysis. $CD4^+$ T cells were gated on (region R1 in A) and their FLICA expression determined under R4 (C). The FSC/SSC location of the $CD4^+$ T cells is indicated by the region R2 (B)

Running the flow cytometer at maximum speed it took several minutes to acquire 10 million events and produced a very large data file that was very slow to load onto analysis software. Additionally this produced a very small $CD4^+$ T cell population as $CD4^+$ T cells make up only 0.2-0.3% of whole blood. With such a high ratio of red cells to white cells it was not possible to collect sufficient $CD4^+$ T cells by this method especially taking into account that FLICA positive cells are rare events. The threshold of the flow cytometer had been set only by size (FSC) to exclude debris therefore erythrocytes were considered as events and constituted most of the 10 million event limit. A decision was therefore taken to include a secondary threshold parameter on the flow cytometer, CD4 expression, such that only $CD4^+$ cells would be considered as events. This allowed an adequate number of $CD4^+$ T cells, at least 1000, to be acquired and recorded by the flow cytometer.

3.4 DISCUSSION

The work in this chapter sought to demonstrate and validate flow cytometry methods to identify and quantify $CD4^+$ T cells and their subsets in peripheral blood from HIV-1 infected children and determine methods to investigate the processes of activation, proliferation and apoptosis within those populations.

$CD4^+$ T lymphocytes are the focus of this body of work and therefore the first crucial result demonstrated their identification by flow cytometry. Within samples of peripheral blood cells (PBMCs) lymphocytes and circulating dendritic cells can be discriminated from other cell populations by just two physical parameters, the forward and side scattering of light. Lymphocytes and circulating dendritic cells show intermediate forward and side scatter in comparison to granulocytes, which show high side and forward scatter, and red blood cells and platelets that show low side and forward scatter. To further discriminate $CD4^+$ T cells from other lymphocytes fluorescently labelled antibodies specific for of CD3 and CD4 are commonly used (Perfetto, Chattopadhyay, & Roederer 2004).

Although increasingly more sophisticated machines are available that can distinguish up to 17 fluorescent parameters for each cell, most researchers do not have need of so many parameters and furthermore such machines are usually priced beyond their reach and require an extremely high level of technical support as the machines are very sensitive and compensation is very complicated. Also it could be argued that there is not a great use in further subdividing cell populations into more and more ever increasing smaller sub-populations especially without functional studies.

I had access to 3 and 4 colour flow cytometry and therefore sought to conserve fluorescent channels for analysing other cell parameters. I was able to demonstrate that a single parameter, CD4 in conjunction with forward and side scatter identified the same cell population as CD4 combined with CD3. CD4 can be expressed by both lymphocytes and monocyte derived cells but it is unlikely that the $CD4^+$ population identified included the latter cell type because analysis revealed two distinct populations with differing fluorescence intensity and intermediate versus high forward and side scatter. Additionally CD3 expression was restricted to the $CD4^{high}$, intermediate side and forward scatter population. The same populations were demonstrated in samples obtained by both density gradient centrifugation and red cell lysis, an important result because both methods would be used for this study and it has been reported that purifying peripheral blood lymphocytes by density gradient centrifugation can produce an unpredictable enrichment and loss of selected lymphocyte populations, however the variability was described amongst the $CD8^+$ T cells, which are not investigated in this study (Renzi and Ginns 1987), (Romeu et al. 1992). Importantly this was shown in both uninfected adults as well as HIV-1 infected children because it has been reported that amongst HIV-1 infected individuals the lymphocyte gate is often and unpredictably contaminated by debris and other cell types (Pacifici et al. 1998), one of the causes being antiretroviral treatment which is associated with increased granulocyte fragility and reduced susceptibility of red blood cells to lysis (CDC 1994).

Perhaps the most commonly used functional subdivision of $CD4^+$ T cells is into a naïve and memory type and therefore identifying means to discriminate between these types by flow cytometry was the next step undertaken. Additionally changes to these

phenotypes have been implicated in HIV-1 infection and is a noted difference between adults and children and this study is chiefly concerned with paediatric HIV-1 infection. It is widely accepted that differentiation from a naïve to memory phenotype is associated with decreased CD45RA and increased CD45RO expression. However as discussed earlier there is some evidence that memory cells can regain expression of CD45RA and that some $CD45RA^+$ cells exhibit a primed phenotype. It would be preferable to use one marker therefore I sought to verify whether $CD45RA^+$ cells included $CD45RO^+$ cells and whether $CD45RA^-$ $CD4^+$ cells were entirely $CD45RO^+$. Amongst $CD45RA^+$ cells from both uninfected adults and uninfected children there was very little CD45RO expression. The $CD45RA^+$ $CD45RO^+$ $CD4^+$ T cells, which have been reported to be primed cells in transition from naïve to memory cells, were found to be a very minor population, less than 4% and a mean size 1.2%. Other studies have reported similar results, means of 3.4% and 2.4%, in healthy controls and HIV-1 infected adults respectively that did not differ significantly (Mahalingam et al. 1996).

Interestingly a not insignificant proportion of $CD45RA^-$ cells did not express CD45RO, 9-11.8%. All $CD4^+$ T cells express some variant of the CD45 antigen because they are leucocytes, which would suggest that that this small population of $CD45RA^-CD45RO^-$ cells are perhaps either not leucocytes or are apoptotic cells or insufficient antibody was used. However, all antibodies used in this study were titrated around the concentration recommended by the manufacturer and used in excess therefore this would seem unlikely. Lysing red blood cells in samples from HIV-1 infected individuals is notoriously difficult. As mentioned previously amongst HIV-1 infected individuals the lymphocyte gate is often and unpredictably contaminated by debris and other cell types (Pacifici et al 1998), which may account for this small $CD45RA^-CD45RO^-$ population. It has also been suggested, based on the size of these cells, that they represent apoptotic cells (McElhaney, Pinkoski, & Meneilly 1995). Apoptosis has been shown to be increased in HIV infection thus the greater proportion of these cells in the HIV-1 infected children compared to the uninfected adults supports this hypothesis. It has been proposed that these apoptotic cells might be derived from memory by virtue of their expansion post influenza vaccine and subsequent influenza virus challenge (McElhaney, Pinkoski, & Meneilly 1995).

A minority of people have been reported to have a CD45 polymorphism, C77G, which results in continuous expression of CD45RA by memory cells. The C77G polymorphism is prevalent in around 1% of the Caucasian population and has an even lower frequency in non Caucasians (Tchilian et al. 2002). It was not found in the 14 children investigated and is unlikely to exist in either of the cohorts described in this study as they are mostly non Caucasian.

Therefore in conclusion defining naïve cells by CD45RA expression includes both $CD45RA^{+}$ $CD45RO^{-}$ and a very small proportion of primed $CD45RA^{+}$ $CD45RO^{+}$ cells and defining memory cells by lack of CD45RA expression both $CD45RA^{-}$ $CD45RO^{+}$ and $CD45RA^{-}$ $CD45RO^{-}$ cells. The phenotype of $CD45RA^{-}$ $CD45RO^{-}$ cells is unknown but they may be a population of apoptotic cells derived from memory cells.

The consensus of the MASIR 2008 conference on the phenotype and function of human T lymphocytes was that there are 2 populations of antigen experienced $CD4^{+}$ T cells that express CD45RA but that they can distinguished from true naïve cells by their lack of CD27 and CCR7 expression (Appay et al. 2008). Though I have shown that $CD45RA^{+}CD45RO^{+}$ cells are a very minor population in the children we tested I also sought to investigate the CD27 and CCR7 expression of $CD45RA^{+}$ cells in these children. We found that CD27 and CCR7 were both expressed by over 99% of $CD45RA^{+}$ cells. Additionally there was no significant difference between the level of CD27 and CCR7 expression in each child. This supports our view that almost all the $CD45RA^{+}$ cells are antigen naïve.

As mentioned in chapter one memory $CD4^{+}$ T cells can be subdivided into two populations based on homing or migratory potential and the presence or absence of effector function (Sallusto et al 1999). These two populations, central and effector memory cells, were shown to differ in CCR7 expression but subsequently CD27 expression was also shown to differ between these populations (Sallusto et al 2000),

(Sallusto, Geginat, & Lanzavecchia 2004). We have shown that there was no significant difference between the percentage of CD27 and CCR7 expressed by $CD45RA^-$ cells in each child.

Naïve $CD4^+$ T cells have been shown to be divided into a TREC content high and TREC content low population by the presence or absence of CD31 expression (Kimmig et al 2002). The $CD31^+$ population and $CD31^-$ populations have been reported to represent RTEs and central naive cells as detailed in chapter one. Due to greater thymic function in children than in adults RTEs would be likely to be a greater proportion of the $CD4^+$ T cell population in children than in adults and accordingly a decrease in the proportion of $CD45RA^+CD31^+$ $CD4^+$ T cells with age has been shown in uninfected individuals (Kimmig et al 2002). Our results show that HIV-1 infected children also have a significantly greater proportion of $CD45RA^+CD31^+$ $CD4^+$ T cells than the uninfected adults. It also known that amongst uninfected individuals the proportion of $CD45RA^-CD31^+$ $CD4^+$ T cells does not change with age (Junge et al 2007). Our results show that HIV-1 infected children also do not have a significantly different proportion of $CD45RA^-CD31^+$ $CD4^+$ T cells than the uninfected adults.

To characterise activation within $CD4^+$ T cells we studied three surface markers commonly used, CD38, CD69 and HLA-DR. CD38 has been found to be expressed at higher levels on neonatal lymphocytes than adults; high levels on mature thymocytes and activated T cells; low levels on resting ($HLA\text{-}DR^-$) naïve cells and undetectable levels on resting memory cells. In HIV CD38 is upregulated on uninfected cells. It was also reported that CD38 expression has better prognostic value if mean fluorescence intensity (MFI) not proportion of cells positive is evaluated because gating of positive cells is subjective (Savarino et al. 2000). Similar to reported data I found CD38 expression to be higher amongst HIV infected children than uninfected adults also amongst both groups a greater proportion of memory cells than naïve cells expressed CD38.

We found that CD38 expression by $CD4^+$ T cells is not a dichotomy of either high or low expression. This made it subjective and less reliable to state the percentage of cells

that expressed CD38. As we have shown stating the difference between the MFI of the CD38 antibody and its isotype control for each child would be more appropriate but given the great number of samples to be processed for this study that would not be feasible. Additionally the suitability of CD38 as a marker of activation must be questioned. CD38 is constitutively expressed by naïve cells but not by memory cells therefore only when detected on a memory cell is it an accurate indicator of activation. Furthermore CD38 is downregulated independently by HIV (Savarino et al 2000).

Expression of CD69 by both the $CD45RA^+$ and $CD45RA^-$ $CD4^+$ T cell populations was extremely low, less than 1% on all populations therefore the ability of the CD69 antibody to bind was verified by demonstrating elevated CD69 expression in stimulated cells. CD69, as a very early marker is expressed at low levels, 0-5%, by T cells and rapidly but transiently induced upon activation (Cosulich et al. 1987), (Lanier et al. 1988), (Sancho, Gomez, & Sanchez-Madrid 2005). CD69 expression by unstimulated $CD4^+$ T cells has been reported in HIV-1 infected adults as less than 1%, and significantly lower than in healthy controls (Perfetto et al. 1997) but has also been reported as up to 42% (mean 15%) in HIV-1 infected children, and was not significantly different from healthy controls (Perfetto et al 1997), (Bohler et al. 1999).

Though the study group used here consisted of children, the range of CD69 expression levels were found to be closer to those reported by *Perfetto et al* among HIV-1 infected adults. Although as reported by *Böhler et al*, I too found no significant difference in CD69 expression between HIV infected children and un-infected adults amongst both the $CD45RA^+$ and $CD45RA^-$ sub-populations. I expected however, to detect higher levels because activation is believed to occur continually in HIV infection and high percentages of $CD69^+$ cells have been reported in other chronic inflammatory conditions such as rheumatoid arthritis and chronic inflammatory liver disease. However in both these conditions the presence of $CD69^+$ cells has been detected within the disease sites i.e. in synovial fluid and in the liver and not peripheral blood (Marzio, Mauel, & Betz-Corradin 1999). Apart from peripheral blood the disease sites for HIV include the gut, lymphoid tissue and the brain. Perhaps in these organs the percentage of $CD69^+$ cells is greater than in peripheral blood. Accordingly a population of dense $CD69^+$ monocytes has been described in patients with HIV associated dementia. This

population was found to be absent or present in much lower numbers in controls without dementia (Pulliam et al. 1997). As we detected a low percentage of $CD69^+$ cells which did not differ significantly between the $CD4^+$ T cell subsets and donor groups investigated we decided not to investigate CD69 expression in the cohorts described later in this thesis.

HLA-DR expression was greater amongst HIV-1 infected children than uninfected adults and greater by memory than naïve cells and additionally lacked the problems of CD69 and CD38 and therefore HLA-DR was used as an indicator of T cell activation for this study.

We used expression of Ki67, CD27 and HLA-DR to investigate the significance of CD31 expression by memory cells. We found only Ki67 expression to differ significantly between $CD31^+$ and $CD31^-$ memory cells. $CD31^+$ memory cells showed higher levels of Ki67 expression therefore they may require different or lower stimulus to proliferate than $CD31^-$ memory cells. The phenotype of this population is further explored in chapter four.

Lastly, the adaptation of a flow cytometric caspase detection assay (method in 2.2.4), designed for single cell populations in suspension, for use on $CD4^+$ T cells in whole blood was described. Initially the FLICA marker was binding non-specifically as confirmed by the camptothecin studies, which showed no difference in FLICA experience between cells cultured with camptothecin and those cultured without. The non-specific binding was successfully resolved by eliminating the use of a lysis buffer and using whole blood. Although to further confirm the specificity of the assay it could be confirmed to other methods of measuring apoptosis.

The methods developed and validated in this chapter have been demonstrated to be suitable for identifying $CD4^+$ T cells subsets and exploring the kinetic processes affecting those subsets, which is the focus of the next chapter of this thesis.

CHAPTER 4

$CD4^+$ T CELL KINETICS IN A COHORT OF HIV-1 INFECTED CHILDREN

4.1 INTRODUCTION

HIV-1 infection in children is associated with a gradual progressive decline in the number of $CD4^+$ T lymphocytes and as a consequence increased vulnerability to opportunistic infections. Effective treatment with a combination of three or more antiretroviral drugs, highly active anti-retroviral therapy (HAART), suppresses viral replication and the fall in plasma viraemia is accompanied by a concomitant increase in the number of $CD4^+$ T cells towards non-disease levels. However the sub-populations of $CD4^+$ T cells which contract during HIV-1 infection and the processes behind their decline are not fully understood in children.

4.1.1 $CD4^+$ T cell kinetics

The size of a cell population is maintained by a balance between input and output thus for the population to contract, input must decrease and/or output must increase. Therefore cell kinetics in this context refers to the collective changes affecting the $CD4^+$ T cell subsets, which together determine the size of the total $CD4^+$ T cell population.

The potential sources of input into the $CD4^+$ T cell pool are thymic output, homeostatic proliferation, activation driven differentiation of cells to a memory/effector phenotype and movement of cells out of the lymph nodes into the periphery. Whereas potential sources of output are death by apoptosis or necrosis, conversion of cells to a memory/effector phenotype and movement of cells from the periphery into lymphoid tissue. These processes may also operate to differing degrees during HAART to restore the $CD4^+$ T cell population.

4.1.2 Effect of HAART on $CD4^+$ T cell kinetics

The administration of HAART is associated with many effects, including an increase in CD4 count, that are unlikely to be solely due to decreased viral replications. HAART has also been associated in HIV infected children with an increase in TREC count (Persaud et al 2000), (de Rossi A. et al 2002) and a decrease in activated CD4 cells

($CD4^+HLA\text{-}DR^+$, $CD4^+HLA\text{-}DR^+CD38^+$ and $CD4^+CD45RO^+HLA\text{-}DR^+$) (Resino et al. 2005), (Rosenblatt et al 2005)

The mechanisms behind the increase in CD4 count are not wholly understood. HAART may indirectly reverse the factors associated with CD4 depletion discussed in 1.4.4. Decreasing CD4 depletion through apoptosis may be one of the mechanisms. T cell apoptosis was shown to decrease after treatment with protease inhibitors (Weichold et al. 1999). Using an RNA protection assay, where single stranded RNA is protected from RNase degradation by hybridisation to RNA probes for apoptosis related genes, Balestrieri et al found that after 12 months of successful HAART, expression of several pro-apoptotic genes including *Fas* and *Caspase 8* were downregulated (Balestrieri et al. 2007).

Decreased rates of CD4 loss are unlikely to entirely account for the increased CD4 count. HAART may also increase CD4 output. *In vivo* labelling techniques in monkeys infected with SIV and humans infected with HIV have been undertaken in an attempt to determine the source. In one study where bromo deoxy uridine (BrdU) was infused into rhesus macaque monkeys a rapid decrease in the proportion of labelled $CD4^+$ T cells occurred. From this it was deduced that labelled cells die faster than they divide. As this was occurring in a steady state there would have to be another source of incoming cells into the population. This could potentially be the thymic output or proliferation within the population. The same study found similar results in HIV infected individuals receiving anti-retroviral therapy (Mohri et al. 2001). This would suggest that HAART is associated with increased input to the CD4 pool either by increased rates of thymic output or increased rates of proliferation or both.

4.1.3 Proliferation as a mechanism of input

Inducing lymphopenia in mouse models results in a peripheral T cell expansion called homeostatic proliferation (Haynes et al 2000) and in the human newborn 50% of daily T

cell generation is due to peripheral T cell expansion (Haynes et al 2000) therefore it would be reasonable to expect proliferation to play a major part in HIV infection and reconstitution on HAART. The proliferation may be induced by lymphopenia or by activation.

Ki67 is a cell cycle protein expressed in the nucleus in cells in G_1, S and G_2 phase. How long Ki67 expression remains after mitosis is not clear but Ki67 expression is usually confined to cycling cells. In healthy adult controls, expression of Ki67 by $CD45RO^-$ $CD27^{high}$ (naïve) cells decreases and therefore cell proliferation has been shown to decrease with increasing age (Douek et al. 2001). In the same study the opposite, i.e. an increase in Ki67 expression, was shown for $CD45RO^+$ (memory) cells. They also showed a 5.9 times greater percentage of $Ki67^+$ memory cells in HIV infected compared to control adults. In the naïve pool proliferation was similar for both uninfected and infected adults, less than 1% of the cells. A different study by Di Mascio *et al* measuring Ki67 expression on $CD45RA^+$ cells showed decreased naïve cell proliferation 18 months after HAART was initiated in 20 adults (Di Mascio et al. 2006). Decreased proliferation by naïve cells may slow recruitment of naïve cells into the memory pool.

4.1.4 Thymic output

Thymic output, especially in children in whom thymic involution has not yet occurred, may be a significant factor in the increased concentration of circulating CD4 T cells seen in HAART. IL-7, a likely regulator of thymic output, has been shown to take part in the differentiation of thymocytes and has been associated with CD4 T cell recovery in children (Correa, Resino, & Munoz-Fernandez 2003).

4.1.4.1 Investigating thymic output by T cell receptor excision content

Thymic output was initially estimated by quantifying the number of T cell receptor excision circles (TRECs) in naïve cells. Studies have shown that TREC counts in HIV infected people declined faster with increasing age than in uninfected adults thus

suggesting thymic output is decreased in HIV. Doubts, however, about the suitability of using TRECs as a measure of thymic output emerged when Hazenberg *et al* demonstrated that in addition to decreasing thymic output a fall in TREC count could also be explained by increased proliferation within the naïve pool which would dilute the TREC count (Hazenberg et al 2000). However a decrease in TRECs occurring in the absence of an increase in naïve cell proliferation would indicate a decrease in thymic output as has been demonstrated in HIV infected adults (Douek et al 2001). In children, however, HAART has been associated in HIV infected children with an increase in TREC count (Persaud et al 2000), (de Rossi A. et al 2002). Increased TREC counts have also been associated with slower disease progression in pathogenic SIV infection (Ho Tsong et al. 2005).

4.1.4.2 Investigating thymic output by CD31 expression

A study carried out by Kimmig *et al* (Kimmig et al 2002) identified two populations of $CD45RA^+$ $CD4^+$ T cells with disparate TREC content. The TREC were highly enriched in the $CD31^+$ population and barely present in the $CD31^-$ population. They also showed a decrease of $CD45RA^+CD31^+$ cells with increasing age. In addition the low production of effector cytokines in $CD45RA^+CD31^+$ cells indicates the suitability of using co-expression of CD31 and CD45RA as a marker of recent thymic emigrants (RTEs).

Kimmig *et al.* put forward a model of naïve $CD4^+$ T cell homeostasis predicated from an *in vitro* study that showed loss of CD31 after TCR triggering. They suggested that naïve cells can be divided into two groups: RTEs that express CD31 and central naïve cells that do not express CD31. In this model, activation of either of these groups within the periphery by foreign antigen leads to their differentiation into $CD45RO^+$ (memory) $CD4^+$ T cells. Whereas when presented with self antigen, RTEs undergo homeostatic proliferation, lose CD31 expression and differentiate into central naïve cells. Unfortunately this work is concerned with naïve cells and does not report on the significance of CD31 expression by $CD45RO^+$ memory cells.

In 2007 Junge *et al* published a study endorsing the results of the initial Kimmig study and additionally showed that telomere length was longest in $CD31^{+}CD45RO^{-}$, then $CD31^{-}CD45\ RO^{-}$, $CD31^{+}CD45RO^{+}$ and least in $CD31^{-}CD45RO^{+}$. They also showed telomerase activity was much higher in $CD31^{+}CD45RO^{-}$ than $CD31^{-}CD45\ RO^{-}$ cells (Junge et al 2007).

A study by Bofill *et al.* used $CD45RA^{+}CD31^{+}$ expression to investigate increased thymic output in $CD4^{+}$ T cell recovery on HAART. They found a non-significant association between increased proportion of $CD45RA^{+}CD31^{+}$ cells and improved $CD4^{+}$ T cell count (Bofill et al. 2006). The study population, however, were adults. In children co-expression of CD45RA and CD31 by $CD4^{+}$ T cells has not been yet been used to investigate increased thymic output as a source of new cells in immune reconstitution.

Only one study has measured $CD45RA^{+}CD31^{+}$ cells in HIV-1 infected children. The study found that children who had been on HAART for over 4 years had comparable proportions of $CD45RA^{+}CD31^{+}$ cells to age matched controls (Vrisekoop et al. 2008). There are no studies known that have followed changes in the $CD45RA^{+}CD31^{+}$ cell population before and upon starting HAART.

The aim of this chapter was to utilise the immunophenotyping methodology developed in chapter 3 to study, within the $CD4^{+}$ T cell sub-populations of a cohort of HIV-1 infected children, some of the processes that may govern the contraction and expansion of the CD4 pool during progressive HIV infection and during the response to HAART, respectively.

4.2 RESULTS

4.2.1 Sample characteristics

The expression of various markers such as CD45RA, CD45RO, CD27, CD31 and CD62L have been used previously to describe $CD4^+$ T cells with differing phenotype and function. To investigate $CD4^+$ T cell subset dynamics in paediatric HIV-1 infection, blood samples from 58 children with vertically acquired HIV-1 infection were incubated with antibodies against CD4, CD45RA and CD31 such that $CD4^+$ T cells could be identified by flow cytometry and divided into subsets defined by expression of CD31 and CD45RA. The characteristics of the cohort are displayed (Table 4.1).

Sample Characteristic	Distribution
Number female	31 (53.4%)
Median age in years	10.5 (7.9-13.0)
Number ART naïve	10 (17.2%)
Number of ART at time of sampling	27 (46.6%)
Median CD4 count	516.5 (352.5-775.5)
Median CD4 % (as % of total lymphocytes)	24 (18.3-32.8)
Median viral load (log RNA copies/ml plasma)*	3.2 (1.7-4.1)

Table 4.1 Patient characteristics at time of sampling

Forty-five children with vertically acquired HIV-1 infection and varying ART experience were recruited to the study. The characteristics of the population, median and IQR in brackets, at the time of sampling are displayed. * Undetectable viral loads were assumed to be 50 copies/ml, which is the limit of detection, for purposes of calculating the median and IQR.

4.2.2 Aging is associated with changes to the distribution of $CD4^+$ T cell subsets

Aging is a normal process, which in healthy children is associated with changes to the size and distribution of lymphocyte populations, however less is known about the effect of age on CD45RA and CD31 defined $CD4^+$ T lymphocytes in HIV infected children therefore in this study the children's ages were compared to the size of the CD4 pool and the distribution of $CD4^+$ T cell subsets.

As has been described in healthy children, the CD4 count was negatively correlated with age, decreasing with advancing age (Figure 4.1). Additionally aging was found to be negatively correlated with the percentages of $CD45RA^+$ and $CD45RA^+CD31^+$ cells, positively correlated with the percentages of $CD45RA^-$ and $CD45RA^-CD31^-$ cells but not associated with the percentages of $CD45RA^+CD31^-$ and $CD45RA^-CD31^+$ cells (Figure 4.2). The proportion of $CD45RA^+CD31^-$ cells were found to be relatively low, compared to the other subsets, in all the children tested whereas a wider variation in the proportion of $CD45RA^-CD31^+$ cells was observed in children of different ages.

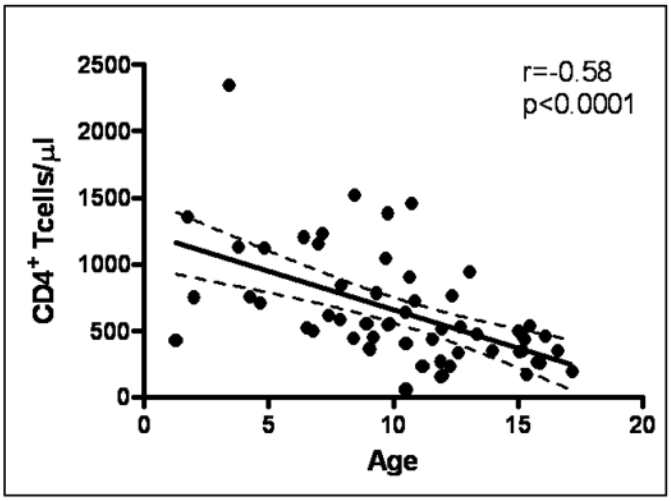

Figure 4.1 Association between age and CD4 count

The CD4 count for each child (n=58) was provided by GOSH diagnostic laboratories and was plotted against the child's age. The strength of the correlation between the age and CD4 count was determined by Spearman's rank coefficient (r). The statistical significance (p) is shown. The solid and broken lines represent lines of regression and 95% confidence interval, respectively.

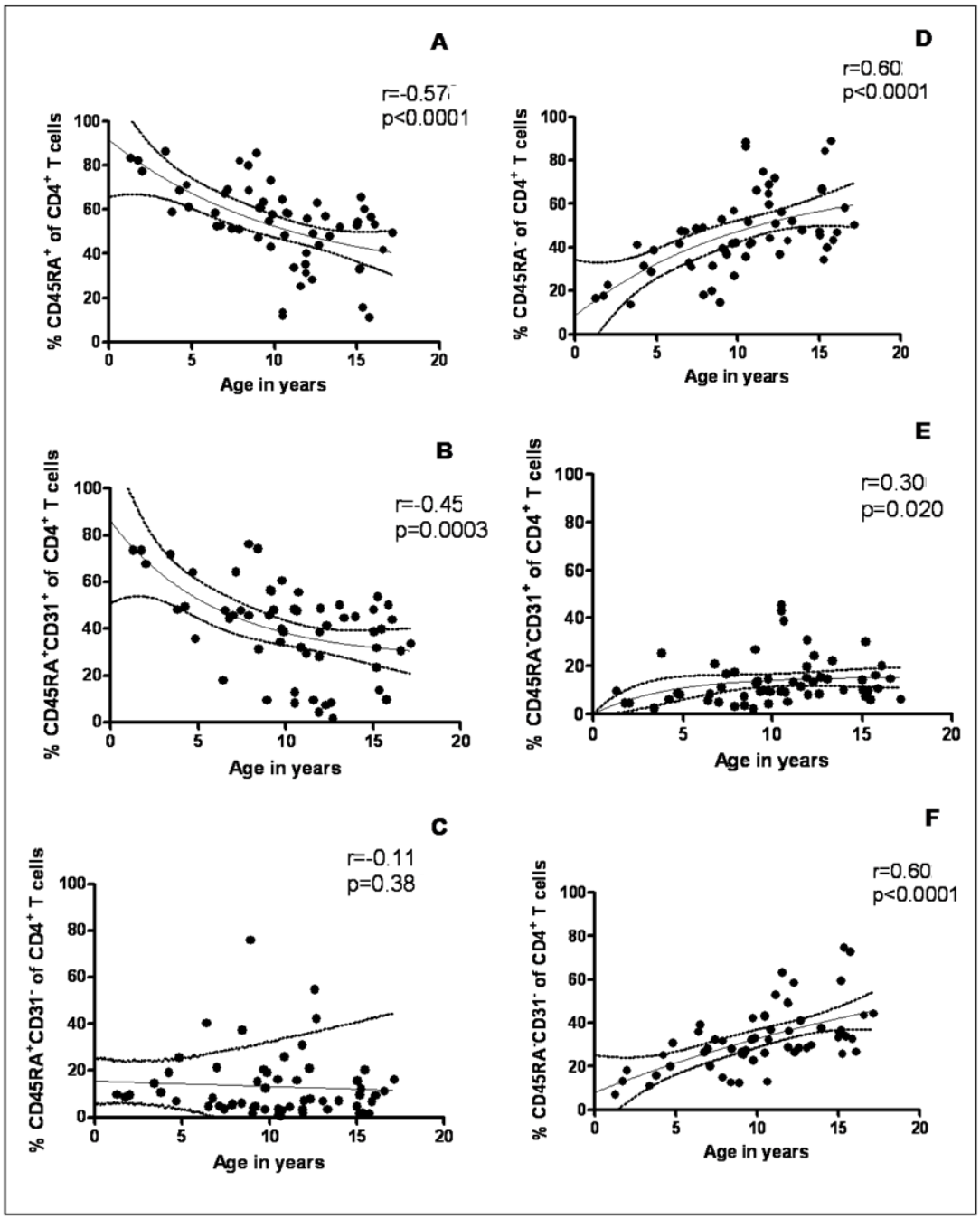

Figure 4.2 Relationship between Age and CD4 Subset distribution

Peripheral blood samples from 46 HIV-1 infected children were incubated with antibodies against human CD4, CD45RA and CD31 and their expressions analysed by flow cytometry. The percentage of $CD4^+$ T cell subsets for each child were plotted against their age. The strength of the correlations were determined by Spearman's rank coefficient (r). The statistical significance (p) is shown. The solid and broken lines represent lines of regression and 95% confidence intervals, respectively.

4.2.3 Patients with detectable viraemia and patients with undetectable viraemia have different CD4 counts and CD4 subset distributions

Although chronic HIV infection is associated with a progressive gradual decline of $CD4^+$ T cells and a concomitant increase in viral load studies have failed to show an association between viral load and CD4 count (Luzuriaga and Sullivan 1998) and none have determined which $CD4^+$ T cell subsets decrease as viral load increases. Viral loads cannot be routinely quantified below 50 copies/ml plasma however detectable plasma viraemia is indicative of unsuppressed viral replication, therefore the children were divided into two groups, those with detectable viraemia (≥50 copies/ml plasma) at time of sampling and those with undetectable viraemia at the time of sampling (<50 copies/ml plasma).Then the $CD4^+$ T cell count and subset distribution were compared between the two groups (Figure 4.3).

The group with detectable viraemia had a lower $CD4^+$ T cell count and lower concentrations of the $CD4^+$ T cell subsets; $CD45RA^-CD31^+$, $CD45RA^-CD31^-$, $CD45RA^-$ and especially $CD45RA^+$ cells. Interestingly, there was no difference in the concentration of RTEs therefore even though CD4 count is significantly lower in the detectable viraemia group, the concentration of RTEs is unchanged, suggesting ongoing thymic output is an important contribution. The detectable viraemia group had a significantly higher mean age and increasing age is well known to be associated with decreasing CD4 count. Therefore the percentage of $CD4^+$ T cells, which is more constant with age, was tested and this too was found to be significantly lower in the group with detectable viraemia. Interestingly, there was no difference between the percentages of $CD4^+$ T cell subsets between the undetectable and detectable viraemia groups.

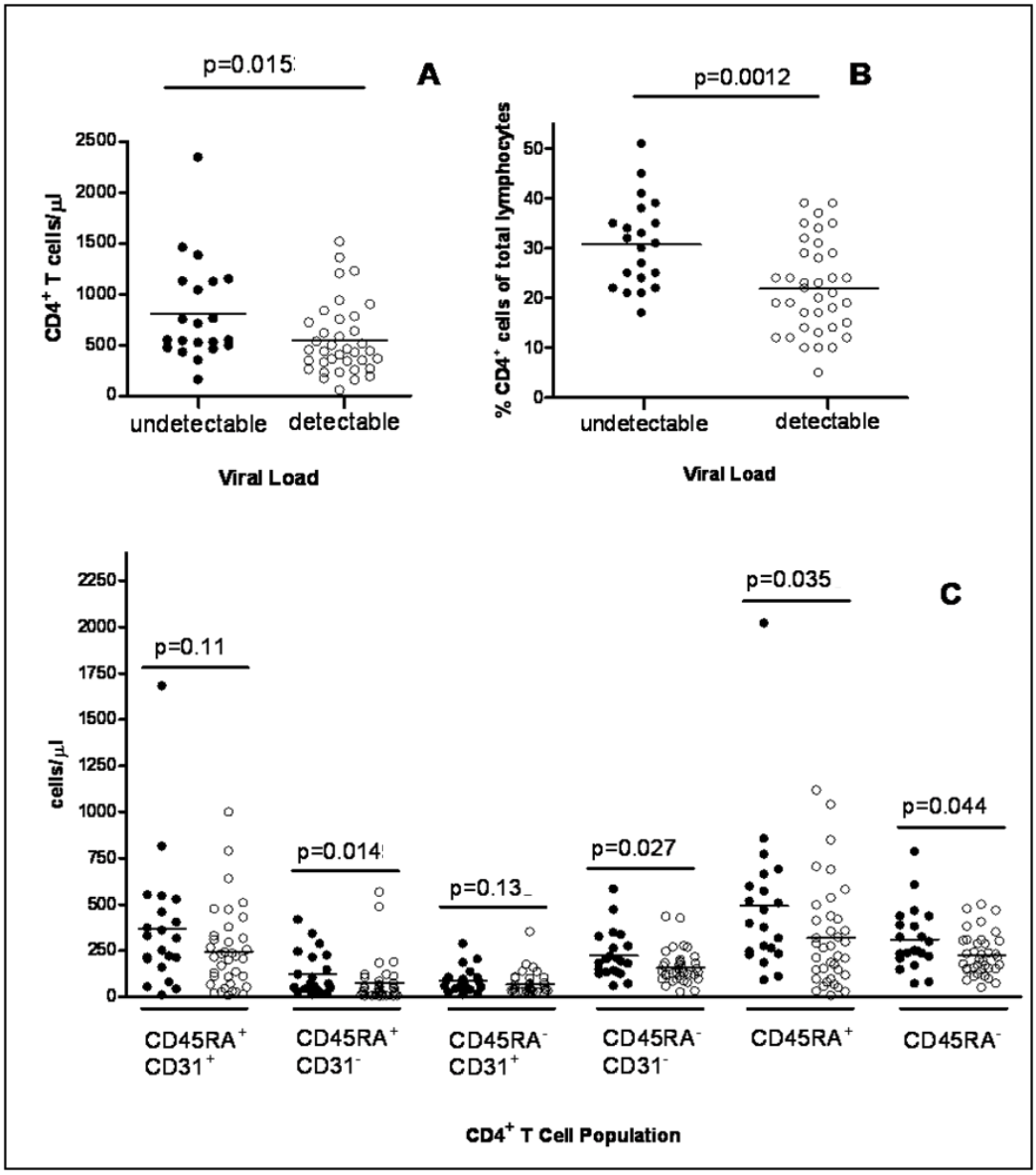

Figure 4.3. Comparison of the $CD4^+$ T cell population and CD4 Subsets in children with detectable versus undetectable viral load.

The children were divided into those with undetectable viral loads (<50 copies/ml of plasma), n=21 and those with detectable viral loads, n=37. Black circles and white circles represent children with undetectable and detectable viral loads respectively. The $CD4^+$ T cell count, percentage of $CD4^+$ T cells and the concentration of the $CD4^+$ T cell sub-populations were compared between the two groups in A, B and C respectively. For each variable shown the difference between the children with undetectable viral load and those with detectable viral load was tested for statistical significance by the Mann Whitney test.

Viral replication is thought to produce the non-specific generalised immune activation seen in HIV infection, although indirectly via CD4 cell depletion from the gut which damages the mucosal barrier allowing bacterial translocation as discussed in section 1.4 but studies have not shown an association between viral load and $CD4^+$ T cell activation and proliferation therefore children with undetectable versus detectable viraemia were compared for differences in $CD4^+$ T cell activation and proliferation as determined by HLA-DR and Ki67 expression respectively (Figure 4.4).

Children with detectable viral load had greater Ki67 expression in the total $CD4^+$ T cell population and within the $CD45RA^-$ subset compared to children with undetectable viraemia. There was however, no difference in Ki67 expression by $CD45RA^+$ cells between the groups. Surprisingly HLA-DR expression by the total $CD4^+$ T cells did not differ between the two viraemia groups but when the $CD4^+$ T cells were subdivided by CD45RA expression HLA-DR expression by both the $CD45RA^+$ and the $CD45RA^-$cells was found to be significantly higher in the group of children with a detectable viral load at time of sampling.

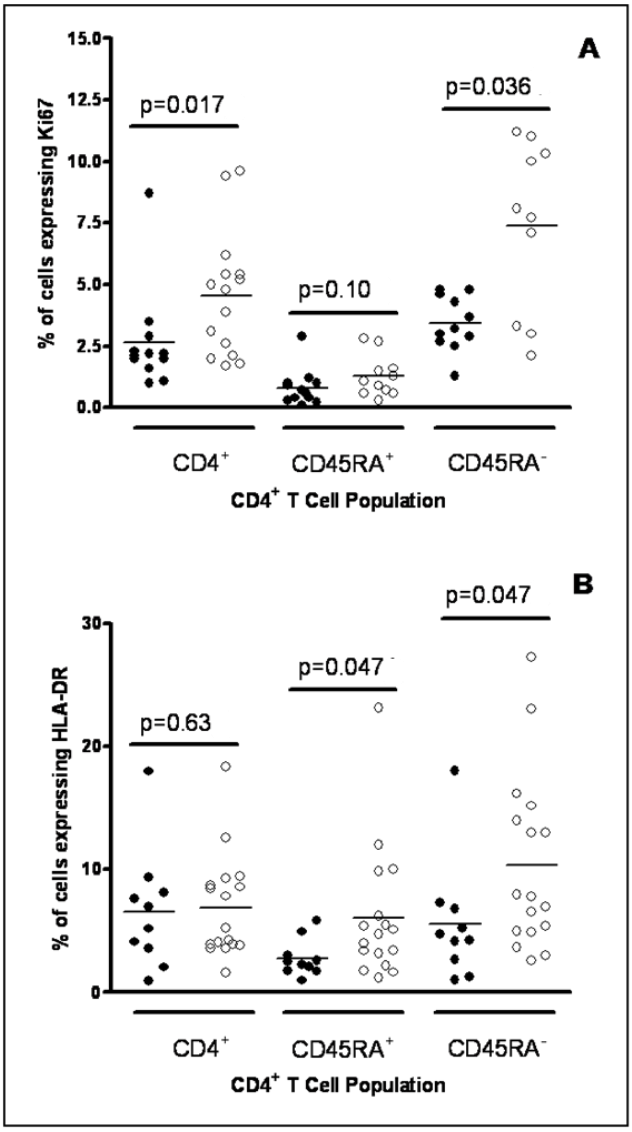

Figure 4.4 Comparison of Ki67 and HLA-DR expression in children with detectable versus undetectable viral load

The children were divided into those with undetectable viral loads (<50 copies/ml of plasma), n=19 and those with detectable viral loads, n=27. Black circles and white circles represent children with undetectable and detectable viral loads respectively. Ki67 and HLA-DR expression by the total $CD4^+$ T cell pool and $CD4^+$ T cell sub-populations were compared between the two groups. For each variable shown the difference between the children with undetectable viral load and those with detectable viral load was tested for statistical significance by the Mann Whitney test.

4.2.4 Levels of Ki67 and HLA-DR expression differ between naïve and memory cells

Proliferation and activation are two processes known to control the size and equilibrium between lymphocyte populations and there is interaction between the two processes; as discussed in section 1.2.5. T cell proliferation can occur in response to activation as well in response to lymphopenia. Therefore to characterise the effect of these processes on $CD4^+$ T cell subsets and their interaction with each other two markers of lymphocyte proliferation and activation, Ki67 and HLA-DR respectively, were used in conjunction. Additional samples were taken from the children and co-incubated with either antibodies against CD4, CD45RA, CD31 and Ki67 or antibodies against CD4, CD45RA, CD31 and HLA-DR.

As was mentioned in chapter one, the memory population is more activated and proliferating than the naïve population, which was also confirmed in section 3.3.7 and 3.3.8 where a greater proportion of memory cells where shown to express HLA-DR and Ki67 compared to naïve cells. However it is not known how CD31 defined naïve and memory subsets compare to each other. Therefore HLA-DR and Ki67 expression was investigated in 28 HIV-1 infected children but only Ki67 expression was found to differ significantly between the sub-populations (Figure 4.5). $CD45RA^+CD31^+$ had the lowest Ki67 expression, followed by $CD45RA^-CD31^+$ then $CD45RA^-CD31^-$ and finally $CD45RA^+CD31^-$.

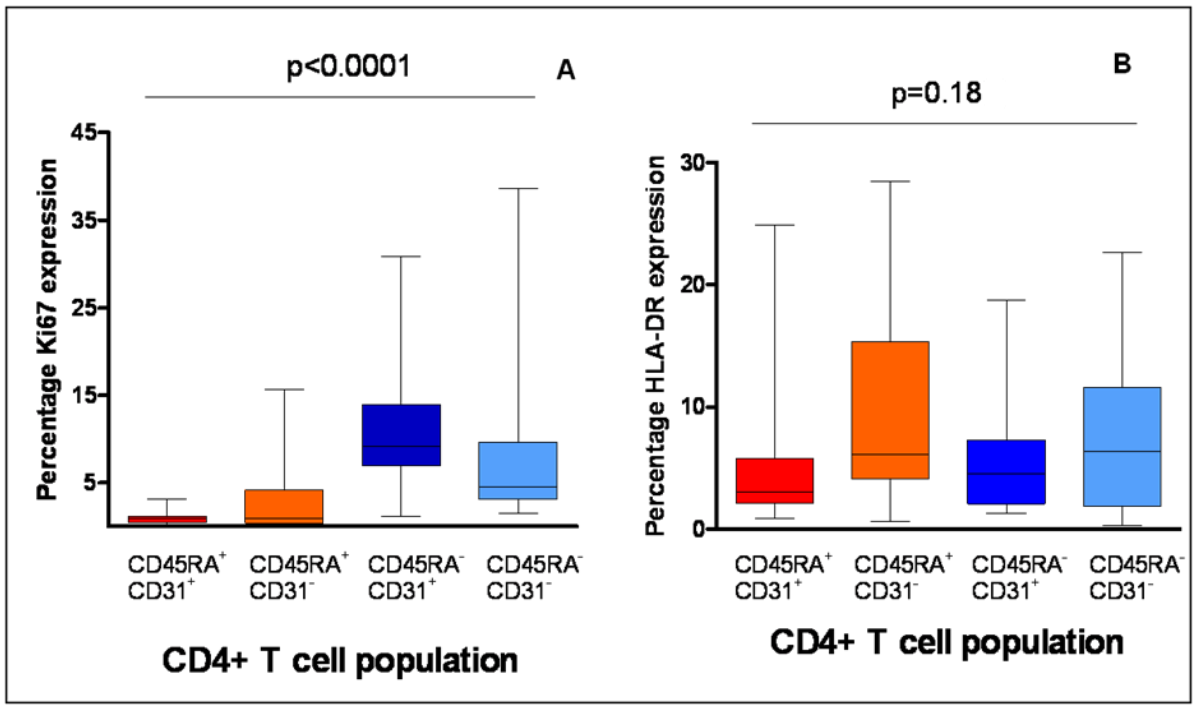

Figure 4.5 Characteristics of CD4 subsets

The box whisker graphs show HLA-DR and Ki67expression in $CD4^+$ T cell sub-populations (n=28). The Ki67 and HLA-DR expression are compared in CD45RA and CD31 delineated $CD4^+$ T cell sub-populations in (A). and (B) respectively The differences between the populations were tested by Kruskall-Wallis.

As discussed in section 1.4 it has been shown that $CD4^+$ T cell activation correlates with CD4 count and progression in adults with HIV-1 infection therefore activation as determined by HLA-DR expression was investigated in the children described here as well as proliferation, which can also affect the size of $CD4^+$ T cell pool (Figure 4.6). There was no significant association between HLA-DR expression and either the CD4 count or the percentage of $CD4^+$ T cells. However the level of Ki67 did correlate with both the CD4 count and the percentage of $CD4^+$ T cells.

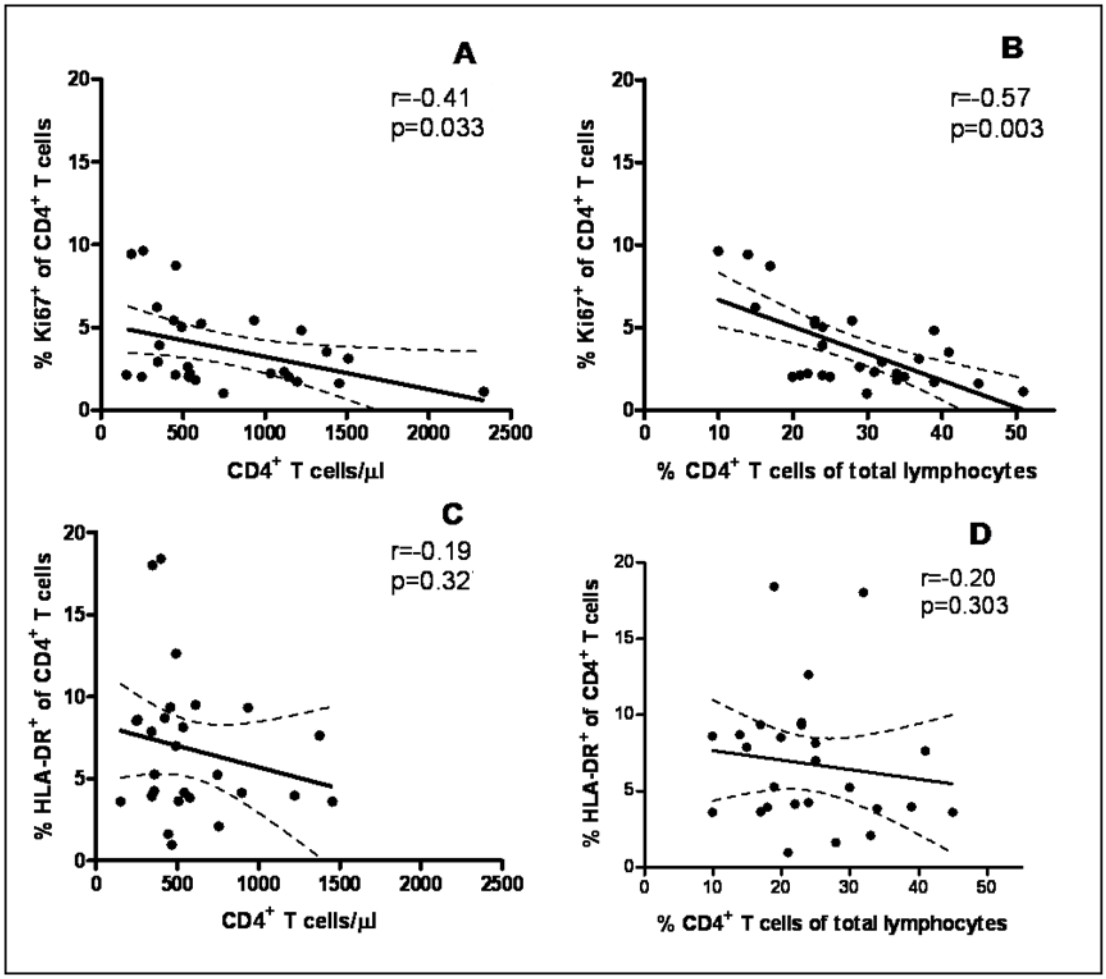

Figure 4.6 Association between the size of the $CD4^+$ T cell population and Ki67 and HLA-DR
Blood samples from 28 children were incubated with antibodies against CD4 and either Ki67 or HLA-DR and the CD4 count and percentage of $CD4^+$ T cells were plotted against the level of Ki67 and HLA-DR expression. An association between CD4 count and percentage of $CD4^+$ T cells and Ki67 and HLA-DR expression was tested by Spearman's rank. The Spearman's rank correlation coefficients, r, and p values are shown. The solid and broken lines represent lines of regression and 95% confidence intervals, respectively.

Activation does not always result in proliferation and proliferation can occur in the absence of activation i.e. lymphopenia induced proliferation versus activation driven proliferation therefore to investigate what proportion of activated cells proliferate and what proportion of proliferating cells are activated in children with HIV blood samples were incubated with antibodies against CD4, CD45RA, HLA-DR and Ki67. $CD45RA^-$ $HLA\text{-}DR^+$ cells were found to express significantly greater levels of Ki67 than

$CD45RA^{+}HLA\text{-}DR^{+}$ cells but there was no significant difference between the level of HLA-DR expression by $CD45RA^{-}Ki67^{+}$ and $CD45RA^{+}Ki67^{+}$cells (Figure 4.7). Almost 50% of $CD45RA^{-}Ki67^{+}$ and $CD45RA^{+}Ki67^{+}$ cells also express HLA-DR.

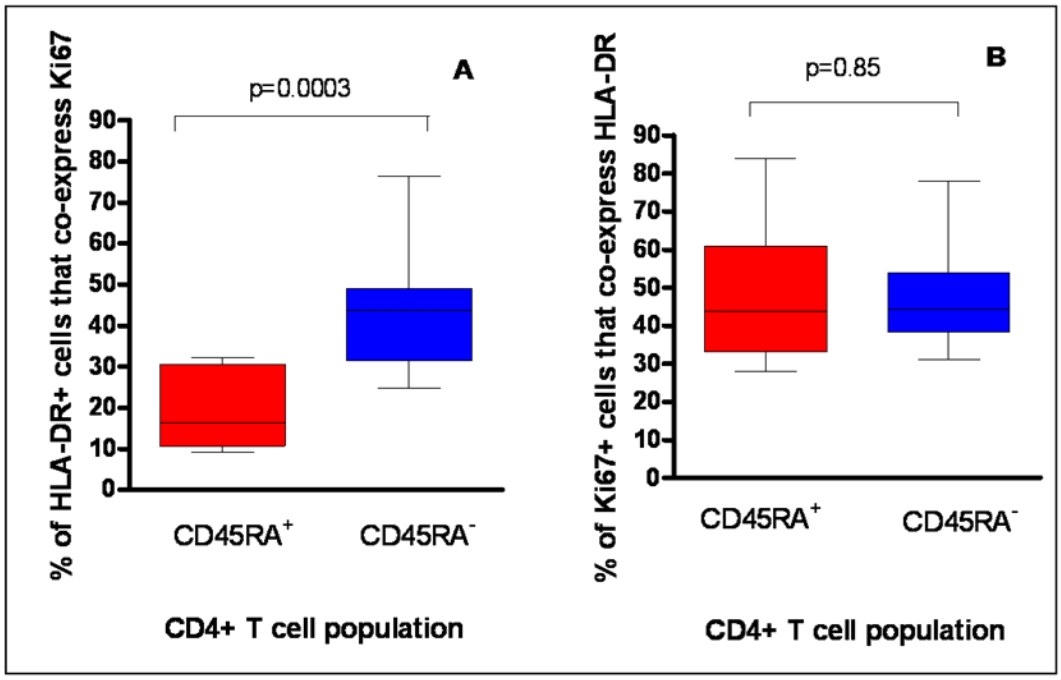

Figure 4.7 Co-expression by HLA-DR and Ki67 by CD4 subsets

In a subset of patients (n=16) peripheral blood samples were co-stained with both anti-HLA-DR and anti-Ki67 antibodies in addition to anti CD4 and anti CD45RA. The level of Ki67 expression was determined and compared for $HLA\text{-}DR^{+}$ $CD45RA^{+}$ versus $HLA\text{-}DR^{+}$ $CD45RA^{-}$ $CD4^{+}$ T cells (A) The level of HLA-DR expression was determined and compared for $Ki67^{+}$ $CD45RA^{+}$ versus $Ki67^{+}$ $CD45RA^{-}$ $CD4^{+}$ T cells (B) The difference between the medians of the populations was tested by Mann-Witney test.

4.2.5 FLICA expression in $CD4^{+}$ T cells

Gougeon and colleagues demonstrated that lymphocytes from HIV infected individuals are more susceptible to spontaneous apoptosis compared to healthy controls and that this susceptibility correlates to the level of activation, determined by HLA-DR and CD38 expression . In their studies apoptotic cells were identified by propidium iodide (P.I.) and 7-amino-actinomycin D (7-AAD) staining and CD4 subpopulations were not

investigated (Gougeon et al 1996). In this present study apoptosis was identified by fluorescent-labelled inhibitor of caspases (FLICA) staining, as described in chapter 2 and was investigated in $CD45RA^+$ and $CD45RA^-$ $CD4^+$ T cells.

Gougeon *et al* reported that apoptosis is low in freshly isolated PBMCs from HIV-1 infected individuals, less than 5%, and is not different from healthy controls (Gougeon et al 1996) therefore initially FLICA staining in $CD45RA^+$ and $CD45RA^-$ $CD4^+$ T cells in freshly drawn whole blood from six children was investigated. FLICA expression by $CD4^+$ T cells was very low, mean of 1.7%, and there was no difference between FLICA expression by $CD45RA^+$ and $CD45RA^-$ $CD4^+$ T cells (Figure 4.8).

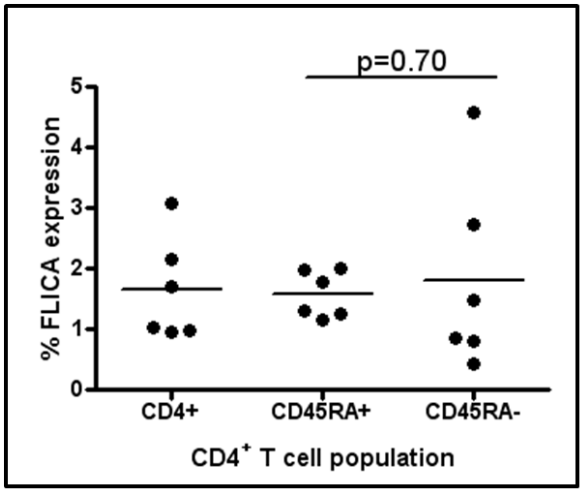

Figure 4.8 FLICA expression by $CD4^+$ T cell sub-populations in freshly drawn whole blood
Freshly drawn whole blood from n=6 children was incubated with antibodies against CD4 and CD45RA and the FLICA reagent. The FLICA expression was determined in the total $CD4^+$ T cell population and in the $CD45RA^+$ and $CD45RA^-$ $CD4^+$ T cell sub-populations. Horizontal lines indicate the mean FLICA expression for each cell population. The difference between FLICA expression by the $CD4^+$ sub-populations was tested for significance by the Mann-Witney test.

As there is little apoptosis present in freshly drawn blood, whole blood from 24 children was incubated at room temperature for 24 hours and then stained with FLICA and anti-CD4 and CD45RA antibodies to determine which subpopulation would be more

susceptible to apoptosis. After 24 hours there was greater FLICA expression and it was significantly higher in the $CD45RA^-$ than in the $CD45RA^+$ $CD4^+$ T cell population (Figure 4.9).

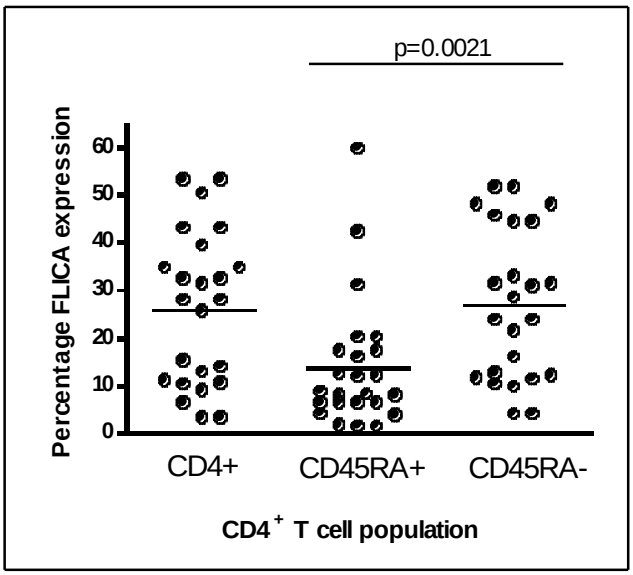

Figure 4.9. FLICA expression by $CD4^+$ T cell sub-populations in whole blood after 24 hours
Freshly drawn whole blood from n=24 children was incubated at room temperature for 24 hours and then with antibodies against CD4 and CD45RA and the FLICA reagent. The FLICA expression was determined in the total $CD4^+$ T cell population and in the $CD45RA^+$ and $CD45RA^-$ $CD4^+$ T cell sub-populations. Horizontal lines indicate the mean FLICA expression for each cell population. The difference between FLICA expression by the $CD4^+$ sub-populations was tested for significance by the Mann-Witney test.

Activated cells are more susceptible to apoptosis (Groux et al 1992), (Meyaard et al 1992), (Estaquier et al 1995) therefore to investigate whether apoptotic cells displayed an activated phenotype whole blood from 24 children was incubated over 24 hours at room temperature and then stained with FLICA and antibodies against CD4, CD45RA and HLA-DR. Over 60% of $FLICA^+$ cells also co-express HLA-DR, and the HLA-DR expression of $CD45RA^-$ $FLICA^+$ cells is significantly higher than the HLA-DR expression of $CD45RA^+FLICA^+$ $CD4^+$ T cells (Figure 4.10). By contrast, when peripheral blood from 3 subjects was stained for FLICA and then stained for Ki67 to

investigate the association of apoptosis and proliferation in $CD4^+$ T cells, only 6.7% of $FLICA^+$ cells were found to express Ki67 (data not shown).

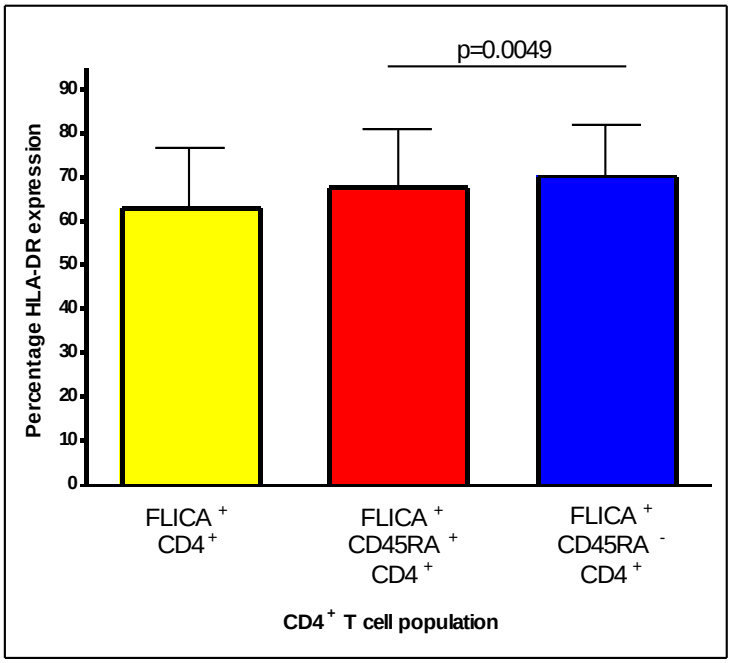

Figure 4.10 HLA-DR expression by FLICA positive cells

Freshly drawn whole blood from n=24 children was incubated at room temperature for 24 hours and then with antibodies against CD4, CD45RA, HLA-DR and the FLICA reagent. The level of FLICA expression by FLICA positive cells was determined by flow cytometry. The mean HLA-DR expression and 95% C.I. for each population of FLICA positive cells is displayed. The difference between the HLA-DR expression by the FLICA positive $CD45RA^+$ and FLICA positive $CD45RA^-$ $CD4^+$ T cells was tested for significance using the Mann-Witney test.

4.2.6 The absolute $CD4^+$ T cell count is associated with the distribution of $CD4^+$ T cell subsets and Ki67 expression

CD4 count is used extensively as a prognostic indicator in the management of HIV infection, where an increase is usually associated with improvement of the clinical picture and a decrease with deterioration. Therefore the CD4 count was compared to the size of each $CD4^+$ T cell subsets (Figure 4.11) to see how the distribution of subsets was affected by changes in the CD4 count. The CD4 count was positively correlated with the

percentage of $CD45RA^{+}CD31^{+}$ cells, though the rate of change was not fixed. When the CD4 count was high, above 600 $CD4^{+}$ T cells/µl, a large change corresponded to a small change in the percentage of $CD45RA^{+}CD31^{+}$ cells. When the CD4 count was lower, below 600 $CD4^{+}$ T cells/µl, a small decrease was associated with a large fall in the percentage of $CD45RA^{+}CD31^{+}$ cells. This is illustrated in Figure 4.11A where children with a higher CD4 count (greater than 600 $CD4^{+}$ T cells/µl) have over 30% of their $CD4^{+}$ T cells in the $CD45RA^{+}CD31^{+}$ sub-population (green box, Figure 4.11A) though for children with a low CD4 count (less than 600 $CD4^{+}$ T cells/µl) one group of children have greater than 30% $CD45RA^{+}CD31^{+}$ (blue box, Figure 4.11A) and the other group less than 30% (red box, Figure 4.11A). There was no correlation between CD4 count and percentage of $CD45RA^{-}CD31^{+}$ cells but the percentage of $CD45RA^{+}$ cells was positively correlated with CD4 count. The CD4 count was negatively correlated with the percentage of $CD45RA^{-}$ $CD31^{+}$, $CD45RA^{-}CD31^{-}$ and $CD45RA^{-}$ sub-populations.

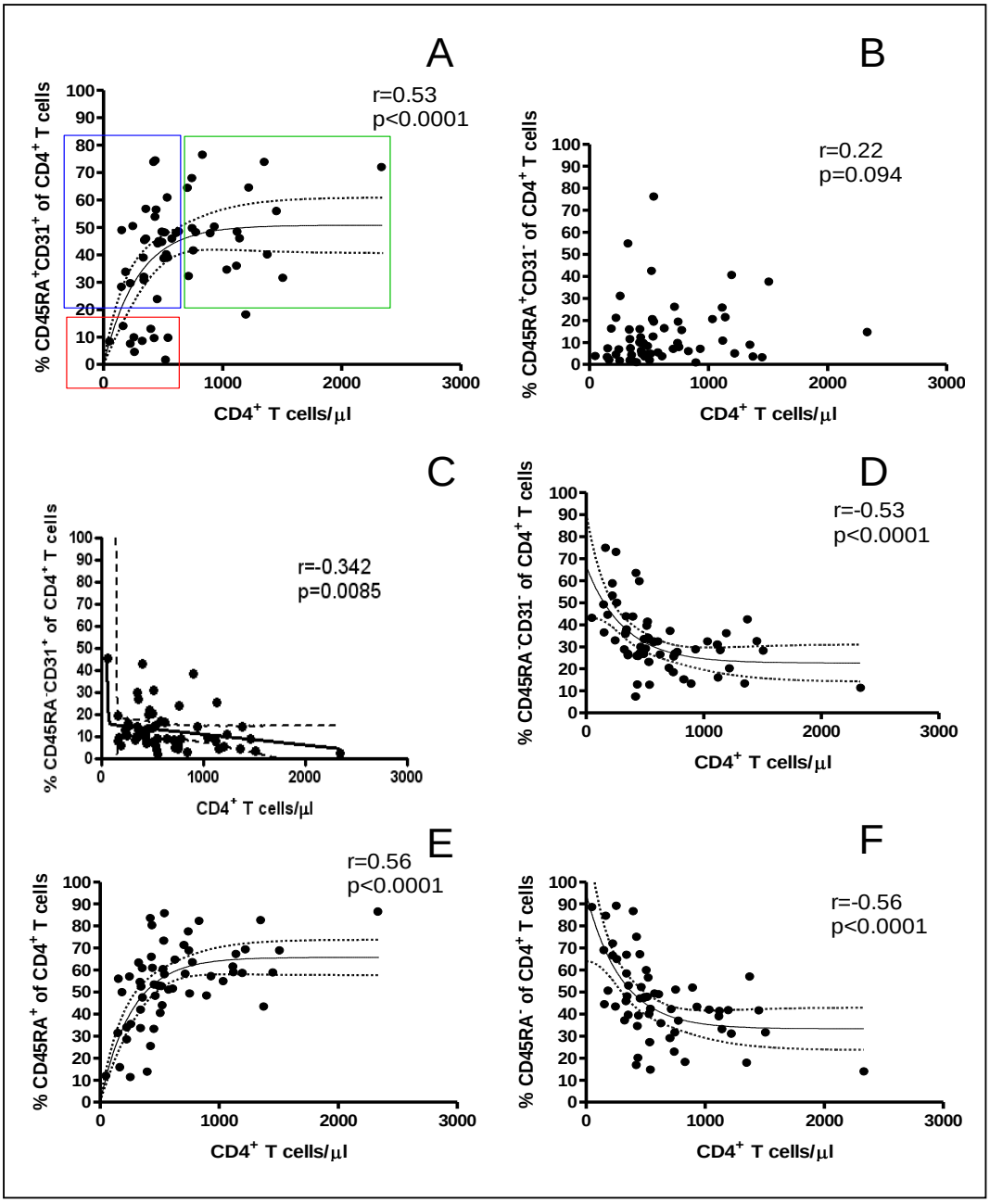

Figure 4.11. Relationship between CD4 count and CD4 Subset distribution.

$CD4^+$ T cell immunophenotyping was performed on 58 children by incubating blood with antibodies against CD4, CD45RA and CD31. The CD4 counts at time of sampling for each child were provided by GOSH diagnostics labs and plotted against the percentage of the $CD4^+$ T cell sub-populations. The strength of the correlations between the CD4 count and the proportion of each sub-population was determined by Spearman's rank. The coefficient (r) is shown with corresponding p values. The solid and broken lines represent lines of regression and 95% confidence intervals, respectively.

As mentioned previously cellular proliferation and viral replication can affect the size of the $CD4^+$ T cell pool. Figure 4.6 showed a negative correlation was found between the CD4 count and the level of Ki67 expressed by $CD4^+$ T cells but did not investigate the association between the CD4 count and level of Ki67 expressed by the $CD45RA^+$ and $CD45RA^-$ $CD4^+$ T cells. Therefore to investigate if the changes in the total CD4 count are associated with changes in the proliferation of $CD4^+$ T cell sub-populations and viral replication the CD4 count for each child was compared to the viral load and the level of proliferation in the $CD4^+$ T cell sub-populations (Figure 4.12). The CD4 count was negatively correlated with the percentage Ki67 expression of $CD45RA^-$ $CD4^+$ T cells but there was no association with the percentage Ki67 expression of $CD45RA^+$ $CD4^+$ T cells. A negative correlation was also established between the CD4 count and viral load.

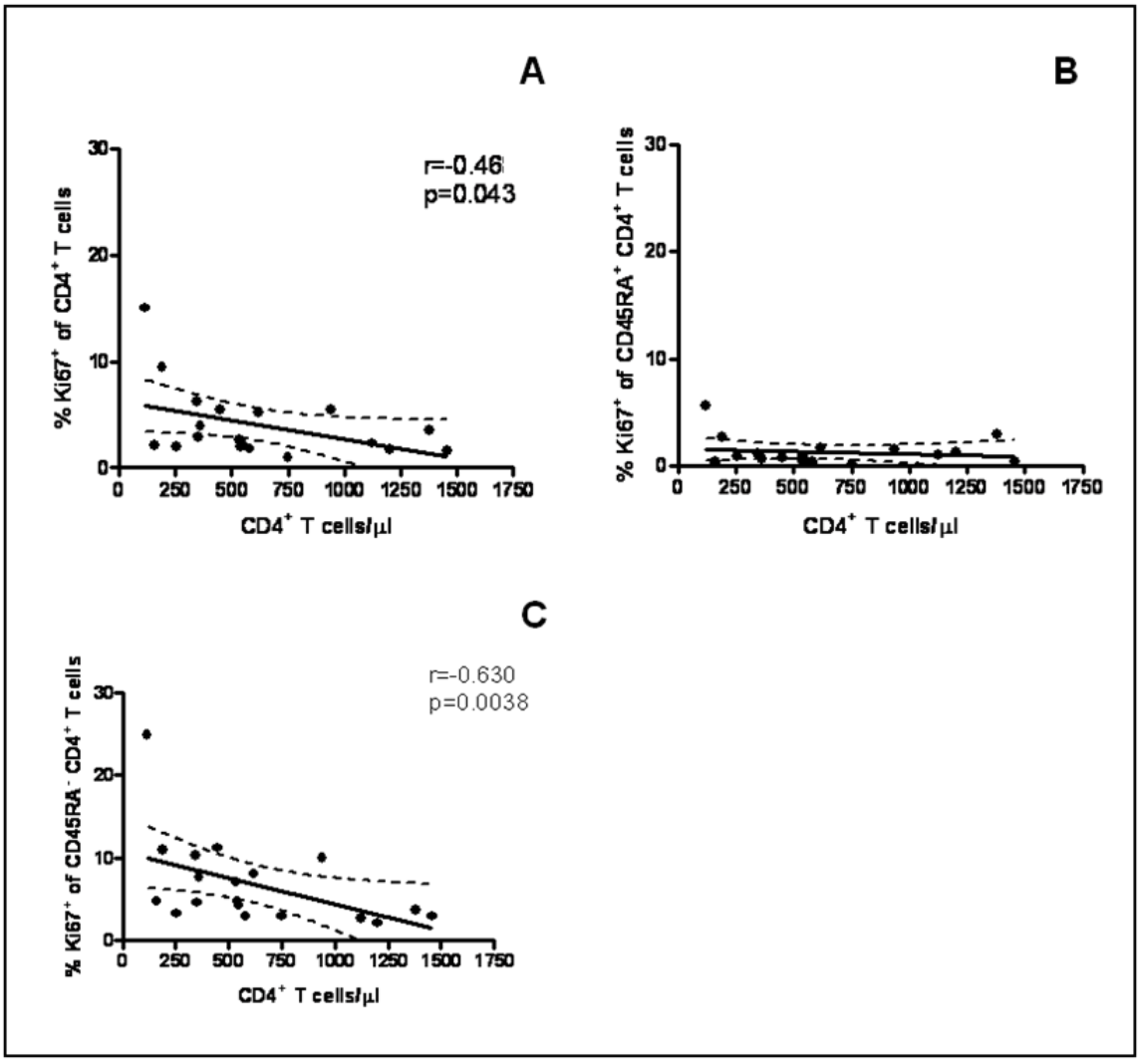

Figure 4.12. Relationship between CD4 count and level of Ki67 expression by CD4 cells and CD4 Subsets

Peripheral blood from 27 HIV-1 infected children were incubated with antibodies against human CD4, CD45RA, CD31 and Ki67 and their expressions analysed by flow cytometry. The CD4 count for each child was obtained from GOSH diagnostic labs and plotted against the level of Ki67 expression by $CD4^+$ T cell subsets and viral load, which was also provided by GOSH diagnostic labs. The strength of the correlations between the CD4 count and the level of Ki67 expression by the sub-populations was determined by Spearman's rank. The coefficient (r) is shown with corresponding p values. The solid and broken lines represent lines of regression and 95% confidence intervals, respectively.

4.3 DISCUSSION

HIV infection is characterised by a progressive decline in the absolute number of $CD4^+$ T cells where the mode of cell death is via apoptosis as was described in chapter one. In this chapter I have shown that FLICA expression, and therefore apoptosis, is greater in $CD45RA^-$ than in $CD45RA^+$ cells (Figure 4.9). More than 60% of apoptotic, $FLICA^+$, cells co-express the marker of activation, HLA-DR, and HLA-DR expression is significantly higher in the $CD45RA^-FLICA^+$ than in the $CD45RA^+FLICA^+$ subpopulation (Figure 4.10). This in agreement with a study of apoptosis and activation in HIV-1 infected individuals, which found that 50-60% of apoptotic $CD4^+$ T cells expressed markers of activation (Gougeon et al 1996). In that study apoptosis was detected by 7-amino-actinomycin D (7-AAD and activation was detected by CD38 and HLA-DR expression. From this, we can infer that activated cells are more susceptible to apoptosis and cells with a memory phenotype, $CD45RA^-$, are preferentially lost during HIV infection over $CD4^+$ T cells with a naïve phenotype, $CD45RA^+$. This is likely due to the higher levels of activation, HLA-DR expression, seen in memory cells.

In early HIV infection the CD4 count remains stable and relatively high despite the loss of CD4 cells therefore this loss must be compensated for by an equal rate of input. The results discussed here suggest that the compensatory mechanisms may include increased proliferation by memory cells because a decrease in CD4 count is associated with increased Ki67 expression by $CD45RA^-$ cells but not by $CD45RA^+$ $CD4^+$ T cells (Figure 4.12). $CD45RA^+$ $CD4^+$ T cells express very little Ki67 (Figure 4.5) and this does not change when the CD4 count increases or decreases (Figure 4.12). Therefore if naïve cell production is increased to compensate for increased loss of $CD4^+$ T cells the source of naïve cell production is likely to be thymic ouput of de novo naïve cells, recent thymic emigrants (RTEs) rather than proliferation of existing cells within the periphery. It is evidently important to maintain naïve cell production as none of the children with a high CD4 count had a low proportion of $CD45RA^+CD31^+$ cells (RTEs). This effect was independent of age.

As HIV infection progresses, perhaps due to decreased drug sensitivity and/or poor adherence to therapy, the viral load increases and the CD4 count begins to decline. The CD4 count may begin to fall either because the loss of CD4 cells increases beyond what the compensatory mechanisms can cope with and/or because the compensatory mechanisms (proliferation of memory cells, naïve cell production and proliferation) fail. The results shown here may suggest that the compensatory mechanisms continue to operate because Ki67 expression by $CD45RA^-$ cells increased with declining CD4 count (Figure 4.12) and there is no difference in the percentage of Ki67 expression, between the group of children with a high CD4 count and high proportion of $CD45RA^+CD31^+$ cells (RTEs) (Figure 4.11A green box) and the group of children with a low CD4 count and a high proportion of $CD45RA^+CD31^+$ cells (Figure 4.11A blue box). Therefore the CD4 count falls because the rate of loss of CD4 cells is increased.

I have shown that as the CD4 count falls the balance between naïve and memory cells is relatively unchanged until it reaches about 600 cells/μl therefore initially thymic output may be able to adequately compensate for differentiation and proliferation, which produce memory cells. As the CD4 count falls below about 600 cells/μl the balance rapidly swings from naïve to memory cells. It may be because at some point thymic output is no longer able to compensate either because it has declined and/or the drive from naïve to memory has increased. If thymic output has declined, the decline is not explained by age as there is no significant difference between the age of children with low CD4 count-low proportion of $CD45RA^+CD31^+$ cells (Figure 4.11A red box) and the age of the children with a low CD4 count-high proportion of $CD45RA^+CD31^+$ cells (Figure 4.11A blue box). Either way the CD4 pool is now mostly composed of memory cells. These cells, as detailed in chapter one, are a rapidly turning over population with shorter half lives and telomeres than naïve cells and are more susceptible to both apoptosis and infection by HIV. Thus unless the loss of cells is reversed or the production of naïve cells is re-instated, by effective HAART, the CD4 count will fall to dangerous levels.

In studying $CD4^+$ T cell kinetics in HIV infected children I have also further elucidated the significance of CD31 expression by $CD4^+$ T cells. $CD45RA^+CD31^+$ $CD4^+$ T cells were first put forward as RTEs by Kimmig *et al*., who also proposed a model of peripheral naive $CD4^+$ T cell homeostasis where RTEs in the periphery, compensate for falling thymic output, by proliferating and differentiating into central naïve cells, $CD45RA^+CD31^-$, in response to self antigen (Kimmig et al 2002). In uninfected individuals Kimmig and other authors have demonstrated a decline in RTEs with age that is initially rapid then slows down. Now within a cohort of HIV-1 infected children I have shown that the same exponential decay kinetics occur in RTEs with increasing age. At the same time also showing the zero order kinetics of central naïve cells where increasing age did not show an association with the size of the central naïve sub-population. The majority of memory cells, which do not express CD31 memory cells, shows a gradual increase with age as has been demonstrated before (Huenecke, Behl, & Zimmerman 2008).

Kimmig *et al*. did not discuss $CD31^+$ memory cells but they have been detected at very low frequencies in healthy individuals of all ages by Junge *et al* (Junge et al 2007). Similarly in the cohort of HIV-1 infected children described here $CD45RA^-CD31^+$ remained a consistently small sub-population, however in contrast to uninfected individuals the percentage of $CD45RA^-CD31^+$ cells showed a significant association with age and were negatively associated with CD4 count. Therefore this population may be expanded during HIV infection. Additionally in chapter 3 we demonstrated that Ki67 expression in this population was higher than in the other $CD4^+$ T cell subsets. Torimoto *et al.* showed in cells in culture that after $CD45RA^+$ cells were activated CD31 expression did not change and that activation of $CD45RO^+$ did not produce CD31 expression (Torimoto et al. 1992). From this we can infer that $CD31^+$ memory $CD4^+$ T cells represent $CD45RA^+CD31^+$ $CD4^+$ T cells post antigenic differentiation and $CD31^-$ memory $CD4^+$ T cells represent $CD45RA^+CD31^-$ $CD4^+$ T cells post antigenic differentiation. Later Prager *et al.* provided data that suggests a suppressor role for $CD31^+$ memory $CD4^+$ T cells (Prager et al. 1996). Therefore $CD31^+$ memory $CD4^+$ T

cells could contribute to the immune dysregulation seen in HIV. The deleterious impact of a decline in CD4 count may be amplified by the expansion of this population.

From the results described here and the studies by Kimmig, Junge, Torimoto and Prager I have proposed a model of T cell kinetics in HIV infection (Figure 4.13). The CD4 count and the balance between the sub-populations are controlled by thymic output, proliferation and antigen driven differentiation. $CD45RA^{+}CD31^{+}$ $CD4^{+}$ T cells are produced by thymic output. In response to activation they can differentiate into either $CD45RA^{-}CD31^{+}$ cells or into $CD45RA^{+}CD31^{-}$, which can themselves differentiate into $CD45RA^{-}CD31^{-}$ cells (red arrows). $CD45RA^{-}CD31^{+}$ and $CD45RA^{-}CD31^{-}$ cells respond to activation by proliferating (green arrows). Death occurs in all populations, though at different rates (black arrows). Viral replication increases activation in all populations and activation increases the death rate in all populations. In addition increased activation drives the differentiation of $CD45RA^{+}CD31^{+}$ and $CD45RA^{+}CD31^{-}$ cells and the proliferation of $CD45RA^{-}CD31^{+}$ and $CD45RA^{-}CD31^{-}$ cells thus moving the equilibrium towards memory cells.

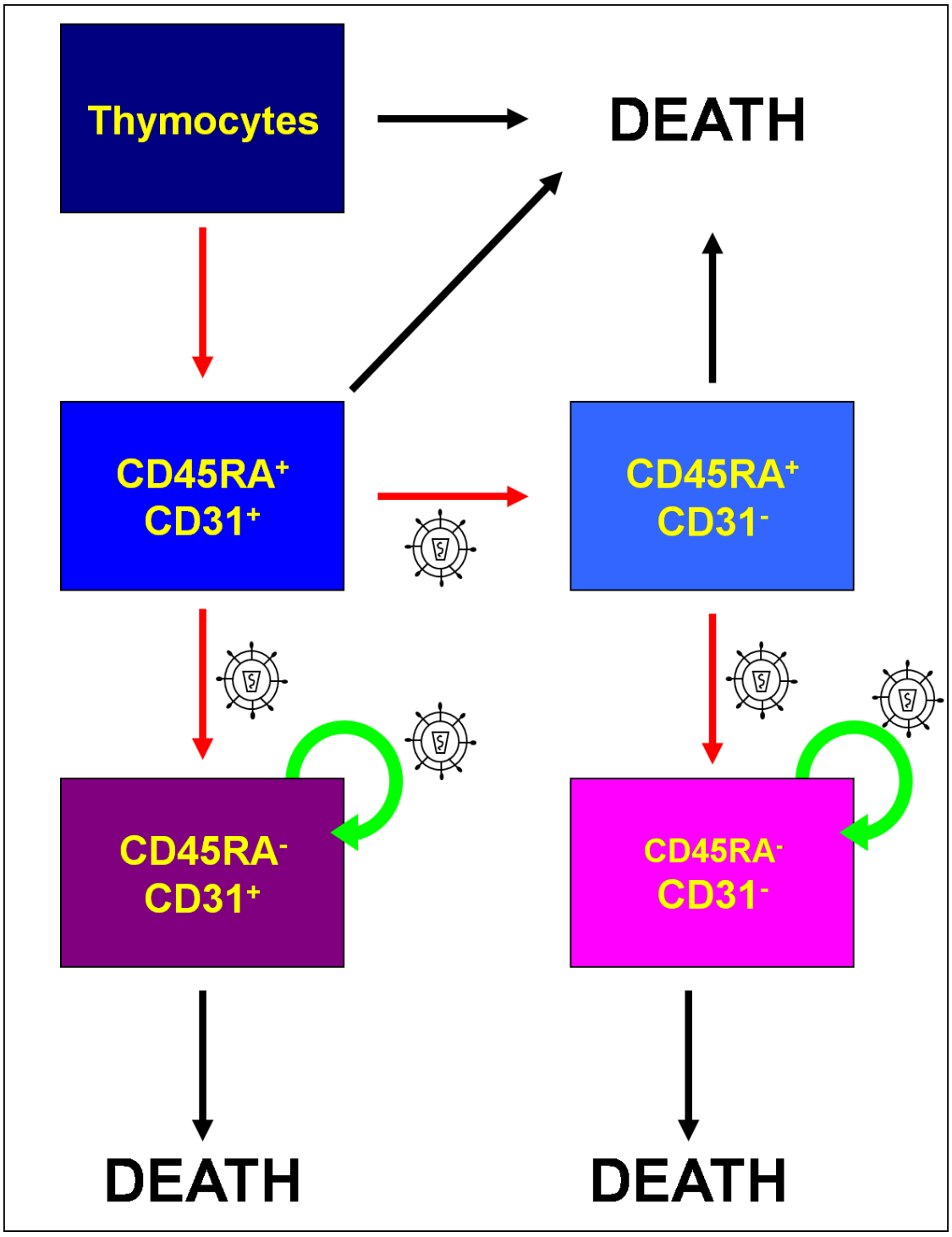

Figure 4.13 Model of T cell kinetics in paediatric HIV infection

The boxes represent the $CD4^+$ T cell populations present in peripheral blood and thymocytes in thymus. Red arrows indicate antigen driven differentiation, green arrows proliferation and black arrows death.

.

CHAPTER 5

IMMUNOLOGICAL STUDY OF PLANNED TREATMENT INTERRUPTION IN A COHORT OF HIV-1 INFECTED CHILDREN

5.1 INTRODUCTION

The optimum of care for HIV infected individuals, as discussed in chapter one, includes continuous long-term administration of three of more anti-retroviral drugs, termed highly active anti-retroviral therapy (HAART). Compliance is difficult because HAART is a rigorous regime of multiple drugs administered several times a day and is associated with toxicities. Yet if therapy is not strictly adhered to, viral strains with mutations that confer drug resistance emerge resulting in virological failure, a loss of viral suppression despite HAART. ARVs are changed in response to virological failure or drug intolerance but there are a limited numbers of drug combinations available and life long treatment is required. Due to these constraints, it may not be possible to achieve life long viral suppression with the current treatments available and it is therefore important to optimise treatment for maximum therapeutic effect balanced against patient quality of life. One of the strategies for optimising HAART is intermittent treatment.

It has been postulated that intermittent therapy would be helpful in conserving treatment options for the lifetime of the patient, increasing adherence, addressing virological failure and decreasing the occurrence of anti-retroviral drug associated toxicities and side effects. Intermittent therapy might also make long term treatment cheaper and more affordable. It could however carry some significant risks, such as increased viral replication and faster disease progression (Miller 2001). Since the introduction of HAART it has not been uncommon for individuals to transiently stop treatment, either by choice due to drug intolerance and other reasons, or under the advice of a physician due to virological failure. The logic being that removing drug pressure would result in the resurgence of ARV sensitive wild type virus because in the absence of ARVs, viruses with resistance-conferring mutations have reduced fitness compared to wildtype virus (Miller et al. 2000b). Additionally viral suppression is associated with decreased numbers of HIV specific CTLs therefore it has also been suggested that intermittent therapy might work like a vaccine to boost the CTL response and thus induce immune mediated control. of HIV-1 (Montaner 2001).

Intermittent therapy has been investigated in various studies. Initial trials were performed with small groups of patients with sustained viral suppression below the standard limit of detection. Use of treatment interruption in such patients would require subsequent therapy to remain effective after the interruption. This was investigated by Neumann *et al*, where a small group of ARV naïve patients received HAART for 28 days, interrupted for 28 days and then restarted with the same regime. They found that upon reinitiating treatment, viral loads declined at a similar rate to that seen following initial treatment and they did not detect resistance-conferring mutations (Neumann et al. 1999). Other investigators have also shown that the ability of HAART to suppress viral replication was not affected by a short period of interruption (Devereux et al. 1999), (Miller et al. 2000a).

The second scenario for the use of treatment interruption was virological failure in treatment experienced individuals. Two such trials in the UK and Germany detected decreased viraemia and increased $CD4^+$ T cell counts after restarting therapy compared to before the interruption. These changes were associated with decreased detection of drug resistant strains. They reported that the longer the interruption period, the higher the peak viraemia and the greater the reduction in drug resistant mutant strains. They also reported a decrease in CD4 count during the interruption to pre-HAART levels (Devereux et al 1999), (Miller et al 2000a).

Recently there have been larger trials of planned treatment interruption (PTI) utilising CD4 count guided entry and restart criteria. They include the SMART trial, Trivacan and DART, all of which were unsuccessful for the most part. They all reported excess risk of opportunistic infections in the group allocated to treatment interruption compared to the group assigned to continuous treatment and had to be prematurely terminated (Danel et al. 2006), (El-Sadr et al. 2006), (DART Trial Team 2008). Additionally the SMART trial did indicate that individuals with low nadir $CD4^+$ T cell count or advanced disease most likely could not tolerate a treatment interruption (El-Sadr et al 2006).

Amongst untreated individuals and those receiving continuous therapy, viral load, does not correlate, as well as CD4 count and level of immune activation with disease progression (Resino et al 2006), (Albuquerque et al 2007). The trials discussed thus far assessed $CD4^+$ T cell count during PTI and mostly found that though $CD4^+$ T cell count declined to some degree during the interruption it could be restored by restarting therapy. However to date, only one trial has looked at immune activation during PTI, and that was in $CD8^+$ T cells, in which an increased CD38 expression was noted following interruption (Ruiz et al. 2000). No PTI trials have assessed immune activation of $CD4^+$ T cells.

The trials described thus far have been conducted in adults yet treatment interruption regimes could be more useful in children than in adults because HIV-1 infected children will probably spend more years on treatment and therefore have a greater need to conserve anti-retroviral combinations. Attaining strict adherence in children can also be harder as they start school and then enter adolescence. Within growing children the toxicities and side effects associated with anti-retroviral treatment can have different or more deleterious effects for example stunted growth which would not be an issue in adults. Additionally as described in chapter one the juvenile immune system is more adaptable and therefore perhaps better able to respond to cycles of treatment interruption and restart. Despite this, investigations of treatment interruption in children have been limited.

There is limited evidence to support the view that treatment interruption in children may be more successful than in adults. The earliest paediatric study was in children undergoing unplanned treatment interruptions and therefore breaks in treatment were of various lengths and children had wide ranges of viral load and CD4 count at treatment cessation. This study looked at children who had interrupted ART for at least 4 weeks and it was observed that although CD4 counts fell during interruption, within 6 months of restarting therapy, they had returned to pre-interruption levels. At this point half the children had viral loads lower than before interruption. However greater inter-person

variability and higher viral load increases than in adults have been reported (Gibb et al. 2004).

As in adults, planned treatment interruption was also considered for children with virological failure and for children with sustained viral suppression. A trial of treatment interruption for virological failure showed that $CD4^+$ T cells declined, as seen in adults, but viral load increases were higher in children (Monpoux et al. 2004).

Studies of planned treatment interruption in children with sustained viral suppression have used interruption periods of a predetermined length or used the CD4 count to guide the length of treatment interruption. Trials with predetermined periods of interruption have used a wide range of interruption durations ranging from a few days to a few months. One trial to induce cellular immunity against HIV in virally suppressed children used alternating cyles of treatment interruption and treatment reintroduction, where the length of the treatment interruption progressively increased with each cycle, starting with an interruption of 3 days and increasing by 2 days with every subsequent cycle leading up to a maximum interruption period of 27 days during the 13^{th} cycle. During each cycle, the period of interruption was followed by, 18 days of treatment. Subjects were allowed to progress to the next cycle if they had been aviraemic at the end of their last treatment interruption otherwise they had to continue treatment until they achieved an undetectable viral load. The study was terminated in patients who were still viraemic after 112 days of treatment. 8 out 14 subjects achieved cycle 13 or greater i.e. they experienced at least a 27 day interruption period. Unfortunately the authors did not assess CD4 counts but did report that median viral loads peaked during the cycle 7, where treatment was interrupted for 15 days (Borkowsky et al. 2008). In another trial where patients were subjected to cycles of 4 weeks of treatment interruptions followed by 12 weeks of treatment, the patients experienced declines in CD4 count and increases in viraemia. (Palacios et al. 2009).

Considering the high degree of inter-person CD4 count variability in children assigned to treatment interruption, a CD4 count guided trial was logical. PENTA 11 was a trial of CD4 count guided planned treatment interruption (PTI) in 109 HIV-1 infected children conducted by the Paediatric European Network for the Treatment of AIDS (PENTA). Excerpts from the trial final report describing study design are provided in the appendix.

The overall aim of the PENTA 11 trial was to evaluate the role of planned treatment interruptions in the management of HIV infected children who have responded well to antiretroviral therapy. Entry criteria included sustained viral suppression below 50 copies/ml and the CD4 criterion in children 2-6 years was percentage $CD4^+$ T cells of 30% or more. For children 7-15 years at least 25% $CD4^+$ T cells and CD4 count of at least 500 cells/µl. Therapy was restarted in children if the percentage of $CD4^+$ T cells fell below 20% in children under 7 years, or less than 20% or a $CD4^+$ T cell count less than 350 cells/µl in children 7-15 years old. Additionally each PTI period could not last longer than 48 weeks and further PTIs could be undertaken only in children who spent more than 10 weeks off therapy during the 1st PTI and then had been back on HAART for 24 weeks. The children were followed for a median period of 130 weeks.

Unlike trials in adults PENTA11 reported no deaths or serious clinical events. During the first PTI just over half the children had to restart therapy early, before 48 weeks had lapsed. A quarter of the children in the PTI arm underwent a 2nd PTI. 4 children on PTI compared to 1 child on CT experienced a primary endpoint, CD4%<15% and CD4 count<200cells/µl for children 7years and older. In contrast to other trials PENTA11 reported an association between nadir CD4 count and restarting early. As expected after 72 weeks fewer children in the PTI arm than in the CT arm were virally suppressed. Interestingly CD4 recovery after PTI was better in younger children (Gibb et al. 2008).

This chapter describes a pilot substudy in a small number of children involved in the PENTA11 trial. It attempts specifically to address whether children with chronic HIV

infection undergoing planned antiretroviral treatment interruptions are disadvantaged immunologically by periods of time without treatment. This was done by comparing the distribution of CD4 subsets and activation and proliferation, as discussed in chapters three and four, in children assigned to the PTI arm, during and after PTI and against the results observed in children assigned to the continuous treatment (CT) arm.

5.2 METHODS

5.2.1 Participants

Detailed information on participant recruitment and ethical approval for the whole study are provided in the appendix. This substudy investigated immunological parameters in 24 children in the UK, 12 assigned to PTI and 12 to CT, and within 12 children in Italy, 7 assigned to PTI and 5 to CT. The study plan for PENTA 11 allowed for multiple interruption periods, however only 5 of the children included this substudy underwent more than one interruption. Data was unavailable for several time points due to non-attendance by the subjects, failure to collect the sample, failure to prepare the sample or dead cells upon thawing of the frozen PBMCs.

5.2.2 Sample collection and storage

10 ml of whole blood were collected by venesection from each child within the predetermined time points in EDTA tubes. Within the day PBMCs were isolated by density gradient centrifugation as described in chapter 2. PBMCs were divided into 3 aliquots and stored at -80°C until use. At each time point viral loads and lymphocytes were also quantified by the GOSH (UK samples) or Padova University Hospital (Italian samples) clinical Immunology and Virology laboratories, and thus were available for analyses.

5.2.3 Immunophenotyping

Single aliquots for every child at every time point, where available, were thawed and resupended in media as described in chapter 2. Samples of dead cells, identified by inability to form cell suspensions and flow cytometric SSC/FSC profiles were excluded from analysis. 100 µl aliquots of cell suspension were incubated with anti-CD4, CD45RA, CD31 antibodies and either anti-HLA-DR antibody or after permeabilisation anti-Ki67 antibody as described in chapter 2. Samples were then acquired and analysed by flow cytometry as described in chapter 4. Sample collection, storage and immunophenotyping of Italian samples were similarly performed by Anita de Rossi's group at the University of Padova.

5.2.4 Analysis

Immunophenotyping protocols used in this thesis and described in chapter 2 were the same as those used by Anita de Rossi's group except that HLA-DR expression was not assessed in the Italian cohort and Ki67 expression was only measured in two populations of $CD4^+$ T cells, the $CD45RA^+$ and $CD45RA^-$ fractions. The results of the UK and Italian cohorts showed similar trends and as they were produced by common methods, the two cohorts were combined to increase total numbers as in both cohorts, some time points had been missed.

14 (74%) of the children in the PTI group only underwent one period of treatment interruption. Measurements taken during the first period of interruption (1^{st} PTI) for all children assigned to PTI were compared to the same variables in children assigned to CT for a similar length of time. Measurements made once children in the PTI arm restarted therapy (1^{st} restart) are compared to the same variables in children on the CT arm for a similar length of time. Measurements were fitted into nominal week windows counted as weeks after interrupting or after restarting therapy. Nominal week windows for the period of interruption were assigned as follows:

- Nominal Week=0 if sample was collected before or at week 0 of interrupting therapy
- Nominal Week=2 if sample collected week>0 & week<3
- Nominal Week=4 if sample collected week>=3 & week<6
- Nominal Week=8 if sample collected week>=6 & week<10
- Nominal Week=12 if sample collected week>=10 & week<18
- Nominal Week=24 if sample collected week>=18 & week<36
- Nominal Week=48 if sample collected week>=36 & week<60
- And so on every 24 weeks.

Nominal week windows for the restart period were the same except that nominal week 0 of restarting treatment only included samples collected during week 0 of restarting treatment and there was no nominal week 8. Therefore nominal week 4 included samples collected at or after week 3 but before week 8 and nominal week 12 included samples collected at or after week 8 but before week 18.

To compare changes to parameters in the PTI group against the CT group, measurements during each nominal week window were transformed into percentage change from baseline, where the baseline was either week 0 of interruption or week 0 of restart, using the equation shown Figure 5.1. Parameter measurements at week 0 of 1st PTI and at week 0 of 1st restart were not made for 3 out of the 19 subjects assigned to the PTI arm of the trial because the samples of PBMCs were dead. Therefore these subjects could not be included in the analysis.

$$\text{\% change from baseline at week } x = \frac{\text{value at week } x - \text{value at week 0}}{\text{value at week 0}} \times 100\%$$

Figure 5.1 Percentage change from baseline equation

A total of 168 samples from the 16 subjects included in the analysis of the PTI arm were thawed, of these 150 (89%) were deemed to be viable. 87 samples were from time points during the 1st interruption period, 57 from the 1st restart period, 3 from the 2nd interruption period and 3 from the 2nd restart period. For each parameter measured, the median percentage change from baseline at each time point is presented, along with the associated IQR where the sample numbers were greater than or equal to four. For each parameter the numbers of samples quantified at each time point are indicated on the graphs.

If children met the restart criteria, a confirmed $CD4^+$ T cell count of less than 20% in children under 7 years, or less than 20% or less than 350 cells/μl in children 7 years and older, they resumed treatment before the full 48 week period had lapsed. Therefore the 18 children included in the analysis of the PTI arm could be divided into two groups; a group of early restarters, 4 (22%) children, who had to restart therapy before 48 weeks and another group of late restarters, 14 (78%) children, who completed the whole 48 week interruption period. Amongst the early restarters, 1 child restarted therapy after 8 weeks, 2 after 12 weeks and 1 after 24 weeks. Results submitted for publication by the PENTA 11 study group found that the nadir $CD4^+$ T cell count before PTI was significantly lower in early versus late restarters. Changes observed in the early restart group are compared to the late restart group for each parameters measured where samples were available.

The concentrations of $CD4^+$ T cell subsets were calculated by multiplying the percentage size of the subsets against the CD4 count. The concentration of HLA-DR^+ and $Ki67^+$ cells of each cell population were determined by multiplying the percentage HLA-DR or Ki67 expression within each population against the concentration of each population.

Lastly results from the children who underwent more than one PTI during the period of follow up are described.

5.3 RESULTS

5.3.1 PTI and CT study populations at randomisation

At randomisation there was no difference between the children assigned to PTI and the children assigned to CT in terms of the ages of children, the $CD4^+$ T cell counts, percentages and concentrations of $CD4^+$ T cell subsets and viral loads (Table 5.1). All participants had an undetectable viral load.

VARIABLE	PTI (n=16)			CT (n=17)		
	MEDIAN	LQ	UQ	MEDIAN	LQ	UQ
Age (years)	8.9	6.05	10.9	9.25	5.75	11.25
CD4 count (cells/µl)	1049	860	1274	1013	841	1075
$CD4^+$ T cells (% of total lymphocytes)	36.6	32.75	40.55	35	33.3	39.6
Total lymphocytes/µl	2765	2325	3385	2827	2410	3200
Log viral load (copies/ml) †	1.7	1.7	1.7	1.7	1.7	1.7

Table 5.1 Characteristics of study populations at randomisation

PBMC samples were obtained from children undergoing a PTI or CT regime. Median value and IQR are given for the PTI and CT arms. † For the purpose of analysis, undetectable VLs (below 50 copies/ml) were considered equivalent to 50 copies/ml.

5.3.2 Effect of interrupting and restarting treatment on HIV viraemia and $CD4^+$ T cells during 1st PTI, 1st restart and CT

When CD4 count was examined over the duration of the PTI (Figure 5.2) it was found to decrease from baseline until the 4th week, and thereafter did not change. Interestingly the decline in the percentage of CD4 cells lagged behind the decline in concentration. Until week 4 the percentage of CD4 cells was close to baseline, then decreased until week 8 and then held steady after that point. The change in viral load from baseline in

the PTI group showed a steep increase until week 4 and then plateau-ed for the remaining time of PTI. During this time, in the CT group, there was almost no change in viral load from baseline.

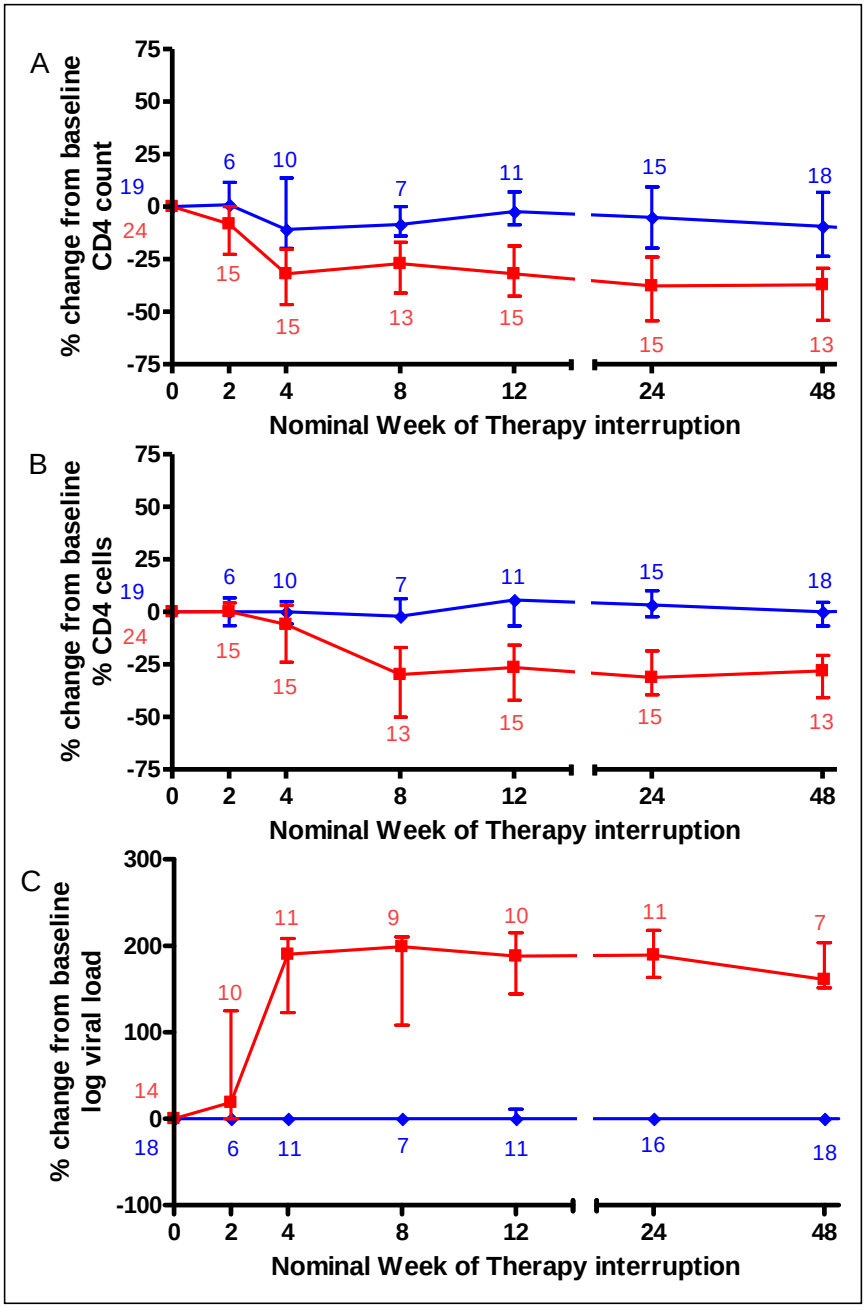

Figure 5.2 Change to the concentration and percentage of $CD4^+$ T cells during 1st PTI

The percentage change from baseline of the absolute concentration and percentage of $CD4^+$ T cells during the 1st PTI (red line and squares) were compared to the percentage change from baseline during CT (blue line and diamonds) of the same duration. Numbers indicate the number of samples available at each time point for both arms and vertical lines show the IQR.

At the end of the interruption period HAART was reintroduced but an increase in the CD4 count was not seen until after the 12th week (Figure 5.3). The CD4 count did not increase in all subjects, indicated by the wide IQRs. The percentage of CD4 cells did not increase upon restarting treatment. Initially no change to viral load was detected upon restarting treatment but by week 4 viral loads had fallen and continued to decrease for several weeks before plateauing though by this point there are only 1-2 subjects therefore it is difficult to comment on this trend.

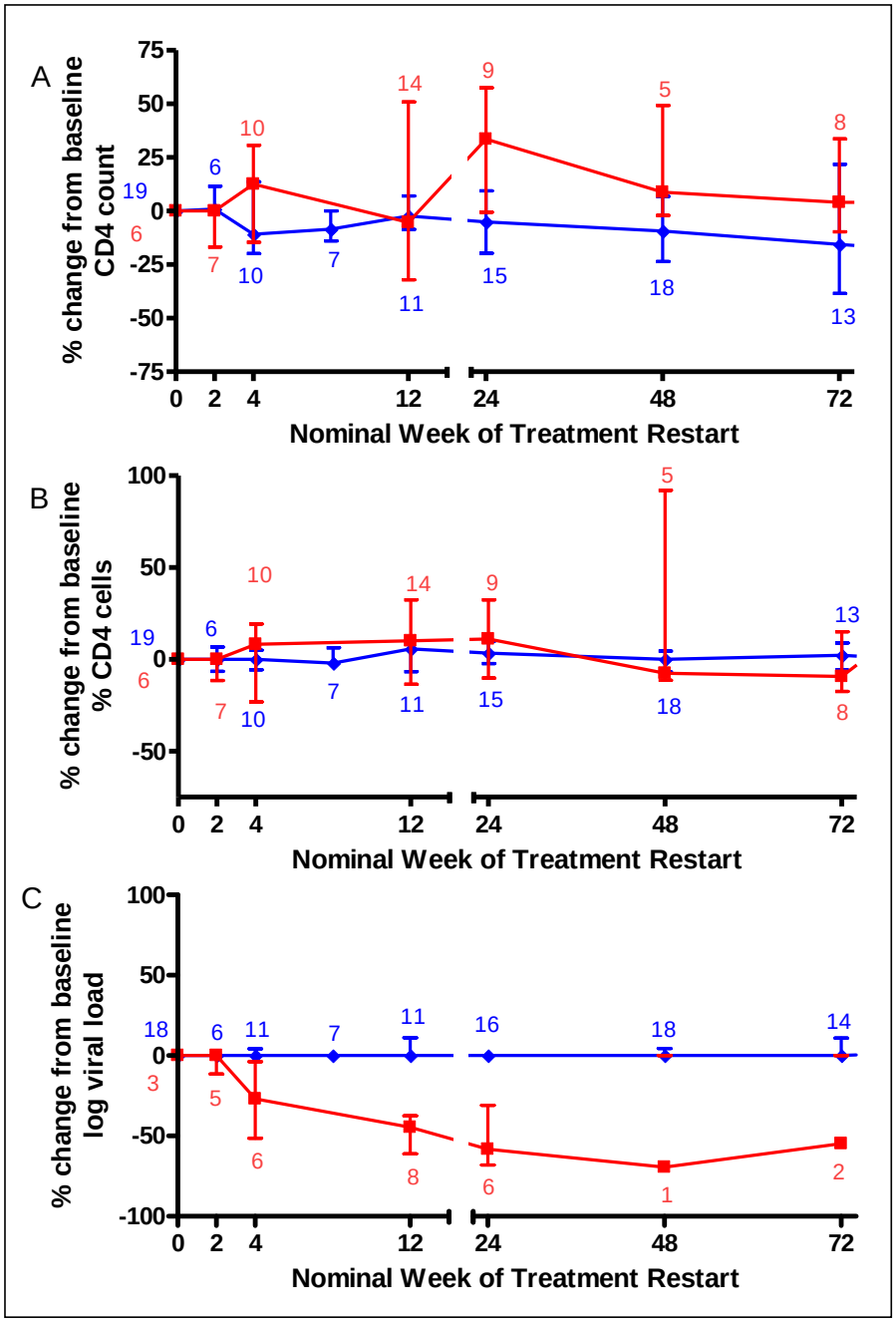

Figure 5.3 Change to the concentration and percentage of CD4$^+$ T cells during treatment restart

The percentage change from baseline of the absolute concentration and percentage of CD4$^+$ T cells during the treatment reintroduction (red line and squares) were compared to the percentage change from baseline during CT (blue line and diamonds) of the same duration. Numbers indicate the number of samples available at each time point for both arms and vertical lines show the IQR.

5.3.3 The major influence of PTI is on concentration and not proportions of CD45RA and CD31 defined subsets

$CD4^+$ T cell subsets were enumerated at specific time points after therapy interruption (weeks 0, 2, 4, 8, 12, 24 and 48); therefore changes to the percentage and concentration of $CD4^+$ T cell subsets during the 1^{st} PTI could be examined by looking at the percentage change from baseline with increasing time off therapy and compared to CT of a similar duration (Figure 5.4 and Figure 5.5).

In the CT group the median percentage of $CD4^+$ T cell subsets appeared to changed little form baseline over 48 weeks, although considering the IQR there was considerable inter-patient variation in the percentage change to the $CD45RA^-CD31^+$ subset over the treatment interruption period (Figure 5.4).

In the PTI arm the percentage of $CD45RA^+CD31^+$ cells decreased at week 4 before stabilising towards baseline levels by week 8 and then decreased again at week 48, however this was within a small subject group. There also appeared to be a transient decline in the percentage of $CD45RA^+CD31^-$ at 2 weeks. There was a transient rise in the percentage of $CD45RA^-CD31^-$ cells at 4 weeks which had returned towards baseline at week 8. The proportion of these cells appeared to increase towards the end of the 48 week period of interruption. As with the CT group there was substantial variation in the percentage change from baseline in the $CD45RA^-CD31^+$ cells during PTI. Therefore overall there is minimal change to the distribution of CD4 subsets during PTI compared to CT.

When the concentration of cells was compared between the two treatment arms (Figure 5.5), by 2-8 weeks all subsets had decreased in the PTI arm compared to CT. Interestingly the concentration of cells appeared to stabilise by week 12 until the end of the 1^{st} PTI.

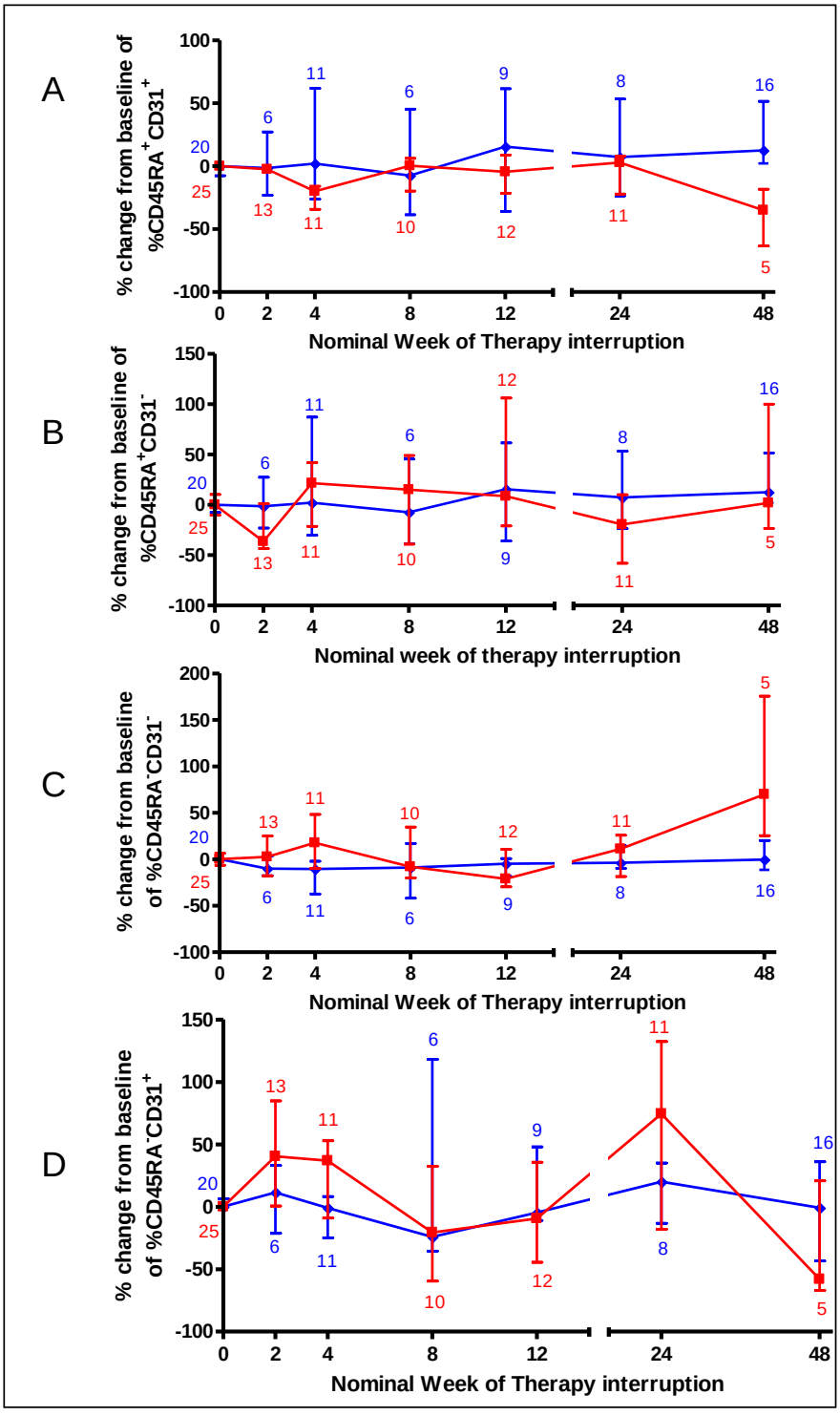

Figure 5.4 Change in $CD4^+$ T cell subset during 1st PTI

The percentage change from baseline of proportions of $CD4^+$ T cell subsets during the 1st PTI (red line and squares) were compared to the percentage change from baseline during CT (blue line and diamonds) of the same duration. Numbers indicate the number of samples available at each time point for both arms and vertical lines show the IQR.

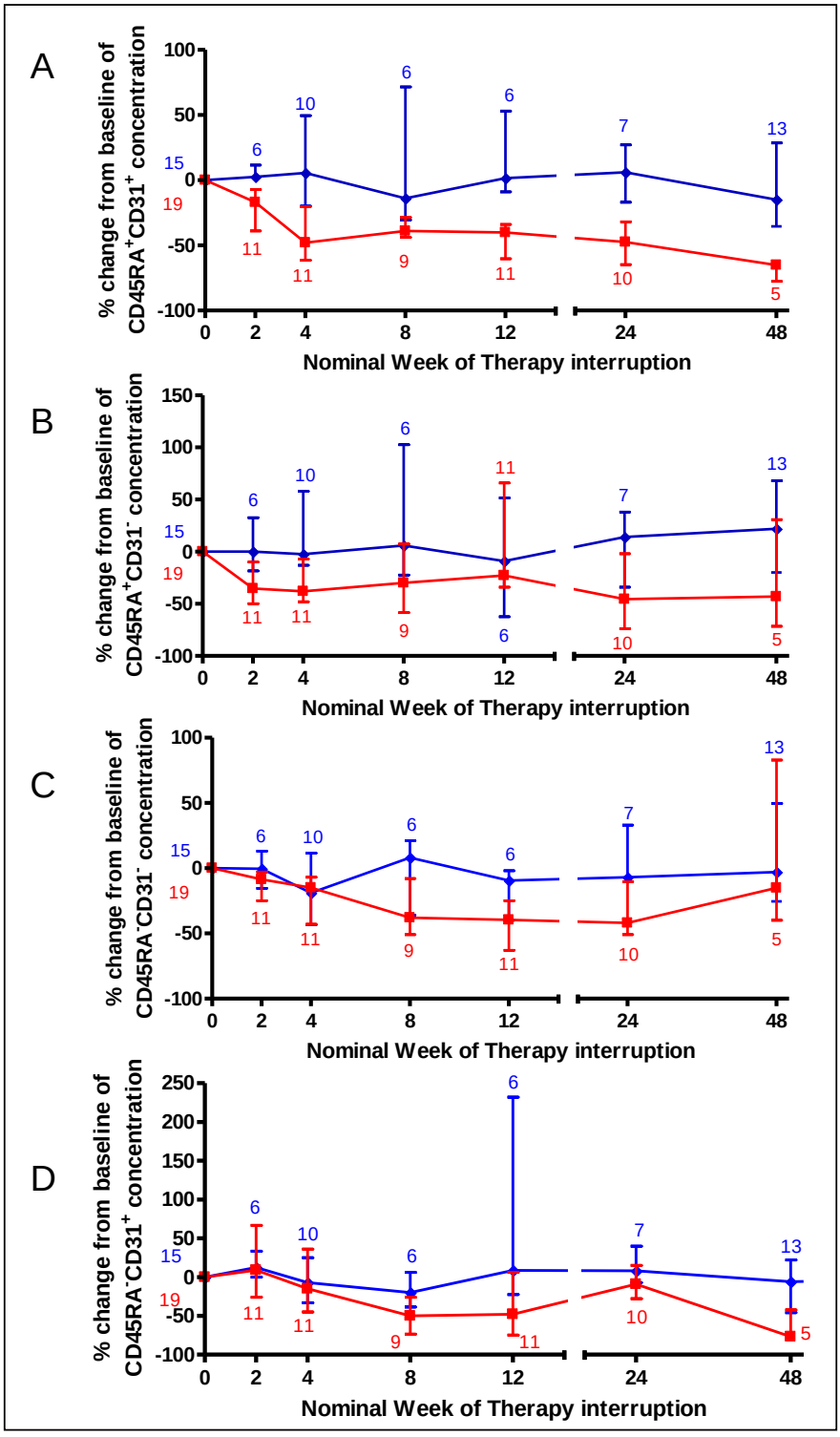

Figure 5.5 Change in concentration of $CD4^+$ T cell subsets during 1st PTI

The percentage changes from baseline of the concentrations of $CD4^+$ T cell subsets during the 1^{st} PTI (red line and squares) were compared to the percentage changes from baseline during CT (blue line and diamonds) of the same duration. Red and blue numbers indicate the number of samples of 1^{st} PTI and CT respectively at each time point and vertical lines show the IQR.

5.3.4 HLA-DR expression during PTI

Changes in the level of HLA-DR expression by $CD4^+$ T cells and subsets from baseline were followed during the 1st PTI and compared to the changes during CT of the same duration. The percentage change in HLA-DR expression by $CD4^+$ T cells and subsets and the concentrations of $HLA\text{-}DR^+$ cells during PTI compared to CT are shown in Figure 5.6 and Figure 5.7. On average HLA-DR expression by $CD4^+$ T cells doubled quickly from baseline by week 2 but decreased towards baseline by week 4. Within the $CD4^+$ T cells subsets a transient increase in HLA-DR expression occurred in all subpopulations. Changes to the concentration of $HLA\text{-}DR^+$ cells during PTI were also assessed and found to be similar to that seen in the CT arm.

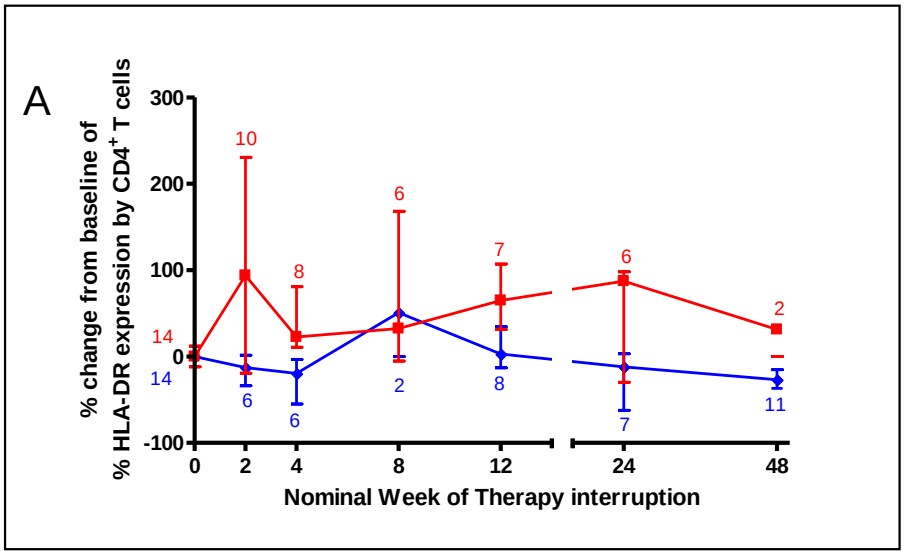

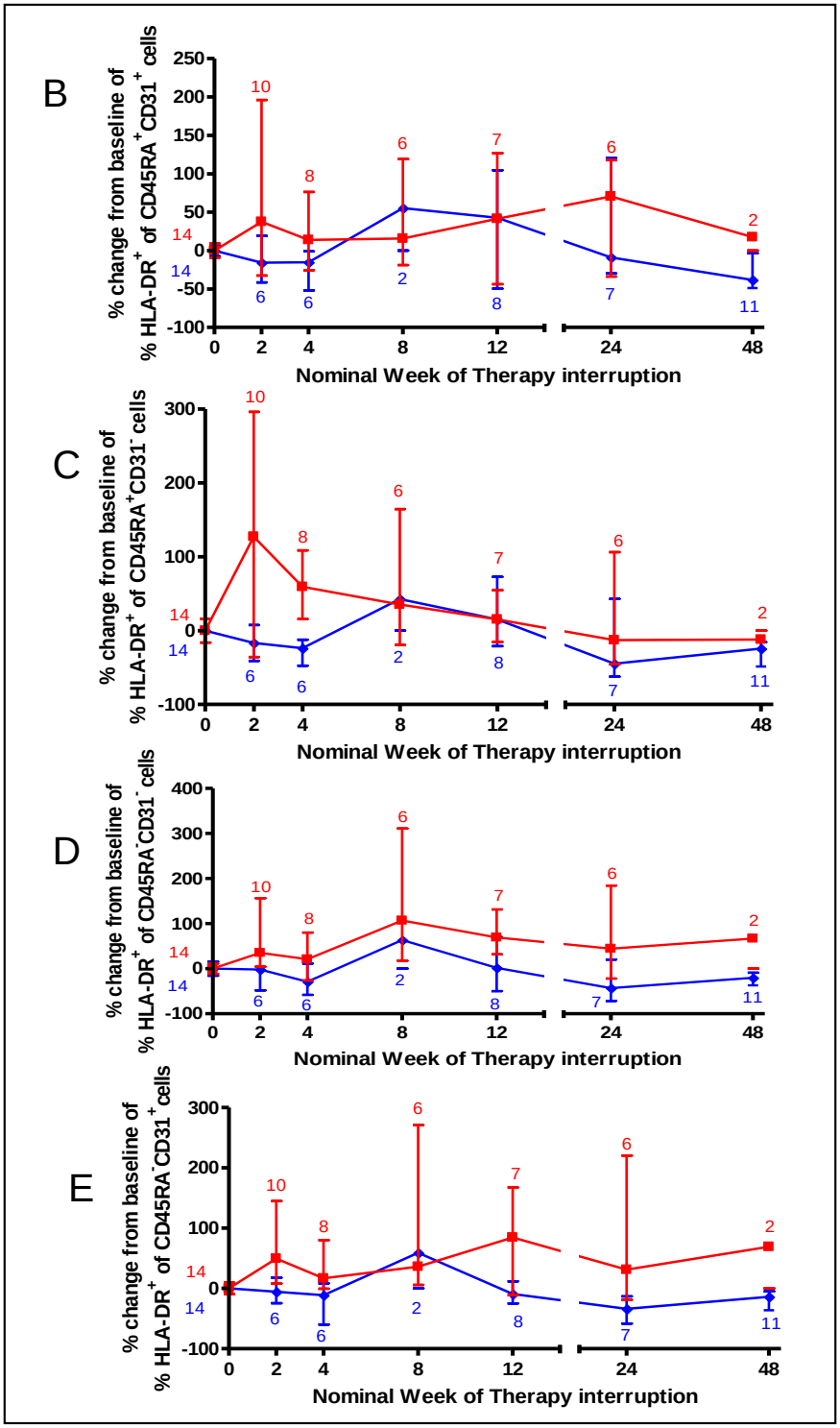

Figure 5.6 Change in HLA-DR expression by $CD4^+$ T cells and subsets during 1st PTI

The percentage changes from baseline of HLA-DR expression by $CD4^+$ T cells and subsets during the 1st PTI (red line and squares) were compared to the percentage changes from baseline during CT (blue line and diamonds) of the same duration. Red and blue numbers indicate the number of samples of 1st PTI and CT respectively at each time point and vertical lines show the IQR.

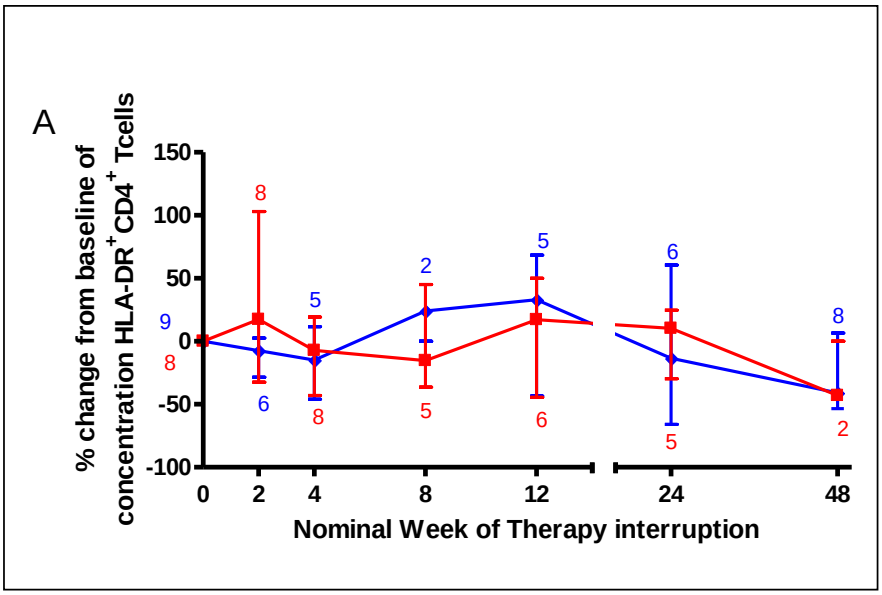
A
% change from baseline of concentration HLA-DR+CD4+ Tcells
150
100
50
0
-50
-100
0
2
4
8
12
24
48
Nominal Week of Therapy interruption

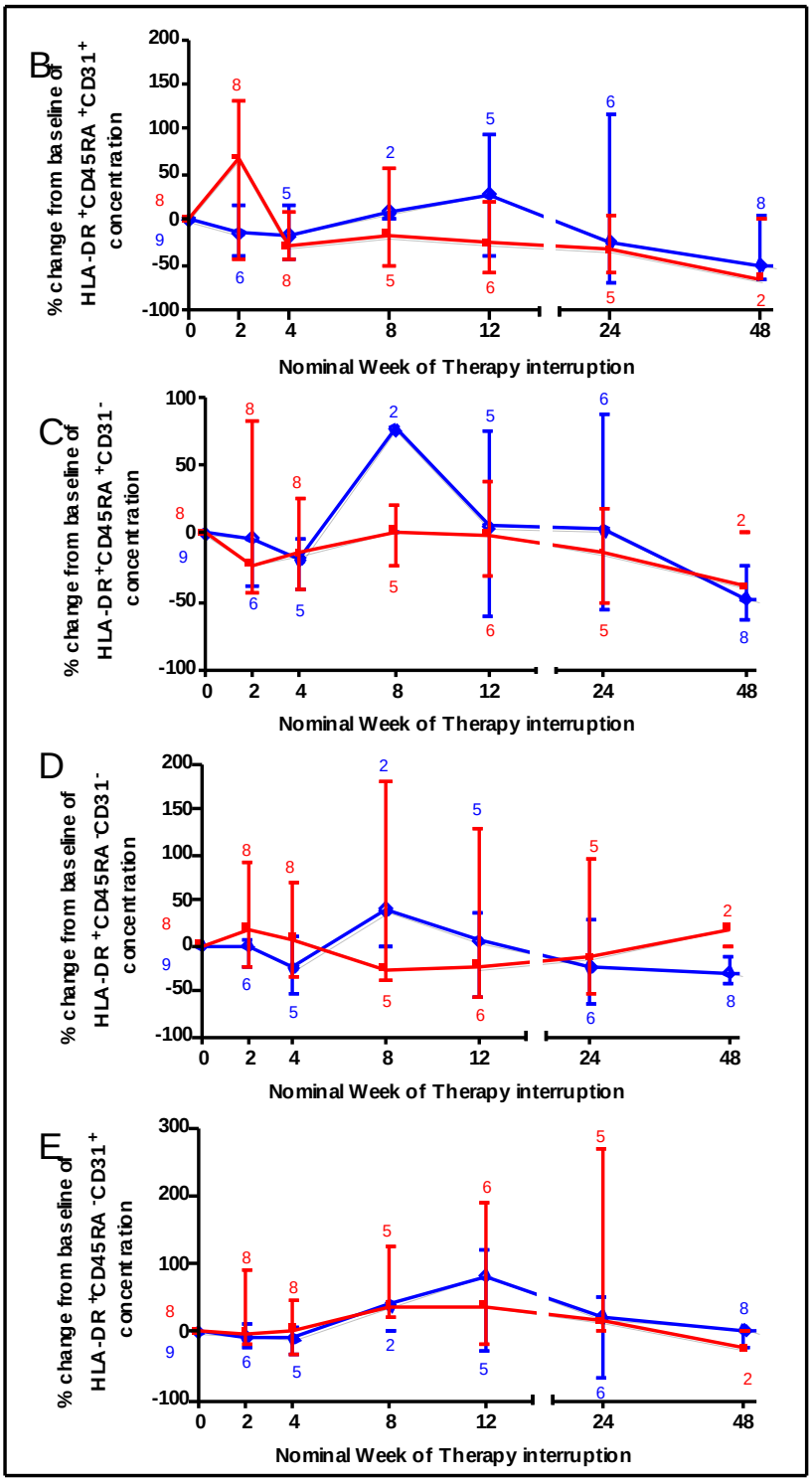

Figure 5.7 Change in concentration of HLA-DR $^{+}$ cells and subsets during 1st PTI

The percentage changes from baseline of the concentrations of HLA-DR $^{+}$ cells during the 1st PTI (red line and squares) were compared to CT (blue line and diamonds) of the same duration. Red and blue numbers indicate the number of samples of 1st PTI and CT respectively at each time point and vertical lines show the IQR.

5.3.5 Ki67 expression increases during PTI

Changes in the level of Ki67 expression by $CD4^+$ T cells and subsets from baseline were followed over the course of the 1st PTI and compared to the changes during CT of the same duration. The percentage change in Ki67 expression by $CD4^+$ T cells and subsets and the concentrations of $Ki67^+$ cells during PTI compared to CT are shown in Figure 5.8 and Figure 5.9.

There was a transient increase in the percentage of $Ki67^+$ $CD4^+$ cells at 4 weeks but decreased to baseline by week 8. This transient increase was predominantly because of Ki67 expression in the $CD45RA^-$ population. Amongst the $CD45RA^-$ subsets, $CD45RA^-CD31^-$ and $CD45RA^-CD31^+$, percentage of Ki67 expression increased in both but remained elevated in $CD45RA^-CD31^+$, throughout PTI.

The change from baseline in the concentration of $Ki67^+$ cells was also assessed in Figure 5.10 and Figure 5.11. The concentration of $Ki67^+CD4^+$ cells increased transiently. Amongst the $Ki67^+CD45RA^+$ and $Ki67^+CD45RA^-$ cells the concentration of $Ki67^+CD45RA^+$ cells increased transiently but the increase in the concentration of was $Ki67^+CD45RA^-$ cells was sustained. The concentration of cells was also elevated amongst the $Ki67^+CD45RA^+CD31^-$, $Ki67^+CD45RA^-CD31^-$ and $Ki67^+CD45RA^-CD31^+$ but not the $Ki67^+CD45RA^+CD31^+$ cells.

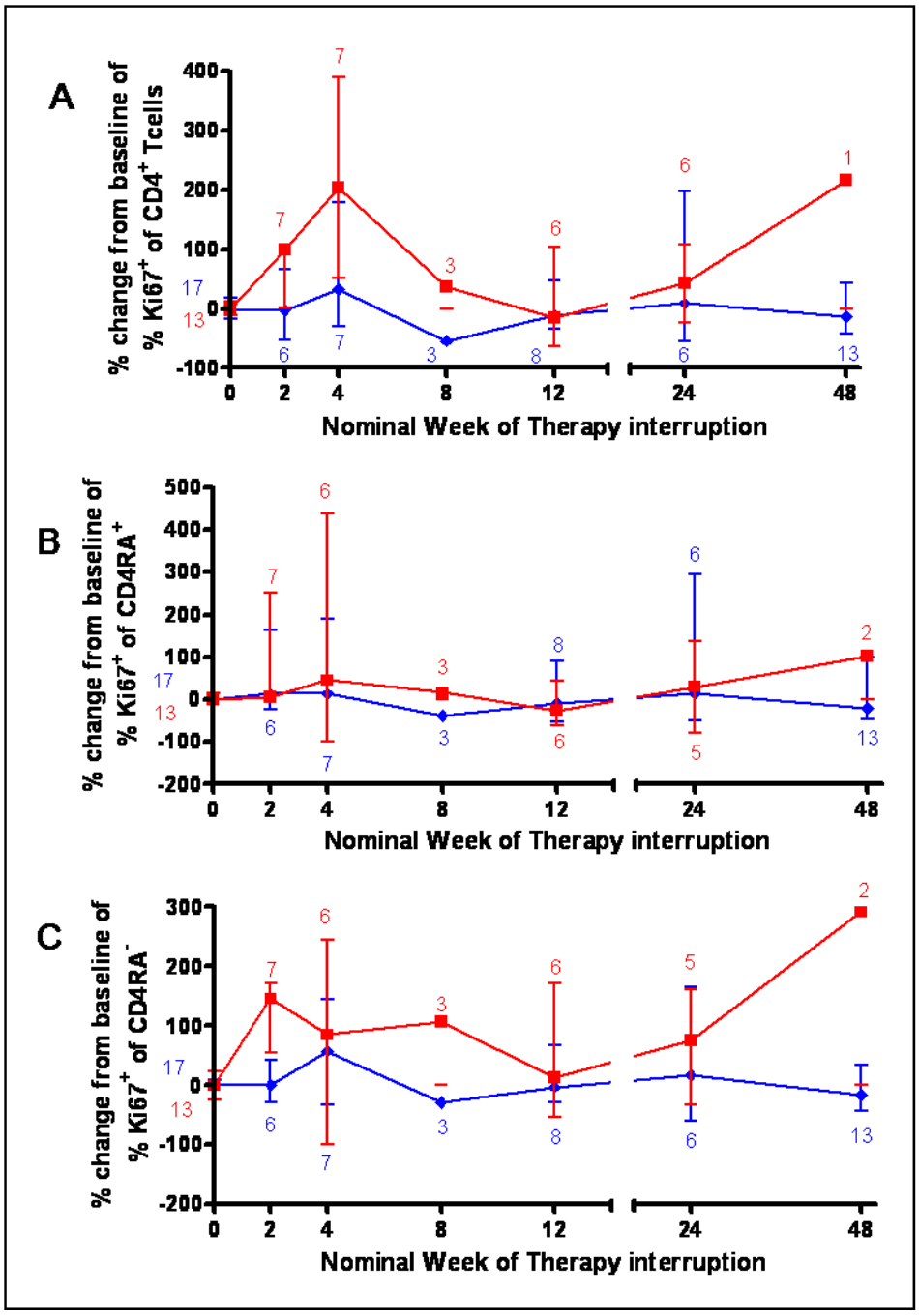

Figure 5.8 Change in Ki67 expression by $CD4^+$ T cells and CD45RA defined subsets during 1st PTI
The percentage changes from baseline of Ki67 expression by $CD4^+$ T cells (A) and $CD45RA^+$ (B) and $CD45RA^-$ (C) subsets during the 1st PTI (red line and squares) were compared to the percentage changes from baseline during CT (blue line and diamonds) of the same duration. Red and blue numbers indicate the number of samples of 1st PTI and CT respectively at each time point and vertical lines show the IQR.

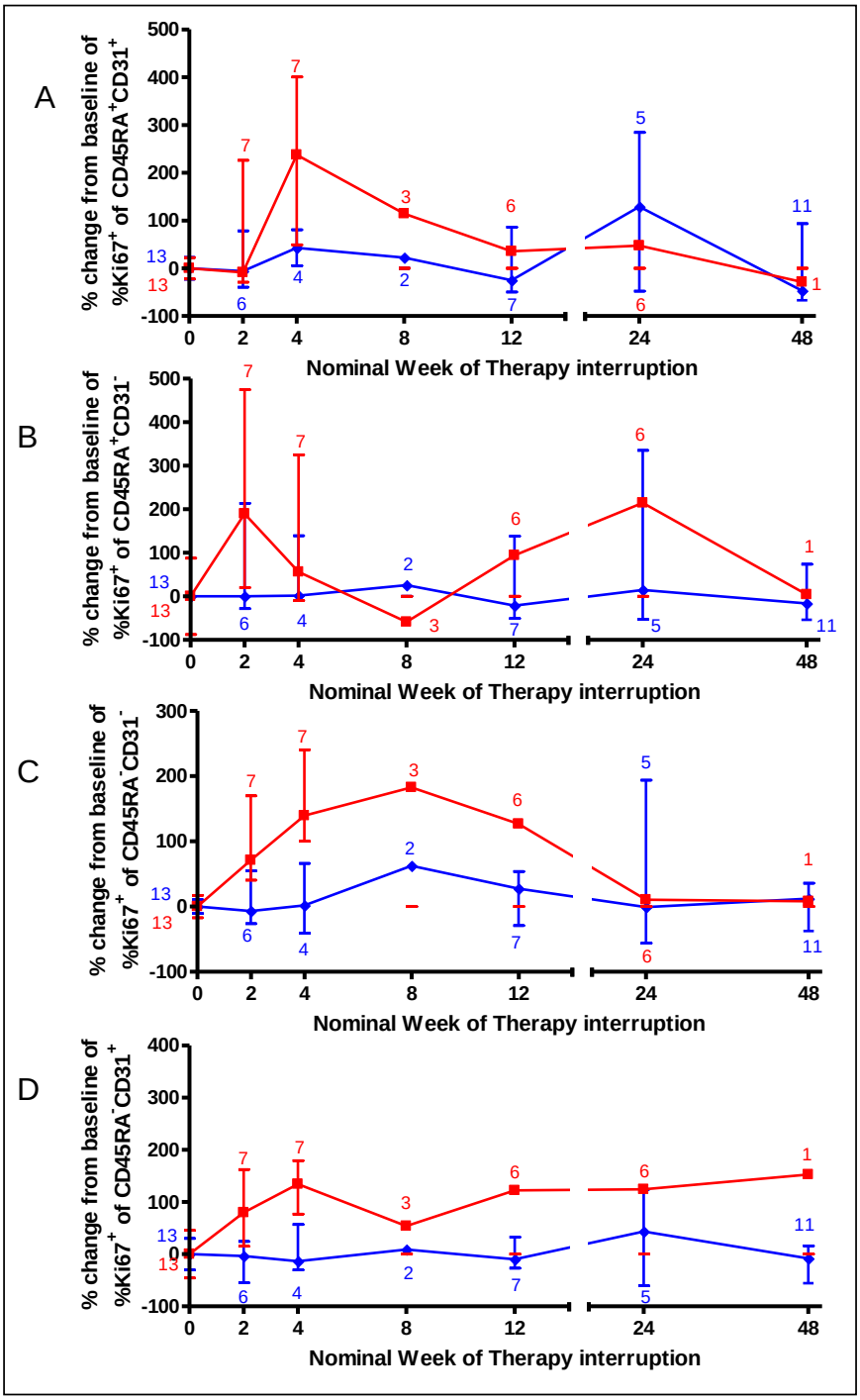

Figure 5.9 Change in Ki67 expression by $CD4^+$ T cells and CD45RA and CD31 defined subsets during 1st PTI

The percentage changes from baseline of Ki67 expression by $CD45RA^+CD31^-$(A), $CD45RA^+CD31^+$ (B), $CD45RA^-CD31^-$ (C) and $CD45RA^-CD31^+$ (D) $CD4^+$ T cells subsets during the 1^{st} PTI (red line and squares) were compared to the percentage changes from baseline during CT (blue line and diamonds) of the same duration. Red and blue numbers indicate the number of samples of 1^{st} PTI and CT respectively at each time point and vertical lines show the IQR.

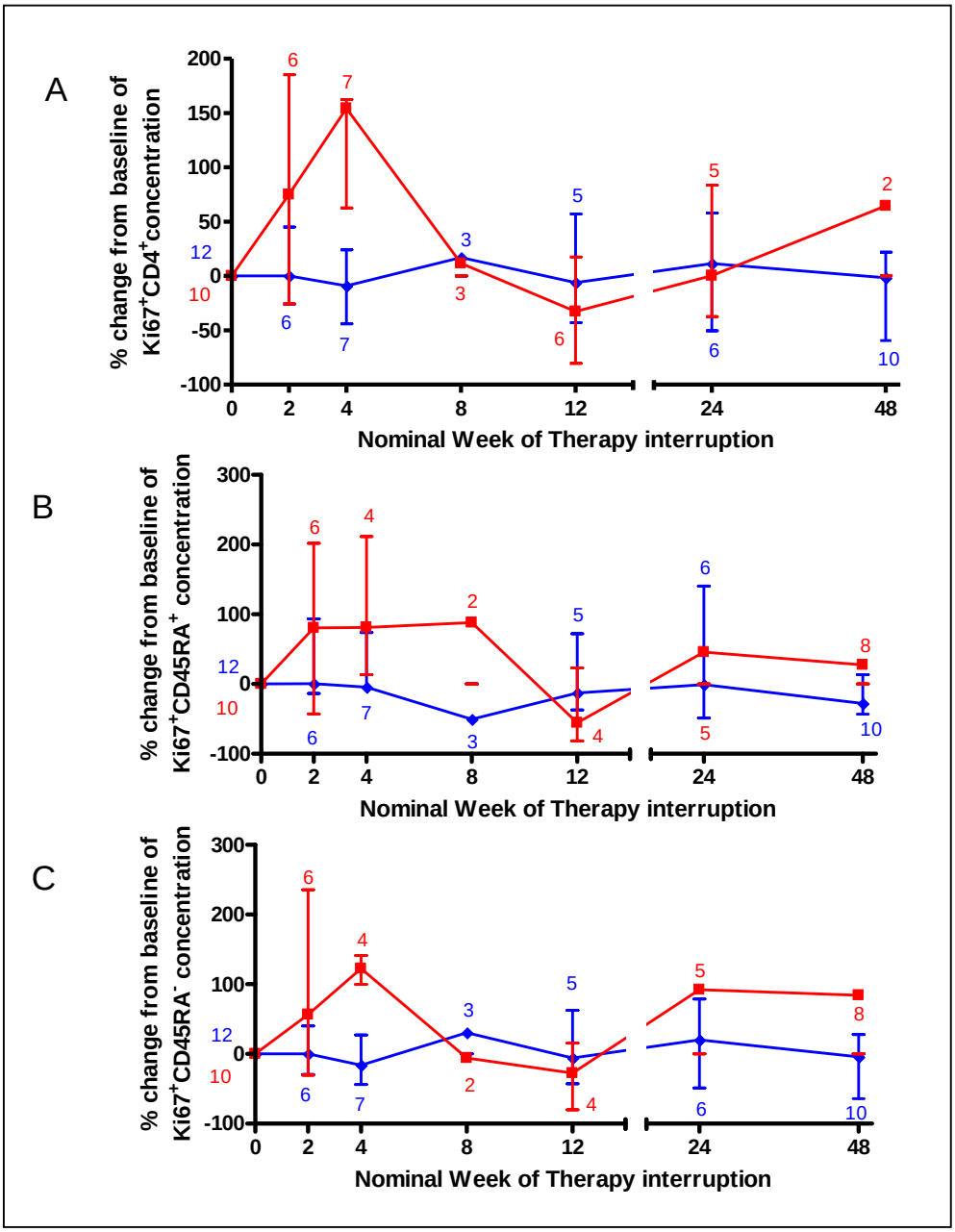

Figure 5.10 Change in the concentration of CD45RA defined Ki67$^+$ cells during 1st PTI

The percentage changes from baseline of the concentrations of Ki67$^+$ CD4$^+$, CD45RA$^+$ and CD45RA$^-$ cells during the 1st PTI (red line and squares) were compared to the percentage changes from baseline during CT (blue line and diamonds) of the same duration. Red and blue numbers indicate the number of samples of 1st PTI and CT respectively at each time point and vertical lines show the IQR.

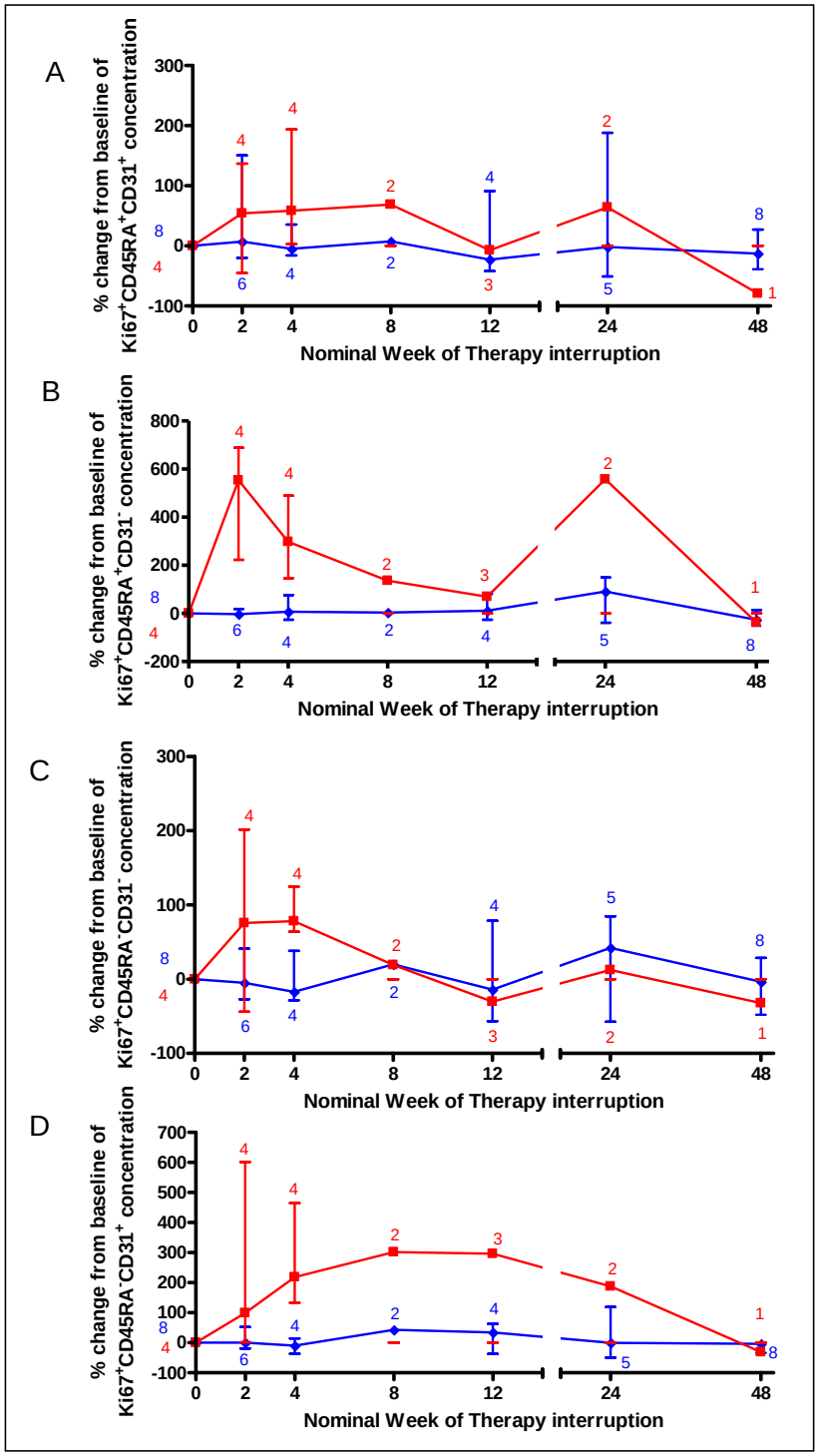

Figure 5.11 Change in the concentration of CD45RA and CD31 defined Ki67$^+$ cells during 1st PTI
The percentage changes from baseline of the concentrations of Ki67$^+$ CD4$^+$, CD45RA$^+$ and CD45RA$^-$ cells during the 1st PTI (red line and squares) were compared to the percentage changes from baseline during CT (blue line and diamonds) of the same duration. Red and blue numbers indicate the number of samples of 1st PTI and CT respectively at each time point and vertical lines show the IQR.

5.3.6 Changes to $CD4^+$ T cell subsets on restarting HAART

When children were reintroduced to treatment after a PTI the changes from baseline, week 0 of treatment restart, to the percentages and concentrations of $CD4^+$ T cells were compared to the changes from baseline in children who had been on CT. The percentage change from baseline of the percentages and concentrations of $CD4^+$ T cell subsets compared to CT are shown in Figure 5.12 and Figure 5.13. The percentages of CD4 subsets, similar to CT, appeared unchanged upon restarting. By week 48 of treatment resumption there was a median increase in CD4 count of 25% but this did not occur in all patients are seen by the wide IQRs (0.3-57%). This is in accordance with observations in the CD4 subsets where at week 48 we detected an increase of 33% (16-130%) in the $CD45RA^+CD31^+$, 41% (10-285%) in the $CD45RA^+CD31^-$, 29% (-21-164%) in the $CD45RA^-CD31^-$ and 100% (24-456%) in the $CD45RA^-CD31^+$.

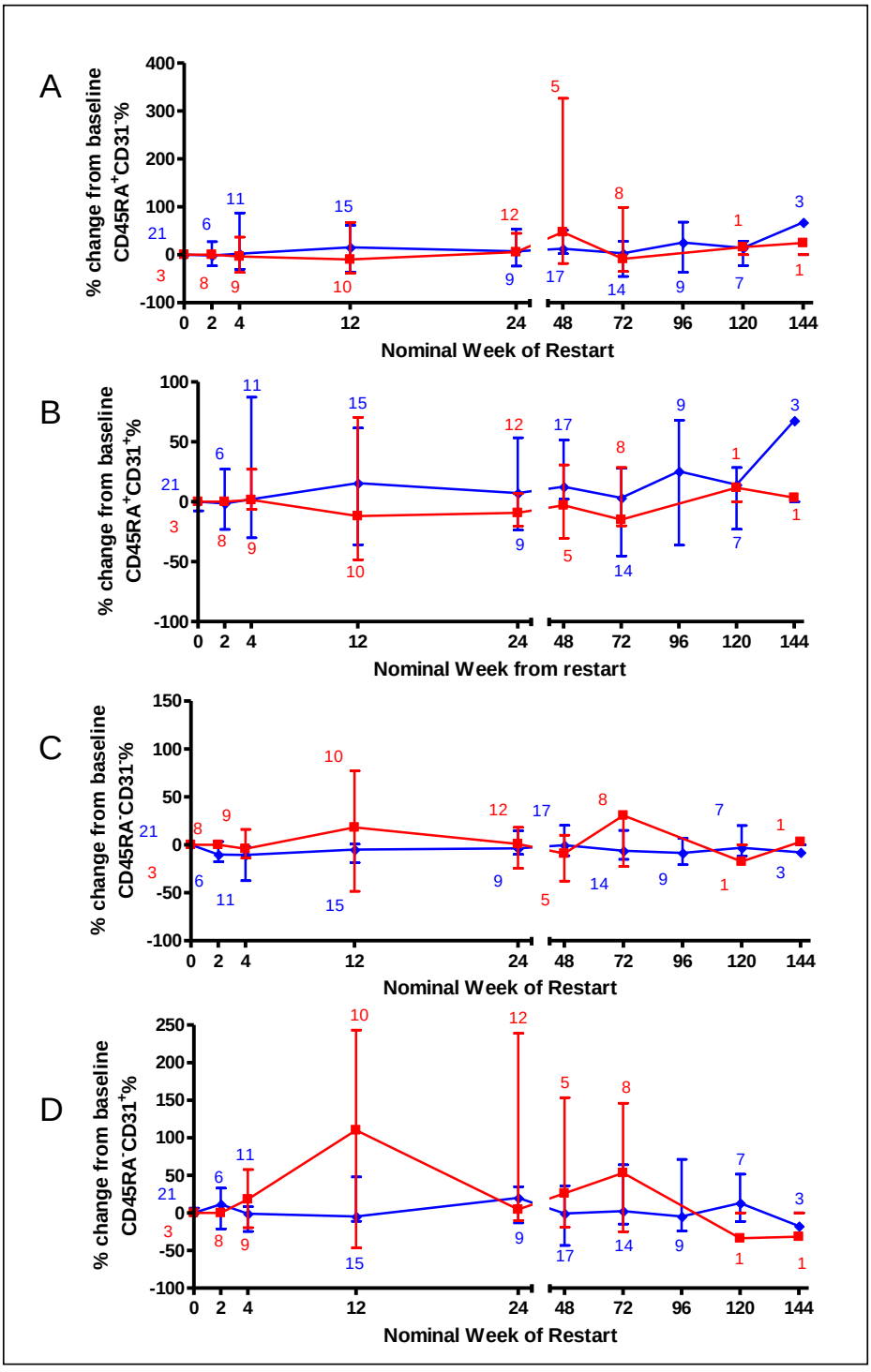

Figure 5.12 Change in CD4$^+$ T cell subset during treatment restart

The percentage change from baseline of proportions of CD4$^+$ T cell subsets during the treatment restart (red line and squares) were compared to the percentage change from baseline during CT (blue line and diamonds) of the same duration. Red and blue numbers indicate the number of samples of 1st PTI and CT respectively at each time point and vertical lines show the IQR.

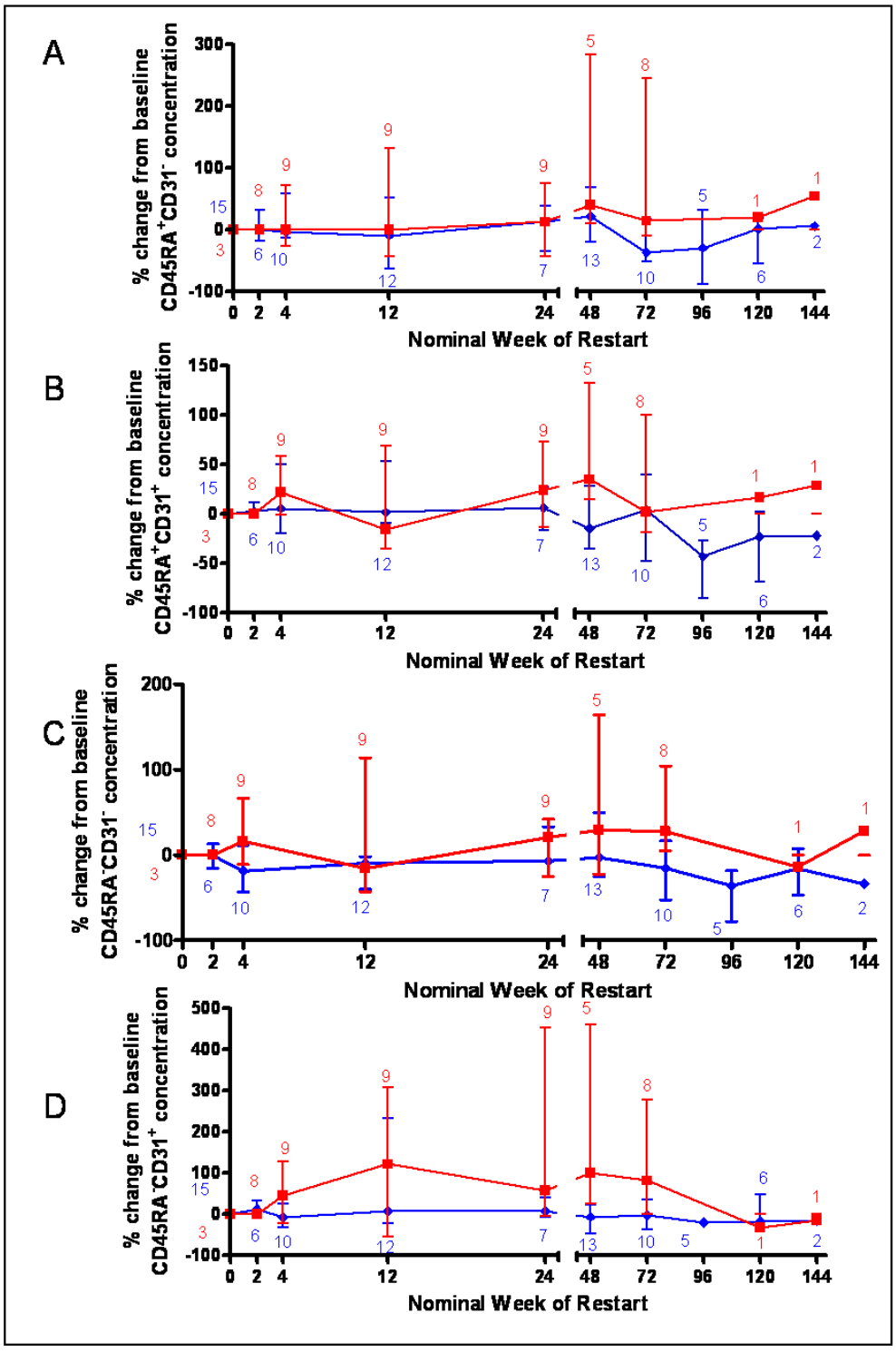

Figure 5.13 Change in concentration of CD4$^+$ T cell subsets during treatment restart

The percentage changes from baseline of the concentrations of CD4$^+$ T cell subsets during the 1st restart (red line and squares) were compared to the percentage changes from baseline during CT (blue line and diamonds) of the same duration. Red and blue numbers indicate the number of samples of 1st restart and CT respectively at each time point and vertical lines show the IQR

5.3.7 HLA-DR expression decreased on restarting HAART

The changes from baseline, week 0 of treatment restart, to HLA-DR expression by $CD4^+$ T cells and subsets in children who were restarting therapy after a PTI were compared to the changes from baseline in children who had been on CT. The percentage change from baseline of HLA-DR expression by $CD4^+$ T cells and subsets and the concentrations of $HLA\text{-}DR^+$ cells compared to CT are shown in Figure 5.14 and Figure 5.15. Upon restarting therapy there was a decrease in the percentage expression of HLA-DR, this was predominantly due to the $CD45RA^-$ subsets, $CD45RA^-CD31^-$ and $CD45RA^-CD31^+$. There was no change in the concentration of $HLA\text{-}DR^+$ cells except $HLA\text{-}DR^+CD45RA^-CD31^+$ cells which appeared to decrease.

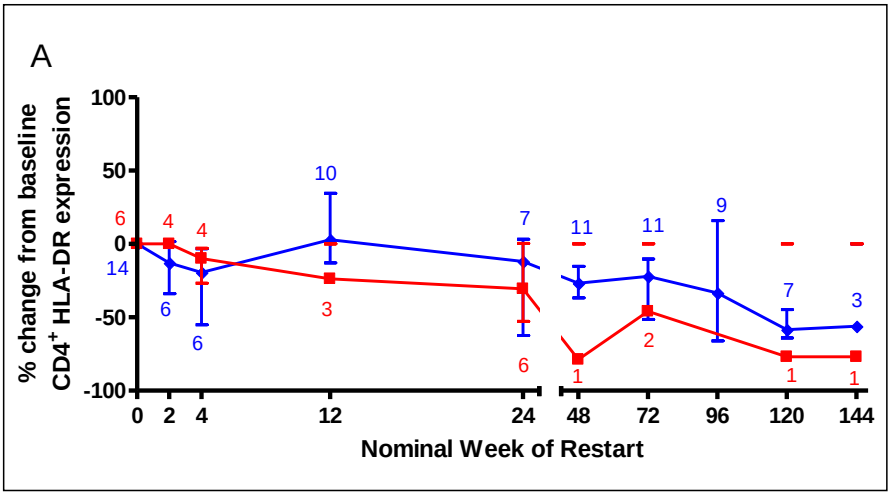

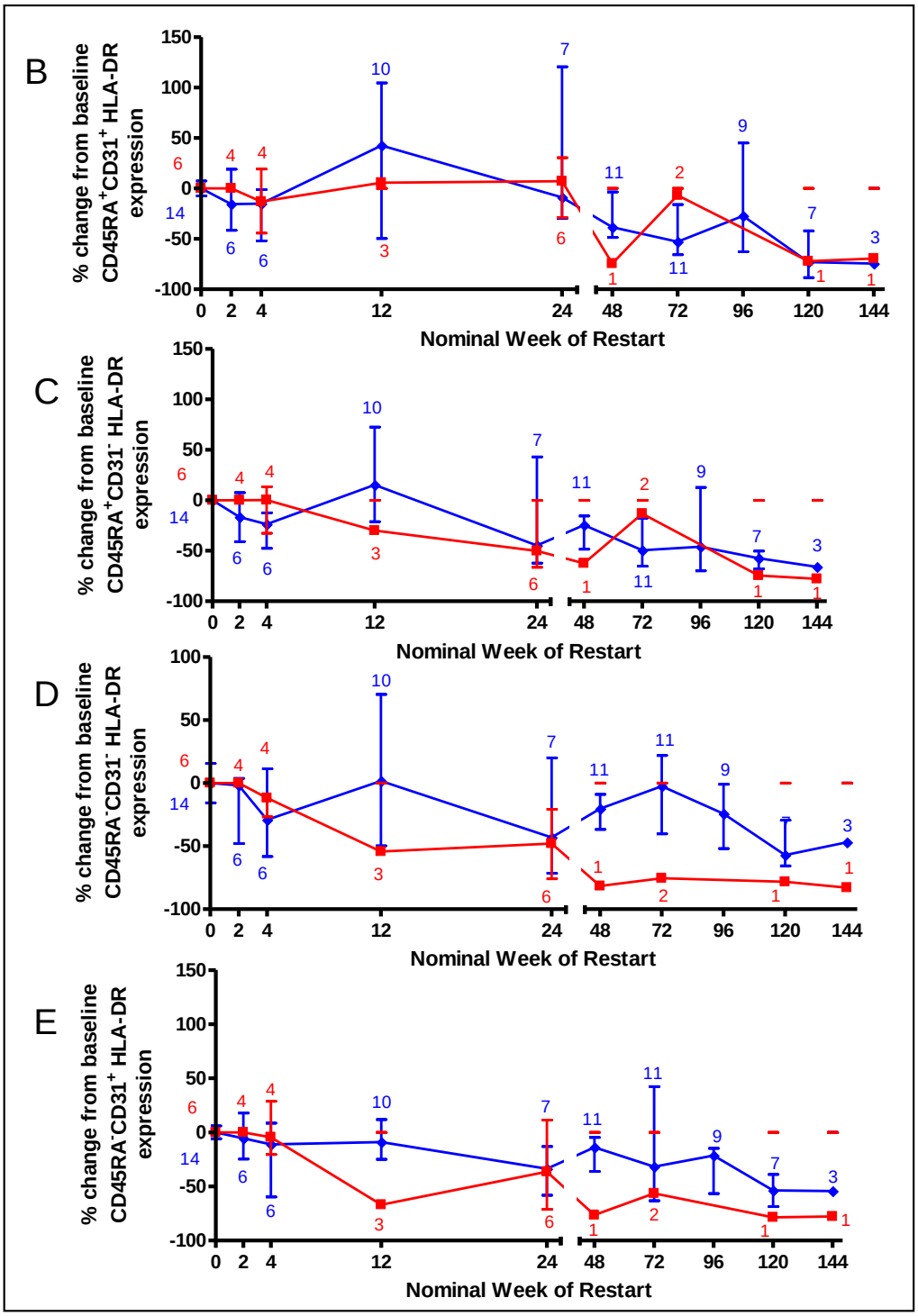

Figure 5.14 Change in HLA-DR expression by $CD4^+$ T cells and subsets during treatment restart

The percentage changes from baseline of HLA-DR expression by $CD4^+$ T cells and subsets during the 1st restart (red line and squares) were compared to the percentage changes from baseline during CT (blue line and diamonds) of the same duration. Red and blue numbers indicate the number of samples of 1st restart and CT respectively at each time point and vertical lines show the IQR.

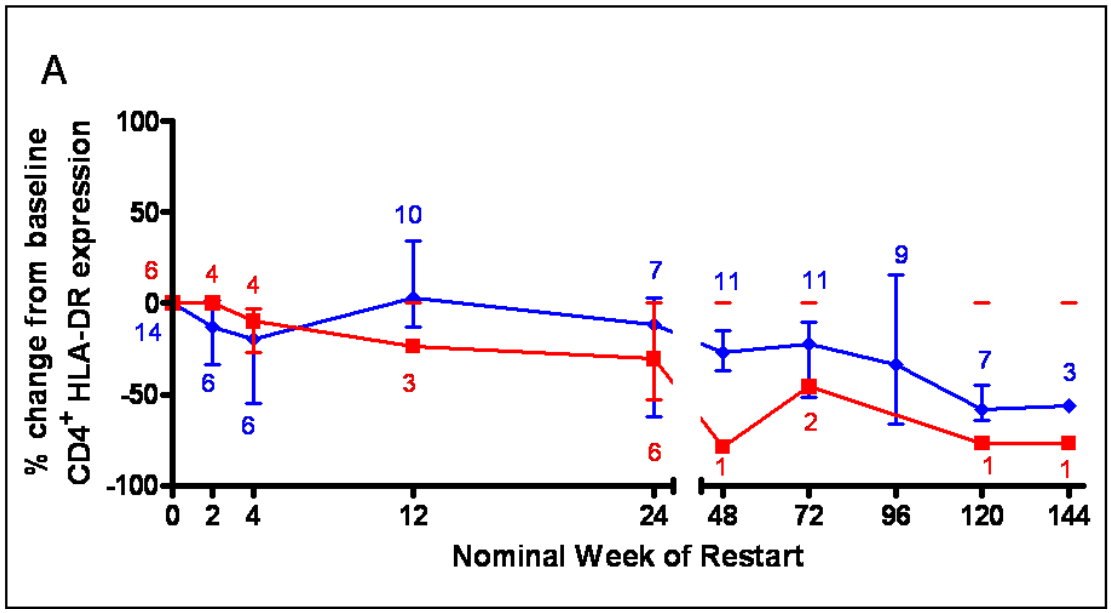
A
% change from baseline
CD4+ HLA-DR expression
100
50
0
-50
-100
6
4
4
10
7
11
11
9
14
6
6
3
6
7
3
1
2
1
1
0
2
4
12
24
48
72
96
120
144
Nominal Week of Restart

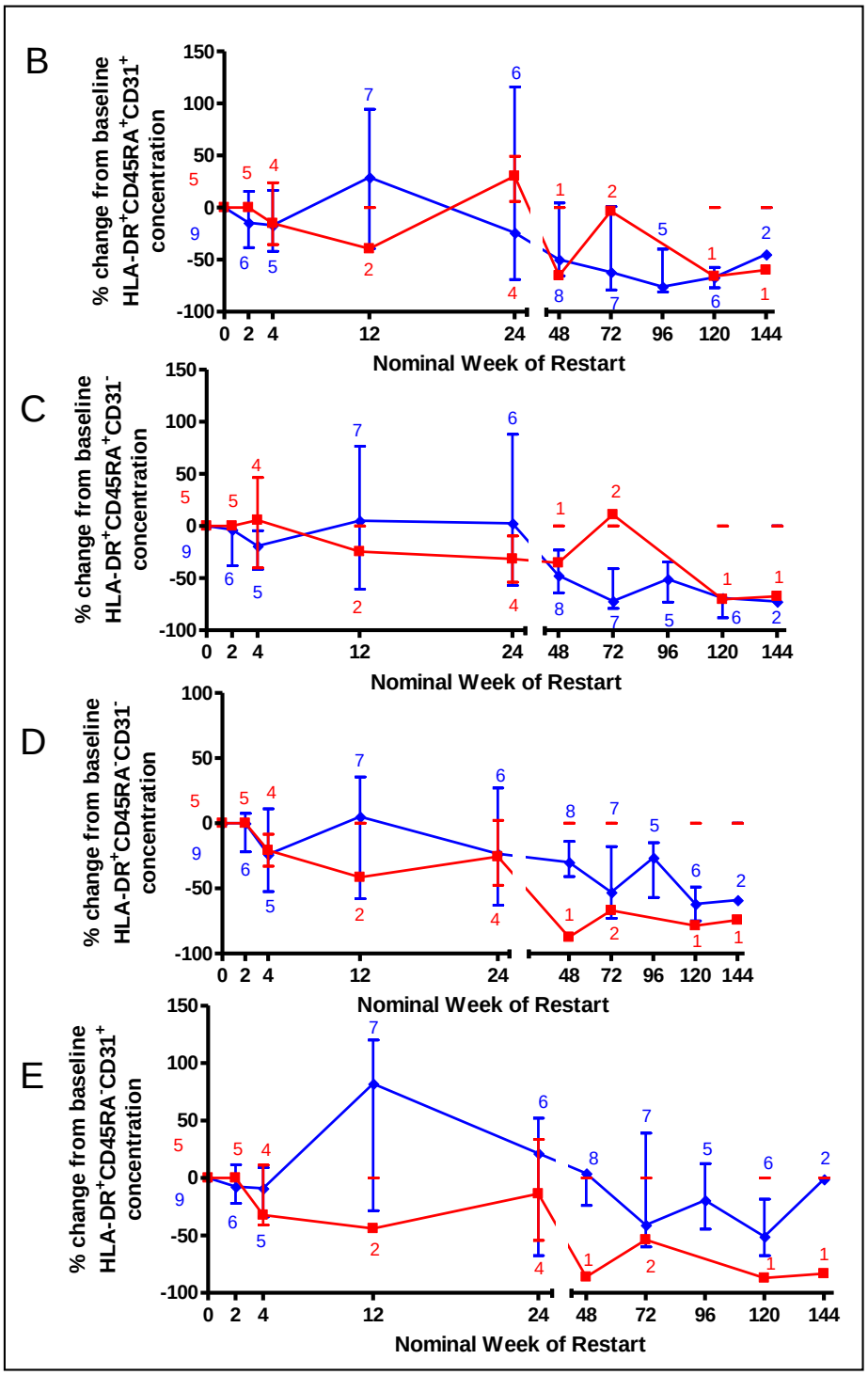

Figure 5.15 Change in concentration of HLA-DR $^{+}$ cells and subsets during treatment restart

The percentage changes from baseline of the concentrations of HLA-DR $^{+}$ cells during the 1st restart (red line and squares) were compared to CT (blue line and diamonds) of the same duration. Red and blue numbers indicate the number of samples of 1st restart and CT respectively at each time point and vertical lines show the IQR

5.3.8 Ki67 expression decreased on restarting HAART

The changes from baseline, week 0 of treatment restart, to Ki67 expression by $CD4^+$ T cells and subsets in children who were restarting therapy after a PTI were compared to the changes from baseline in children who had been on CT. Figure 5.16 and Figure 5.17 show that upon restarting treatment the percentage of $Ki67^+$ cells decreased, specifically in the $CD45RA^-$ cells. Similarly the concentrations of $Ki67^+$ cells also decreased following treatment restart.

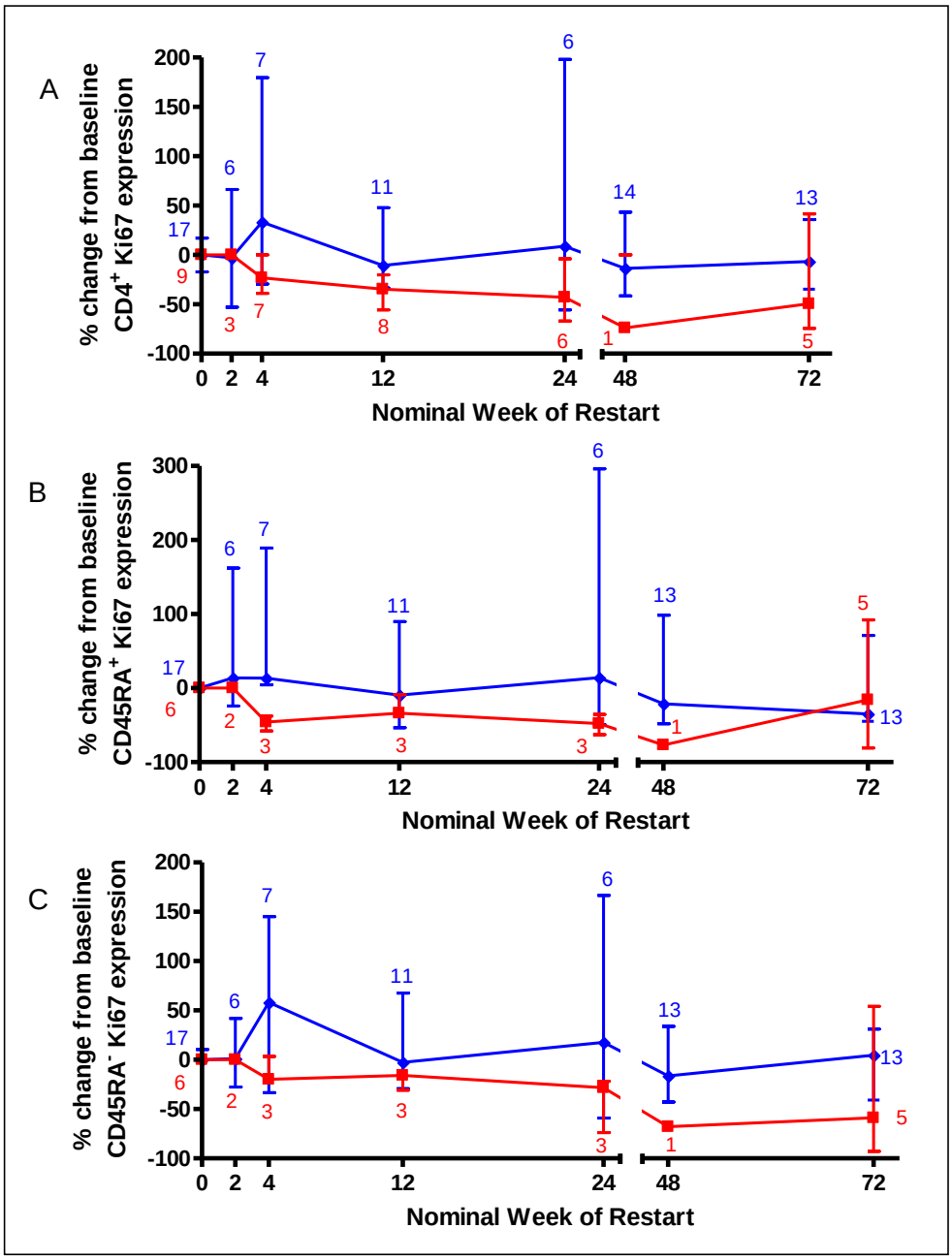

Figure 5.16 Change in Ki67 expression by $CD4^+$ T cells and CD45RA defined subsets during treatment restart

The percentage changes from baseline of Ki67 expression by $CD4^+$ T cells (A) and $CD45RA^+$ (B) and $CD45RA^-$ (C) subsets during the 1st restart (red line and squares) were compared to the percentage changes from baseline during CT (blue line and diamonds) of the same duration. Red and blue numbers indicate the number of samples of 1st restart and CT respectively at each time point and vertical lines show the IQR

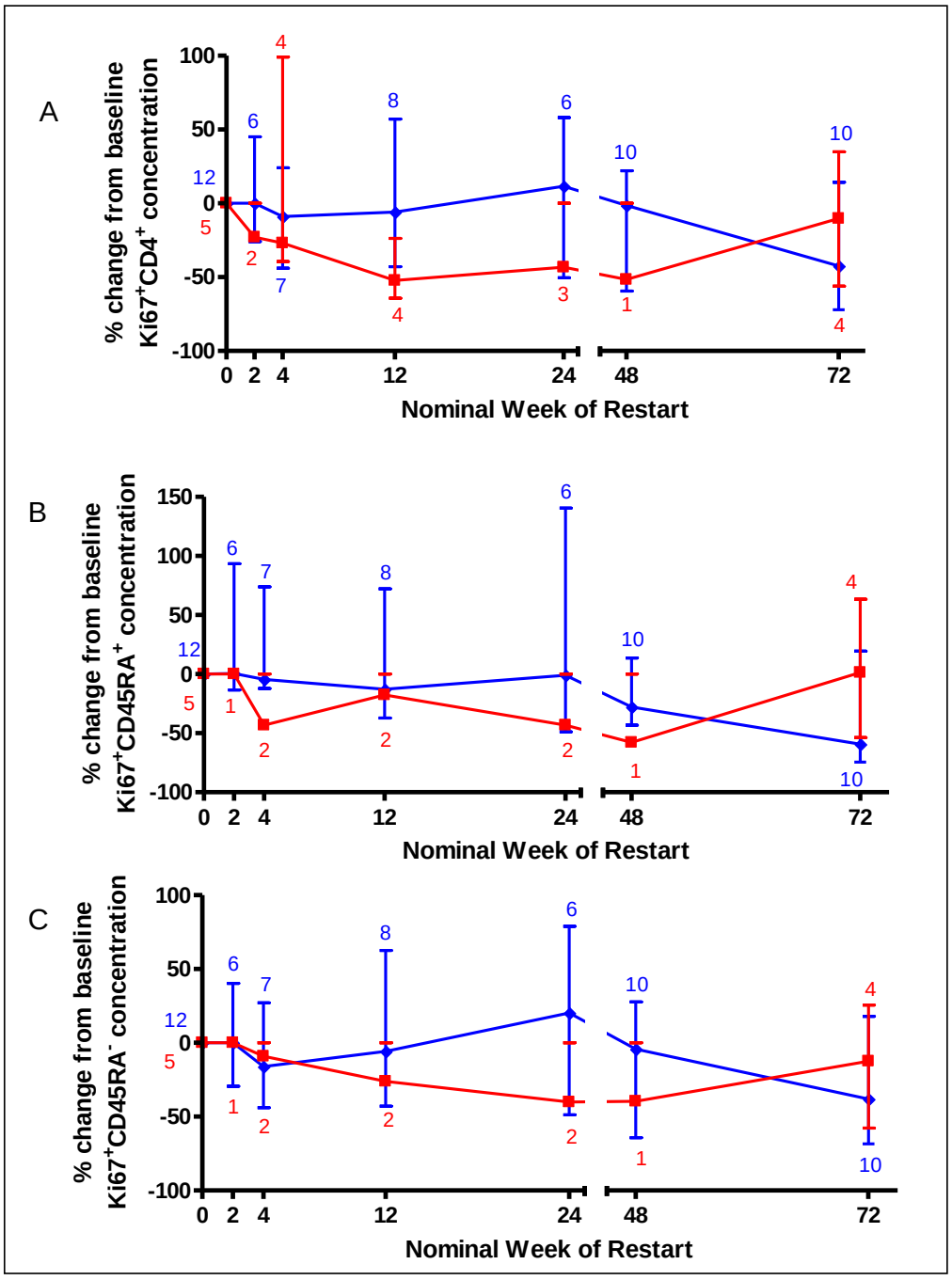

Figure 5.17 Change in the concentration of Ki67$^+$ cells and CD45RA defined subsets during treatment restart

The percentage changes from baseline of the concentrations of Ki67$^+$ CD4$^+$, CD45RA$^+$ and CD45RA$^-$ cells during the 1st restart (red line and squares) were compared to the percentage changes from baseline during CT (blue line and diamonds) of the same duration. Red and blue numbers indicate the number of samples of 1st restart and CT respectively at each time point and vertical lines show the IQR

5.3.9 Early versus late restarters

Of the 18 children assigned to PTI, 4 ‘early restarters’ experienced a decline in $CD4^+$ T cells below 20% and therefore had to restart therapy within 48 weeks, 14 ‘late restarters’ completed the full 48 weeks of PTI. Starting age, $CD4^+$ T cell count and percentage, $CD4^+$ T cell subsets counts and percentages, level of HLA-DR and Ki67 expression at start were investigated as possible predictors of time to restart in children assigned to PTI. However the sample sizes were too small to yield statistically significant results. There is however, a tentative suggestion that changes to the relative sizes of $CD4^+$ T cell subsets during PTI and subsequent treatment restart, do not appear dissimilar between the two groups. It also appears that both groups experience transient increases in HLA-DR and Ki67 expression, levels were higher amongst the early restarters (Figure 5.18 and Figure 5.19).

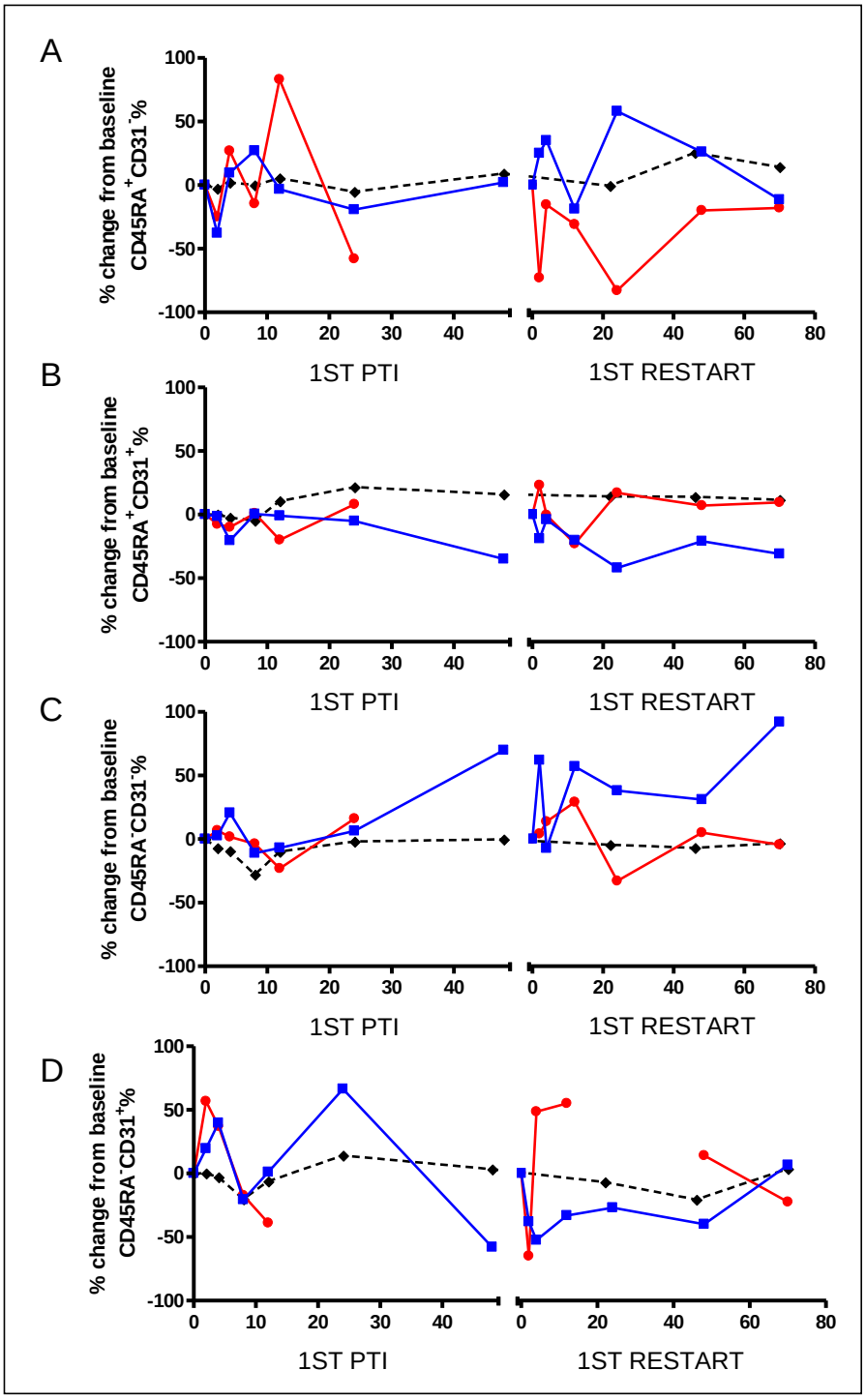

Figure 5.18 Comparison of 'early' and 'late' restarters CD4$^+$ T cell subsets during PTI and treatment restart

The median changes from the PTI and restart baselines of CD4$^+$ T cell subsets during 1st PTI and 1st restart were compared between 'early' restarters, indicated by red circles and solid lines and 'late' restarters indicated by blue squares and solid lines. For comparison median baseline changes during CT are included (black diamonds and broken lines).

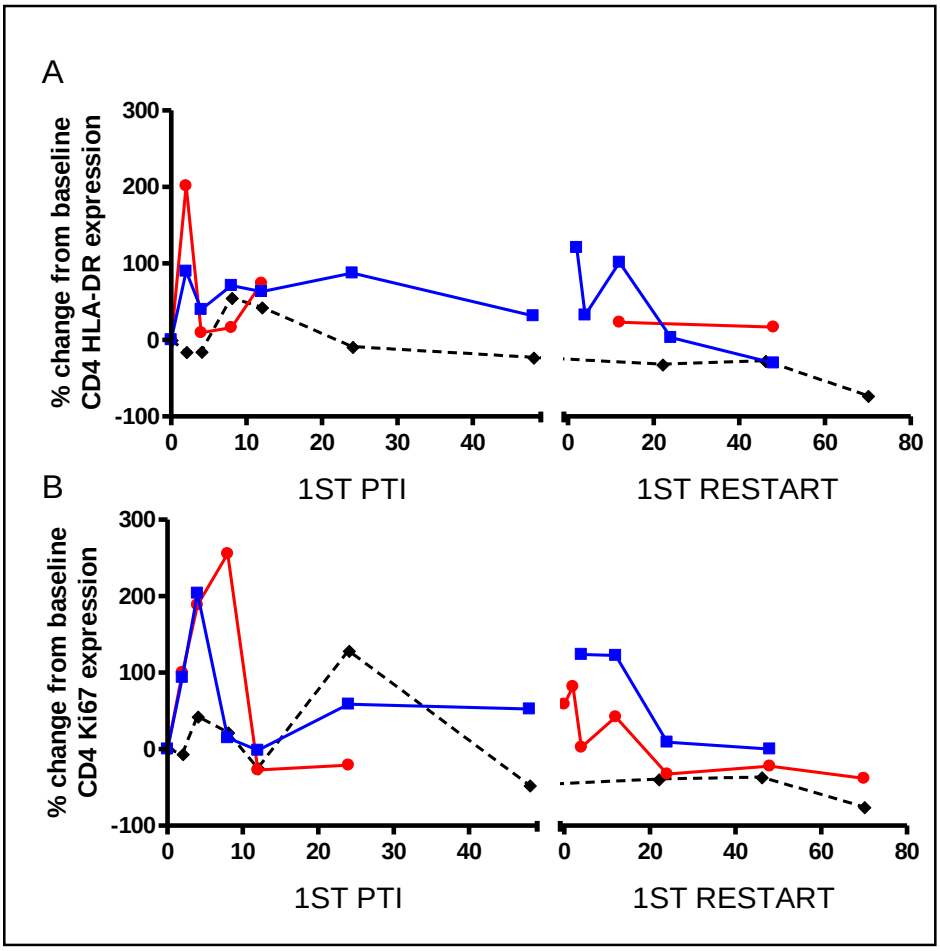

Figure 5.19 Comparison between 'early' and 'late' restarters of HLA-DR and Ki67 expression by CD4$^+$ T cells during PTI and treatment restart

The median changes from the PTI and restart baselines of percentage HLA-DR and Ki67 expression by CD4$^+$ T cells during 1st PTI and 1st restart were compared between 'early' restarters, indicated by red circles and solid lines and 'late' restarters indicated by blue squares and solid lines. For comparison the median baseline changes during CT are included (black diamonds and broken lines)

5.3.10 Serial interruptions

Individuals who maintained their CD4$^+$ T cells above 20% during the full 48 week PTI were allowed to undergo a second interruption after restarting treatment for at least 24 weeks. 5 out of the 18 children assigned to PTI underwent a second further PTI during the follow up period. In one child CD4$^+$ T cell subsets, HLA-DR and Ki67 parameters were measured during the 1st PTI, 1st restart, the 2nd PTI and 2nd restart. The variation of

$CD4^+$ T cell subsets, HLA-DR and Ki67 with time of follow up are shown in Figure 5.20, Figure 5.21 and Figure 5.22 respectively.

Apart from during the 1^{st} PTI there seemed to be little change to the proportions of $CD4^+$ T cell subsets during the whole study period. During the 1^{st} PTI there seemed to be a transient increase in the percentage of $CD45RA^-$ cells and a transient decrease in $CD45RA^+$ cells within the first 4 weeks. Thereafter there was little change during 1^{st} restart, 2^{nd} PTI and 2^{nd} restart.

The absolute counts of $CD4^+$ T cell subsets declined during both 1^{st} and 2^{nd} PTI except for the concentration of $CD45RA^+CD31^-$ cells, which appeared constant throughout. The decline in the $CD4^+$ T cell concentrations experienced during the 1^{st} interruption is greater than the 2^{nd} interruption. During the 1^{st} PTI cell counts declined until week 12 and held steady thereafter. Initiating the 1^{st} restart the absolute counts increased back towards baseline. The declines in CD4 subset count during the 2^{nd} PTI were smaller than during the 1^{st} PTI but once again increased during the 2^{nd} restart.

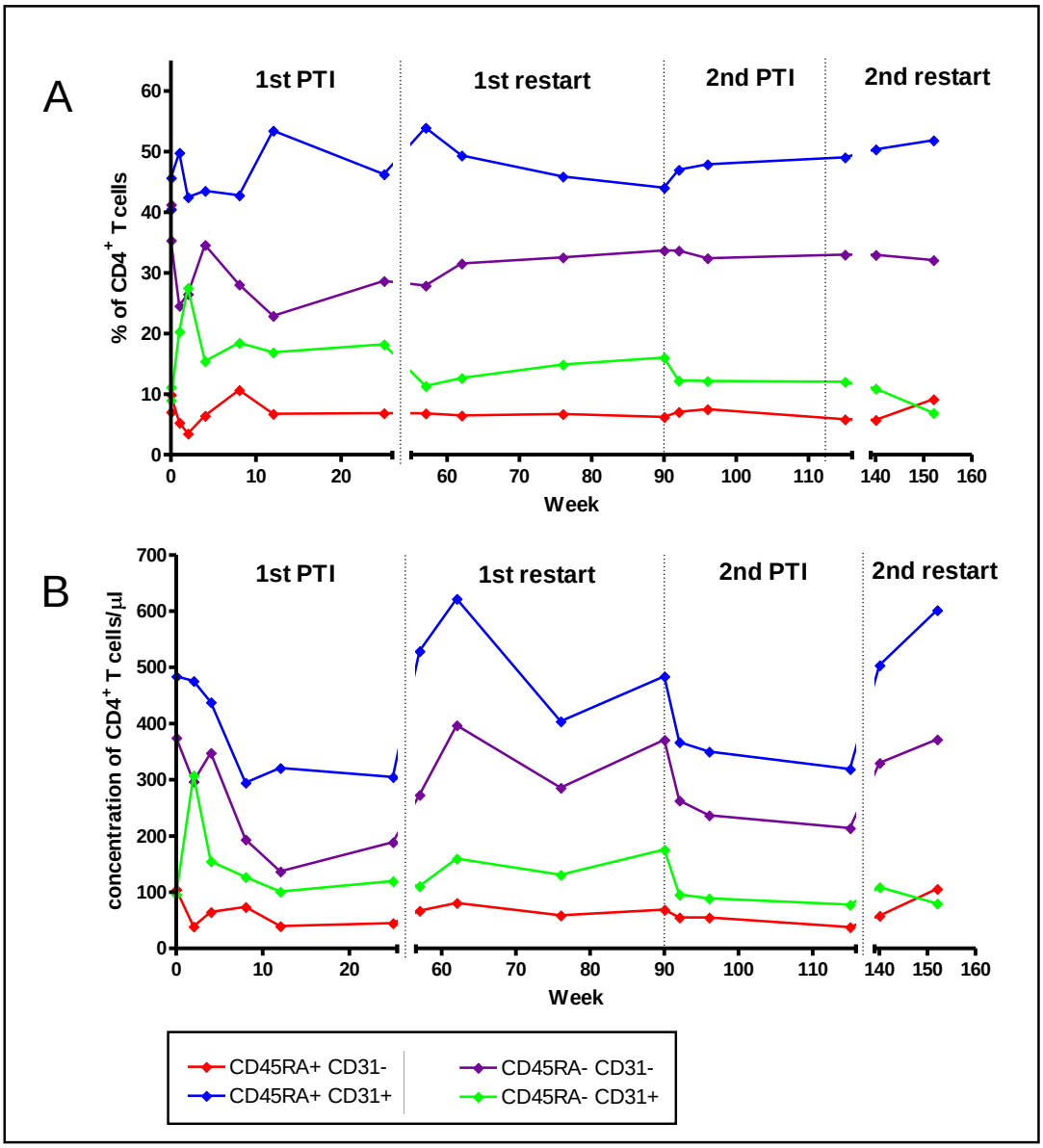

Figure 5.20 Variation of $CD4^+$ T cell subsets during serial interruptions

Percentage size and concentrations of $CD4^+$ T cell subsets are shown for a child who underwent 2 PTIs during the follow up period. $CD45RA^+CD31^-$, $CD45RA^+CD31^+$, $CD45RA^-CD31^-$ and $CD45RA^-CD31^+$ cells are shown in red, blue, purple and green respectively.

Percentage HLA-DR expression by $CD4^+$ T cells increased transiently during the 1st PTI and then reduced after the 1st restart. During the 2nd PTI the increase in HLA-DR expression was less than during the 1st PTI but was sustained before declining slightly during the 2nd restart. Within the $CD4^+$ T cell pool the largest increases in HLA-DR

expression occurred in the $CD45RA^{-}CD31^{-}$ subset, then the $CD45RA^{+}CD31^{-}$ subset and least in the $CD45RA^{+}CD31^{+}$ and $CD45RA^{-}CD31^{+}$ subsets.

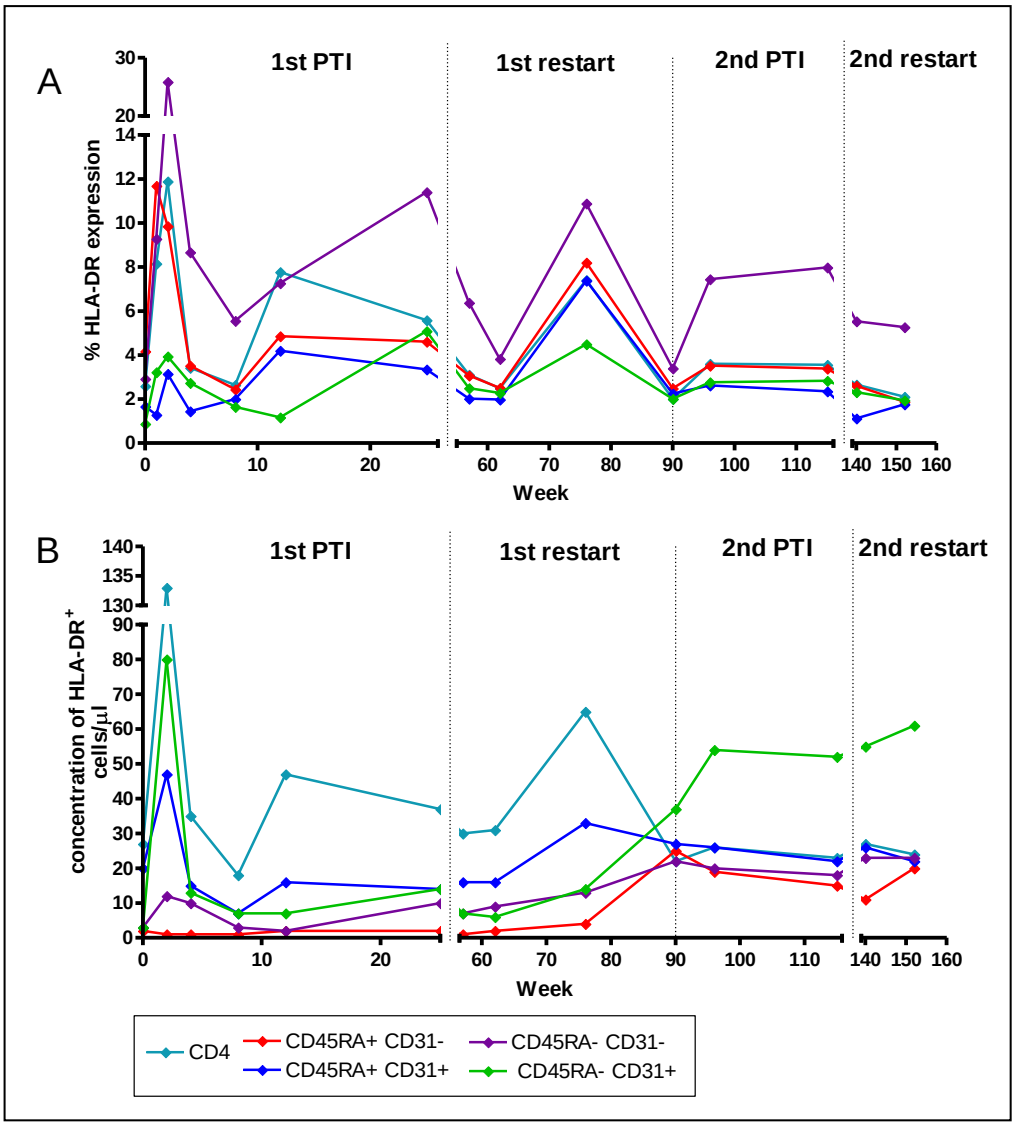

Figure 5.21 Variation in HLA-DR expression during serial interruptions

Percentage HLA-DR expression by $CD4^{+}$ T cells and concentration of $HLA\text{-}DR^{+}$ $CD4^{+}$ T cells (light blue) are shown for a child who underwent 2 PTIs during the follow up period. Percentage HLA-DR expression and concentration of $HLA\text{-}DR^{+}$ cells are also shown for the specific subsets $CD45RA^{+}CD31^{-}$, $CD45RA^{+}CD31^{+}$, $CD45RA^{-}CD31^{-}$ and $CD45RA^{-}CD31^{+}$ cells in red, blue, purple and green respectively.

The pattern seen with Ki67 was similar to HLA-DR. Specifically percentage Ki67 expression by $CD4^+$ T cells increased transiently during the 1st PTI and then again during the 1st restart. The increase during the 2nd PTI was smaller but declined again by the end of the 2nd PTI. Within the $CD4^+$ T cell pool the largest increases occurred in the $CD45RA^-$ subsets followed by the $CD45RA^+CD31^-$ subset. Ki67 expression by $CD45RA^+CD31^+$ cells appeared unchanged throughout. During the 1st PTI there was a transient increase in the concentration of $Ki67^+CD45RA^-$ cells against a decline in the total subset but this had declined by the 8th week and held steady until the 2nd PTI when they again increased transiently. The concentration of $Ki67^+CD45RA^+$ cells remained low throughout.

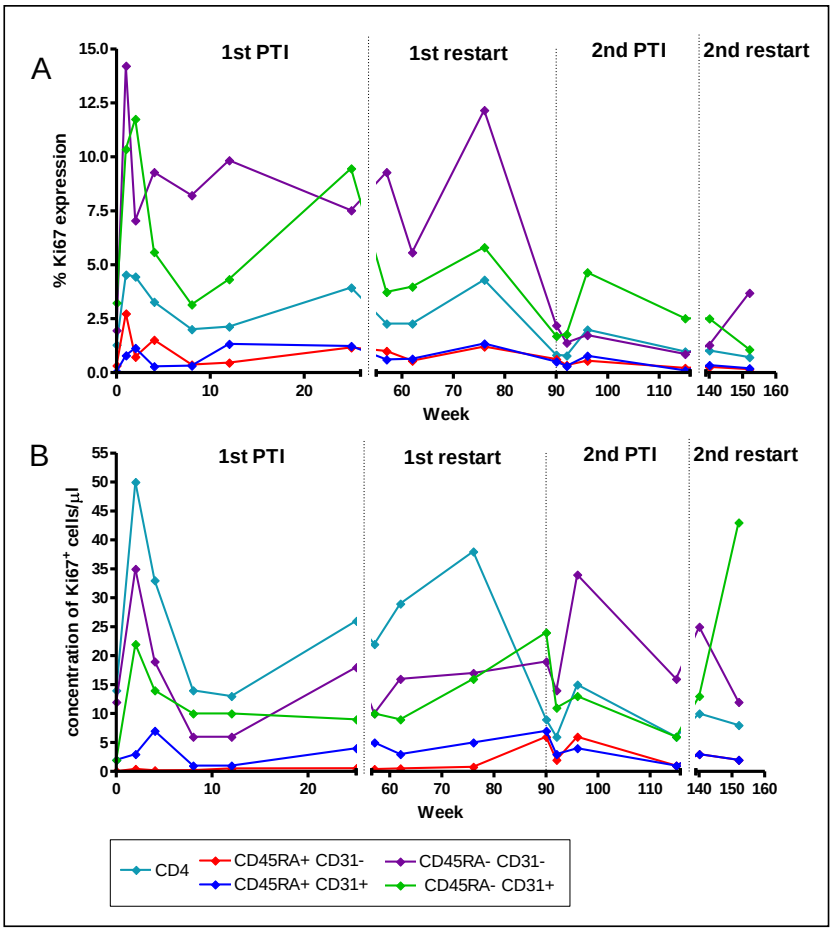

Figure 5.22 Variation in Ki67 expression during serial interruptions

Percentage Ki67 expression by $CD4^+$ T cells and concentration of $Ki67^+$ $CD4^+$ T cells (light blue) are shown for a child who underwent 2 PTIs during the study. Expression and concentration are also shown for the subsets $CD45RA^+CD31^-$, $CD45RA^+CD31^+$, $CD45RA^-CD31^-$ and $CD45RA^-CD31^+$ cells in red, blue, purple and green respectively.

5.4 DISCUSSION

This chapter describes the results of the first immunology study of its kind, in a trial of CD4 guided planned treatment interruption in children with sustained viral suppression, PENTA 11. Changes in proliferation and activation as determined by Ki67 and HLA-DR expression were investigated in CD45RA and CD31 defined $CD4^+$ T cell subsets during sequential periods of interruption and restart. Results were analysis was performed by assessing the relative change from baseline at various timepoints during both PTI and restart and compared to changes from baseline in the CT arm.

Most of the variables measured displayed a wide distribution in both the PTI and CT group and therefore their IQRs often overlapped. In fact CD4 count has been reported to be more variable in children undergoing unplanned PTI than in adults undergoing unplanned PTI (Gibb et al 2004).

Changes from baseline were detected in the PTI group for most parameters but interestingly even in the CT group parameters tended to show some variation from baseline during the study. These changes may reflect the dynamic nature of the $CD4^+$ T cell pool. The study was long, in excess of 2 years; therefore it was important to compare trends in the PTI group to age associated changes which would also occur in the CT group.

Changes to viral loads and lymphocytes were assessed in children assigned to CT and PTI using the values quantified by the GOSH and Padova University Hospital Clinical Immunology and Virology Laboratories. Over the follow up period there was a slow gradual decrease in the concentration of $CD4^+$ T cells in the CT arm, median 15% decrease from baseline at week 72 but there was no change to the percentage of CD4 cells during this time. The viral load was also unchanged in the CT group, remaining undetectable in almost all subjects. In comparison, both $CD4^+$ T cells and viral load

changed considerably in the PTI arm. By weeks 4 and 8 of PTI the concentration and percentage of $CD4^+$ T cells had decreased by a median of over 25% from baseline. Interestingly they did not fall any further after this point but remained at this level for the remainder of the PTI period. Similarly viral load increased by a median of almost 200% by week 4 of the PTI and stayed at this level for the duration of the PTI period.

Within 4 weeks of restarting treatment in the PTI arm, the CD4 concentration and percentage began to increase although only by a median of 12 and 10% respectively. However by week 24 of restarting treatment the median CD4 concentration had increased by over 25% but the median CD4 percentage had not increased any further. The IQRs ranges for percentage change in CD4 count were wide therefore some children experienced much larger increases than others and this in addition to the fact that children were older after restarting therapy than they were at the beginning of the PTI could explain why the median CD4 count experienced during treatment restart was less than that experienced in the CT arm and also lower than experienced during the PTI. Furthermore, in accordance with the results published for the whole PENTA 11 trial, the largest increases from base line occurred in the younger children, for example after 24 weeks of restarting therapy half the children were under 8 years and had a percentage change from baseline approximately 8-fold greater than in children 8 years and older. Viral load fell slowly upon restarting treatment, by week 24 of restarting treatment the median viral load had decreased by 75%. After this timepoint numbers were too small to draw further conclusions.

$CD4^+$ T cell subsets defined by CD45RA and CD31 were enumerated in children assigned to CT and children assigned to PTI. Over the follow up period the median percentages of subsets were unchanged in the CT group though there was some variation to the proportion of $CD45RA^-CD31^+$ cells. In the PTI arm there were transient changes to the median percentage of each subset by week 4, specifically decreases in the percentages of $CD45RA^+CD31^+$ and $CD45RA^+CD31^-$ cells and increases in the percentages of $CD45RA^-CD31^+$ and $CD45RA^-CD31^-$ cells. Where after the subset

percentages returned to baseline until at least week 24 of PTI. After week 24 of PTI the $CD45RA^{+}CD31^{+}$ and $CD45RA^{-}CD31^{-}$ cells decreased and increased respectively from baseline.

The absolute concentrations of the CD4 subsets were also determined for both treatment groups. In the CT group there was a slow gradual decline in the median concentration of $CD45RA^{+}CD31^{+}$ cells but the concentrations of the other subsets seemed unchanged. During PTI the concentrations of all $CD4^{+}$ T cell subsets appeared to decrease.

Upon treatment restart there did not appear to be any changes to the proportions of $CD4^{+}$ T cell subsets. However after 24 weeks of resuming treatment increases to the concentrations of CD4 subsets were observed. Although there was significant inter-patient variation the greatest percentage increases from baseline were in the $CD45RA^{-}CD31^{+}$ subset though this is partly a reflection of the small size of this subset i.e. a modest absolute increase would translate into a large percentage increase. The increased concentrations of $CD4^{+}$ T cell subsets upon treatment restart are more marked when compared to children undergoing CT who experienced decreased percentage changes from baseline.

$CD4^{+}$ T cell activation was monitored during the study by measuring the percentage HLA-DR expression in the total $CD4^{+}$ T cell population as well as in the subsets. In the CT arm there appeared to be little change from baseline to HLA-DR expression except for unexpected increase at week 8, which is most likely an anomaly. During PTI there were transient increases in the percentage expression of HLA-DR at week 2 which quickly returned to baseline and were unchanged for the rest of the PTI period. Intriguingly the transient increases were of higher magnitude in the $CD45RA^{+}$ subsets. During PTI there were decreases in the concentrations of $CD4^{+}$ T cells yet the concentration of $HLA\text{-}DR^{+}$ cells did not appear to change which would suggest that gain of $HLA\text{-}DR^{+}CD4^{+}$cells offsets loss of $HLA\text{-}DR^{+}CD4^{+}$cells.

Upon restarting treatment with HAART there was a slow and gradual decrease in the percentage HLA-DR expression and in the concentration of $HLA\text{-}DR^+$ cells.

$CD4^+$ T cell proliferation was monitored during the study by measuring the percentage Ki67 expression in the total $CD4^+$ T cell population as well as in the subsets. In the CT arm there was little change to Ki67 expression however during treatment interruption in the PTI arm Ki67 expression increased. Within the $CD45RA^+$ subsets there were transient early increases but in the $CD45RA^-$ subsets the increases were sustained for longer. The concentration of $Ki67^+$ cells was unchanged in the CT arm but increased during PTI despite decreased concentrations of all subsets. This would suggest that gain of $Ki67^+CD4^+$ cells exceeds loss of $Ki67^+CD4^+$ cells.

Upon restarting treatment there were moderate percentage decreases from baseline to both the percentage Ki67 expression and to the concentration of $Ki67^+$ cells.

Perhaps the most important theme to consistently emerge from these data is the importance of set points in HIV infection. Although treatment interruption results in initial perturbations to the percentage size of the CD4 subsets they quickly return to their baseline levels, their set point levels. Also the CD4 count and viral load only fell and rose respectively for the first few weeks of treatment interruption until they reach a set point. It is likely that processes controlling cell numbers such as activation and proliferation are important in re-establishing these set points because we detected early increases in HLA-DR and Ki67 expression in the $CD4^+$ T cell subsets, especially within the memory populations. A key to optimising PTI and HAART may to working out when these set points are established, how they are established and how they could be altered in favour of higher CD4 counts and lower viral loads.

Upon restarting treatment, Ki67 expression decreased but cell numbers increased which may suggest that the recovery is due to decreased loss rather than increased production.

In some children CD4 cells fell below 20% and therefore they resumed therapy after a shortened PTI but children who maintained CD4 cells above 20% were permitted to complete the full 48 week PTI. These children were termed ‘early’ and ‘late’ restarters respectively. 25% of children assigned to PTI in PENTA11 were early restarters, which is reflected in this substudy where 22% of the children on PTI therapy fell into this group. The starting values of age, CD4 count, CD4 subsets and HLA-DR and Ki67 expression were compared between the two groups in order to identify predictors of response to PTI i.e. factors associated with children who had to restart early but we found no statistically significant associations. However it is not clear if this is because none of these factors are predictors or because the numbers of children, especially in the early restart group, were too small.

An attempt was made to determine whether early and late restarters underwent dissimilar changes in response to interruption and restart. This could not realistically be interpreted because of small numbers and missing time points within subjects though the results may tentatively suggest that the transient increases in HLA-DR and Ki67 expression during PTI mentioned previously are steeper in early restarters than in late restarters, though this must be confirmed with more children and more samples. In this case higher HLA-DR expression in early restarters may explain why they experience a quicker fall in CD4 count and hence had to restart treatment sooner.

Data was also provided on a 2nd further PTI and 2nd restart period for one child. The decrease in absolute cell numbers was around 15% smaller in the 2nd PTI compared to the 1st PTI. Smaller increases to HLA-DR and Ki67 expression occurred during the 2nd PTI compared to the 1st. Although data from more than one child is required to make any conclusions the data does suggest that there may be an improvement to cell loss and the

degree of immune activation and proliferation as measured by HLA-DR and Ki67 expression respectively, during subsequent PTIs. This has also been suggested by an adult PTI trial that employed several short cycles of treatment interruption (Borkowsky et al 2008). Therefore it would be interesting to assess further periods of interruption in more children. The child described here was followed for 3 years so any trial investigating more periods of interruption would be liable to run for over 5 years.

This study was constrained by low numbers and this is most evident in the analysis of 'early' and 'late' restarters. Greater numbers were required therefore ideally we would have liked to extend the study by obtaining aliquots of PBMCs from other PENTA11 trial sites within Europe specifically biased towards children who restarted early. Equal numbers of early and late restarters of adequate sample size would have strengthened the results of any analysis. A number of time points had been missed for the various reasons discussed. This was especially problematic if baseline PTI and baseline restart values were not available because changes during PTI and restart could not be investigated. A significant number of the time points missed were for samples that contained mostly dead cells and were not viable.

$CD4^+$ T cell sub-populations, immune activation and proliferation have not been investigated in paediatric PTI trials. However a recent adult PTI trial conducted by Libois et al investigated immune activation and naïve and memory cell dynamics during cycles of PTI (Libois et al. 2006). They used 5 cycles of 2 weeks off and 8 weeks on therapy followed by a 12 week treatment interruption after which most patients remained off therapy until viral load peaked. They assessed immune activation of $CD4^+$ T by CD38 expression and found no significant increase in CD38 expression during neither the short nor the long treatment interruptions, compared to period of HAART before the interruption. (Libois et al 2006). However this trial featured much shorter PTI periods, 2 weeks compared to the 48 weeks used for the PENTA trial and we did not detect increased HLA-DR expression until week 2-4. We presented data from the 2^{nd} interruption period for one child in PENTA 11 where HLA-DR expression was around

80% lower than during the 1st PTI therefore we propose that multiple interruption cycles decrease the sensitivity of $CD4^+$ T cells to immune activation which may explain why Libois et al found CD38 expression unchanged after the long interruption.

Libois et al assessed naïve and memory cells by CD45RO, CD45RA and CD62L and found that that during the 2 week PTI periods the percentage of naïve cells was higher and the percentage of memory cells were lower than during the prior 8 week HAART. During the 12 week treatment interruption they found that the percentage of naïve cells was unchanged and the percentage of memory cells had decreased and when the viral load peaked after 50-106 weeks of interruption they found that the percentage of naïve cells and memory cells had decreased and increased respectively (Libois et al 2006). By comparison we found that percentages of naïve and memory cells appeared unchanged after 48 weeks of interruption. However as we determined the concentrations of the subsets we noted that the concentrations of naïve and memory subsets fell during interruption. The concentration of naïve and memory cells were not provided by Libois et al therefore the increased naïve and decreased memory percentages could be associated naïve cell concentration falling slower than the memory cell concentration or the memory cell concentration rising faster than the naïve cell concentration.

The increased immune activation during PTI that we reported in this study appeared to be transient but immune activation is associated with CD4 depletion as discussed in chapter one. Garcia et al have proposed that the therapeutic use of treatment interruption might be improved by use of immuomodulating agents such as corticosteroids to decrease non-specific activation without blunting the anti-HIV CTL response (Garcia, Fumero, & Gatell 2008).

The results of this study cannot strongly advocate the use of PTI as part of the management of HIV infection in children. Greater sample numbers and a longer follow up period are required to look for any long term consequences. However the study does suggest that in the short term there are unlikely to be any major deleterious effects of PTI especially in younger children and that most changes are transient or at least

reversed by re-introducing treatment. Therefore weighed against the prospect of running out of ARV combinations as HIV-infected children grow into adulthood and toxic effects of ARVs, PTI should be given serious consideration as a long term treatment modality.

CHAPTER 6

QUANTIFICATION OF HIV DNA IN $CD4^+$ T CELL SUB-POPULATIONS

6.1 INTRODUCTION

As described in chapter one, most anti-retroviral drugs prevent the infection of new cells and virus production by interference with either HIV viral enzymes or structural proteins (Pomerantz and Horn 2003). Therefore, HAART is only usually efficacious against replicating virions. This allows non-replicating viruses to make up the latent viral reservoir. Virions can enter this latent phase at any point after target cell entry. The virion can be found in RNA or DNA forms, generated by reverse transcription. Unintegrated RNA and DNA forms of HIV are highly labile and are not transmitted to daughter cells during mitosis. However, the viral genome is stabilised following integration into the host genome, which permits HIV transmission to daughter cells during cell division. During this phase, the integrated virus, known as the provirus, requires active transcription and translation by host cellular machinery to generate new virions. The provirus is lost when the host cell dies (Blankson, Persaud, & Siliciano 2002). HIV infection is higher in populations of cells that have a high turnover. Homeostatic proliferation in the absence of new infection will dilute the proviral concentration. As such the concentration of the latent HIV reservoir in CD4 cell populations is at least partly determined by the rate of cell turnover.

6.1.1 The viral reservoir

Shortly after implementation of HAART, it was predicted that long-term HAART treatment would lead to complete eradication of HIV from the body. During effective HAART, HIV RNA could not be detected in the plasma by commercially available assays with detection limits of 50 copies/ml.

By contrast, ultrasensitive assays which can detect a single copy have demonstrated a low level viraemia and ongoing replication in virally-suppressed individuals. Without treatment, viral suppression is not sustained, and HAART discontinuation leads to rapid resurgence of viral load, which may be due to the latent persistence of replication-competent virus in long-lived populations of resting memory cells (Garcia et al. 1999), (Stephenson 1999).

In section 1.4.1, the evolution of plasma viral load during untreated HIV-1 infection from first an acute phase of high-level viraemia, which then declines to a set point that exists for an extremely variable length of time before finally a steep increase of viral load occurs was described. HAART alters the natural course of viral load. During HAART the plasma viral load decreases over three distinct phases, as shown in Figure 6.1. During the first phase, an exponential decrease in viral load by 1-2 logs, during the first 2 weeks of therapy is seen, due to rapid viral clearance and turnover of short-lived productively infected $CD4^+$ T cells. The second phase is slower and reflects turnover in longer lived populations if HIV infected cells; these include infected macrophages and less activated $CD4^+$ T cells which permit limited viral replication. The third phase occurs several months after initiating HAART and can last for several years. At this time plasma viral load is below the limit of detection but low level viraemia persists in plasma and other compartments such as semen while replication competent virus persists in latently infected cells (Kim and Perelson 2006).

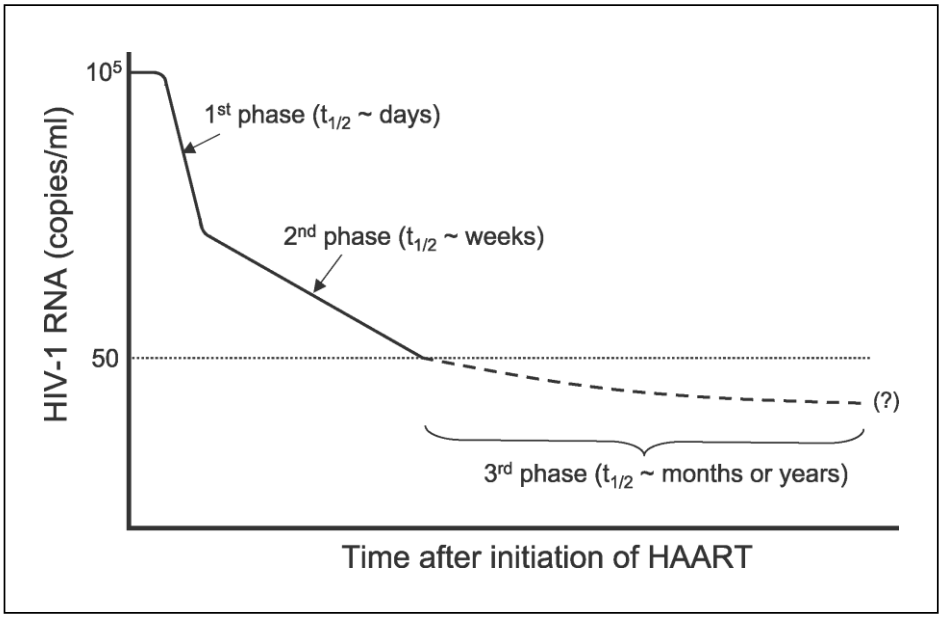

Figure 6.1 Schematic illustrating the dynamics of HIV-1 decay upon initiating HAART
The graph shows the decay in plasma viral load over three phases. From (Kim and Perelson 2006)

Mathematical models of the decay of the latent HIV reservoir have been formulated, which take into account entry of newly infected cells into the latent reservoir, latent cell activation and homestatic proliferation of latently infected cells. They suggest that the stability of the latent reservoir is unlikely to be due to ongoing replication during HAART and that therefore intensification of HAART is unlikely to have significant effects on the decay of the latent reservoir (Sedaghat et al. 2007), (Kim and Perelson 2006).

Large populations of HIV infected cells reside in lymphoid tissue in the gut in gut associated lymphoid tissue (GALT). It has been proposed that progressive loss of $CD4^+$ T cells from the gut may irreversibly damage the immune barrier required to prevent bacterial translocation into the bloodstream (Douek 2007). Vulnerability to bacterial translocation increases the risk of opportunistic infection and the levels of bacterial products which can increase T cell activation in the blood and lymphoid tissue. It is not generally feasible, however, to investigate the HIV viral reservoirs outside the circulation and therefore this study is limited to studying intracellular HIV in $CD4^+$ T cells sampled from peripheral blood.

The majority of the latent reservoir resides in central memory cells as these are both preferentially infected, and have a longer life-span than effect memory cells.

It is not known if planned treatment interruption (PTI), previously discussed in chapter 5, affects the size of the viral reservoir in different $CD4^+$ T cell populations. Initially the loss of viral suppression might result in expansion of the latent viral reservoir if replication is free to occur.

The aim of this chapter was to

1. Develop methods to separate naïve and memory $CD4^+$ T cells from PBMCs

2. Develop methods to quantify intracellular HIV within these cells.

These techniques were then applied to a group of children participating in a PTI trial (see chapter 5).

6.2 METHODS

6.2.1 Isolating Naïve and Memory $CD4^+$ T cells

As discussed in chapters one and three, the transition of $CD4^+$ T cells from a naïve to memory phenotype is associated with decreased expression of CD45RA and increased expression of CD45RO (Akbar et al 1988). Therefore a population of naïve cells can be defined as a group of $CD4^+$ T cells that highly express CD45RA and a population of memory cells as cells that highly express CD45RO. Antibodies specific for the CD4, CD45RA and CD45RO cell surface proteins can be used to separate these populations from PBMCs either by fluorescence activated cell (FACS) sorting or immuno-magnetic cell separation.

To comply with safety regulations, HIV infected samples must be fixed with formaldehyde before introduction to the fluorescence activated cell sorting facility at the Institute of Child Health (ICH). However it is difficult to extract viable DNA from formaldehyde fixed samples because formaldehyde cross links DNA to protein and formaldehyde residue inhibits PCR by reacting with the cytosine, guanine and adenine bases (Schander and Kenneth 2003). As such it was not feasible to employ a FACS sorting method at ICH and therefore an immuno-magnetic method was employed (Miltenyi) which uses antibodies covalently bound to metal beads to separate cells within a magnetic field. Cells which express the target epitope of the antibody are separated from those not expressing the target antigen by passing the cell-antibody-bead suspension through a column matrix within a

magnetic field. The magnetically labelled cells are retained in the column (positive selection) and unlabelled cells pass through into a collection vessel (negative selection) Cells retained in the magnetic field can be collected by removing the cell column from the field and washing the cells into a suitable container. The process is shown in Figure 6.2.

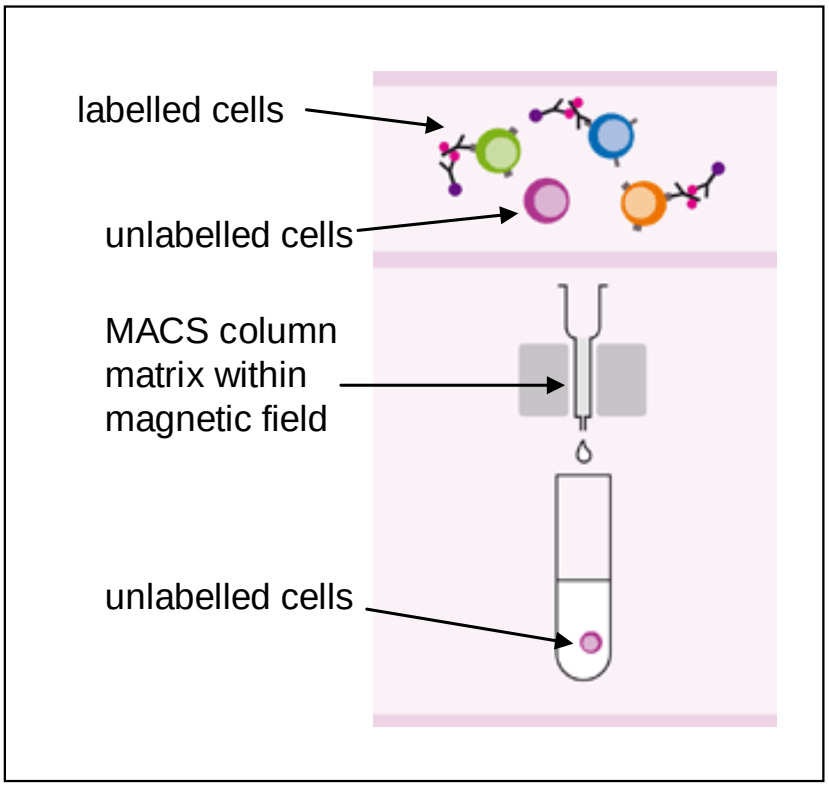

Figure 6.2 Principle of immuno-magnetic separation with Miltenyi reagents
The diagram shows how after incubation with antibody bound microbeads labelled cells are retained on the column and unlabelled cells pass through. Adapted from (Miltenyi Biotech 2009)

Ideally, if sufficient PBMCs are available, naïve and memory populations can be obtained using the 4 step separation shown in Figure 6.3. A cocktail of antibodies is used to negatively select $CD4^+$ T cells followed by CD45RO microbeads to obtain relatively pure populations of naïve, $CD45RO^-$, and memory, $CD45RO^+$ cells. These populations can then be further purified using CD45RA microbeads. However this four step separation protocol was not feasible in this study because of the small numbers of cells available. As CD45RA

and CD45RO expression is almost reciprocal, contamination with cells positive for both CD45RA and CD45RO is low. In chapter 3 $CD45RA^{+}CD45RO^{+}$ cells were found to make up less than 5% of the $CD4^{+}$ T cell population and therefore the first two steps, the CD4 negative selection and the CD45RO separation, were considered sufficient.

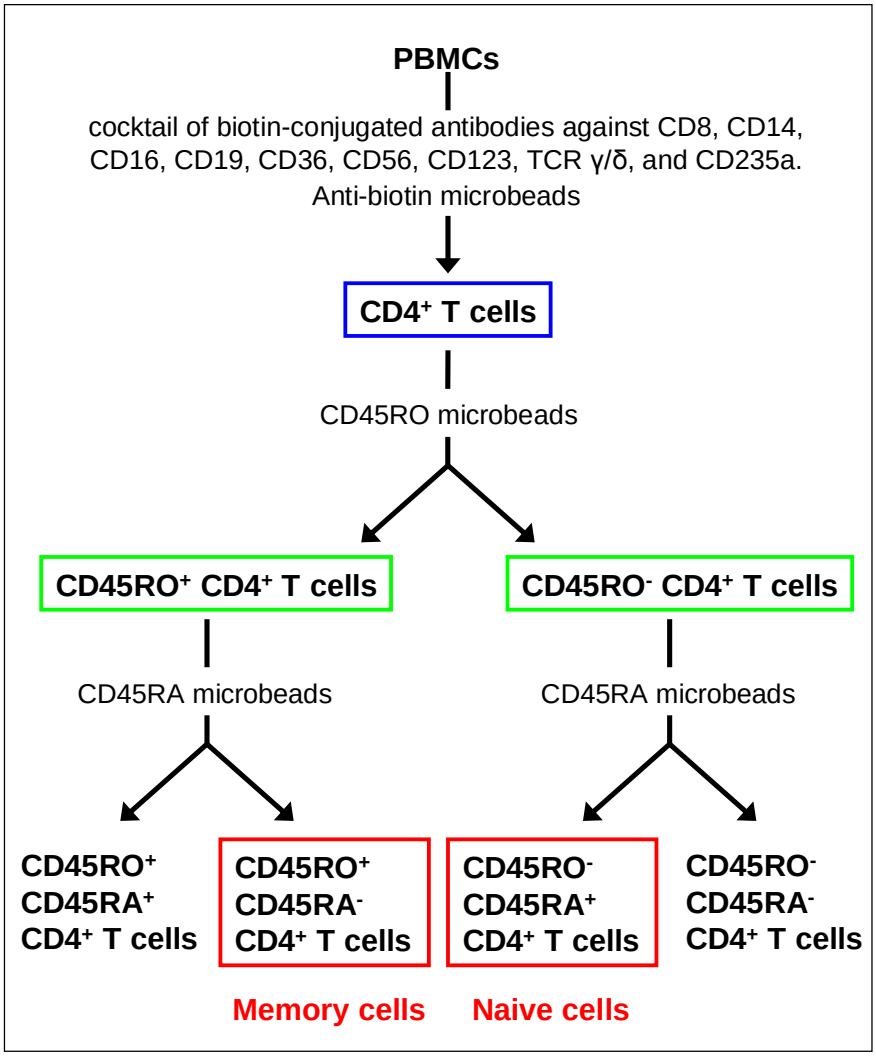

Figure 6.3 Schematic of naive and memory separation

The diagram shows how 4 immuno-magnetic separations, a CD4 negative selection, a CD45RO selection and two CD45RA selections could be used to obtain populations of naïve and memory cells.

6.2.2 Separation of naïve and memory populations and assessment of purity

Isolation of PBMCs from whole blood, and the separation of naïve and memory populations, were carried out as described in methods and materials section 2.2.1 and 2.2.5. The purity of the enriched $CD45RA^+$ $CD4^+$ T cells and $CD45RA^-$ $CD4^+$ T cells was determined and compared to PBMCs by incubating 10^5 cells with antibodies against CD4 and CD45RA and analysed by flow cytometry. Typically 70% and 80% purity were achieved for $CD45RA^+$ $CD4^+$ T cells and $CD45RA^-$ $CD4^+$ T cells respectively compared to less than 20% before separation (Figure 6.4).

In accurately assessing purity it was important that the epitopes of the fluorescently tagged antibody did not coincide with the epitopes of the metallic bead tagged antibody. As the clones used by the manufacturer could not be disclosed purity was assessed using a CD45RA antibody instead of both CD45RO and CD45RA antibodies. Figure 6.4 showed that contamination of naïve cells and memory cells would be $CD45RA^-CD45RO^-$ cells and $CD45RA^+$ $CD45RO^+$ cells therefore the use of a CD45RA antibody enabled that contamination to be assessed.

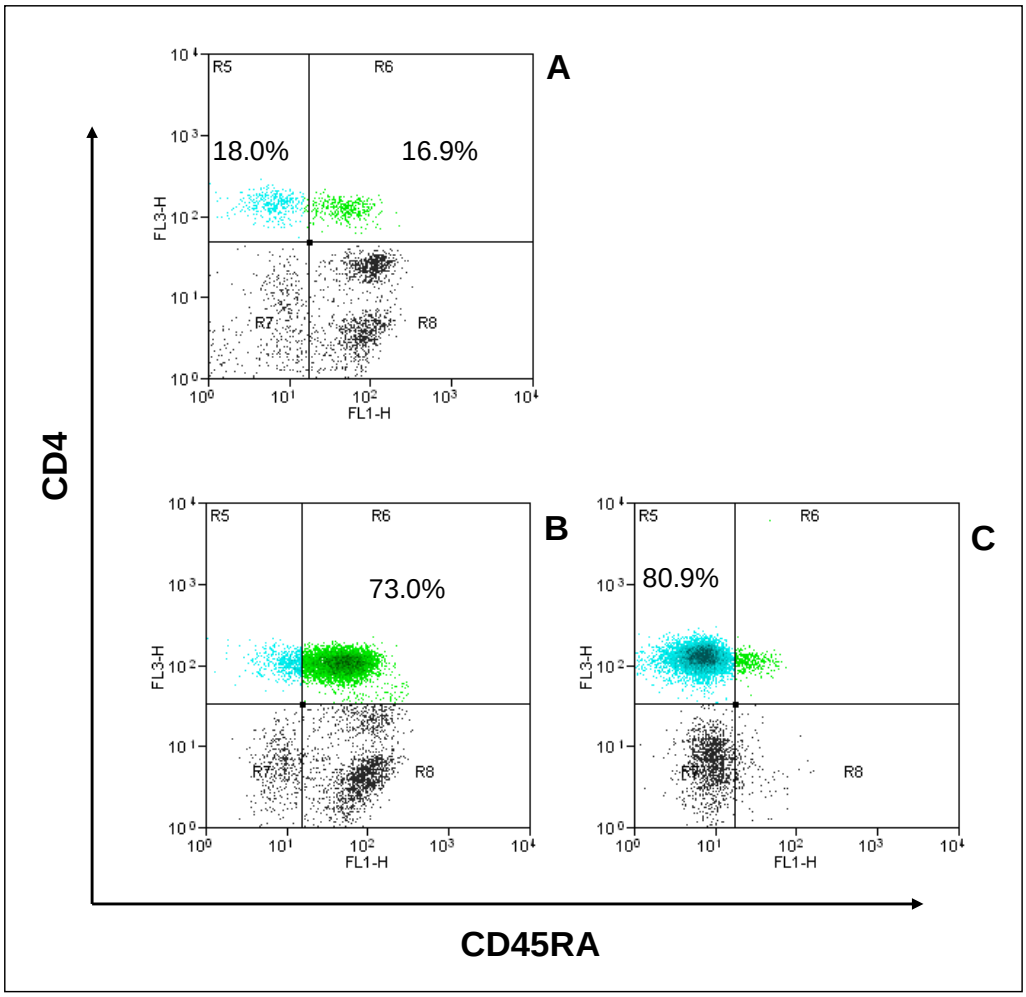

Figure 6.4. Flow cytometric analysis of pre and post separation $CD4^+$ T cell sub populations.
PBMCs pre separation and cell post separation were incubated with antibodies against CD4 and CD45RA and analysed by flow cytometry. A) Pre separation $CD45RA^+$ $CD4^+$ T cells and $CD45RA^-$ $CD4^+$ T cells were 16.9% and 18.0% respectively. B) After $CD4^+$ T cell selection and CD45RA positive selection $CD45RA^+$ $CD4^+$ T cells were 73%. C) After $CD4^+$ T cell selection and CD45RA depletion $CD45RA^-$ $CD4^+$ T cells were 80.9%.

This method of separation resulted in a population purity considered to be insufficient to accurately quantify the HIV DNA in the cell populations of interest. This was primarily caused by CD4- cells passing through the column in the first step and contaminating the population. Thus, the $CD4^+$ T cell negative selection step was optimised, as described below in section 6.2.3.

6.2.3 Optimisation of CD4 selection

Initially, the $CD4^+$ T cell isolation was carried out according to the manufacturer's instructions, as described in materials and methods section 2.2.5. This included incubating the PBMCs with a biotin-antibody cocktail for 10 minutes. To investigate whether I could improve the purity of separation by increasing the length of this incubation, so increasing the chance of antibody interaction with cell surface antigens, I incubated aliquots of the PBMCs with the biotin-antibody cocktail for 10, 30 or 60 minutes. The remainder of the protocol was carried out according to the manufacturer's protocol.

The purity/enrichment of $CD4^+$ T cells was compared across the 3 incubation periods by flow cytometric analysis. It was possible that increasing the incubation time could have increased the amount of non-specific binding and as such, $CD4^+$ T cells would have been retained within the magnetic field. Therefore the proportion of $CD4^+$ T cells retained in the $CD4^-$ fraction was also assessed, and compared across the 3 incubation periods. Dot plots of the results are displayed in Figure 6.5. After 30 and 60 minutes the purity of $CD4^+$ T cells was much greater than after 10 min: 95.7% and 94.0% compared to 85.2% respectively. The proportion of $CD4^+$ T cells within the $CD4^-$ fraction, a measure of non-specific binding, did not increase greatly as the incubation period was extended from 10 minutes to 30 minutes and 60 minutes: 1.7% to 1.8% and 1.9% respectively. As a result of these studies the 30 minute incubation was used for subsequent studies.

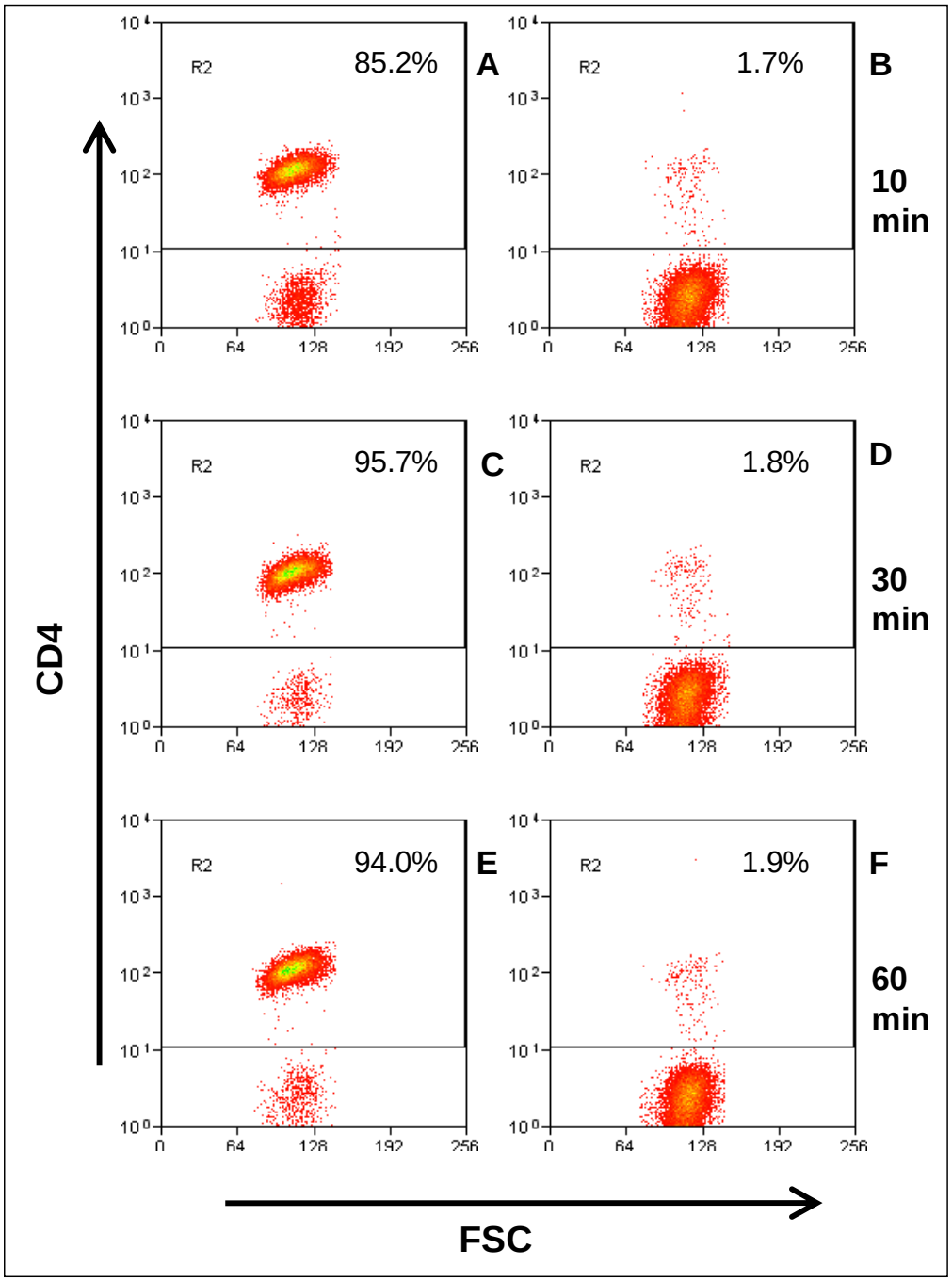

Figure 6.5 Purity of $CD4^+$ cells recovered with different incubations

PBMCs were incubated with a cocktail of antibodies for 10, 30 or 60 min. The purity of $CD4^+$ T cells obtained for each period and the percentage of $CD4^+$ T cells within the $CD4^-$ fraction, lost by non-specific binding, were assessed by flow cytometry. The purity of cells recovered using a 10 min incubation is shown in A and the corresponding proportion of cells in the $CD4^-$ fraction is shown in B. C and D, and E and F show the same results from a 30 and 60 min incubation respectively.

6.2.4 Assessment of separation of frozen PBMCs

The PBMC samples from the PENTA11 cohort were only available as frozen cells, therefore it was important to ascertain that a high level of purity could also be attained using frozen PBMCs. With this in mind, PBMCs from a healthy donor were frozen and thawed using the same conditions as those used for the PENTA11 samples, described in materials and methods section 2.2.1. Once assessed for viability and separated as described in materials and methods sections 2.2.1.4 and 2.2.5, but with an initial incubation time of 10 minutes instead of 30 minutes. The purity of the naïve and memory cells obtained was assessed by flow cytometric analysis of CD4 and CD45RA expression as shown in Figure 6.6.

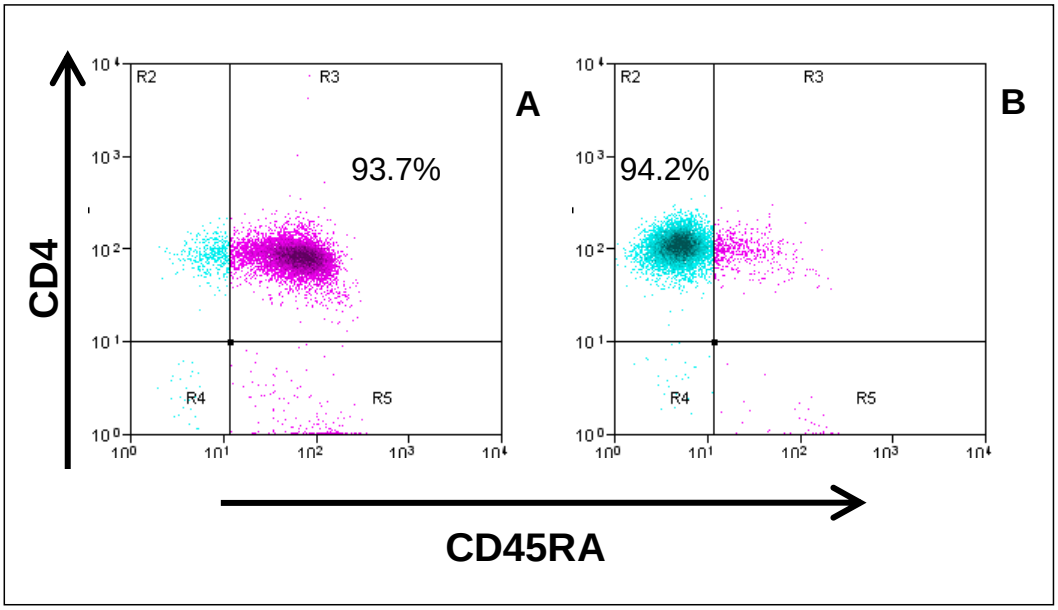

Figure 6.6 Purity of naive and memory CD4$^+$ T cells obtained from frozen PBMCs
Frozen PBMCs from a healthy donor were thawed and naïve and memory CD4$^+$ T cells separated out. The purity of the populations was assessed by flow cytometric analysis of CD4 and CD45RA expression. The naïve and memory cells are shown in A and B respectively.

As only a small number of PBMCs were available for each time point for each child in the PENTA11 trial it was not possible to assess the purity of the separated naïve and memory

cells for every sample. Two PENTA 11 and four healthy donor samples were assessed to determine if the purities obtained could be reliably generated with other samples. The lowest and highest purities of naïve cells were 93.1 and 99.7% $CD4^+CD45RA^+$ respectively. The lowest and highest purities of memory cells were 93.8 and 96.5% $CD4^+CD45RA^-$ respectively.

However, it is important to remember that a population of memory cells obtained in this manner, with 100% CD45RO expression, would also have low level CD45RA expression.

6.3 DNA EXTRACTION AND PURITY

Following separation of the CD4 cells into CD45RA and CD45RO population, DNA was extracted. The microbeads used for the separation do not affect subsequent experiments with the cells, as stated by the manufacturer and demonstrated in (Rambaldi et al. 1998). DNA extraction and quantification was performed and DNA purity assessed as described in materials and methods section 2.2.6. However, the DNA was eluted in Tris EDTA (TE) buffer instead of water to minimise degradation during storage at -80°C (Kaneko and Nakagata 2006). Although the negatively selected naïve cells CD45RO- did not have bound microbeads, the positively selected memory cells did. However, both the naïve and memory cells had 260/280 ratios, as assessed by nanodrop spectrophotometry, of between 1.78 and 1.82. A ratio of 1.8 is considered to be the ratio obtained with pure DNA.

6.4 QUANTIFICATION OF HIV DNA

6.4.1 Aims of assay

The following sections of this chapter describe the development of a quantitative real-time polymerase chain reaction assay. The assay was adapted from a semi-quantitative protocol used by University College Hospital (UCH) Diagnostic Virology Services to diagnose HIV infection in newborns. The following features were considered desirable in the assay required for the intended studies:

- To quantify the number of cells (equivalent to the DNA present in the reaction) and the number of copies of HIV DNA in the same tube at the same time so the concentration of HIV DNA could be assessed.
- To be specific so that no pseudogenes would be amplified while all HIV-1 virus subtypes could be amplified and accurately quantified
- To linearly amplify a wide range of template quantities for accurate and reliable quantification
- To be sensitive enough that even very small template quantities could be amplified and accurately quantified
- To be reproducible when repeated with multiple different samples

6.4.2 Introduction to multiplex real-time PCR

Quantitative real-time Polymerase Chain Reaction (qPCR) follows the general principles of PCR in that large quantities of a specific nucleotide sequence are generated using a DNA polymerase enzyme, usually *Taq*, a heat-stable DNA polymerase originally isolated from *Thermus Aquaticus*. First heat is applied to DNA to separate the strands, referred to as the template, then two short lengths of nucleotide sequence, around 20 bases, called primers or oligonucleotides anneal to their complementary sequence on the template. The DNA polymerase, which is usually heat activated (hot start PCR) attaches to a primer-template hybrid and synthesizes a complementary strand from the 5’ end until it reaches the primer-

template hybrid at the 3’ end when it detaches. Multiple cycles result in an exponential increase in the amount of DNA template.

In qPCR a DNA sequence is simultaneously amplified and quantified by coupling PCR amplification to the principle of fluorescence resonance energy transfer (FRET). Thus in addition to a pair of primers, the system includes another oligonucleotide. This probe bears a fluorescent reporter at one end and a fluorescence quencher at the other. Like the primers, the probe hybridises to a complementary sequence on the template located between the binding sites of the primers. While the probe remains intact fluorescence is quenched by the proximity of the quencher to the reporter. However during PCR the probe is degraded by *Taq* and fluorescence is emitted and detected by the fluorescent spectrophotometer of a real-time PCR thermal cycler (Figure 6.7). Thus an increase in fluorescence is proportional to an increase in the probe’s target sequence i.e. the amount of amplicon produced. Real time refers to the fact that after each cycle, the amplified DNA is quantified. The data is reported as a cycle threshold (CT), the number of cycles after which the level of fluorescence exceeds the background fluorescence threshold, set within the exponential phase of the PCR. In reactions with low target sequence abundance enough PCR cycles must be allowed to achieve the CT.

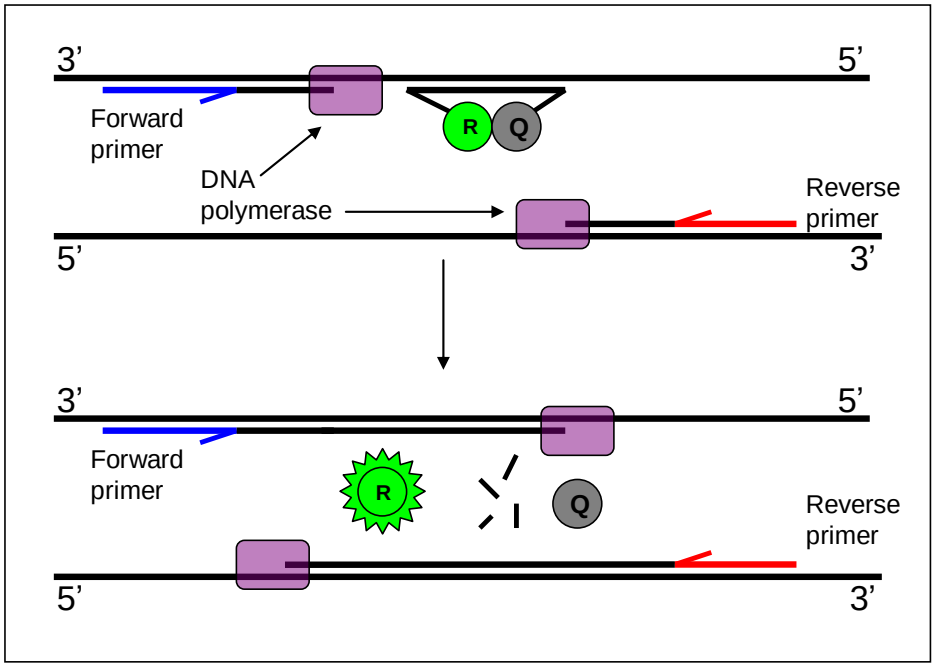

Figure 6.7 Principle of quantitative PCR

DNA polymerase is shown moving along the template and synthesising the nascent strand. Upon encountering the probe the exonuclease activity degrades the probe, liberating the reporter molecule (R) from the quencher molecule (Q) and fluorescence is emitted.

Multiplex PCR, where two or more targets are simultaneously amplified, enables the quantity of HIV to be compared to a cell number by amplifying both cellular and viral targets in the same reaction. Thus a concentration can be obtained which can be compared between children and between different time-points of the same child. Multiplex also has added advantages of reducing the amount of template used because multiple genes are quantified in the same reaction tube. In addition errors in the amplification of one target are usually cancelled out by errors in the amplification of the other target if multiplex reactions are used.

The assay used by UCH Diagnostic Virology Services was used to confirm HIV infection in newborns. As explained in section 1.5.2 detection of anti-HIV antibodies by ELISA is unreliable in infants because maternally derived antibodies are present in the circulation.

Therefore diagnosis is made by detecting the presence of HIV virions using PCR. The HIV virions contain an RNA genome therefore the UCH assay is an RT-qPCR assay because first the RNA target template is reverse transcribed to DNA then the DNA is amplified and quantified. HIV RNA is much more abundant than HIV DNA therefore a high level of sensitivity was not required for diagnostic purposes and the assay did not produce linear amplification of the targets. Therefore, as it stood, it could not be used to accurately quantify the concentration of HIV DNA in DNA extracted from naïve and memory cells. Therefore, the RT step was removed and the assay was adapted as described in the following sections, using the reagents and reaction conditions described in materials and methods section 2.1.3, 2.1.4 and 2.2.7.

6.4.3 PDH primer titration

The multiplex HIV DNA assay developed consisted of two reactions, amplification of the HIV target gene and amplification of an internal reference gene also called a housekeeping gene. The housekeeping gene is present as two copies in every somatic human cell. Therefore the number of copies of the gene present in the reaction corresponds directly to the cell number.

Pyruvate dehydrogenase (PDH) is an enzyme within the PDH complex involved in the process of transforming pyruvate into acetyl-CoA for use in the citric acid cycle (Patel and Roche 1990). Aliquots of *PDH* forward and reverse primers and probe were kindly provided by UCH Diagnostic Virology Services, who use *PDH* as the housekeeping gene in their in-house semi-quantitative HIV DNA assay. *PDH* also serves as a positive internal control for the HIV gene amplification reaction as *PDH* would always be present providing cellular DNA was present.

As the RT step was removed and the target sequences would be much less abundant than in the original UCH assay, all reagent concentrations were re-titrated around the

concentrations used by the UCH assay but within the ranges recommended for the *Taq* enzyme formulations used. To determine the concentration of the *PDH* primers to use, a set of reactions with a 2-fold range of effective *PDH* primer concentration from 300 nM down to 18.75 nM were set up in duplicate to amplify 6 ng of human placental DNA (equivalent to 1 000 cells). An additional pair of reactions with *PDH* primers used at a final concentration of 300 nM were set up as a non-template control (NTC) with water instead of the human placental DNA template. The concentration of *PDH* probe was unchanged and all other reaction conditions were as used by the UCH diagnostic virology service: 400nM *PDH* probe, 12.5 µl of 2X Stratagene Brilliant II QPCR mastermix, 6 ng of human placental DNA, equivalent to 1 000 cells, distilled water to make up a final reaction volume of 25 µl. The thermal cycling conditions for the Stratagene Brilliant II QPCR mastermix are shown in Table 2.4.

The results of the qPCR reactions were displayed as amplification plots as shown in Figure 6.8. Fluorescence above the threshold was detected for each pair of reactions at all concentrations of *PDH* primer, except the NTC. This indicated that that the reaction mixtures were unlikely to be contaminated. The CT increased and the relative fluorescence decreased with decreased concentrations of *PDH* primers. From these experiments 300 nM was accepted as the best *PDH* primer concentration in the series as it had the lowest CT and greatest amplitude of fluorescence. However, the range of concentrations only extended up to 300 nM therefore it was possible that a concentration higher than 300 nM might have produced better results.

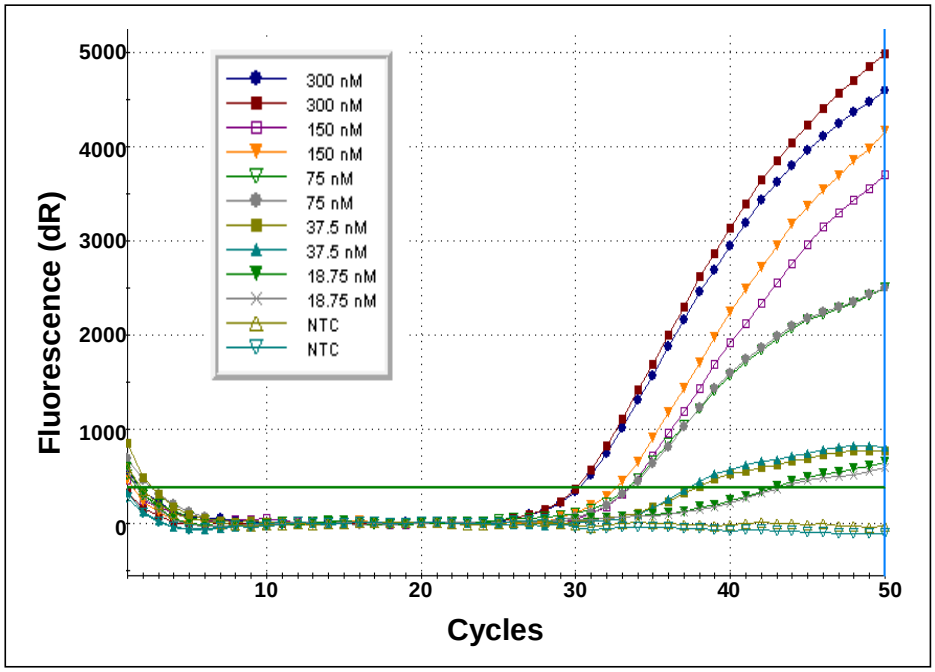

Figure 6.8 Amplification plots of *PDH* primer titration

QPCR reactions to amplify DNA equivalent to 1000 human placental cells were set up with decreasing concentrations of *PDH* primers. The amplification curves generated at each concentration are indicated on the graph. No product was produced in the non-template control (NTC) reactions.

6.4.4 PDH probe and further primer titration

A further titration of the PDH primers was performed over the range 600 nM to 300 nM to determine if higher concentrations would produce lower CTs. This was combined with a titration of the *PDH* probe concentration from 400 nM to 100 nM. For each primer-probe combination the reaction was set up in duplicate. 6 ng human placental DNA was amplified as before.

The results of the qPCR reactions are displayed as amplification plots in Figure 6.9. There was little to distinguish the primer-probe combinations in CT as they all occurred between 30 and 31 cycles. There was however some difference in the amplitude of relative fluorescence. The 3 highest amplitudes were produced by reactions where the *PDH* probe concentration was 400 nM and the primer concentrations were 450nM or 600 nM. The 6

lowest curves were all produced by reactions where the *PDH* probe concentration was 100 nM and the primer concentrations were 600 nM, 450 nM and 300 nM. These results suggest over the ranges tested the optimum concentrations for the *PDH* probe and primers were 400 nM and 600 nM respectively.

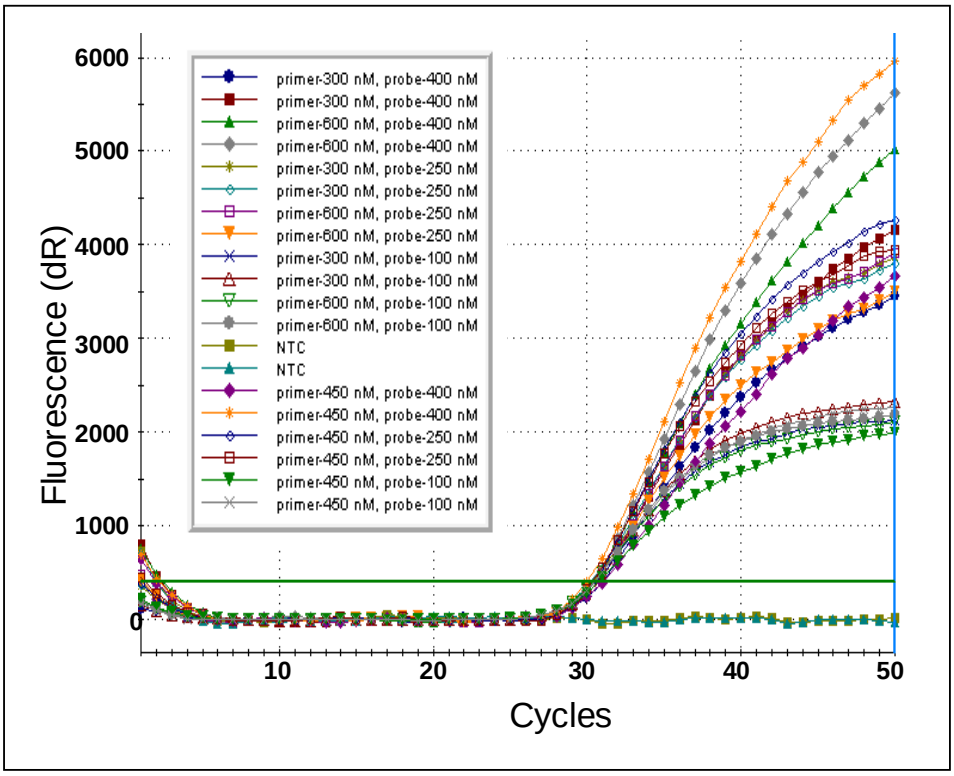

Figure 6.9 Titration of *PDH* probe and primers concentration

QPCR reactions to amplify DNA equivalent to 1000 human placental cells were set up at varying concentrations of *PDH* probe and primers. The amplification curves generated with a probe concentration of 400 nM and 100 nM are indicated on the graph. The green horizontal line indicates the fluorescence threshold and NTC indicates the pair of the non-template controls.

6.4.5 Standard curve to calibrate assay for cell number

The *PDH* qPCR reaction was to be used to quantify the cell number equivalent in each well. Therefore the following experiments were performed to assess if a wide range of template quantities could be amplified linearly and thus generate an accurate standard curve

to quantify cell number. A 10-fold dilution series of human placental DNA was made up with distilled water. PCR reactions for each template quantity were set up in duplicate and an additional pair of NTC reactions using distilled water instead of human placental DNA. PDH probe and primers were used at the optimised concentrations obtained from the previous experiments, 400 nM and 600 nM respectively. In the previous experiment where the template quantity was equivalent to 1000 cells, the CT was approximately 30 cycles therefore the CT for 1 cell would be 40 cycles, because when PCR is efficient there is a doubling of amplicon after each cycle. With this in mind the reaction was reduced from 50 cycles to 40 cycles, otherwise reaction conditions and thermal cycling conditions remained unchanged. Increasing the number of cycles in a PCR reaction increases the likelihood of generating spurious products however increasing the number of cycles in this study would not affect accuracy of quantification because Taqman probes will only hybridize to true targets in a PCR reaction and not to primer-dimers or other spurious products. The resulting amplification curves generated are shown in Figure 6.10. Fluorescence above the threshold was detected for every DNA template quantity except the 1 cell equivalent. This established that a wide range of template quantities could be amplified. Though the 1 cell equivalent was not successfully amplified, this was not an obstacle to using the assay because the PENTA 11 patient samples would have DNA equivalent to approximately 10 000 cells.

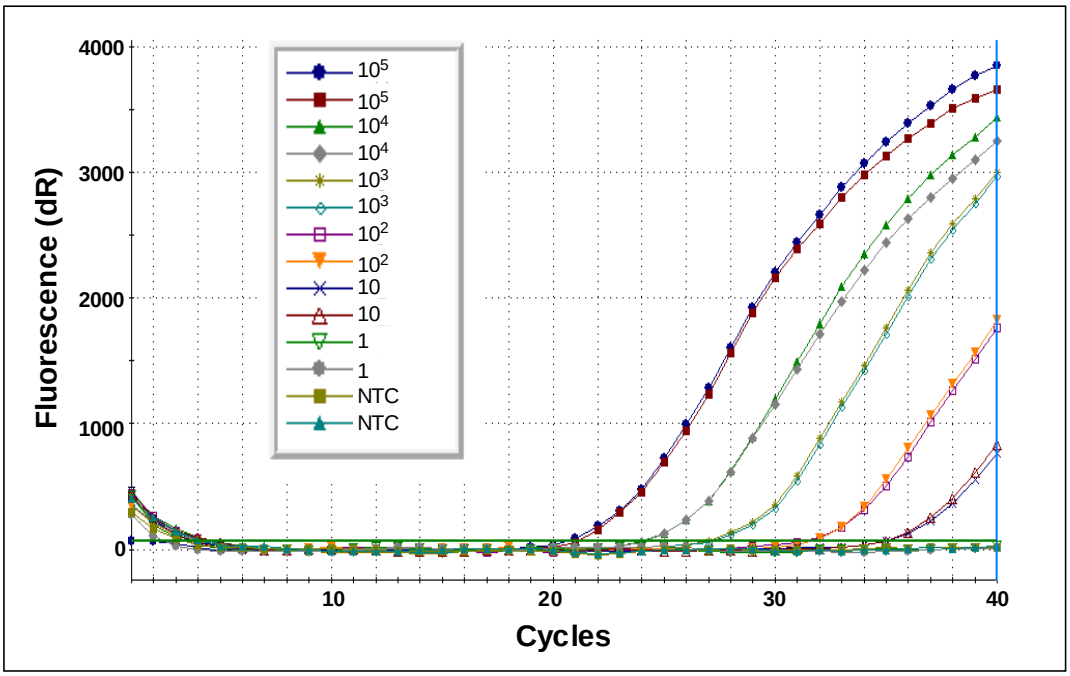

Figure 6.10 amplification plots for 10-fold dilution series of human placental DNA

QPCR reactions to amplify varying quantities of human placental DNA were set up. The amplification curves generated by each cell number equivalent are indicated on the graph. The green horizontal line indicates the fluorescence threshold and NTC indicates the pair of the non-template controls.

To produce a calibration curve to quantify unknown template quantities by their CT, amplification of the DNA dilution series would have to be linear. In Figure 6.11 each quantity was plotted against CT to assess the linear relationship between template quantity and CT. The PCR efficiency of the amplification reaction was 90.0%, which is determined by comparing the number of cycles between each pair of CTs to the number expected under ideal conditions. The R^2 value was 0.996, which indicates how closely the CTs obtained fit the linear line of regression, where 1 is a perfect fit.

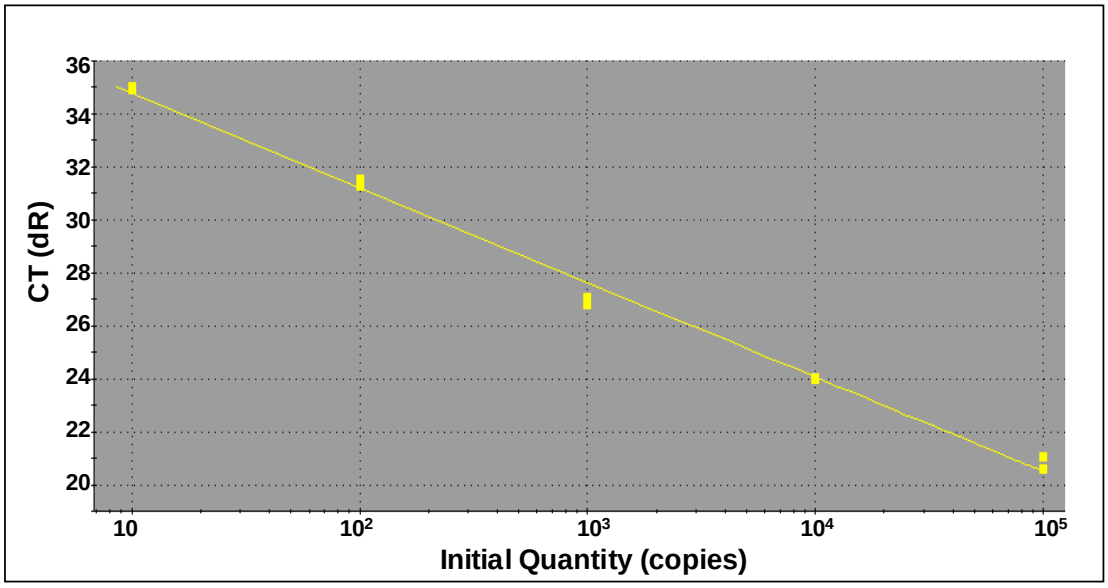

Figure 6.11 Standard curve of *PDH* template quantity

The standard curve was generated by plotting each template quantity against the CT obtained during qPCR amplification and fitting a linear regression line. PCR effiency was 90% and R^2 was 0.996.

6.4.6 Titration of LTR primers

The second reaction in the UCH multiplex assay utilises primers and probe specific for sequences of the HIV-1 *long terminal repeat* (*LTR*) were used to amplify and quantify the HIV DNA copy number. As described in section 1.3.3 LTRs are sequences of repeated nucleotides generated during reverse transcription and found at the ends of viral DNA. They regulate synthesis of viral RNA. The concentrations of the *LTR* primers were titrated using a 2-fold dilution series, ranging from a final reaction concentration of 600 nM to 75 nM. HIV DNA was obtained from the 8e5 cell line, cloned by Folks *et al*., which is a lymphocyte derived cell line containing one provirus per cell (Folks et al. 1985). Reactions were set up in duplicate using each primer concentration and template, 8e5 DNA extract equivalent to 100 HIV copies. The *LTR* probe was added at a final reaction concentration of 200 nM. Reaction conditions and thermal cycling conditions were unchanged. The amplification curves generated for each concentration are shown in Figure 6.12. There was little difference in CT or fluorescent amplitude over the range of concentrations tested therefore the primer concentration remained 300 nM as used by UCH Diagnostic Virology

Services. At all primer concentrations tested the amplification curves were weak and of low amplitude (less than 2000). It was assumed that optimising the concentration of the *LTR* probe might improve the amplification.

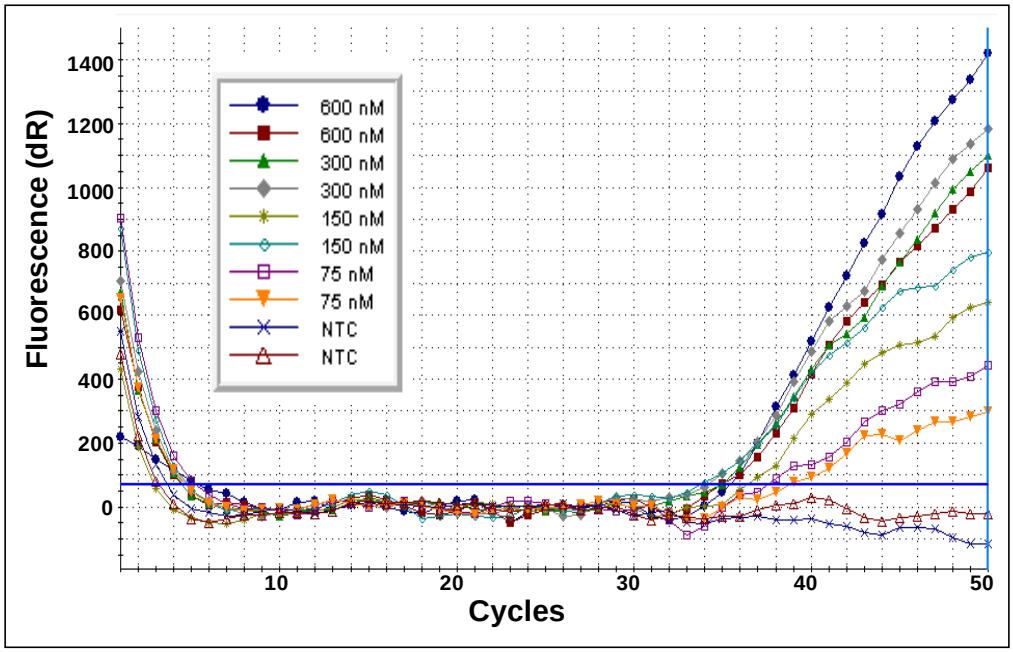

Figure 6.12 Amplification plots of *LTR* primer titration

QPCR reactions to amplify DNA equivalent to 100 human copies of HIV provirus were set up with varying concentrations of *LTR* primers. The amplification curves generated at each concentration are indicated on the graph. The blue horizontal line indicates the fluorescence threshold.

6.4.7 Titration of LTR probe

Using the optimised primer concentration a set of reactions were set up with varying concentrations of LTR probe ranging from 500 nM to 100 nM. Reaction and thermal cycling conditions were unchanged. The resulting amplification curves are shown in Figure 6.13. There was little difference in CT or fluorescent amplitude over the range of concentrations tested therefore the probe concentration remained 350 nM as used by UCH Diagnostic Virology Services. No probe concentration improved improved the

amplification reaction, at all probe concentrations tested the amplification curves remained weak and of low amplitude (less than 2000).

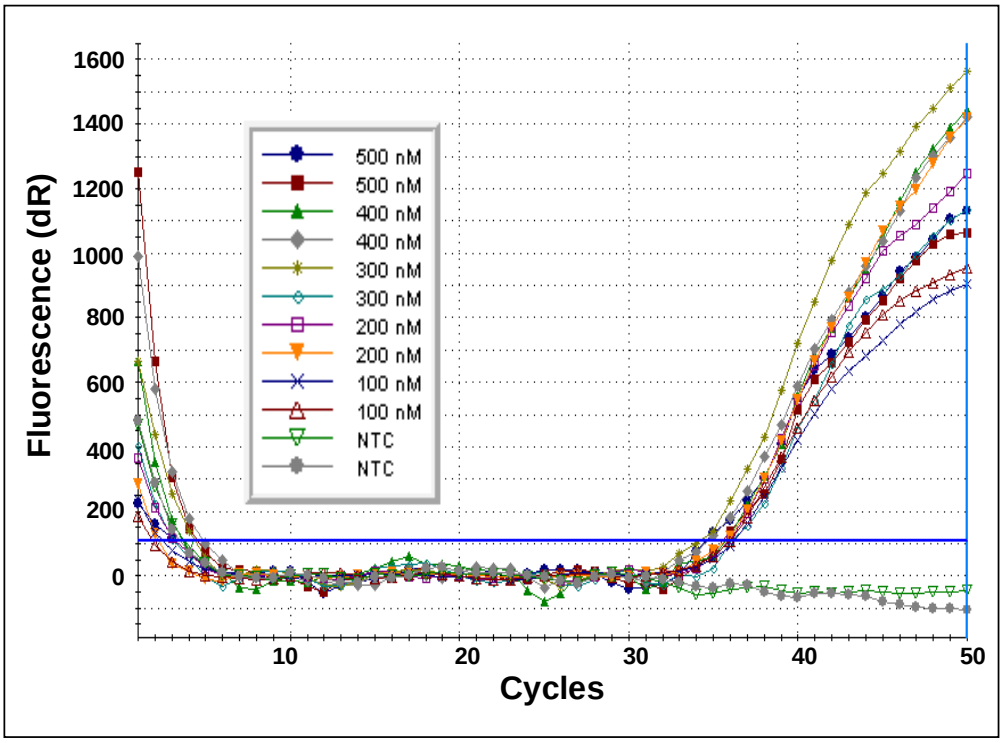

Figure 6.13 Titration of *LTR* probe concentration

QPCR reactions to amplify DNA equivalent to 100 human copies of HIV provirus were set up at varying concentrations of *PDH* probe. The amplification curves generated at each concentration are indicated on the graph. The blue horizontal line indicates the fluorescence threshold.

6.4.8 Calibration of HIV copy number

Despite the poor amplification of 1000 copies of HIV DNA, the following experiment was performed to assess if a wide range of template quantities could be amplified linearly and thus generate an accurate standard curve to quantify HIV proviral copy number. A 4-fold dilution series of 8E5 DNA from 1000 to 0.24 copies was generated with distilled water. PCR reactions for each template quantity were set up in duplicate and an additional pair of NTC reactions using distilled water instead of 8E5 DNA. The amplification curves

generated are shown in Figure 6.14. Only high copy numbers could be detected, above 60 copies, and amplification was not linear.

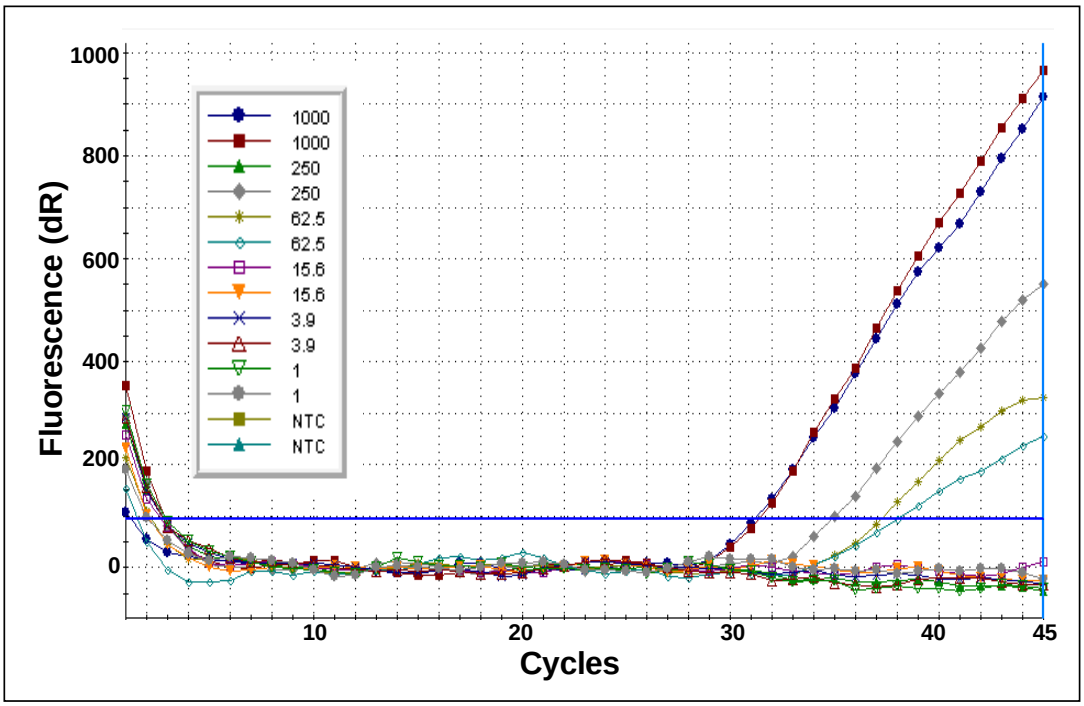

Figure 6.14 Amplification plots for 4-fold dilution series of 8E5 DNA

QPCR reactions to amplify varying quantities of 8E5 DNA were set up. The amplification curves generated by each proviral copy number equivalent are indicated on the graph. The blue horizontal line indicates the fluorescence threshold.

6.4.9 Comparison of 2 qPCR enzyme formulations

Despite titrating the *LTR* probe and primers and testing new syntheses of the oligonucleotides (data not shown), the amplification of 8E5 DNA remained poor. Amplification of a range of template quantity was not linear and at the lower range of template quantity detection was not possible. Therefore a different qPCR enzyme formulation, Quantitect QPCR mastermix (Qiagen), was evaluated against the Brilliant II QPCR mastermix (Stratagene) used thus far in the study. Additionally the Magnesium chloride ($MgCl_2$) concentration was titrated for Brilliant II QPCR mastermix (Stratagene).

The concentration of $MgCl_2$ in the Brilliant mastermix is 5.5 mM. By adding varying dilutions of $MgCl_2$ solution to aliquots of the mastermix, a series of mastermix solutions with effective $MgCl_2$ concentrations of 6.0 mM, 6.5 mM and 7.0 mM were produced. Using the optimised concentrations of *LTR* probe and primers and adding 8E5 DNA equivalent to 1000 proviral copies qPCR reactions were set up in duplicate with Quantitect mastermix and Brilliant mastermix with varying concentrations of $MgCl_2$. The resulting amplification curves are displayed in Figure 6.15. Varying the $MgCl_2$ concentration between 5.5 mM and 7.0 mM had no impact on either CT or the level of fluorescence emitted. There was minimal difference in CT between the reactions amplified with either mastermix, however higher levels of fluorescence were detected where the Quantitect master mix was used.

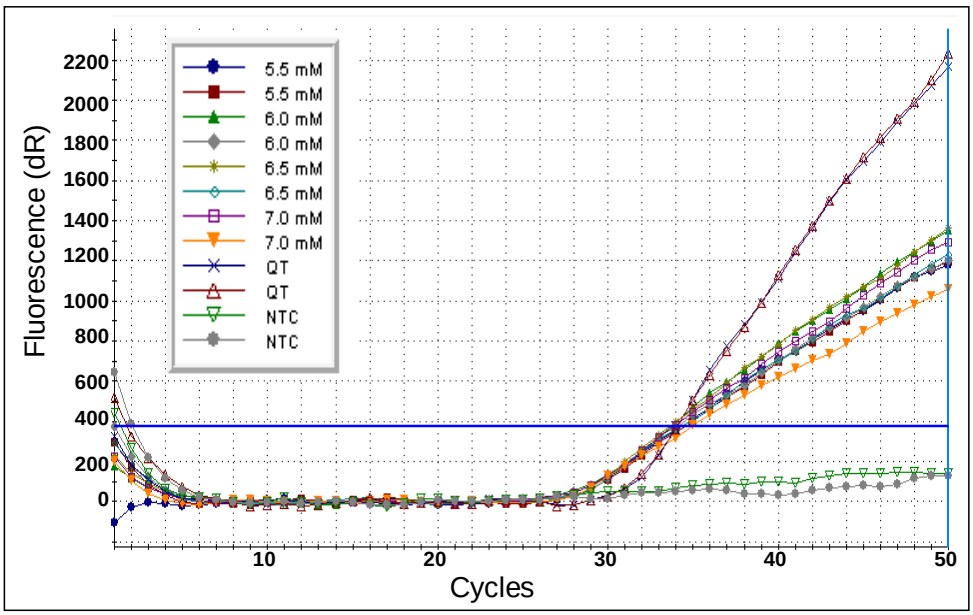

Figure 6.15 QPCR amplification using Quantitect versus Brilliant mastermix

8E5 DNA equivalent to 1 000 proviral copies was amplified with LTR targeted primers and probe using either Quantitect mastermix (QT) or Brilliant mastermix (BR). The BR mastermix was made up with MgCl2 concentrations of 5.5 mM, 6.0 mM, 6.5 mM and 7.0 mM. The blue horizontal line indicates the fluorescence threshold and NTC the pair of the non-template controls.

Further experiments were performed using the Quantitect mastermix and new thermal cycling conditions as recommended by the manufacturer, which were 10 min activation at 95°C, followed by 50 cycles of 10s denaturation at 95°C and 1 min annealing and elongation at 65°C. The *PDH* and *LTR* probes and primers were re-titrated within the range recommended by the manufacturers to find the optimum concentrations for the new reaction and thermal cycling conditions (data not shown). These were 350 nM for both *PDH* and *LTR* probes and 600 nM for both pairs of *PDH* and *LTR* primers.

6.4.10 New HIV-1 target sequences

A number of parameters were altered to improve the sensitivity of the HIV DNA assay. These included optimising the concentrations of *LTR* probe and primers, comparing these oligonucleotides to other batches to ensure correct synthesis, changing the qPCR enzyme mastermix and thermal cycling conditions. However none of these substantially improved the sensitivity, CT or level of fluorescence emitted. Therefore the quality of the *LTR* primers were evaluated with primer analysis software Primer 3 (available from Sourceforge, http://sourceforge.net/) and Beacon Designer (available from http://www.premierbiosoft.com/molecular_beacons/index.html)and compared to 2 other pairs of primers, available in the lab, specific for sequences within HIV-1 *Pol* and *Gag*. The *LTR* and *Pol* primers were rated low to fair. The *Gag* sequence specific primers, *GagF* and *GagR*, were rated good additionally a BLAST search (http://www.ncbi.nlm.nih.gov/BLAST) showed efficacy against A, B, C and D HIV-1 subtype viruses.

This was also tested experimentally by set up qPCR reactions, in duplicate, to amplify 1000 copies of 8E5 with either the *Gag* or *LTR* primers. The reactions using the *Gag* primers were set up at varying concentrations, 600 nM, 500 nM and 400 nM, to determine the optimum concentration. The amplification plots generated are shown in Figure 6.16. Fluorescence amplitude was much greater for reactions using the *Gag* primers instead of *LTR* primers. Amongst the qPCR reactions with *Gag* primers, there was a moderate

difference in level of fluorescence with varying concentrations, with the highest fluorescence achieved at 400 nM. The concentration of the Gag probe was also titrated, but there was no difference in fluorescence over the range tested, 350 nM to 200 nM, (data not shown) and therefore the probe was used at a concentration of 200 nM.

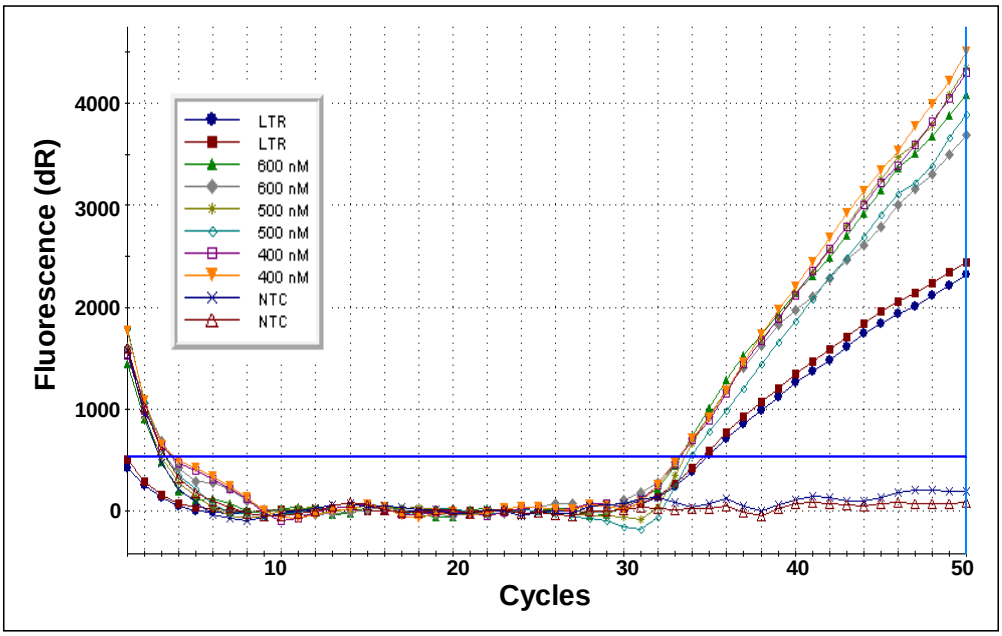

Figure 6.16 Amplification plots for qPCR reactions with either Gag or LTR primers
8E5 DNA equivalent to 1,000 proviral copies was amplified with either LTR targeted or Gag targeted primers. Gag primers were used at varying concentrations. The amplification plots generated using each primer pair and the concentrations of Gag primers, 600nM, 500 nM and 400 nM are indicated on the graph. The blue horizontal line indicates the fluorescence threshold and NTC the pair of the non-template controls.

6.4.11 HIV calibration curve

After individually optimising both the HIV and housekeeping reactions these reactions were combined together in a multiplex reaction to ensure both HIV and cell copy numbers over a wide range could be simultaneously amplified in a linear fashion. Reactions were set up with Quantitect mastermix and the optimised concentrations of Gag and PDH probes and primers. 8E5 DNA template was added to each reaction at either 1000, 333, 111, 37,

12.3 or 4.1 copy number. As mentioned previously the 8E5 cell line contains exactly one integrated HIV provirus per cell and one pair of the *PDH* gene thus the cell number and proviral copy number are equal. An additional pair of NTC reactions were set up with distilled water. For ease of viewing, the *Gag* amplification plots are shown on a separate graph (Figure 6.17A) from the *PDH* amplification plots (Figure 6.17B). The full range of proviral copy or cell number, from 1,000 to 4.1 copies were successfully amplified, this amplification was not linear over the whole concentration range. Therefore only the first four values in the range were plotted against CT to test the strength of the linear relationship. The standard curve for both *Gag* and *PDH* are shown in Figure 6.18. The PCR efficiency and R^2 for *Gag* were 99.2% and 0.924 respectively. The PCR efficiency and R^2 for *PDH* were 91.3% and 0.966 respectively.

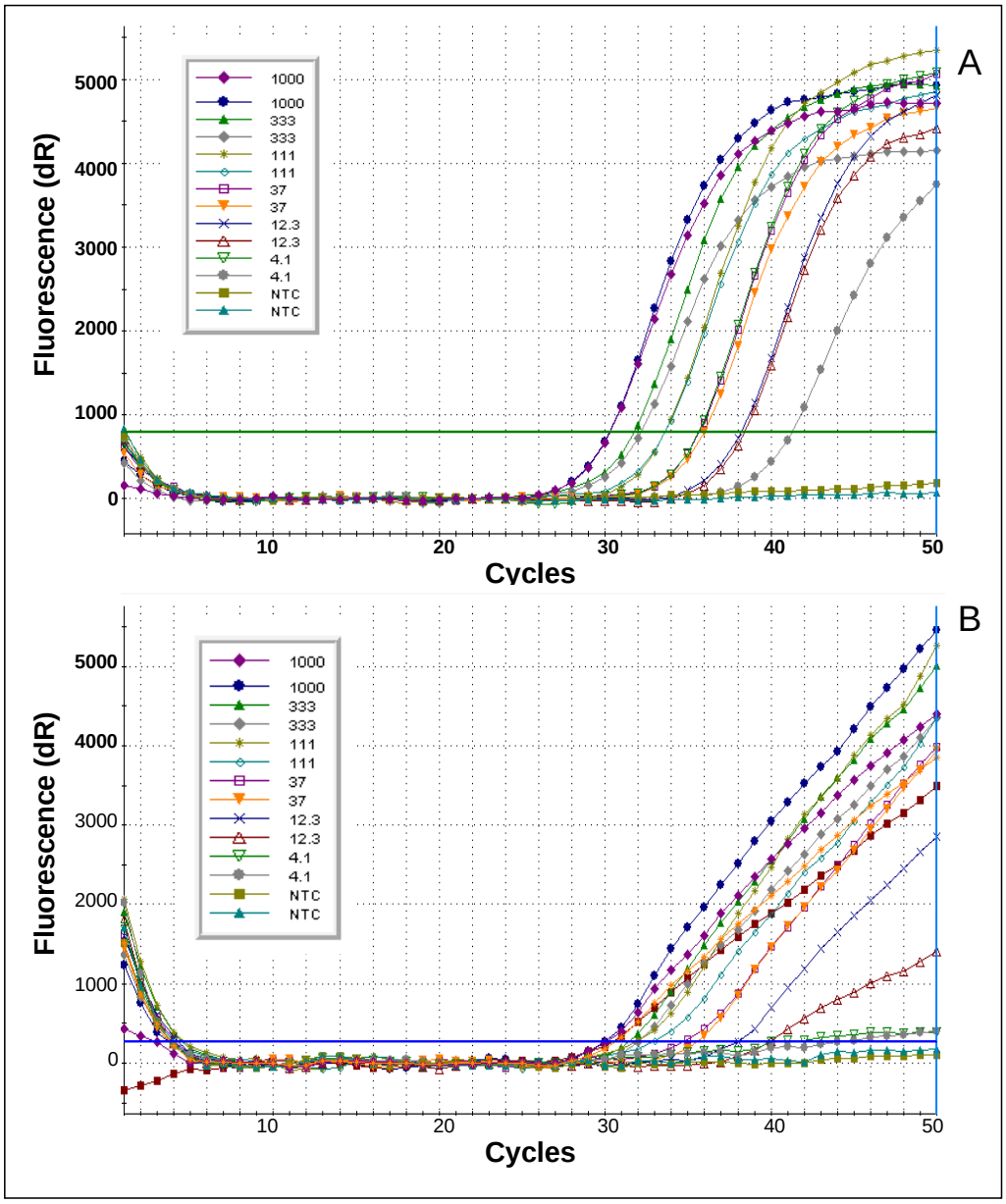

Figure 6.17 Amplification plots for 3-fold dilution series of 8E5 DNA

QPCR reactions to amplify varying quantities of 8E5 DNA were set up. The amplification curves generated for *PDH* and *gag* at each equivalent cell number and proviral copy number are shown in (A) and (B) respectively. The horizontal lines indicate the fluorescence threshold and NTC the pair of the non-template controls.

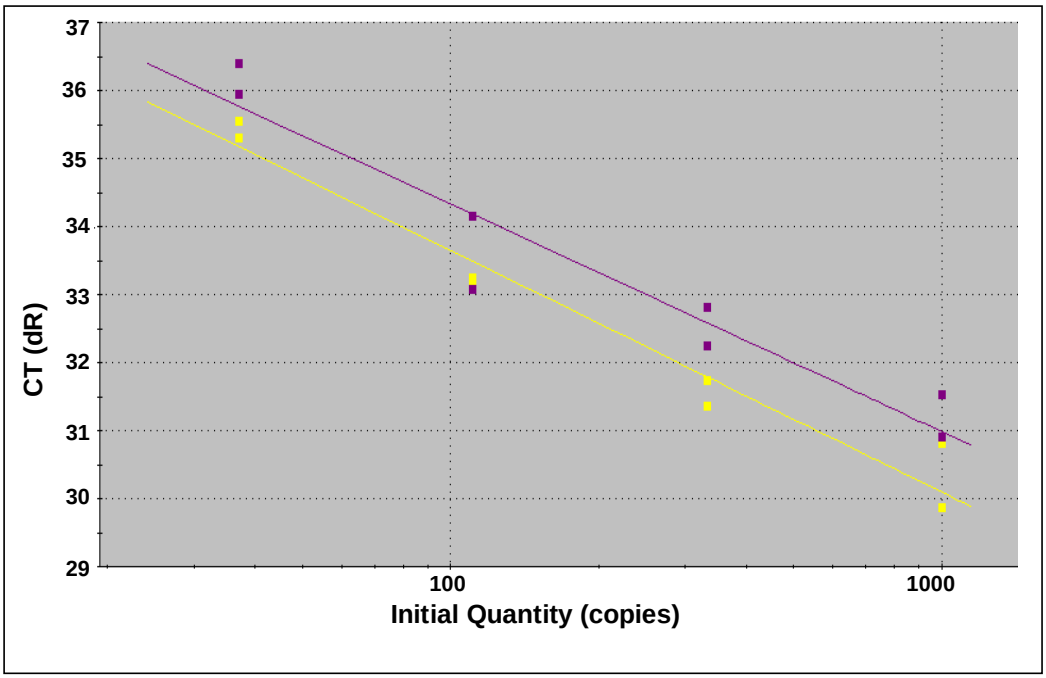

Figure 6.18 Standard curve of PDH and Gag template quantity

The intial template quantity of each well for each well were plotted against the CT produced during the reaction. The yellow squares and line are the PDH standard curve and the purple squares and line, the Gag standard curve.

6.4.12 Amplification of 8E5 with excess placental DNA

The multiplex qPCR assay developed with 8E5 DNA does not reflect HIV-1 infection *in vivo*. In the 8E5 cell line every cell contains an integrated provirus therefore there is one copy of provirus to each pair of *PDH* genes, *in vivo* the majority of $CD4^+$T cells are not infected with virus therefore in DNA extracted from a sample of $CD4^+$T cells there are thousands of copies of the *PDH* to each *Gag* gene. Therefore to establish if the assay could work in the scenario of HIV-1 infection, experiments were performed in which inhibition of *Gag* in the presence of excessive *PDH* was investigated.

HIV-1 multiplex qPCR reactions of 50 copies of 8E5 DNA with or without the presence of human placental DNA were set up. Human placental DNA was added at amounts equivalent to cells numbers, between 6.25×10^3 and 1×10^5 cells. The *Gag* amplification

plots generated are shown in Figure 6.19. For the *PDH* amplification curves (data not shown) the difference in CT between each pair of curves was approximately one cycle, as expected for a 2-fold dilution series. Reactions in the presence of placental DNA had higher CTs for *Gag* than the reactions without. In fact, in the presence of 25, 000 copies or more of placental DNA, *Gag* could not be detected. This limit is equivalent to an HIV DNA concentration of 1 proviral copy per 500 cells or 200 copies per 10^5 cells. These results suggested inhibition of the *Gag* PCR reaction by *PDH* PCR reaction because there is much more substrate available for the *PDH* reaction.

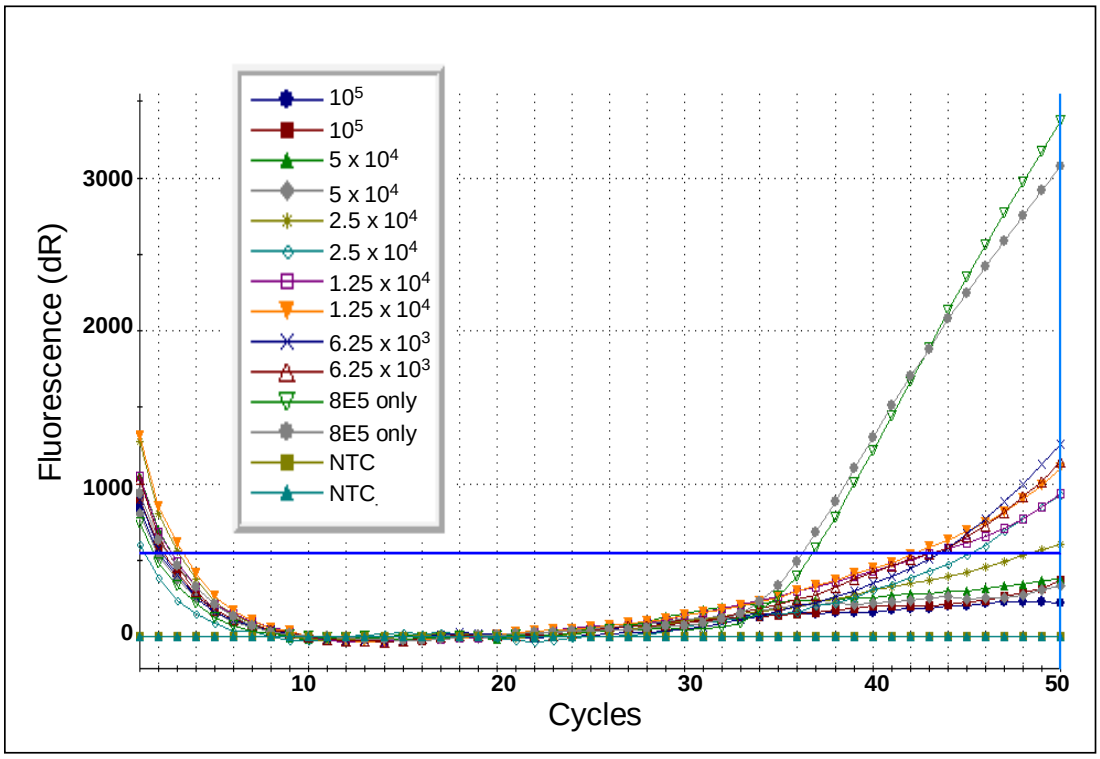

Figure 6.19 Amplification plots of 50 copies of 8E5 combined with human placental DNA
Varying concentrations of placental DNA were added to qPCR reactions of 50 copies of 8E5 DNA. The cell number equivalents of the amount of placental DNA added are indicated on the graph. The blue line indicates the fluorescence threshold.

6.4.13 Detuning the PDH signal

A method for overcoming the inhibition of a component within a multiplex PCR reaction is to alter the reaction conditions as to modify the signal of the inhibiting component. This is called detuning. To detune the *PDH* signal, and thus overcome its inhibition of *Gag*, the previous experiment was repeated with progressively lower concentration of *PDH* primers 100, 75 or 50 nM. Inhibition of *Gag*, confirmed by higher CTs, increased in the presence of increasing concentrations of placental DNA therefore the upper range of placental DNA, equivalent to 10^5, $5x10^4$ and $2.5x10^4$cells, were used.

The effect of *PDH* primer concentration on inhibition is shown in Figure 6.20. The CTs for reactions with placental DNA decreased with decreasing *PDH* concentration. At a *PDH* primer concentration of 100 nM the difference in CT between the reactions of 8E5 alone and 8E5 in the presence of placental DNA was more than 3 cycles. The difference in CT was less at 75 nM. Finally at a *PDH* primer concentration was 50 nM the CTs for 8E5 DNA alone and 8E5 DNA combined with placental DNA were approximately equal. Therefore inhibition of *Gag* by *PDH* was removed at this concentration.

However, as concentration of the *PDH* primers decreased, the amplification efficiency of *PDH* also decreased. At 50 nM the PCR efficiency and R^2 were 92% and 0.99 respectively compared to 100% and 1 respectively for 75 nM and 100 nM. The optimum concentration would therefore appear to lie between 50 and 75 nM. The HIV-1 qPCR multiplex assay was carried out using the *PDH* primers at a concentration of 75, 60 or 50 nM on a 3-fold dilution series of 8E5 DNA from 3,000 to 4.1 copies. Every template quantity was detected and the 4 upper values in the 8E5 series were used to produce standard curves for *Gag* and *PDH* by plotting the initial template copy number for each reaction against the associated CT. The efficiencies of the PCR reaction at each *PDH* primer concentration are displayed along with the R^2 value in Figure 6.21. The PCR efficiency and R^2 for both *PDH* and *Gag* were highest at 60 nM and therefore this was chosen as the optimum PDH primer

concentration. The limit of detection for the assay was 4.1 copies of HIV DNA per 10^5 cells or 1 copy per $2.5x10^5$ cells.

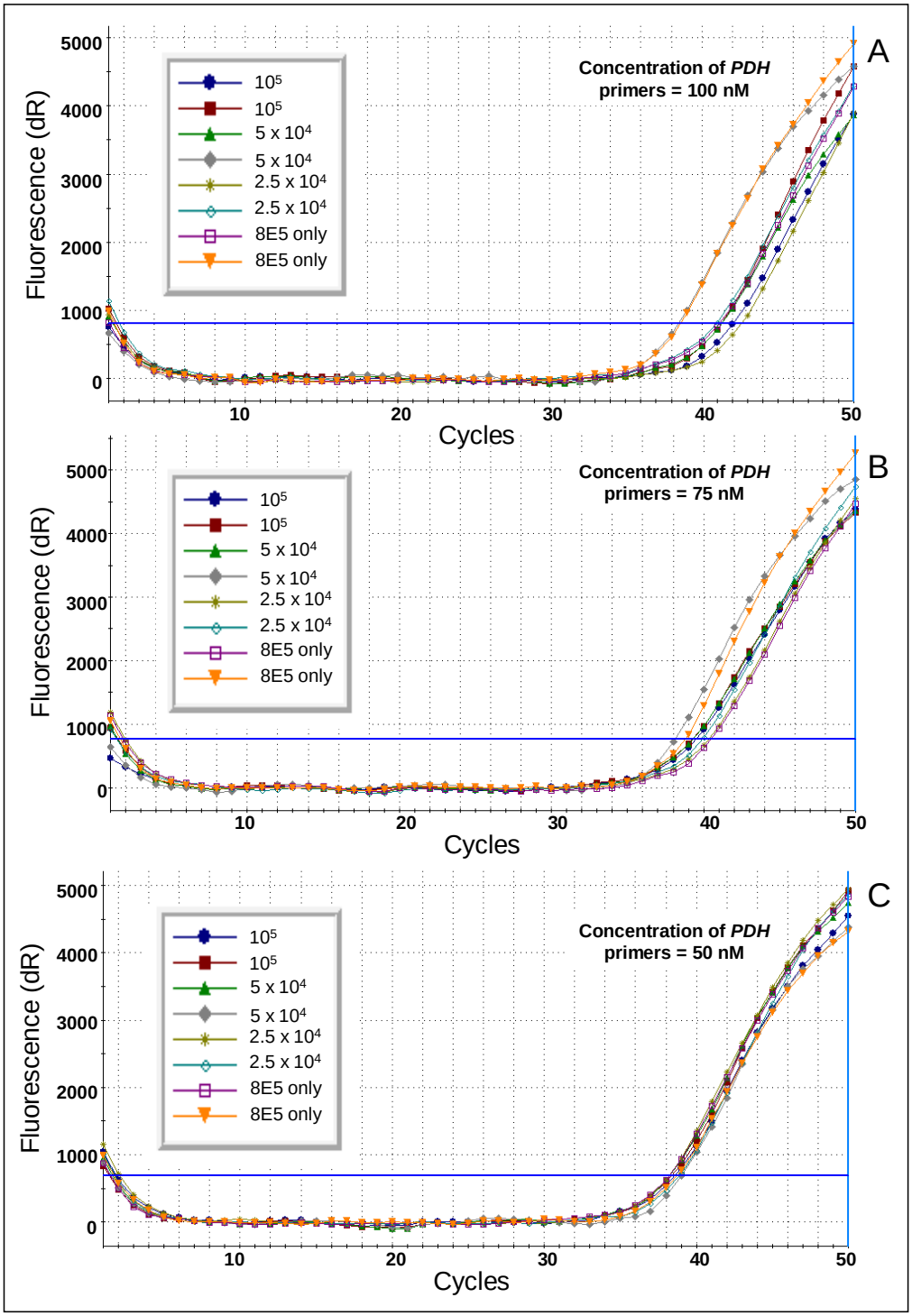

Figure 6.20 Titration of *PDH* primers for amplification of 8E5 DNA with human placental DNA

The HIV assay was performed with a template of 50 copies of 8E5 DNA combined with varying quantities of placental DNA. The reactions were carried out with PDH primer concentrations of 100 nM in A, 75 nM in B and 50 nM in C. The curves for 8E5 DNA alone and combined with placental DNA are indicated.

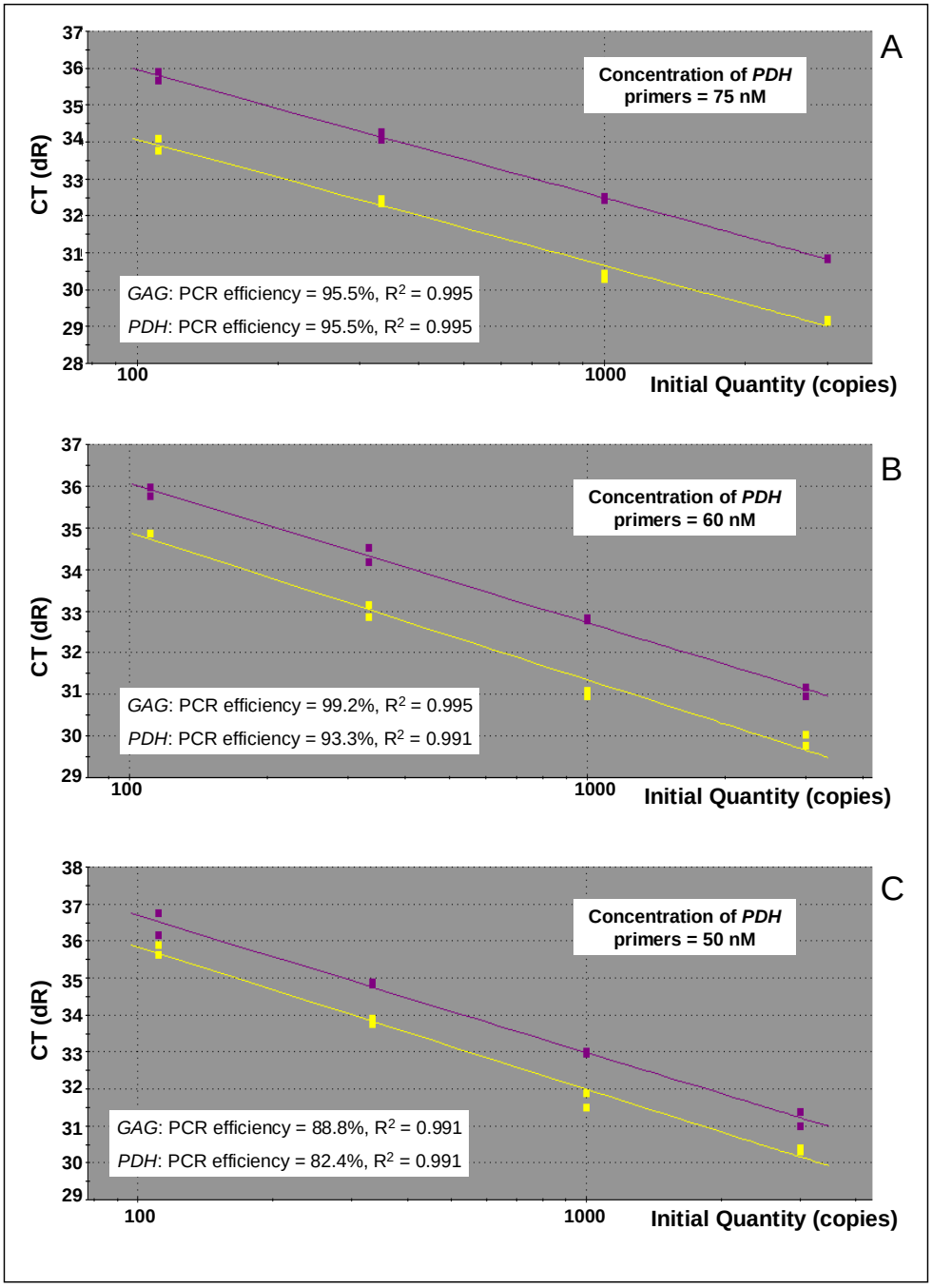

Figure 6.21 *PDH* and *Gag* standard curves produced by various concentrations of *PDH* primers

The HIV-1 qPCR assay was carried out using the PDH primers at a concentration of 75 (A), 60 (B) or 50 nM (C) on a 3-fold dilution series of 8E5 DNA from 3 000 to 4.1 copies. The 4 upper values in the 8E5 series were used to produce standard curves for Gag (purple) and PDH (yellow) by plotting the intial template copy number for each reaction against the associated CT. The efficiencies of the PCR reaction at each concentration of PDH primer are displayed with the R2 value, which indicates how closely the points fit the regression line.

6.4.14 Dissolving 8E5 DNA in a solution of carrier RNA

The results of section 6.4.13 showed that PCR efficiency in the assay decreased with lower template quantities. In tubes with a low DNA concentration, the DNA molecules may adsorb to the plastic of the tube where the PCR reaction is unlikely to occur. Carrier RNA can be added to PCR reactions containing low concentrations of template DNA to reduce/prevent non-specific binding of target DNA to the tube and also provides an alternative target for any RNase that might be present in the sample. PCR plastics that are non-DNA binding were already in use therefore the assay was carried out with 8E5 DNA diluted in distilled water or a solution of carrier RNA to determine if the addition of carrier RNA improved PCR efficiency at low template concentration. The standard curves generated are shown in Figure 6.22. The PCR efficiency was much higher when carrier RNA was used, 95% and 99% for Gag and PDH respectively, compared to 75% and 77% for Gag and PDH respectively, when distilled water was used. In the following sections the 8E5 standards were generated by dissolving 8E5 DNA in a solution of carrier RNA.

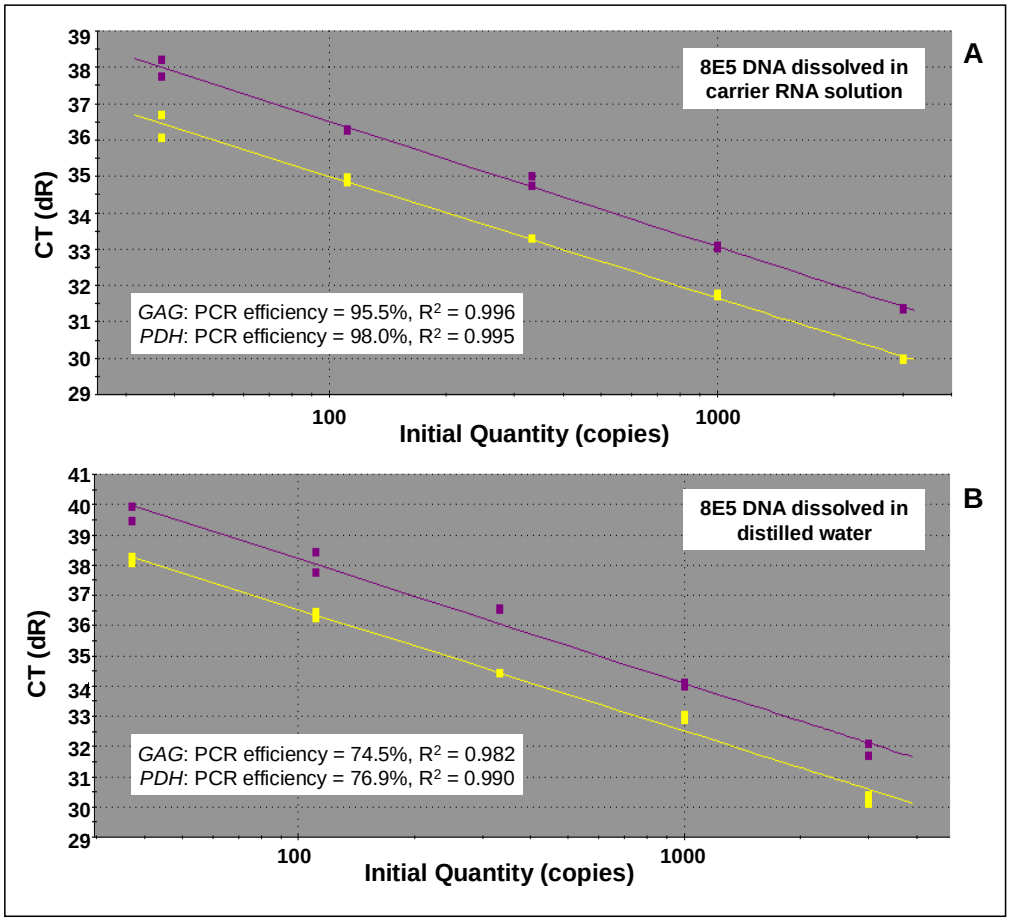

Figure 6.22 Gag and PDH standard curves produced from 8E5 DNA dissolved in carrier RNA solution or distilled water

The HIV-1 qPCR multiplex assay was performed on a 3-fold dilution series of 8E5 DNA dissolved either in carrier RNA solution or in distilled water. The 5 upper values in the 8E5 series were used to produce calibration curves for *Gag* and *PDH* by plotting the initial Gag and PDH template quantities against the associated CTs. The calibration curves produced using carrier RNA solution and distilled water are shown in A and B. The efficiencies of the PCR reactions when carrier RNA solution and distilled water were used are displayed with the R^2 value, which indicates how closely the points fit the regression line.

6.5 QUANTIFICATION OF HIV DNA IN CD4 SUBSETS FROM CHILDREN UNDERGOING TREATMENT INTERRUPTION

6.5.1 Methods

As explained previously aliquots of PBMCs isolated from children at various stages of treatment interruption were thawed and subjected to immuno-magnetic separation to isolate populations of $CD45RA^+$ and $CD45RA^-$ $CD4^+$ T cells, referred to as naïve and memory cells respectively. DNA was extracted from these naïve and memory $CD4^+$T cell sub-populations and amplified in duplicate in a HIV-1 DNA qPCR multiplex assay alongside a series of known concentrations of 8E5 DNA also in duplicate. PBMCs were separated from 6 ml whole blood and divided into three aliquots, one of which was used for the HIV DNA study described here. qPCR was carried out according to the methods described in methods and materials section 2.2.7, with 9µl template DNA (equivalent to the extraction from approximately 10,000 cells).

6.5.2 Sample characteristics

The HIV DNA concentration was quantified in 29 PBMC samples. The characteristics of the samples are shown in Table 6.1. Results from 2 samples from subject QUT036011 were excluded from further analysis. This was because when DNA from these samples was amplified the slopes of the amplification curves were flatter than slopes for other samples or for the 8E5 DNA series. This indicated that amplification was less efficient, most likely due to mismatching between the template sequence and the *Gag* primers or probe. Values reported by the assay would therefore underestimate the true concentrations. As stated in chapter 5 the inclusion criteria for the trial required 2 consecutive undetectable viral load tested 1-4 months apart therefore all children had an undetectable viral load (less than 50 copies/ml of plasma) at the start of trial. HIV DNA was quantified in nine baseline samples at which time viral load had been undetectable. The median viral load and IQR given in the table therefore refer to detectable viral loads measured after the start of therapy interruption. The immunological inclusion criterion for the trial was a percentage $CD4^+$ T

cell ≥30% in children 2-6 and in children 7-15 a percentage $CD4^+$ T cell ≥25% and a CD4 count ≥500 cells/mm^3.

VARIABLE	MEDIAN	IQR
Age at start (years)	8.9	6.5-10.9
Age at sample (years)	9.0	6.7-11.4
Viral load (log genomes/ml)	4.7	3.8-5.4
CD4 count (cells/µl)	870	550-1060
$CD4^+$ T cells (as % of total lymphocytes)	33.0	22.0-41.9
$CD4^+$ T cell subsets (as % of total $CD4^+$ T cell count):		
$CD45RA^+CD31^-$	12.7	7.2-19.7
$CD45RA^+CD31^+$	47.8	42.5-53.7
$CD45RA^-CD31^-$	24.5	21.1-35.0
$CD45RA^-CD31^+$	9.0	5.2-15.4
Concentration of $CD4^+$ T cell subsets (cells/ µl):		
$CD45RA^+CD31^-$	98	45.0-181.5
$CD45RA^+CD31^+$	320	204-560.5
$CD45RA^-CD31^-$	213	148.5-269.5
$CD45RA^-CD31^+$	52	31.5-147.0

Table 6.1 Characteristics of sample population for HIV DNA quantification

HIV DNA was quantified in 29 samples. The median and IQR of characteristics of this population are given in the table. The viral load refers to viral loads in samples after week 0.

6.5.3 Comparison of HIV-1 DNA concentration in naïve and memory CD4+ T cells

In the 27 samples of memory cell DNA analysed, the HIV DNA concentration in all samples was quantified. In the 27 samples of naïve cell DNA extract, *Gag* was detected in 22 samples although in 1 of these samples, *Gag* was detected in only one of the duplicate qPCR reactions. Amplification may have failed in the 5 samples because there was no HIV DNA in the sample. However it could also have been because there was insufficient template in the tube to enable an effective reaction. Of the 5 samples, 2 had low template

numbers (equivalent to 800 and 1,000 cells) and 3 had sufficient template (equivalent to 5,000, 6,000 and 9,000 cells) but an undetectable viral load at the time of sampling. The mean amount and IQR of naïve cell DNA used in the reactions was equivalent to 9,400 cells and 5 200-109 300 cells.

The range of HIV DNA concentrations in the total $CD4^+$ T cell pool and in the naïve and memory sub-populations are shown in Figure 6.23. A very wide range of concentrations were found in the naïve population but the concentration of HIV DNA in the memory population was usually significantly higher (Mann-Whitney test, p=0.0012). The median concentration of HIV DNA in the memory cell population was just over 10 times greater than that detected in the naïve cells from the same PBMC sample.

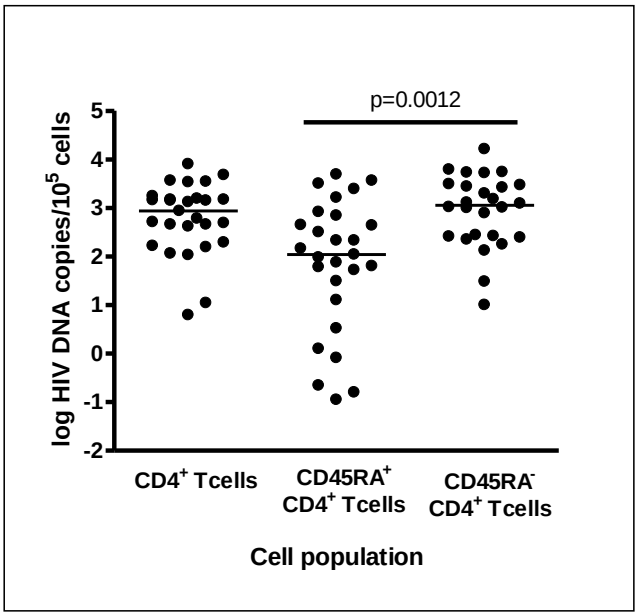

Figure 6.23 Scatter graph of HIV DNA concentration in $CD4^+$ T cell pool and sub-populations
The log of the concentration of HIV DNA in the total $CD4^+$ T cell pool and in the $CD45RA^+$ and $CD45RA^-$ sub-populations taken from 27 treatment interruption samples were plotted on a scatter graph.

6.5.4 Changes in levels of intracellular HIV DNA during treatment interruption

There were insufficient sample numbers to analyse changes in the concentration of HIV DNA at each time point, therefore it was decided to group the time points into nominal periods of early (weeks 0 and 2), mid (weeks 4 and 12) and late phases of treatment interruption (weeks 24 and 48). The changes in concentration of HIV DNA during this time are shown in Figure 6.24. In all 3 populations the HIV DNA concentration increased with time. The difference between the medians was found to be statistically significant by Kruskall Wallis test.

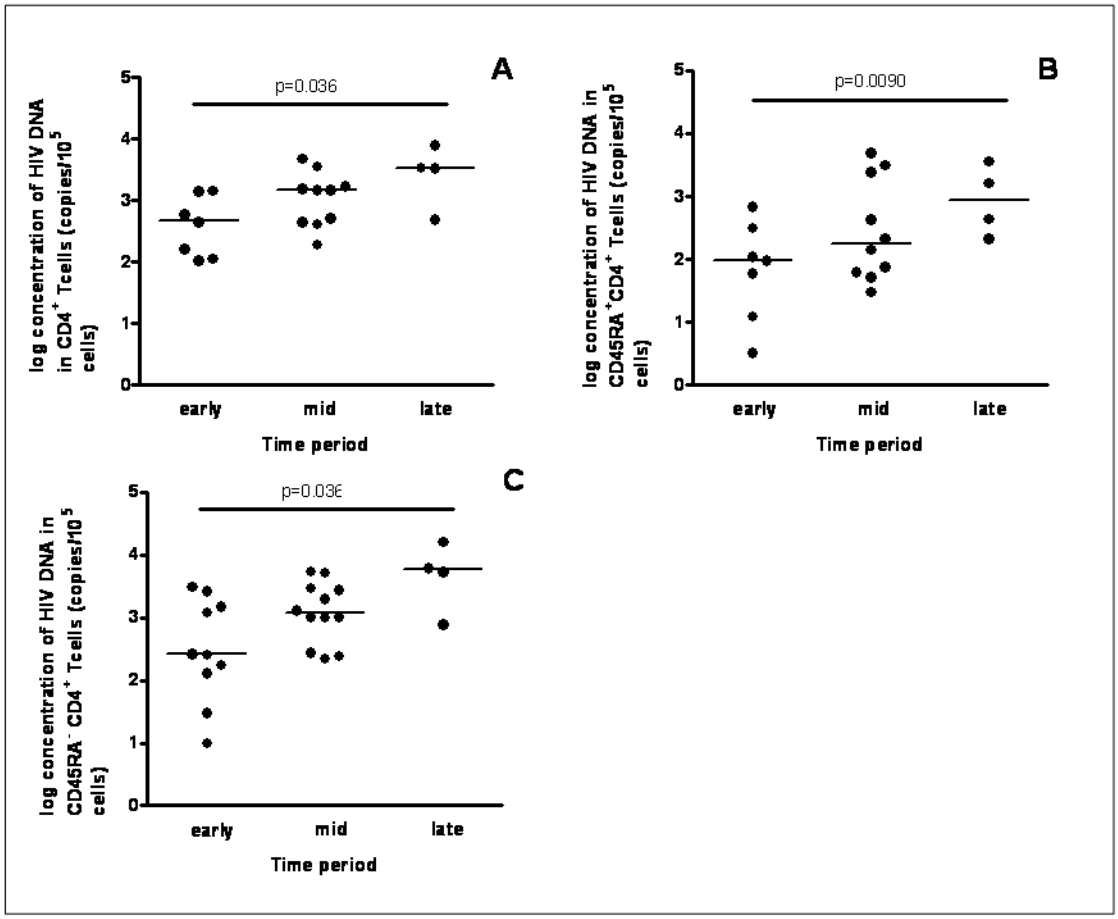

Figure 6.24 Concentration of HIV DNA in $CD4^+$ T cells and sub-populations at different time points
DNA samples were assigned to 3 time points early (weeks 0 and 2), mid(weeks 4 and 12) and late (weeks 24 and 48) based on week of treatment interruption they were obtained. For the total CD4 T cell pool, the $CD45RA^+$ and $CD45RA^-$ populations the median HIV DNA concentrations were compared across the 3 time points by Kruskal-Wallis test for statistical significance, p values are indicated.

6.5.5 Association between CD45RA$^-$ T cell HIV DNA concentration and sample characteristics

The CD4, CD45RA$^-$, CD45RA$^+$ HIV DNA concentration for each sample was plotted against the respective age, viral load, CD4 count, percentage of CD4$^+$T cells, proportion and concentrations of CD4$^+$T cell subsets to investigate for associations between the variables. No statistically significant results were found for the CD4 and CD45RA$^+$ HIV DNA concentrations. However, the CD45RA$^-$ CD4$^+$T cell HIV DNA concentration was significantly correlated with the viral load, the percentage of CD4$^+$T cells and the concentration of CD45RA$^-$CD31$^-$ CD4$^+$T cells as shown in Figure 6.25.

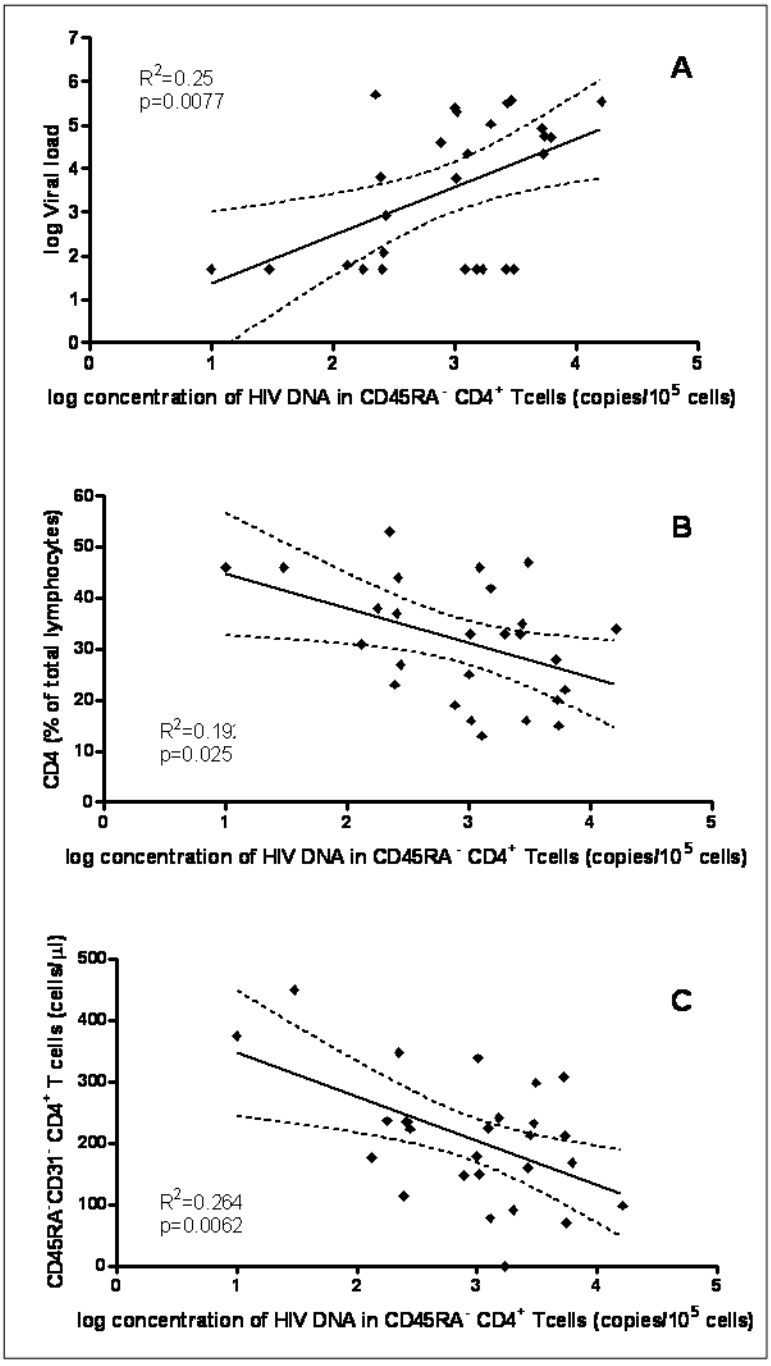

Figure 6.25 Correlation between CD45RA$^-$CD4$^+$ T cell HIV DNA concentration and sample characteristics

The concentration of HIV DNA in CD45RA$^-$ CD4$^+$ T cells was found to correlate significantly with the viral load, CD4 percentage and concentration of CD45RA$^-$CD31$^-$ CD4$^+$ T cells at the time of sampling. Solid and dashed lines are the lines of linear regression and 95% confidence interval respectively. R2 and p values given indicate the goodness of fit and statistical significance.

6.6 DISCUSSION

I have described the optimisation of an immuno-magnetic separation method to obtain high purity populations of naïve and memory $CD4^+$T cells ideal for use where cell numbers are limited and FACS sorting is not possible. I also described the development and successful of application of an HIV-1 DNA multiplex qPCR assay to samples of naïve and memory $CD4^+$T cell DNA.

The purity of the naïve and memory populations has been demonstrated to be on average 95%, ranging from 93-99%. Although this is very high purity any contamination of the naïve population could affect the reliability of the HIV DNA concentration measured because the concentration of HIV DNA in the memory population is over 10-fold greater. However it is unlikely that greater purity could be attained without FACS sorting.

The limit of sensitivity of the qPCR assay developed was 4 copies of HIV DNA. No assays thus far developed have a lower limit than 4 copies.

Most of the $CD4^+$ T cells that contain HIV DNA have a memory phenotype. To the best of my knowledge HIV DNA has not been quantified in CD4 subsets in HIV-1 infected children but the results of this study are similar to data published for HIV-1 infected adults. In agreement with HIV literature I found that most HIV DNA was located in the memory $CD4^+$T cell population. Indeed the median HIV DNA concentration in the memory is over 10 times greater than in the naïve $CD4^+$T cell sub-population. I also found that with increasing time without treatment the HIV DNA concentration increased significantly in all populations. At each time point there was a lot of variation in the HIV DNA concentration, which would likely be affected by changes in the size of the cell population and viral replication. Thus we found that the memory cell HIV DNA concentration was significantly associated with the CD4 percentage, the plasma viral load and the concentration of

$CD45RA^{-}CD31^{-}$ $CD4^{+}$T cells, which is the likely reservoir of HIV DNA amongst the $CD4^{+}$T cell subsets.

Although these preliminary results are very interesting little can be concluded due to the small number of samples tested as well as the lack of treatment restart samples because although I have shown that the concentration of HIV DNA increases with increased time off treatment, what is more important is the effect of restarting treatment on the HIV DNA concentration. Does it decrease on resuming treatment and if so does it decrease to baseline levels or perhaps even lower? Also if more samples were evaluated it would be interesting to determine if the baseline HIV DNA concentration predicts peak rebound viraemia during treatment interruption in children in this study as has been reported in adults in the Swiss cohort study (Yerly et al. 2004). Therefore future work would concentrate on testing more samples both during treatment interruption and upon resuming treatment. Additionally if viral load set point data from before the children were ever treated with HAART were available, I could assess investigate if viral load set point predicts the concentrations of HIV DNA measured during treatment interruption.

CHAPTER 7

GENERAL DISCUSSION

The overall aim of this thesis was the study of how sub-populations are involved in changes to size of the $CD4^+$ T cell population in HIV-1 infection in children with or without treatment and the processes controlling those changes.

7.1 IMPORTANCE OF THIS STUDY

This study is very important because it included the first investigation of recent thymic emigrants (RTEs) and central naïve, $CD4^+$ T cells, as defined by CD31 expression in HIV-1 infected children. It also shed greater understanding on the differences between $CD31^+$ and $CD31^-$ memory cells and their possible roles and origins. Furthermore these populations were investigated in a trial of planned treatment interruption (PTI), the first of its kind to carried out in children and also the first to included a detailed immunological study. This seminal trial also led to the development of a uniquely sensitive assay to quantify intracellular HIV DNA in highly purified populations of naïve and memory $CD4^+$ T cells, showing the effect of ceasing treatment on the proviral load and showing for the first time the possible importance of naïve cells as an important reservoir of HIV viral latency in children.

7.2 RECENT THYMIC EMIGRANTS

In uninfected individuals RTEs have been shown to constitute a greater proportion of the peripheral $CD4^+$ T cell population in children than in adults and to decrease as a proportion of the $CD4^+$ T cell population with increasing age (Kimmig et al 2002), (Junge et al 2007). This present work shows for the first time that also in HIV-1 infected children RTEs comprise a significantly greater proportion of the $CD4^+$ T cell population than un-infected adults. Additionally the relationship of a decreased percentage of RTEs with increased age is also seen in HIV-1 infected children.

RTEs by virtue of their telomere length and telomerase measurement are believed to have very limited replicative history (Junge et al 2007), which is supported by the findings from this present work that in both uninfected adults and HIV-1 infected children even when treatment is interrupted, with detectable viral replication or increased activation, the proportion of RTEs that proliferate remains extremely low, much lower than the other sub-populations investigated. This would also further support the belief that $CD45RA^{+}CD31^{+}$ cells are truly RTEs as they are unlikely to be produced by proliferation of existing $CD45RA^{+}CD31^{+}$ cells.

Although the proportion of RTEs proliferating remained low despite changing parameters such as viral replication and CD4 count this was not so for the activation level of RTEs. Increased proportions of RTEs expressing the activation marker HLA-DR did appear to be associated with decreased CD4 counts, viral replication, and interrupting treatment.

From this present study it could also be proposed that the percentage of RTEs is a useful indicator of disease progression because in the children studied, both ART naïve and ART experienced, increased CD4 counts were associated with increased percentage of RTEs, independent of age.

7.3 CENTRAL NAÏVE CELLS

With the focus of researchers naturally directed at RTEs there has been limited study of central naïve cells. Throughout this work central naïve cells come across as a population of cells in dynamic equilibrium. Firstly the difference in the proportions of central naïve cells between HIV-1 infected children and uninfected adults is only just statistically significant and is much smaller than the difference in RTEs. Accordingly the proportion of central naïve cells within the $CD4^{+}$ T cell peripheral population appears unchanged with increased age. It also appears unchanged with increased total proliferation in the

$CD4^+$ T cell population. Taken together these findings would suggest that although cell parameters and the proportions of the $CD4^+$ T cell peripheral pool composed of RTEs and memory cells may change, the percentage of central naïve cells remains fairly constant. As this study has also shown changed levels of proliferation and activation in the central naïve population we would suggest that increased loss from this population.

7.4 $CD31^+$ AND $CD31^-$ MEMORY CELLS

The proportion of the $CD4^+$ T cell peripheral pool composed of memory cells has been shown to increase with age and with decreased CD4 count in HIV-1 infection in children and adults. More recently the percentage of $CD31^+$ memory cells has been reported to be unchanged with increased age in uninfected individuals (Junge et al 2007) thus inferring that it is the percentage of $CD31^-$ memory cells that increases with age. The results discussed in this thesis support and add to these described by Junger and colleagues. I have shown for the first time that there is no significant difference between the percentage of $CD31^+$ memory cells between HIV-1 infected children and uninfected adults and that with increased age of HIV-1 infected children the proportion of $CD31^-$ memory cells increases and the proportion of $CD31^+$ memory cells is unchanged.

The finding from this study that Ki67 expression in significantly greater in $CD31^+$ memory cells than $CD31^-$ memory cells supports the proposal that $CD31^+$ memory cells have a longer replicative history than $CD31^-$ memory cells (Junge et al 2007).

7.5 RELATIONSHIP BETWEEN THE $CD4^+$ T CELL SUB-POPULATIONS

From the results obtained by us and other researchers (Torimoto et al 1992), (Prager et al 1996), (Kimmig et al 2002), (Junge et al 2007), we have proposed a model of T cell

dynamics in HIV infection The CD4 count and the balance between the sub-populations are controlled by thymic output, proliferation and antigen driven differentiation. RTEs are produced by thymic output. In response to activation they can differentiate into either $CD31^+$ memory cells or into central naïve cells, which can themselves differentiate into $CD31^-$ memory cells. $CD31^+$ and $CD31^-$ memory cells respond to activation by proliferating. Death occurs in all populations, though at different rates, being higher in the memory population. Viral replication indirectly produces increased activation, perhaps as been suggested due to increased bacterial translocation from the gut (Douek 2007), in all populations and via activation induced cell death, the death rate in all populations increases. In addition increased activation drives the differentiation of RTEs and central naïve cells and the proliferation of memory cells thus moving the equilibrium towards memory cells.

7.6 THE IMPORTANCE OF THE SET POINT IN HIV-1 INFECTION

We undertook the first immunological study of planned treatment interruption (PTI) in children. We showed that even in virally suppressed children on continuous therapy (CT) who maintain their CD4 count, in a year there is still considerable variation in most parameters, a finding which highlights the dynamic equilibrium in stable HIV infection.

Perhaps the most important theme to consistently emerge from these data is the importance of set points in HIV infection. Although treatment interruption resulted in initial perturbations to the percentage size of the CD4 subsets; specifically decreases in the proportions of RTEs and central naive cells and increases in the proportions of $CD31^+$ and $CD31^-$ memory cell; however the distribution of these cells quickly returned to their baseline levels, their set point contribution to the CD4 pool. Also the CD4 count and viral load only fell and rose respectively for the first few weeks of treatment interruption until they too reached set points. It is likely that processes controlling cell numbers such as activation and proliferation are important in re-establishing these set

points because we detected early increases in HLA-DR and Ki67 expression in the $CD4^+$ T cell subsets, especially within the memory populations. A key to optimising PTI and HAART may be to determine when these set points are established, how they are established and how they could be altered in favour of higher CD4 counts and lower viral loads.

7.7 INTRACELLULAR HIV DNA

In this study we described the development of a highly sensitive qPCR assay to quantify intracellular HIV DNA in highly purified naïve and memory $CD4^+$ T cells. Thus we quantified for the first time in HIV-1 infected children the concentration of HIV DNA and found that as in adults almost all the HIV DNA is located in the memory pool, over 90%. This is a very interesting result as suggests that even though naïve cells make up a much greater proportion of the $CD4^+$ T cell pool in children, naïve cells are still infected at much lower rates than memory cells.

HIV DNA was quantified in children who had stopped anti-retroviral treatment and therefore we were able to confirm that in children as has already been reported in adults the concentration of HIV DNA increases with increasing time off treatment. This finding would suggest that PTI is associated with increased latent viral load during the interruption period. It would, however, be interesting and important to determine what happens to the concentration of HIV DNA upon resuming treatment, which has been reported in adult patients to decrease again when treatment is resumed.

7.8 LIMITATIONS OF THE STUDY

Although the findings in this work, describing a dynamic relationship between $CD4^+$ T cell sub-populations and the importance of the set point in controlling changes in this

relationship, are valuable contributions to the understanding of $CD4^+$ T cell dynamics in HIV-1 infected children their strength is limited because only the peripheral $CD4^+$ T cell pool was studied, most explanations were extrapolated from associations between sub-populations and parameters rather than direct causal relationships and small sample groups were used especially in the investigations of PTI.

7.9 FUTURE WORK

Further work should certainly focus on testing the explanations proposed herein for causal relationships such as for example studies to showing the direct effect of activation on the sub-populations discussed. More samples from the PTI trial should be tested and it would be fascinating to determine the effect of intracellular HIV DNA concentration in naïve and memory cells upon recommencing anti-retroviral treatment and even more interesting to undertake a study of the HIV DNA genotypes before treatment interruption, during treatment interruption and after restarting treatment again. The proposed intracellular HIV DNA study would be even more noteworthy if performed in the RTE, central naïve and $CD31^+$ and $CD31^-$ $CD4^+$ T cell sub-populations. This would however require development of a method to isolate highly purified populations and either a great number of cells would be required and/or a more sensitive qPCR assay developed.

CHAPTER 8

APPENDIX

8.1 SUPPLEMENTARY FIGURES

8.1.1 CD3 and CD4 expression in PBMCs from an HIV-1 infected child

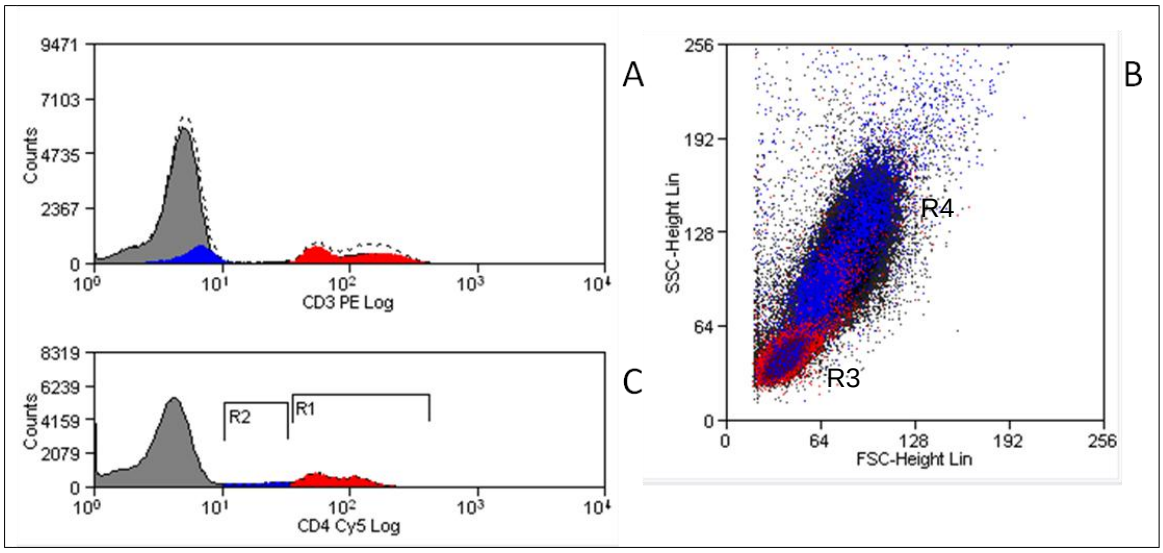

Figure 8.1 CD3 and CD4 expression in PBMCs from an HIV-1 infected child

A) A $CD4^{high}$ (red peak, R1) and $CD4^{low}$ (blue peak, R2) population are marked on the histogram and applied to the FSC versus SSC dot plot, B). The $CD4^{high}$ cells are almost exclusively located in R3, a region of low FSC and SSC and the $CD4^{low}$ cells are mostly located in R4, a region of high FSC and SSC. C) The $CD4^{high}$ (red peak, R1) and $CD4^{low}$ (blue peak, R2) populations are then applied to a histogram of CD3 expression showing that all the $CD4^{high}$ cells also express CD3.

8.1.2 CD3 and CD4 expression in red cell lysed whole blood from an HIV-1 infected child

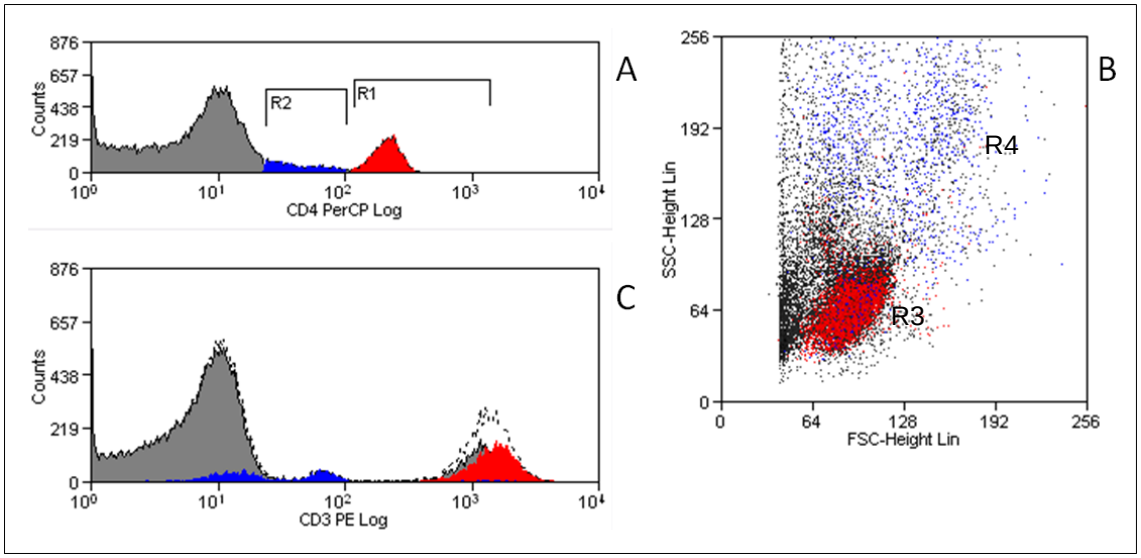

Figure 8.2 CD3 and CD4 expression in red cell lysed whole blood from an HIV-1 infected child

A) A $CD4^{high}$ (red peak, R1) and $CD4^{low}$ (blue peak, R2) population are marked on the histogram and applied to the FSC versus SSC dot plot, B). The $CD4^{high}$ cells are almost exclusively located in R3, a region of low FSC and SSC and the $CD4^{low}$ cells are mostly located in R4, a region of high FSC and SSC. C) The $CD4^{high}$ (red peak, R1) and $CD4^{low}$ (blue peak, R2) populations are then applied to a histogram of CD3 expression showing that all the $CD4^{high}$ cells also express CD3.

8.1.3 Failed ammonium chloride mediated red cell lysis in whole blood from an HIV-1 infected child

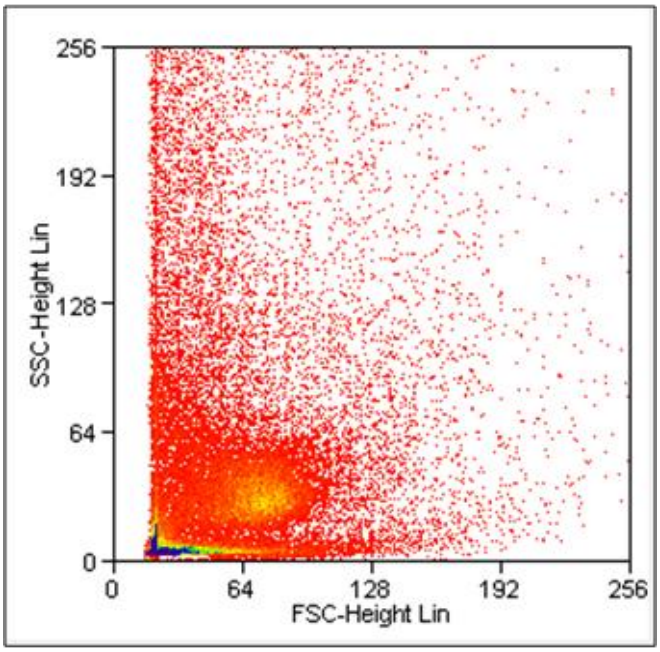

Figure 8.3 Failed ammonium chloride mediated red cell lysis in whole blood from an HIV-1 infected child The scatter plot is an example of failed red cell lysis in an HIV-1 infected child. The bottom left shows the characteristic high density of cell debris and poor separation of leukocyte populations.

8.2 PENTA 11 TRIAL SUMMARY

8.2.1 Aim and Objectives

The overall aim of the PENTA 11 trial is to evaluate the role of planned treatment interruptions in the management of HIV infected children who have responded well to antiretroviral therapy.

The specific objectives are:

- To determine whether children with chronic HIV infection undergoing planned antiretroviral (ART) treatment interruptions are disadvantaged clinically, immunologically or virologically by periods of time off ART.

- To assess HIV-specific immune responses during and after interruptions of ART, compared with continuous ART, in an immunology/virology substudy.

8.2.2 Design

An open, randomised, controlled phase II exploratory trial in HIV-1 infected children on antiretroviral therapy (ART) with HIV-1 RNA <50 copies/ml and

- in children aged 2-6 years: CD4 percent ≥30%
- in children aged 7-15 years: CD4 percent ≥25% and CD4≥500 cells/mm^3

to compare the effect of intermittent versus continuous antiretroviral therapy (ART) on disease progression, CD4 percent, HIV-1 RNA and toxicity in children in whom clinicians would consider interrupting treatment until

- in children aged 2-6 years: CD4 percent declines to below 20%
- in children aged 7-15 years: CD4 percent declines to below 20% **or** CD4 declines to below 350 cells/mm^3

Immunological and virological eligibility criteria must be met at the screening visit and at the prior visit between 1 and 4 months before; immunological re-start criteria should be confirmed on a second sample as soon as possible and **within 4 weeks**.

100 children will be randomised to continue on their current ART regimen or to a strategy of CD4-driven planned treatment interruption(s) (PTI) for 72 weeks. Children randomised to PTI will stop all ART, and will restart ART if the CD4 percent falls to <20% (age 2-6) or CD4 percent falls to <20%, or CD4 falls to < 350 cells/mm^3 (age ≥7).

Children should spend no more than 48 weeks off therapy and should be restarted at their week 48 visit if they have not already reached the immunological restart threshold.

Once HIV-1 RNA is again suppressed <50 copies/ml and either CD4 percent has increased above ≥30% (age 2-6) or CD4 percent ≥25% and CD4≥500 cells/mm^3 (age ≥7) ART should be interrupted again if these results are confirmed at 2 visits, 1- 3 months apart and the child has been back on therapy for at least 24 weeks.

Enrolment will take place over 24 months and follow-up will continue until the last randomised child has completed 72 weeks follow-up.

8.2.3 Population

100 HIV-1 infected children, aged 2 to 15 years old inclusive, on any ART regimen containing 3 or more drugs which they have taken for at least 24 weeks with confirmed (on 2 occasions at least one month apart) HIV-1 RNA <50 copies/ml and either CD4 percent ≥30% (age 2-6 years) or CD4 percent ≥25% and CD4≥500 cells/mm^3 (age ≥ 7).

8.2.4 Primary Outcome

Any of

- CD4 percent <15% (age 2-6)
- CD4 percent <15% and CD4<200 cells/mm^3 (age ≥7)
- new CDC stage C diagnosis
- death

8.2.5 Secondary Outcomes

- change in ART (defined as any change from the ART regimen at randomisation)
- acute retroviral syndrome (see section 9.7)
- ART-related grade 3 and 4 clinical and laboratory adverse events
- HIV-1 RNA ≥400 copies/ml at week 72 having received ART continuously for the preceding 12 weeks
- HIV-1 RNA ≥50 copies/ml at week 72 having received ART continuously for the preceding 12 weeks
- number of HIV mutations present at 72 weeks conferring resistance to drugs taken at entry or during the trial
- adherence to ART as assessed by caregiver completed questionnaire
- acceptability of the two strategies of ART administration to families as assessed by caregiver completed questionnaire

8.2.6 Follow-up

All children will be seen at weeks –2 and 0 (screening and trial entry/randomisation), 12, 24, 36, 48, 60 and 72. All children starting a PTI, and at least 20 children in the continuous therapy arm in the immunology/virology substudy, will also be seen at weeks 2, 4 and 8. CD4 and viral load measurements will be performed locally and plasma stored at each assessment.

Additional visits should be undertaken as clinically indicated (particularly in the PTI arm), and will be at the discretion of the clinician. Any child approaching a re-start threshold (i.e CD4% <22% or CD4 count <400 cells/mm^3) should be seen every 4 weeks.

Children in the PTI group should remain off ART until they meet one of the following conditions:

- age 2-6 years: CD4% <20% (confirmed on a separate sample)
- age ≥7 years: CD4% <20% or absolute CD4 <350 cells/mm^3 (confirmed on a separate sample)
- new or recurrent CDC stage C or severe stage B event
- the child has spent 48 weeks on the current PTI.

Any child who reaches a primary endpoint should restart immediately without a confirmatory test and should not undergo a further PTI:

- CD4% <15% (age 2-6)
- CD4% <15% and CD4 < 200 cells/mm^3 (age ≥7),
- new CDC Stage C diagnosis

In addition children whose CD4 drops rapidly reaching re-start criteria within 10 weeks of stopping should NOT undergo further PTIs.

Children can undergo a further PTI, if, after at least 24 weeks back on therapy:

- age 2-6 years: the CD4 percent increases to ≥30% and HIV RNA is <50 c/ml (both at 2 visits, 3 months apart) or
- age ≥ 7 years: the CD4 percent increases to ≥25% and CD4≥500 cells/mm^3 and HIV-1 RNA < 50 copies/ml (all at 2 visits, 3 months apart).

References

Abbey, JL & O'Neill, HC 2008. Expression of T-cell receptor genes during early T-cell development. *Immunol.Cell Biol.*, 86, (2) 166-174 available from: PM:17955035

Akbar, AN, Terry, L, Timms, A, Beverley, PC, & Janossy, G 1988. Loss of CD45R and gain of UCHL1 reactivity is a feature of primed T cells. *J.Immunol.*, 140, (7) 2171-2178 available from: PM:2965180

Albuquerque, AS, Foxall, RB, Cortesao, CS, Soares, RS, Doroana, M, Ribeiro, A, Lucas, M, Antunes, F, Victorino, RM, & Sousa, AE 2007. Low CD4 T-cell counts despite low levels of circulating HIV: insights from the comparison of HIV-1 infected patients with a discordant response to antiretroviral therapy to patients with untreated advanced HIV-2 disease. *Clin.Immunol*, 125, (1) 67-75 available from: PM:17692571

Alkhatib, G, Combadiere, C, Broder, CC, Feng, Y, Kennedy, PE, Murphy, PM, & Berger, EA 1996. CC CKR5: a RANTES, MIP-1alpha, MIP-1beta receptor as a fusion cofactor for macrophage-tropic HIV-1. *Science*, 272, (5270) 1955-1958 available from: PM:8658171

Altomonte, M, Pucillo, C, & Maio, M 1999. The overlooked "nonclassical" functions of major histocompatibility complex (MHC) class II antigens in immune and nonimmune cells. *J.Cell Physiol*, 179, (3) 251-256 available from: PM:10228943

Ameisen, JC & Capron, A 1991. Cell dysfunction and depletion in AIDS: the programmed cell death hypothesis. *Immunol.Today*, 12, (4) 102-105 available from: PM:1676268

Andersen, MH, Becker, JC, & Straten, P 2005. Regulators of apoptosis: suitable targets for immune therapy of cancer. *Nat.Rev.Drug Discov.*, 4, (5) 399-409 available from: PM:15864269

Appay, V 2004. The physiological role of cytotoxic CD4(+) T-cells: the holy grail? *Clin.Exp.Immunol.*, 138, (1) 10-13 available from: PM:15373899

Appay, V, Dunbar, PR, Callan, M, Klenerman, P, Gillespie, GM, Papagno, L, Ogg, GS, King, A, Lechner, F, Spina, CA, Little, S, Havlir, DV, Richman, DD, Gruener, N, Pape, G, Waters, A, Easterbrook, P, Salio, M, Cerundolo, V, McMichael, AJ, & Rowland-Jones, SL 2002. Memory CD8+ T cells vary in differentiation phenotype in different persistent virus infections. *Nat.Med.*, 8, (4) 379-385 available from: PM:11927944

Appay, V, van Lier, RA, Sallusto, F, & Roederer, M 2008. Phenotype and function of human T lymphocyte subsets: consensus and issues. *Cytometry A*, 73, (11) 975-983 available from: PM:18785267

Arlettaz, L, Barbey, C, Dumont-Girard, F, Helg, C, Chapuis, B, Roux, E, & Roosnek, E 1999. CD45 isoform phenotypes of human T cells: CD4(+)CD45RA(-)RO(+) memory T cells re-acquire CD45RA without losing CD45RO. *Eur.J.Immunol.*, 29, (12) 3987-3994 available from: PM:10602008

Ashorn, PA, Berger, EA, & Moss, B 1990. Human immunodeficiency virus envelope glycoprotein/CD4-mediated fusion of nonprimate cells with human cells. *The Journal of Virology*, 64, (5) 2149-2156 available from: PM:2109100

Asquith, B, Debacq, C, Macallan, DC, Willems, L, & Bangham, CR 2002. Lymphocyte kinetics: the interpretation of labelling data. *Trends Immunol.*, 23, (12) 596-601 available from: PM:12464572

Bahbouhi, B, Landay, A, & Al-Harthi, L 2004. Dynamics of cytokine expression in HIV productively infected primary CD4+ T cells. *Blood*, 103, (12) 4581-4587 available from: PM:14764521

Bains, I, Antia, R, Callard, R, & Yates, AJ 2009. Quantifying the development of the peripheral naive CD4+ T-cell pool in humans. *Blood*, 113, (22) 5480-5487 available from: PM:19179300

Balestrieri, E, Grelli, S, Matteucci, C, Minutolo, A, d'Ettorre, G, Di, SF, Montella, F, Vullo, V, Vella, S, Favalli, C, Macchi, B, & Mastino, A 2007. Apoptosis-associated gene expression in HIV-infected patients in response to successful antiretroviral therapy. *J.Med Virol.*, 79, (2) 111-117 available from: PM:17177302

Balk, SD, Morisi, A, & Gunther, HS 1984. Phorbol 12-myristate 13-acetate, ionomycin or ouabain, and raised extracellular magnesium induce proliferation of chicken heart mesenchymal cells. *Proc.Natl.Acad.Sci.U.S.A*, 81, (20) 6418-6421 available from: PM:6333683

Banda, NK, Bernier, J, Kurahara, DK, Kurrle, R, Haigwood, N, Sekaly, RP, & Finkel, TH 1992. Crosslinking CD4 by human immunodeficiency virus gp120 primes T cells for activation-induced apoptosis. *J.Exp.Med*, 176, (4) 1099-1106 available from: PM:1402655

Basu, VP, Song, M, Gao, L, Rigby, ST, Hanson, MN, & Bambara, RA 2008. Strand transfer events during HIV-1 reverse transcription. *Virus Res.*, 134, (1-2) 19-38 available from: PM:18279992

Baumler, CB, Bohler, T, Herr, I, Benner, A, Krammer, PH, & Debatin, KM 1996. Activation of the CD95 (APO-1/Fas) system in T cells from human immunodeficiency virus type-1-infected children. *Blood*, 88, (5) 1741-1746 available from: PM:8781430

Berzins, SP, Boyd, RL, & Miller, JF 1998. The role of the thymus and recent thymic migrants in the maintenance of the adult peripheral lymphocyte pool. *J.Exp.Med*, 187, (11) 1839-1848 available from: PM:9607924

Bieniasz, PD 2009. The cell biology of HIV-1 virion genesis. *Cell Host.Microbe*, 5, (6) 550-558 available from: PM:19527882

Bird, GW 1972. The red cell. *Br.Med J.*, 1, (5795) 293-297 available from: PM:4550379

Blankson, JN, Persaud, D, & Siliciano, RF 2002. The Challenge of viral reservoirs in HIV-1 infection. *Annu.Rev.Immunol.*, 53, 557-593

Bofill, M, Martinez-Picado, J, Ruiz-Hernandez, R, Cabrera, C, Marfil, S, Erkizia, I, Bellido, R, Romeu, J, Clotet, B, & Ruiz, L 2006. Naive CD4(+) T cells and recent thymic emigrant

levels in treated individuals with HIV: clinical relevance. *AIDS Res.Hum.Retroviruses*, 22, (9) 893-896 available from: PM:16989615

Bohler, T, Walcher, J, Holzl-Wenig, G, Schnitzler, P, Geiss, M, Buchholz, B, Linde, R, Rutschle, H, & Debatin, KM 1999. Expression of CD69 on T-cells from HIV-1-infected children and adolescents increases with increasing viral load. *Eur.J.Pediatr.*, 158, (8) 638-644 available from: PM:10445342

Borkowsky, W, Yogev, R, Muresan, P, McFarland, E, Frenkel, L, Fenton, T, Capparelli, E, Moye, J, Harding, P, Ellis, N, Heckman, B, & Kraimer, J 2008. Planned multiple exposures to autologous virus in HIV type 1-infected pediatric populations increases HIV-specific immunity and reduces HIV viremia. *AIDS Res.Hum.Retroviruses*, 24, (3) 401-411 available from: PM:18327977

Bowen, A, Palasanthiran, P, & Sohn, AH 2008. Global challenges in the development and delivery of paediatric antiretrovirals. *Drug Discov.Today*, 13, (11-12) 530-535 available from: PM:18549980

Brenchley, JM, Price, DA, Schacker, TW, Asher, TE, Silvestri, G, Rao, S, Kazzaz, Z, Bornstein, E, Lambotte, O, Altmann, D, Blazar, BR, Rodriguez, B, Teixeira-Johnson, L, Landay, A, Martin, JN, Hecht, FM, Picker, LJ, Lederman, MM, Deeks, SG, & Douek, DC 2006. Microbial translocation is a cause of systemic immune activation in chronic HIV infection. *Nat Med*, 12, (12) 1365-1371 available from: PM:17115046

Brenchley, JM, Schacker, TW, Ruff, LE, Price, DA, Taylor, JH, Beilman, GJ, Nguyen, PL, Khoruts, A, Larson, M, Haase, AT, & Douek, DC 2004. CD4+ T cell depletion during all stages of HIV disease occurs predominantly in the gastrointestinal tract. *J.Exp.Med*, 200, (6) 749-759 available from: PM:15365096

Briant, L, Coudronniere, N, Robert-Hebmann, V, Benkirane, M, & Devaux, C 1996. Binding of HIV-1 virions or gp120-anti-gp120 immune complexes to HIV-1-infected quiescent peripheral blood mononuclear cells reveals latent infection. *J.Immunol.*, 156, (10) 3994-4004 available from: PM:8621941

Buchschacher, GL 2001. Introduction to retroviruses and retroviral vectors. *Somat.Cell Mol.Genet.*, 26, (1-6) 1-11 available from: PM:12465459

Buseyne, F & Riviere, Y 1993. HIV-specific CD8+ T-cell immune responses and viral replication. *AIDS*, 7 Suppl 2, S81-S85 available from: PM:7909230

Butel, JS 2000. Viral carcinogenesis: revelation of molecular mechanisms and etiology of human disease. *Carcinogenesis*, 21, (3) 405-426 available from: PM:10688861

Capitini, CM, Chisti, AA, & Mackall, CL 2009. Modulating T-cell homeostasis with IL-7: preclinical and clinical studies. *J.Intern.Med*, 266, (2) 141-153 available from: PM:19623690

Carbone, J, Gil, J, Benito, JM, Navarro, J, Munoz-Fernandez, A, Bartolome, J, Zabay, JM, Lopez, F, & Fernandez-Cruz, E 2000. Increased levels of activated subsets of CD4 T cells add to the prognostic value of low CD4 T cell counts in a cohort of HIV-infected drug users. *AIDS*, 14, (18) 2823-2829 available from: PM:11153663

Carter, N. P. & Ormerod, M. G. 2000, "Introduction to the principles of flow cytometry," *In Flow cytometry: A practical approach*, 3 ed. M. G. Ormerod, ed., Oxford: Oxford University Press, pp. 1-22.

Castro, HC, Loureiro, NI, Pujol-Luz, M, Souza, AM, Albuquerque, MG, Santos, DO, Cabral, LM, Frugulhetti, IC, & Rodrigues, CR 2006. HIV-1 reverse transcriptase: a therapeutical target in the spotlight. *Curr.Med.Chem.*, 13, (3) 313-324 available from: PM:16475939

CDC 1981. Kaposi's sarcoma and Pneumocystis pneumonia among homosexual men--New York City and California. *morbidity and mortality weekly report*

CDC 1994. 1994 revised guidelines for the performance of CD4+ T-cell determinations in persons with human immunodeficiency virus (HIV) infections. Centers for Disease Control and Prevention. *MMWR Recomm.Rep.*, 43, (RR-3) 1-21 available from: PM:7908403

CDC. Organisation of the HIV-1 virion. Centers for Disease Control and Prevention . 3-9-2008. 16-8-2009.
Ref Type: Online Source

Centlivre, M, Sala, M, Wain-Hobson, S, & Berkhout, B 2007. In HIV-1 pathogenesis the die is cast during primary infection. *AIDS*, 21, (1) 1-11 available from: PM:17148962

Chermann, JC, Barre-Sinoussi, F, Dauguet, C, Brun-Vezinet, F, Rouzioux, C, Rozenbaum, W, & Montagnier, L 1983. Isolation of a new retrovirus in a patient at risk for acquired immunodeficiency syndrome. *Antibiot.Chemother.*, 32, 48-53 available from: PM:6205626

Chomont, N, El-Far, M, Ancuta, P, Trautmann, L, Procopio, FA, Yassine-Diab, B, Boucher, G, Boulassel, MR, Ghattas, G, Brenchley, JM, Schacker, TW, Hill, BJ, Douek, DC, Routy, JP, Haddad, EK, & Sekaly, RP 2009. HIV reservoir size and persistence are driven by T cell survival and homeostatic proliferation. *Nat.Med.*, 15, (8) 893-900 available from: PM:19543283

Choudhary, SK, Vrisekoop, N, Jansen, CA, Otto, SA, Schuitemaker, H, Miedema, F, & Camerini, D 2007. Low Immune Activation despite High Levels of Pathogenic Human Immunodeficiency Virus Type 1 Results in Long-Term Asymptomatic Disease. *The Journal of Virology*, 81, (16) 8838-8842 available from: http://jvi.asm.org/cgi/content/abstract/81/16/8838

Chougnet, CA & Shearer, GM 2007. Regulatory T cells (Treg) and HIV/AIDS: summary of the September 7-8, 2006 workshop. *AIDS Res.Hum.Retroviruses*, 23, (7) 945-952 available from: PM:17678480

Chun, TW, Carruth, L, Finzi, D, Shen, X, DiGiuseppe, JA, Taylor, H, Hermankova, M, Chadwick, K, Margolick, J, Quinn, TC, Kuo, YH, Brookmeyer, R, Zeiger, MA, Barditch-Crovo, P, & Siliciano, RF 1997. Quantification of latent tissue reservoirs and total body viral load in HIV-1 infection. *Nature*, 387, (6629) 183-188 available from: PM:9144289

Cocohoba, J & Dong, BJ 2008. Raltegravir: the first HIV integrase inhibitor. *Clin.Ther.*, 30, (10) 1747-1765 available from: PM:19014832

Cohen Stuart, JW, Slieker, WA, Rijkers, GT, Noest, A, Boucher, CA, Suur, MH, de, BR, Geelen, SP, Scherpbier, HJ, Hartwig, NG, Hooijkaas, H, Roos, MT, de Graeff-Meeder, B, &

de, GR 1998. Early recovery of CD4+ T lymphocytes in children on highly active antiretroviral therapy. Dutch study group for children with HIV infections. *AIDS*, 12, (16) 2155-2159 available from: PM:9833856

Collins, AR, Oscoz, AA, Brunborg, G, Gaivao, I, Giovannelli, L, Kruszewski, M, Smith, CC, & Stetina, R 2008. The comet assay: topical issues. *Mutagenesis*, 23, (3) 143-151 available from: PM:18283046

Correa, R, Resino, S, & Munoz-Fernandez, MA 2003. Increased interleukin-7 plasma levels are associated with recovery of CD4+ T cells in HIV-infected children. *J.Clin.Immunol.*, 23, (5) 401-406 available from: PM:14601648

Cosulich, ME, Rubartelli, A, Risso, A, Cozzolino, F, & Bargellesi, A 1987. Functional characterization of an antigen involved in an early step of T-cell activation. *Proc.Natl.Acad.Sci.U.S.A*, 84, (12) 4205-4209 available from: PM:3295878

Croft, M 2009. The role of TNF superfamily members in T-cell function and diseases. *Nat Rev.Immunol.*, 9, (4) 271-285 available from: PM:19319144

Cyster, JG 2003. Lymphoid organ development and cell migration. *Immunol.Rev.*, 195, 5-14 available from: PM:12969306

Dalgleish, AG, Beverley, PC, Clapham, PR, Crawford, DH, Greaves, MF, & Weiss, RA 1984. The CD4 (T4) antigen is an essential component of the receptor for the AIDS retrovirus. *Nature*, 312, (5996) 763-767 available from: PM:6096719

Danel, C, Moh, R, Minga, A, Anzian, A, Ba-Gomis, O, Kanga, C, Nzunetu, G, Gabillard, D, Rouet, F, Sorho, S, Chaix, ML, Eholie, S, Menan, H, Sauvageot, D, Bissagnene, E, Salamon, R, & Anglaret, X 2006. CD4-guided structured antiretroviral treatment interruption strategy in HIV-infected adults in west Africa (Trivacan ANRS 1269 trial): a randomised trial. *Lancet*, 367, (9527) 1981-1989 available from: PM:16782488

DART Trial Team 2008. Fixed duration interruptions are inferior to continuous treatment in African adults starting therapy with CD4 cell counts < 200 cells/microl. *AIDS*, 22, (2) 237-247 available from: PM:18097226

de Rossi A., Walker, AS, Klein, N, De, FD, King, D, & Gibb, DM 2002. Increased thymic output after initiation of antiretroviral therapy in human immunodeficiency virus type 1-infected children in the Paediatric European Network for Treatment of AIDS (PENTA) 5 Trial. *J.Infect.Dis.*, 186, (3) 312-320 available from: PM:12134227

De Rossi, A, Franchini, G, Aldovini, A, Del Mistro, A, Chieco-Bianchi, L, Gallo, RC, & Wong-Staal, F 1986. Differential response to the cytopathic effects of human T-cell lymphotropic virus type III (HTLV-III) superinfection in T4+ (helper) and T8+ (suppressor) T-cell clones transformed by HTLV-I. *Proc.Natl.Acad.Sci.U.S.A*, 83, (12) 4297-4301 available from: PM:2424024

de Vries, JE, Cornain, S, & Rumke, P 1974. Cytotoxity of non-T versus T-lymphocytes from melanoma patients and healthy donors on short- and long-term cultured melanoma cells. *Int.J.Cancer*, 14, (4) 427-434 available from: PM:4549213

Delelis, O, Carayon, K, Saib, A, Deprez, E, & Mouscadet, JF 2008. Integrase and integration: biochemical activities of HIV-1 integrase. *Retrovirology.*, 5, 114 available from: PM:19091057

Denucci, CC, Mitchell, JS, & Shimizu, Y 2009. Integrin function in T-cell homing to lymphoid and nonlymphoid sites: getting there and staying there. *Crit Rev.Immunol.*, 29, (2) 87-109 available from: PM:19496742

Devereux, HL, Youle, M, Johnson, MA, & Loveday, C 1999. Rapid decline in detectability of HIV-1 drug resistance mutations after stopping therapy. *AIDS*, 13, (18) F123-F127 available from: PM:10630517

Di Mascio, M, Sereti, I, Matthews, LT, Natarajan, V, Adelsberger, J, Lempicki, R, Yoder, C, Jones, E, Chow, C, Metcalf, JA, Sidorov, IA, Dimitrov, DS, Polis, MA, & Kovacs, JA 2006. Naive T-cell dynamics in human immunodeficiency virus type 1 infection: effects of highly active antiretroviral therapy provide insights into the mechanisms of naive T-cell depletion. *The Journal of Virology*, 80, (6) 2665-2674 available from: PM:16501076

Dooms, H & Abbas, AK 2006. Control of CD4+ T-cell memory by cytokines and costimulators. *Immunol.Rev.*, 211, 23-38 available from: PM:16824114

Douek, D 2007. HIV disease progression: immune activation, microbes, and a leaky gut. *Top.HIV.Med*, 15, (4) 114-117 available from: PM:17720995

Douek, DC, Betts, MR, Hill, BJ, Little, SJ, Lempicki, R, Metcalf, JA, Casazza, J, Yoder, C, Adelsberger, JW, Stevens, RA, Baseler, MW, Keiser, P, Richman, DD, Davey, RT, & Koup, RA 2001. Evidence for increased T cell turnover and decreased thymic output in HIV infection. *J.Immunol.*, 167, (11) 6663-6668 available from: PM:11714838

Douek, DC, Brenchley, JM, Betts, MR, Ambrozak, DR, Hill, BJ, Okamoto, Y, Casazza, JP, Kuruppu, J, Kunstman, K, Wolinsky, S, Grossman, Z, Dybul, M, Oxenius, A, Price, DA, Connors, M, & Koup, RA 2002. HIV preferentially infects HIV-specific CD4+ T cells. *Nature*, 417, (6884) 95-98 available from: PM:11986671

Ebert, LM, Schaerli, P, & Moser, B 2005. Chemokine-mediated control of T cell traffic in lymphoid and peripheral tissues. *Mol.Immunol.*, 42, (7) 799-809 available from: PM:15829268

Echaniz, P, de, J, & Cuadrado, E 1995. DNA staining changes associated with apoptosis and necrosis in blood lymphocytes of individuals with HIV infection. *Cytometry*, 19, (2) 164-170 available from: PM:7538065

El-Sadr, WM, Lundgren, JD, Neaton, JD, Gordin, F, Abrams, D, Arduino, RC, Babiker, A, Burman, W, Clumeck, N, Cohen, CJ, Cohn, D, Cooper, D, Darbyshire, J, Emery, S, Fatkenheuer, G, Gazzard, B, Grund, B, Hoy, J, Klingman, K, Losso, M, Markowitz, N, Neuhaus, J, Phillips, A, & Rappoport, C 2006. CD4+ count-guided interruption of antiretroviral treatment. *N.Engl.J.Med*, 355, (22) 2283-2296 available from: PM:17135583

Estaquier, J, Idziorek, T, Zou, W, Emilie, D, Farber, CM, Bourez, JM, & Ameisen, JC 1995. T helper type 1/T helper type 2 cytokines and T cell death: preventive effect of interleukin 12 on activation-induced and CD95 (FAS/APO-1)-mediated apoptosis of CD4+ T cells from

human immunodeficiency virus-infected persons. *J.Exp.Med*, 182, (6) 1759-1767 available from: PM:7500020

European Collaborative Study 1994. Natural history of vertically acquired human immunodeficiency virus-1 infection. The European Collaborative Study. *Pediatrics*, 94, (6 Pt 1) 815-819 available from: PM:7970995

Evans, RL, Faldetta, TJ, Humphreys, RE, Pratt, DM, Yunis, EJ, & Schlossman, SF 1978. Peripheral human T cells sensitized in mixed leukocyte culture synthesize and express Ia-like antigens. *J.Exp.Med.*, 148, (5) 1440-1445 available from: PM:152800

Fallen, PR, Duarte, RF, McGreavey, L, Potter, M, Ethell, M, Prentice, HG, Madrigal, JA, & Travers, PJ 2003. Identification of non-naive CD4+CD45RA+ T cell subsets in adult allogeneic haematopoietic cell transplant recipients. *Bone Marrow Transplant.*, 32, (6) 609-616 available from: PM:12953134

Feng, Y, Broder, CC, Kennedy, PE, & Berger, EA 1996. HIV-1 entry cofactor: functional cDNA cloning of a seven-transmembrane, G protein-coupled receptor. *Science*, 272, (5263) 872-877 available from: PM:8629022

Fenyo, EM, Albert, J, & Asjo, B 1989. Replicative capacity, cytopathic effect and cell tropism of HIV. *AIDS*, 3 Suppl 1, S5-12 available from: PM:2514754

Fernandez-Botran, R. & Vetvicka, V. 2001. *Methods in Cellular Immunology* CRC Press.

Finkel, TH, Tudor-Williams, G, Banda, NK, Cotton, MF, Curiel, T, Monks, C, Baba, TW, Ruprecht, RM, & Kupfer, A 1995. Apoptosis occurs predominantly in bystander cells and not in productively infected cells of HIV- and SIV-infected lymph nodes. *Nat Med*, 1, (2) 129-134 available from: PM:7585008

Fisher, AG, Collalti, E, Ratner, L, Gallo, RC, & Wong-Staal, F 1985. A molecular clone of HTLV-III with biological activity. *Nature*, 316, (6025) 262-265 available from: PM:2410792

Flexner, C 1998. HIV-protease inhibitors. *N.Engl.J.Med*, 338, (18) 1281-1292 available from: PM:9562584

Folks, T, Benn, S, Rabson, A, Theodore, T, Hoggan, MD, Martin, M, Lightfoote, M, & Sell, K 1985. Characterization of a continuous T-cell line susceptible to the cytopathic effects of the acquired immunodeficiency syndrome (AIDS)-associated retrovirus. *Proceedings of the National Academy of Sciences of the United States of America*, 82, (13) 4539-4543 available from: http://www.pnas.org/content/82/13/4539.abstract

Freed, EO 2001. HIV-1 replication. *Somat.Cell Mol.Genet.*, 26, (1-6) 13-33 available from: PM:12465460

Freed, EO & Mouland, AJ 2006. The cell biology of HIV-1 and other retroviruses. *Retrovirology.*, 3, 77 available from: PM:17083721

French, M 2009. HIV/AIDS: Immune Reconstitution Inflammatory Syndrome: A Reappraisal. *Clinical Infectious Diseases*, 48, (1) 101-107 available from: http://dx.doi.org/10.1086/595006

Fu, SM, Chiorazzi, N, Wang, CY, Montrazeri, G, Kunkel, HG, Ko, HS, & Gottlieb, AB 1978. Ia-bearing T lymphocytes in man. Their identification and role in the generation of allogeneic helper activity. *J.Exp.Med.*, 148, (5) 1423-1428 available from: PM:309915

Furman, PA & Barry, DW 1988. Spectrum of antiviral activity and mechanism of action of zidovudine. An overview. *Am.J.Med*, 85, (2A) 176-181 available from: PM:3044082

Garcia, F, Fumero, E, & Gatell, JM 2008. Immune modulators and treatment interruption. *Curr.Opin.HIV.AIDS*, 3, (2) 124-130 available from: PM:19372953

Garcia, F, Plana, M, Vidal, C, Cruceta, A, O'Brien, WA, Pantaleo, G, Pumarola, T, Gallart, T, Miro, JM, & Gatell, JM 1999. Dynamics of viral load rebound and immunological changes after stopping effective antiretroviral therapy. *AIDS*, 13, (11) F79-F86 available from: PM:10449278

Garcia-Peydro, M, de Yebenes, VG, & Toribio, ML 2006. Notch1 and IL-7 receptor interplay maintains proliferation of human thymic progenitors while suppressing non-T cell fates. *J.Immunol.*, 177, (6) 3711-3720 available from: PM:16951331

Gartner, S, Markovits, P, Markovitz, DM, Kaplan, MH, Gallo, RC, & Popovic, M 1986. The role of mononuclear phagocytes in HTLV-III/LAV infection. *Science*, 233, (4760) 215-219 available from: PM:3014648

Gerdes, J, Schwab, U, Lemke, H, & Stein, H 1983. Production of a mouse monoclonal antibody reactive with a human nuclear antigen associated with cell proliferation. *Int.J.Cancer*, 31, (1) 13-20 available from: PM:6339421

Gibb, DM, Duong, T, Leclezio, VA, Walker, AS, Verweel, G, & Dunn, DT 2004. Immunologic changes during unplanned treatment interruptions of highly active antiretroviral therapy in children with human immunodeficiency virus type 1 infection. *Pediatr.Infect.Dis.J.*, 23, (5) 446-450 available from: PM:15131469

Gibb, DM, Newberry, A, Klein, N, de, RA, Grosch-Woerner, I, & Babiker, A 2000. Immune repopulation after HAART in previously untreated HIV-1-infected children. Paediatric European Network for Treatment of AIDS (PENTA) Steering Committee. *Lancet*, 355, (9212) 1331-1332 available from: PM:10776748

Gibb, DM, Compagnucci, A, Green, H, Lallemant, M, & et al. 2008. Treatment Interruption in Children with Chronic HIV-infection: the results of the Paediatric European Network for Treatment of AIDS (PENTA) 11 trial. *Journal of the International AIDS Society*, 11, (S1) O21

Gordon, SN, Klatt, NR, Bosinger, SE, Brenchley, JM, Milush, JM, Engram, JC, Dunham, RM, Paiardini, M, Klucking, S, Danesh, A, Strobert, EA, Apetrei, C, Pandrea, IV, Kelvin, D, Douek, DC, Staprans, SI, Sodora, DL, & Silvestri, G 2007. Severe depletion of mucosal CD4+ T cells in AIDS-free simian immunodeficiency virus-infected sooty mangabeys. *J.Immunol.*, 179, (5) 3026-3034 available from: PM:17709517

Gougeon, ML, Lecoeur, H, Dulioust, A, Enouf, MG, Crouvoiser, M, Goujard, C, Debord, T, & Montagnier, L 1996. Programmed cell death in peripheral lymphocytes from HIV-infected persons: increased susceptibility to apoptosis of CD4 and CD8 T cells correlates with

lymphocyte activation and with disease progression. *J.Immunol.*, 156, (9) 3509-3520 available from: PM:8617980

Grant, MD, Smaill, FM, & Rosenthal, KL 1993. Lysis of CD4+ lymphocytes by non-HLA-restricted cytotoxic T lymphocytes from HIV-infected individuals. *Clin.Exp.Immunol.*, 93, (3) 356-362 available from: PM:8103717

Grasl-Kraupp, B, Ruttkay-Nedecky, B, Koudelka, H, Bukowska, K, Bursch, W, & Schulte-Hermann, R 1995. In situ detection of fragmented DNA (TUNEL assay) fails to discriminate among apoptosis, necrosis, and autolytic cell death: a cautionary note. *Hepatology*, 21, (5) 1465-1468 available from: PM:7737654

Gregersen, JP, Mehdi, S, Baur, A, & Hilfenhaus, J 1990. Antibody- and complement-mediated lysis of HIV-infected cells and inhibition of viral replication. *J.Med Virol.*, 30, (4) 287-293 available from: PM:1973445

Grimm, TA, Beer, BE, Hirsch, VM, & Clouse, KA 2003. Simian immunodeficiency viruses from multiple lineages infect human macrophages: implications for cross-species transmission. *J.Acquir.Immune.Defic.Syndr.*, 32, (4) 362-369 available from: PM:12640192

Groux, H, Torpier, G, Monte, D, Mouton, Y, Capron, A, & Ameisen, JC 1992. Activation-induced death by apoptosis in CD4+ T cells from human immunodeficiency virus-infected asymptomatic individuals. *J.Exp.Med*, 175, (2) 331-340 available from: PM:1346269

Hainaut, M, Ducarme, M, Schandene, L, Peltier, CA, Marissens, D, Zissis, G, Mascart, F, & Levy, J 2003. Age-related immune reconstitution during highly active antiretroviral therapy in human immunodeficiency virus type 1-infected children. *Pediatric Infectious Disease Journal*, 22, (1) 62-69 available from: ISI:000180455900011

Hamann, D, Baars, PA, Hooibrink, B, & van Lier, RW 1996. Heterogeneity of the human CD4+ T-cell population: two distinct CD4+ T-cell subsets characterized by coexpression of CD45RA and CD45RO isoforms. *Blood*, 88, (9) 3513-3521 available from: PM:8896418

Hamann, D, Kostense, S, Wolthers, KC, Otto, SA, Baars, PA, Miedema, F, & van Lier, RA 1999. Evidence that human CD8+CD45RA+CD27- cells are induced by antigen and evolve through extensive rounds of division. *Int.Immunol.*, 11, (7) 1027-1033 available from: PM:10383934

Hansasuta, P & Rowland-Jones, SL 2001. HIV-1 transmission and acute HIV-1 infection. *Br.Med Bull.*, 58, 109-127 available from: PM:11714627

Hartigan-O'Connor, DJ, Abel, K, & McCune, JM 2007. Suppression of SIV-specific CD4+ T cells by infant but not adult macaque regulatory T cells: implications for SIV disease progression. *J.Exp.Med*, 204, (11) 2679-2692 available from: PM:17954571

Hayday, AC & Pennington, DJ 2007. Key factors in the organized chaos of early T cell development. *Nat Immunol.*, 8, (2) 137-144 available from: PM:17242687

Haynes, BF, Markert, ML, Sempowski, GD, Patel, DD, & Hale, LP 2000. The role of the thymus in immune reconstitution in aging, bone marrow transplantation, and HIV-1 infection. *Annu.Rev.Immunol.*, 18, 529-560 available from: PM:10837068

Hazenberg, MD, Otto, SA, Cohen Stuart, JW, Verschuren, MC, Borleffs, JC, Boucher, CA, Coutinho, RA, Lange, JM, Rinke de Wit, TF, Tsegaye, A, van Dongen, JJ, Hamann, D, de Boer, RJ, & Miedema, F 2000. Increased cell division but not thymic dysfunction rapidly affects the T-cell receptor excision circle content of the naive T cell population in HIV-1 infection. *Nat.Med.*, 6, (9) 1036-1042 available from: PM:10973325

Hazenberg, MD, Otto, SA, van Rossum, AM, Scherpbier, HJ, de, GR, Kuijpers, TW, Lange, JM, Hamann, D, de Boer, RJ, Borghans, JA, & Miedema, F 2004. Establishment of the CD4+ T-cell pool in healthy children and untreated children infected with HIV-1. *Blood*, 104, (12) 3513-3519 available from: PM:15297312

Hellerstein, M, Hanley, MB, Cesar, D, Siler, S, Papageorgopoulos, C, Wieder, E, Schmidt, D, Hoh, R, Neese, R, Macallan, D, Deeks, S, & McCune, JM 1999. Directly measured kinetics of circulating T lymphocytes in normal and HIV-1-infected humans. *Nat.Med.*, 5, (1) 83-89 available from: PM:9883844

Hendriks, J, Gravestein, LA, Tesselaar, K, van Lier, RA, Schumacher, TN, & Borst, J 2000. CD27 is required for generation and long-term maintenance of T cell immunity. *Nat.Immunol.*, 1, (5) 433-440 available from: PM:11062504

Hermiston, ML, Xu, Z, & Weiss, A 2003. CD45: a critical regulator of signaling thresholds in immune cells. *Annu.Rev.Immunol.*, 21, 107-137 available from: PM:12414720

Heumann, D & Roger, T 2002. Initial responses to endotoxins and Gram-negative bacteria. *Clin.Chim.Acta*, 323, (1-2) 59-72 available from: PM:12135807

Hicks, CB, Gay, C, & Ferrari, G 2007. Acute HIV infection: the impact of anti-retroviral treatment on cellular immune responses. *Clin.Exp.Immunol.*, 149, (2) 211-216 available from: PM:17590167

Hintzen, RQ, de, JR, Lens, SM, & van Lier, RA 1994. CD27: marker and mediator of T-cell activation? *Immunol.Today*, 15, (7) 307-311 available from: PM:8086099

Ho Tsong, FR, Khatissian, E, Monceaux, V, Cumont, MC, Beq, S, Ameisen, JC, Aubertin, AM, Israel, N, Estaquier, J, & Hurtrel, B 2005. Disease progression in macaques with low SIV replication levels: on the relevance of TREC counts. *AIDS*, 19, (7) 663-673 available from: PM:15821392

Hotchkiss, RS, Strasser, A, McDunn, JE, & Swanson, PE 2009. Cell death. *N.Engl.J.Med*, 361, (16) 1570-1583 available from: PM:19828534

Huenecke, S, Behl, M, & Zimmerman, S 2008. Age-matched lymphocyte subpopulation reference values in childhood and adolescence: application of exponential regression analysis. *European Journal of Haematology*, 80, (6) 532-539

Jacob, MC, Favre, M, & Bensa, JC 1991. Membrane cell permeabilization with saponin and multiparametric analysis by flow cytometry. *Cytometry*, 12, (6) 550-558 available from: PM:1764979

Jaffar, S, Grant, AD, Whitworth, J, Smith, PG, & Whittle, H 2004. The natural history of HIV-1 and HIV-2 infections in adults in Africa: a literature review. *Bull.World Health Organ*, 82, (6) 462-469 available from: PM:15356940

Johannisson, A & Festin, R 1995. Phenotype transition of CD4+ T cells from CD45RA to CD45R0 is accompanied by cell activation and proliferation. *Cytometry*, 19, (4) 343-352 available from: PM:7796699

Jones, PL, Korte, T, & Blumenthal, R 1998. Conformational changes in cell surface HIV-1 envelope glycoproteins are triggered by cooperation between cell surface CD4 and co-receptors. *J.Biol.Chem.*, 273, (1) 404-409 available from: PM:9417096

Jordan, KA, Furlan, SN, Gonzalez, VD, Karlsson, AC, Quigley, MF, Deeks, SG, Rosenberg, MG, Nixon, DF, & Sandberg, JK 2006. CD8 T cell effector maturation in HIV-1-infected children. *Virology*, 347, (1) 117-126 available from: ISI:000236531600011

Junge, S, Kloeckener-Gruissem, B, Zufferey, R, Keisker, A, Salgo, B, Fauchere, JC, Scherer, F, Shalaby, T, Grotzer, M, Siler, U, Seger, R, & Gungor, T 2007. Correlation between recent thymic emigrants and CD31+ (PECAM-1) CD4+ T cells in normal individuals during aging and in lymphopenic children. *Eur.J.Immunol.*, 37, (11) 3270-3280 available from: PM:17935071

Kaneko, T & Nakagata, N 2006. Improvement in the long-term stability of freeze-dried mouse spermatozoa by adding of a chelating agent. *Cryobiology*, 53, (2) 279-282 available from: PM:16870171

Kaufman, JF, Auffray, C, Korman, AJ, Shackelford, DA, & Strominger, J 1984. The class II molecules of the human and murine major histocompatibility complex. *Cell*, 36, (1) 1-13 available from: PM:6198089

Kawamoto, H & Katsura, Y 2009. A new paradigm for hematopoietic cell lineages: revision of the classical concept of the myeloid-lymphoid dichotomy. *Trends Immunol.*, 30, (5) 193-200 available from: PM:19356980

Keogan, T., Wallace, E., & O'Leary, P. 2006, "Basic Immunology," *In Concise Clinical Immunology for healthcare professionals*, Routledge, pp. 1-105.

Kim, CH, Rott, L, Kunkel, EJ, Genovese, MC, Andrew, DP, Wu, L, & Butcher, EC 2001. Rules of chemokine receptor association with T cell polarization in vivo. *J.Clin.Invest*, 108, (9) 1331-1339 available from: PM:11696578

Kim, H & Perelson, AS 2006. Viral and latent reservoir persistence in HIV-1-infected patients on therapy. *PLoS.Comput.Biol.*, 2, (10) e135 available from: PM:17040122

Kimmig, S, Przybylski, GK, Schmidt, CA, Laurisch, K, Mowes, B, Radbruch, A, & Thiel, A 2002. Two subsets of naive T helper cells with distinct T cell receptor excision circle content in human adult peripheral blood. *J.Exp.Med.*, 195, (6) 789-794 available from: PM:11901204

Kitahata, MM, Gange, SJ, Abraham, AG, Merriman, B, Saag, MS, Justice, AC, Hogg, RS, Deeks, SG, Eron, JJ, Brooks, JT, Rourke, SB, Gill, MJ, Bosch, RJ, Martin, JN, Klein, MB, Jacobson, LP, Rodriguez, B, Sterling, TR, Kirk, GD, Napravnik, S, Rachlis, AR, Calzavara, LM, Horberg, MA, Silverberg, MJ, Gebo, KA, Goedert, JJ, Benson, CA, Collier, AC, Van Rompaey, SE, Crane, HM, McKaig, RG, Lau, B, Freeman, AM, & Moore, RD 2009. Effect of early versus deferred antiretroviral therapy for HIV on survival. *N.Engl.J.Med*, 360, (18) 1815-1826 available from: PM:19339714

Klatzmann, D, Champagne, E, Chamaret, S, Gruest, J, Guetard, D, Hercend, T, Gluckman, JC, & Montagnier, L 1984. T-lymphocyte T4 molecule behaves as the receptor for human retrovirus LAV. *Nature*, 312, (5996) 767-768 available from: PM:6083454

Kleeberger, CA, Lyles, RH, Margolick, JB, Rinaldo, CR, Phair, JP, & Giorgi, JV 1999. Viability and recovery of peripheral blood mononuclear cells cryopreserved for up to 12 years in a multicenter study. *Clin.Diagn.Lab Immunol.*, 6, (1) 14-19 available from: PM:9874657

Kohler, S, Wagner, U, Pierer, M, Kimmig, S, Oppmann, B, Mowes, B, Julke, K, Romagnani, C, & Thiel, A 2005. Post-thymic in vivo proliferation of naive CD4+ T cells constrains the TCR repertoire in healthy human adults. *Eur.J.Immunol.*, 35, (6) 1987-1994 available from: PM:15909312

Kong, FK, Chen, CL, Six, A, Hockett, RD, & Cooper, MD 1999. T cell receptor gene deletion circles identify recent thymic emigrants in the peripheral T cell pool. *Proc.Natl.Acad.Sci.U.S.A*, 96, (4) 1536-1540 available from: PM:9990059

Kornfeld, C, Ploquin, MJ, Pandrea, I, Faye, A, Onanga, R, Apetrei, C, Poaty-Mavoungou, V, Rouquet, P, Estaquier, J, Mortara, L, Desoutter, JF, Butor, C, Le, GR, Roques, P, Simon, F, Barre-Sinoussi, F, Diop, OM, & Muller-Trutwin, MC 2005. Antiinflammatory profiles during primary SIV infection in African green monkeys are associated with protection against AIDS. *J.Clin.Invest*, 115, (4) 1082-1091 available from: PM:15761496

Kostrikis, LG, Neumann, AU, Thomson, B, Korber, BT, McHardy, P, Karanicolas, R, Deutsch, L, Huang, Y, Lew, JF, McIntosh, K, Pollack, H, Borkowsky, W, Spiegel, HM, Palumbo, P, Oleske, J, Bardeguez, A, Luzuriaga, K, Sullivan, J, Wolinsky, SM, Koup, RA, Ho, DD, & Moore, JP 1999. A polymorphism in the regulatory region of the CC-chemokine receptor 5 gene influences perinatal transmission of human immunodeficiency virus type 1 to African-American infants. *The Journal of Virology*, 73, (12) 10264-10271 available from: PM:10559343

Krogstad, P, Uittenbogaart, CH, Dickover, R, Bryson, YJ, Plaeger, S, & Garfinkel, A 1999. Primary HIV infection of infants: The effects of somatic growth on lymphocyte and virus dynamics. *Clinical Immunology*, 92, (1) 25-33 available from: ISI:000081452100005

Krueger, A, Willenzon, S, Lyszkiewicz, M, Kremmer, E, & Forster, R 2010. CC chemokine receptor 7 and 9 double-deficient hematopoietic progenitors are severely impaired in seeding the adult thymus. *Blood*, 115, (10) 1906-1912 available from: PM:20040757

Krzysiek, R, Rudent, A, Bouchet-Delbos, L, Foussat, A, Boutillon, C, Portier, A, Ingrand, D, Sereni, D, Galanaud, P, Grangeot-Keros, L, & Emilie, D 2001. Preferential and persistent depletion of CCR5+ T-helper lymphocytes with nonlymphoid homing potential despite early treatment of primary HIV infection. *Blood*, 98, (10) 3169-3171 available from: PM:11698309

Kvale, D, Ormaasen, V, Kran, AM, Johansson, CC, Aukrust, P, Aandahl, EM, Froland, SS, & Tasken, K 2006. Immune modulatory effects of cyclooxygenase type 2 inhibitors in HIV patients on combination antiretroviral treatment. *AIDS*, 20, (6) 813-820 available from: PM:16549964

Lanier, LL, Buck, DW, Rhodes, L, Ding, A, Evans, E, Barney, C, & Phillips, JH 1988. Interleukin 2 activation of natural killer cells rapidly induces the expression and phosphorylation of the Leu-23 activation antigen. *J.Exp.Med.*, 167, (5) 1572-1585 available from: PM:3259252

Lanzavecchia, A & Sallusto, F 2005. Understanding the generation and function of memory T cell subsets. *Curr.Opin.Immunol.*, 17, (3) 326-332 available from: PM:15886125

Laurent-Crawford, AG, Krust, B, Muller, S, Riviere, Y, Rey-Cuille, MA, Bechet, JM, Montagnier, L, & Hovanessian, AG 1991. The cytopathic effect of HIV is associated with apoptosis. *Virology*, 185, (2) 829-839 available from: PM:1683728

Lazzarin, A 2005. Enfuvirtide: the first HIV fusion inhibitor. *Expert.Opin.Pharmacother.*, 6, (3) 453-464 available from: PM:15794736

Lees, O, Ramzaoui, S, Gilbert, D, Borsa, F, Humbert, G, Leblanc, D, Lagarde, M, & Tron, F 1993. The impaired in vitro production of interleukin-2 in HIV infection is negatively correlated to the number of circulating CD4+DR+ T cells and is reversed by allowing T cells to rest in culture: arguments for in vivo CD4+ T cell activation. *Clin.Immunol.Immunopathol.*, 67, (3 Pt 1) 185-191 available from: PM:8500265

Lewis, MG, Zack, PM, Elkins, WR, & Jahrling, PB 1992. Infection of rhesus and cynomolgus macaques with a rapidly fatal SIV (SIVSMM/PBj) isolate from sooty mangabeys. *AIDS Res.Hum.Retroviruses*, 8, (9) 1631-1639 available from: PM:1457209

Li, Q, Duan, L, Estes, JD, Ma, ZM, Rourke, T, Wang, Y, Reilly, C, Carlis, J, Miller, CJ, & Haase, AT 2005. Peak SIV replication in resting memory CD4+ T cells depletes gut lamina propria CD4+ T cells. *Nature*, 434, (7037) 1148-1152 available from: PM:15793562

Libman, H 1992. Pathogenesis, natural history, and classification of HIV infection. *Prim.Care*, 19, (1) 1-17 available from: PM:1594691

Libois, A, Lopez, A, Garcia, F, Castro, P, Maleno, MJ, Garcia, A, Climent, N, Arnedo, M, Gallart, T, Gatell, JM, & Plana, M 2006. Dynamics of T cells subsets and lymphoproliferative responses during structured treatment interruption cycles and after definitive interruption of HAART in early chronic HIV type-1-infected patients. *AIDS Res.Hum.Retroviruses*, 22, (7) 657-666 available from: PM:16831090

Lim, SG, Condez, A, Lee, CA, Johnson, MA, Elia, C, & Poulter, LW 1993. Loss of mucosal CD4 lymphocytes is an early feature of HIV infection. *Clin.Exp.Immunol.*, 92, (3) 448-454 available from: PM:8099858

Litvak, S, Sarih-Cottin, L, Fournier, M, Andreola, M, & Tarrago-Litvak, L 1994. Priming of HIV replication by tRNA(Lys3): role of reverse transcriptase. *Trends Biochem.Sci.*, 19, (3) 114-118 available from: PM:7515521

Loken, M. R., Green, C. L., & Wells, D. A. 2000, "Immunofluorescence of surface markers," *In flow cytometry*, 3rd ed. M. G. Ormerod, ed., Oxford: Oxford University Press, pp. 61-82.

Loos, B & Engelbrecht, AM 2009. Cell death: a dynamic response concept. *Autophagy.*, 5, (5) 590-603 available from: PM:19363298

Luzuriaga, K, Bryson, Y, Krogstad, P, Robinson, J, Stechenberg, B, Lamson, M, Cort, S, & Sullivan, JL 1997. Combination treatment with zidovudine, didanosine, and nevirapine in infants with human immunodeficiency virus type 1 infection. *N.Engl.J.Med.*, 336, (19) 1343-1349 available from: PM:9134874

Luzuriaga, K, McQuilken, P, Alimenti, A, Somasundaran, M, Hesselton, R, & Sullivan, JL 1993. Early viremia and immune responses in vertical human immunodeficiency virus type 1 infection. *J.Infect.Dis.*, 167, (5) 1008-1013 available from: PM:8486935

Luzuriaga, K & Sullivan, JL 1998. Prevention and treatment of pediatric HIV infection. *JAMA*, 280, (1) 17-18 available from: PM:9660351

Lyons, AB & Parish, CR 1994. Determination of lymphocyte division by flow cytometry. *J.Immunol.Methods*, 171, (1) 131-137 available from: PM:8176234

Macallan, DC, Asquith, B, Irvine, AJ, Wallace, DL, Worth, A, Ghattas, H, Zhang, Y, Griffin, GE, Tough, DF, & Beverley, PC 2003. Measurement and modeling of human T cell kinetics. *Eur.J.Immunol.*, 33, (8) 2316-2326 available from: PM:12884307

Macallan, DC, Fullerton, CA, Neese, RA, Haddock, K, Park, SS, & Hellerstein, MK 1998. Measurement of cell proliferation by labeling of DNA with stable isotope-labeled glucose: studies in vitro, in animals, and in humans. *Proc.Natl.Acad.Sci.U.S.A*, 95, (2) 708-713 available from: PM:9435257

Macallan, DC, Wallace, D, Zhang, Y, De Lara, C, Worth, AT, Ghattas, H, Griffin, GE, Beverley, PC, & Tough, DF 2004. Rapid turnover of effector-memory CD4(+) T cells in healthy humans. *J.Exp.Med.*, 200, (2) 255-260 available from: PM:15249595

Mackay, CR, Marston, WL, & Dudler, L 1990. Naive and memory T cells show distinct pathways of lymphocyte recirculation. *J.Exp.Med*, 171, (3) 801-817 available from: PM:2307933

Mahalingam, M, Peakman, M, Davies, ET, Pozniak, A, McManus, TJ, & Vergani, D 1993. T cell activation and disease severity in HIV infection. *Clin.Exp.Immunol.*, 93, (3) 337-343 available from: PM:8103715

Mahalingam, M, Pozniak, A, McManus, TJ, Senaldi, G, Vergani, D, & Peakman, M 1996. Abnormalities of CD45 isoform expression in HIV infection. *Clin.Immunol.Immunopathol.*, 81, (2) 210-214 available from: PM:8906753

Malavasi, F, Deaglio, S, Ferrero, E, Funaro, A, Sancho, J, Ausiello, CM, Ortolan, E, Vaisitti, T, Zubiaur, M, Fedele, G, Aydin, S, Tibaldi, EV, Durelli, I, Lusso, R, Cozno, F, & Horenstein, AL 2006. CD38 and CD157 as receptors of the immune system: a bridge between innate and adaptive immunity. *Mol.Med.*, 12, (11-12) 334-341 available from: PM:17380201

Markovic, I & Clouse, KA 2004. Recent advances in understanding the molecular mechanisms of HIV-1 entry and fusion: revisiting current targets and considering new options for therapeutic intervention. *Curr.HIV.Res.*, 2, (3) 223-234 available from: PM:15279586

Marzio, R, Mauel, J, & Betz-Corradin, S 1999. CD69 and regulation of the immune function. *Immunopharmacol.Immunotoxicol.*, 21, (3) 565-582 available from: PM:10466080

McCarthy, D. A. 2001, "Introduction to the general principles of sample preparation," *In Cytometric analysis of cell phenotype and function*, D. A. McCarthy & M. G. Macey, eds., Cambridge: Cambridge University Press, pp. 15-44.

McCarthy, D. A. 2007, "cell preparation," *In Flow cytometry: principles and applications*, M. G. Macey, ed., Totowa: Humana, pp. 17-59.

McElhaney, JE, Pinkoski, MJ, & Meneilly, GS 1995. Changes in CD45 isoform expression vary according to the duration of T-cell memory after vaccination. *Clin.Diagn.Lab Immunol.*, 2, (1) 73-81 available from: PM:7719917

Meyaard, L, Otto, SA, Jonker, RR, Mijnster, MJ, Keet, RP, & Miedema, F 1992. Programmed death of T cells in HIV-1 infection. *Science*, 257, (5067) 217-219 available from: PM:1352911

Miedema, F, Meyaard, L, Koot, M, Klein, MR, Roos, MT, Groenink, M, Fouchier, RA, Van't Wout, AB, Tersmette, M, Schellekens, PT, & . 1994. Changing virus-host interactions in the course of HIV-1 infection. *Immunol.Rev.*, 140, 35-72 available from: PM:7821927

Miller, V 2001. Structured treatment interruptions in antiretroviral management of HIV-1. *Curr.Opin.Infect.Dis.*, 14, (1) 29-37 available from: PM:11979112

Miller, V, Cozzi-Lepri, A, Hertogs, K, Gute, P, Larder, B, Bloor, S, Klauke, S, Rabenau, H, Phillips, A, & Staszewski, S 2000a. HIV drug susceptibility and treatment response to mega-HAART regimen in patients from the Frankfurt HIV cohort. *Antivir.Ther.*, 5, (1) 49-55 available from: PM:10846593

Miller, V, Sabin, C, Hertogs, K, Bloor, S, Martinez-Picado, J, D'Aquila, R, Larder, B, Lutz, T, Gute, P, Weidmann, E, Rabenau, H, Phillips, A, & Staszewski, S 2000b. Virological and immunological effects of treatment interruptions in HIV-1 infected patients with treatment failure. *AIDS*, 14, (18) 2857-2867 available from: PM:11153667

Milson, TJ, Patrick, CW, Torke, NJ, & Keller, RH 1986. Holding medium for cell surface phenotypic analysis. *J.Immunol.Methods*, 87, (2) 155-159 available from: PM:3485157

Miltenyi Biotech. CD4+ T cell isolation kit II (#130-091-155). Miltenyi Biotech website . 2009. 7-8-2009.
Ref Type: Online Source

Milush, JM, Reeves, JD, Gordon, SN, Zhou, D, Muthukumar, A, Kosub, DA, Chacko, E, Giavedoni, LD, Ibegbu, CC, Cole, KS, Miamidian, JL, Paiardini, M, Barry, AP, Staprans, SI, Silvestri, G, & Sodora, DL 2007. Virally Induced CD4+ T Cell Depletion Is Not Sufficient to Induce AIDS in a Natural Host. *The Journal of Immunology*, 179, (5) 3047-3056 available from: http://www.jimmunol.org/cgi/content/abstract/179/5/3047

Min, B, McHugh, R, Sempowski, GD, Mackall, C, Foucras, G, & Paul, WE 2003. Neonates support lymphopenia-induced proliferation. *Immunity.*, 18, (1) 131-140 available from: PM:12530982

Misumi, S, Inoue, M, Dochi, T, Kishimoto, N, Hasegawa, N, Takamune, N, & Shoji, S 2010. Uncoating of human immunodeficiency virus type 1 requires prolyl isomerase PIN1. *J.Biol.Chem.* available from: PM:20529865

Mo, H, Monard, S, Pollack, H, Ip, J, Rochford, G, Wu, L, Hoxie, J, Borkowsky, W, Ho, DD, & Moore, JP 1998. Expression patterns of the HIV type 1 coreceptors CCR5 and CXCR4 on CD4+ T cells and monocytes from cord and adult blood. *AIDS Res.Hum.Retroviruses*, 14, (7) 607-617 available from: PM:9591715

Mobley, PW, Curtain, CC, Kirkpatrick, A, Rostamkhani, M, Waring, AJ, & Gordon, LM 1992. The amino-terminal peptide of HIV-1 glycoprotein 41 lyses human erythrocytes and CD4+ lymphocytes. *Biochim.Biophys.Acta*, 1139, (4) 251-256 available from: PM:1355363

Mohri, H, Bonhoeffer, S, Monard, S, Perelson, AS, & Ho, DD 1998. Rapid turnover of T lymphocytes in SIV-infected rhesus macaques. *Science*, 279, (5354) 1223-1227 available from: PM:9469816

Mohri, H, Perelson, AS, Tung, K, Ribeiro, RM, Ramratnam, B, Markowitz, M, Kost, R, Hurley, A, Weinberger, L, Cesar, D, Hellerstein, MK, & Ho, DD 2001. Increased turnover of T lymphocytes in HIV-1 infection and its reduction by antiretroviral therapy. *J.Exp.Med.*, 194, (9) 1277-1287 available from: PM:11696593

Moir, S & Fauci, AS 2008. Pathogenic mechanisms of B-lymphocyte dysfunction in HIV disease. *J.Allergy Clin.Immunol.*, 122, (1) 12-19 available from: PM:18547629

Monini, P, Sgadari, C, Toschi, E, Barillari, G, & Ensoli, B 2004. Antitumour effects of antiretroviral therapy. *Nat Rev.Cancer*, 4, (11) 861-875 available from: PM:15516959

Monpoux, F, Tricoire, J, Lalande, M, Reliquet, V, Bebin, B, & Thuret, I 2004. Treatment interruption for virological failure or as sparing regimen in children with chronic HIV-1 infection. *AIDS*, 18, (18) 2401-2409 available from: PM:15622316

Montaner, LJ 2001. Structured treatment interruptions to control HIV-1 and limit drug exposure. *Trends Immunol.*, 22, (2) 92-96 available from: PM:11286710

Moretti, S, Marcellini, S, Boschini, A, Famularo, G, Santini, G, Alesse, E, Steinberg, SM, Cifone, MG, Kroemer, G, & De, SC 2000. Apoptosis and apoptosis-associated perturbations of peripheral blood lymphocytes during HIV infection: comparison between AIDS patients and asymptomatic long-term non-progressors. *Clin.Exp.Immunol.*, 122, (3) 364-373 available from: PM:11122242

Morris, L 2002. Neutralizing antibody responses to HIV-1 infection. *IUBMB.Life*, 53, (4-5) 197-199 available from: PM:12120994

Murphy, K., Travers, P. J., & Walport, M. 2008, "Antigen presentation to T Lymphocytes," *In Janeway's immunobiology*, 7th ed. New York: Garland Science, pp. 181-218.

Naylor, K, Li, G, Vallejo, AN, Lee, WW, Koetz, K, Bryl, E, Witkowski, J, Fulbright, J, Weyand, CM, & Goronzy, JJ 2005. The influence of age on T cell generation and TCR diversity. *J.Immunol.*, 174, (11) 7446-7452 available from: PM:15905594

Neese, RA, Siler, SQ, Cesar, D, Antelo, F, Lee, D, Misell, L, Patel, K, Tehrani, S, Shah, P, & Hellerstein, MK 2001. Advances in the stable isotope-mass spectrometric measurement of DNA synthesis and cell proliferation. *Anal.Biochem.*, 298, (2) 189-195 available from: PM:11700973

Neumann, AU, Tubiana, R, Calvez, V, Robert, C, Li, TS, Agut, H, Autran, B, & Katlama, C 1999. HIV-1 rebound during interruption of highly active antiretroviral therapy has no deleterious effect on reinitiated treatment. Comet Study Group. *AIDS*, 13, (6) 677-683 available from: PM:10397562

Newell, ML, Patel, D, Goetghebuer, T, & Thorne, C 2006. CD4 cell response to antiretroviral therapy in children with vertically acquired HIV infection: is it associated with age at initiation? *J.Infect.Dis.*, 193, (7) 954-962 available from: PM:16518757

Nielsen, MH, Pedersen, FS, & Kjems, J 2005. Molecular strategies to inhibit HIV-1 replication. *Retrovirology.*, 2, 10 available from: PM:15715913

Notermans, DW, Pakker, NG, Hamann, D, Foudraine, NA, Kauffmann, RH, Meenhorst, PL, Goudsmit, J, Roos, MT, Schellekens, PT, Miedema, F, & Danner, SA 1999. Immune reconstitution after 2 years of successful potent antiretroviral therapy in previously untreated human immunodeficiency virus type 1-infected adults. *J.Infect.Dis.*, 180, (4) 1050-1056 available from: PM:10479130

Okada, R, Kondo, T, Matsuki, F, Takata, H, & Takiguchi, M 2008. Phenotypic classification of human CD4+ T cell subsets and their differentiation. *Int.Immunol.*, 20, (9) 1189-1199 available from: PM:18635582

Oswald-Richter, K, Grill, SM, Leelawong, M, & Unutmaz, D 2004. HIV infection of primary human T cells is determined by tunable thresholds of T cell activation. *Eur.J.Immunol.*, 34, (6) 1705-1714 available from: PM:15162441

Pacifici, R, Zuccaro, P, Cozzi-Lepre, A, di, CS, Bacosi, A, & Fattorossi, A 1998. Quantification of the variation due to lysing technique in immunophenotyping of healthy and HIV-infected individuals. *Clin.Biochem.*, 31, (3) 165-172 available from: PM:9629490

Paiardini, M, Cervasi, B, Sumpter, B, McClure, HM, Sodora, DL, Magnani, M, Staprans, SI, Piedimonte, G, & Silvestri, G 2006. Perturbations of cell cycle control in T cells contribute to the different outcomes of simian immunodeficiency virus infection in rhesus macaques and sooty mangabeys. *The Journal of Virology*, 80, (2) 634-642 available from: PM:16378966

Pakker, NG, Notermans, DW, de Boer, RJ, Roos, MT, de, WF, Hill, A, Leonard, JM, Danner, SA, Miedema, F, & Schellekens, PT 1998. Biphasic kinetics of peripheral blood T cells after triple combination therapy in HIV-1 infection: a composite of redistribution and proliferation. *Nat.Med.*, 4, (2) 208-214 available from: PM:9461195

Palacios, GC, Sanchez, LM, Briones, E, Ramirez, TJ, Castillo, H, Rivera, LG, Vazquez, CA, Rodriguez-Padilla, C, & Holodniy, M 2009. Structured interruptions of highly active antiretroviral therapy in cycles of 4 weeks off/12 weeks on therapy in children having a chronically undetectable viral load cause progressively smaller viral rebounds. *Int.J.Infect.Dis.* available from: PM:19467895

Pantaleo, G, Graziosi, C, & Fauci, AS 1993. New concepts in the immunopathogenesis of human immunodeficiency virus infection. *N.Engl.J.Med.*, 328, (5) 327-335 available from: PM:8093551

Patel, D., Ford, T. C., & Rickwood, D. 1998, "Fractionation of cells by sedimentation methods," *In Cell Separation A Practical Approach*, D. Fisher, G. E. Francis, & D. Rickwood, eds., Oxford: Oxford University Press, pp. 43-89.

Patel, MS & Roche, TE 1990. Molecular biology and biochemistry of pyruvate dehydrogenase complexes. *FASEB J.*, 4, (14) 3224-3233 available from: PM:2227213

Patki, AH, Georges, DL, & Lederman, MM 1997. CD4+-T-cell counts, spontaneous apoptosis, and Fas expression in peripheral blood mononuclear cells obtained from human immunodeficiency virus type 1-infected subjects. *Clin.Diagn.Lab Immunol.*, 4, (6) 736-741 available from: PM:9384300

Patki, AH, Zielske, SP, Sieg, SF, & Lederman, MM 2000. Preferential S phase entry and apoptosis of CD4(+) T lymphocytes of HIV-1-infected patients after in vitro cultivation. *Clin.Immunol.*, 97, (3) 241-247 available from: PM:11112363

Pavia, A. 2008, "Managing HIV infection in children and adolescents," *In Global HIV/AIDS medicine*, P. Volberding et al., eds., Philadelphia: Saunders Elsevier, pp. 475-485.

Penninger, JM, Irie-Sasaki, J, Sasaki, T, & Oliveira-dos-Santos, AJ 2001. CD45: new jobs for an old acquaintance. *Nat.Immunol.*, 2, (5) 389-396 available from: PM:11323691

Perfetto, SP, Chattopadhyay, PK, & Roederer, M 2004. Seventeen-colour flow cytometry: unravelling the immune system. *Nat Rev.Immunol.*, 4, (8) 648-655 available from: PM:15286731

Perfetto, SP, Hickey, TE, Blair, PJ, Maino, VC, Wagner, KF, Zhou, S, Mayers, DL, St, LD, June, CH, & Siegel, JN 1997. Measurement of CD69 induction in the assessment of immune function in asymptomatic HIV-infected individuals. *Cytometry*, 30, (1) 1-9 available from: PM:9056736

Persaud, D, Pierson, T, Ruff, C, Finzi, D, Chadwick, KR, Margolick, JB, Ruff, A, Hutton, N, Ray, S, & Siliciano, RF 2000. A stable latent reservoir for HIV-1 in resting CD4(+) T lymphocytes in infected children. *J.Clin.Invest*, 105, (7) 995-1003 available from: PM:10749578

Plaeger-Marshall, S, Isacescu, V, O'Rourke, S, Bertolli, J, Bryson, YJ, & Stiehm, ER 1994. T cell activation in pediatric AIDS pathogenesis: three-color immunophenotyping. *Clin.Immunol.Immunopathol.*, 71, (1) 19-26 available from: PM:7511081

Poiesz, BJ, Ruscetti, FW, Gazdar, AF, Bunn, PA, Minna, JD, & Gallo, RC 1980. Detection and isolation of type C retrovirus particles from fresh and cultured lymphocytes of a patient with cutaneous T-cell lymphoma. *Proc.Natl.Acad.Sci.U.S.A*, 77, (12) 7415-7419 available from: PM:6261256

Pomerantz, RJ & Horn, DL 2003. 20 years of therapy for HIV-1 infection. *Nat Med*, 9, (7) 867-873

Poveda, E, Briz, V, Quinones-Mateu, M, & Soriano, V 2006. HIV tropism: diagnostic tools and implications for disease progression and treatment with entry inhibitors. *AIDS*, 20, (10) 1359-1367 available from: PM:16791010

Prager, E, Sunder-Plassmann, R, Hansmann, C, Koch, C, Holter, W, Knapp, W, & Stockinger, H 1996. Interaction of CD31 with a heterophilic counterreceptor involved in downregulation of human T cell responses. *J.Exp.Med.*, 184, (1) 41-50 available from: PM:8691148

Prince, AL, Yin, CC, Enos, ME, Felices, M, & Berg, LJ 2009. The Tec kinases Itk and Rlk regulate conventional versus innate T-cell development. *Immunol.Rev.*, 228, (1) 115-131 available from: PM:19290924

Pulliam, L, Gascon, R, Stubblebine, M, McGuire, D, & McGrath, MS 1997. Unique monocyte subset in patients with AIDS dementia. *Lancet*, 349, (9053) 692-695 available from: PM:9078201

Rambaldi, A, Borleri, G, Dotti, G, Bellavita, P, Amaru, R, Biondi, A, & Barbui, T 1998. Innovative two-step negative selection of granulocyte colony-stimulating factor-mobilized circulating progenitor cells: adequacy for autologous and allogeneic transplantation. *Blood*, 91, (6) 2189-2196 available from: PM:9490708

Read, JS 2007. Diagnosis of HIV-1 infection in children younger than 18 months in the United States. *Pediatrics*, 120, (6) e1547-e1562 available from: PM:18055670

Read, SW, Lempicki, RA, Di, MM, Srinivasula, S, Burke, R, Sachau, W, Bosche, M, Adelsberger, JW, Sereti, I, Davey, RT, Jr., Tavel, JA, Huang, CY, Issaq, HJ, Fox, SD, Lane, HC, & Kovacs, JA 2008. CD4 T cell survival after intermittent interleukin-2 therapy is predictive of an increase in the CD4 T cell count of HIV-infected patients. *J.Infect.Dis.*, 198, (6) 843-850 available from: PM:18684102

Renzi, P & Ginns, LC 1987. Analysis of T cell subsets in normal adults. Comparison of whole blood lysis technique to Ficoll-Hypaque separation by flow cytometry. *J.Immunol.Methods*, 98, (1) 53-56 available from: PM:2951443

Resino, S, Galan, I, Perez, A, Ramos, JT, Bellon, JM, Fontelos, PM, de Jose, MI, Gutierrez, MD, Cabrero, E, & Munoz-Fernandez, MA 2005. Immunological changes after highly active antiretroviral therapy with lopinavir-ritonavir in heavily pretreated HIV-infected children. *AIDS Res.Hum.Retroviruses*, 21, (5) 398-406 available from: PM:15929702

Resino, S, Seoane, E, Gutierrez, MD, Leon, JA, & Munoz-Fernandez, MA 2006. CD4(+) T-cell immunodeficiency is more dependent on immune activation than viral load in HIV-infected children on highly active antiretroviral therapy. *J.Acquir.Immune.Defic.Syndr.*, 42, (3) 269-276 available from: PM:16810122

Richards, D, Chapman, MD, Sasama, J, Lee, TH, & Kemeny, DM 1997. Immune memory in CD4+ CD45RA+ T cells. *Immunology*, 91, (3) 331-339 available from: PM:9301520

Riviere, Y, Tanneau-Salvadori, F, Regnault, A, Lopez, O, Sansonetti, P, Guy, B, Kieny, MP, Fournel, JJ, & Montagnier, L 1989. Human immunodeficiency virus-specific cytotoxic responses of seropositive individuals: distinct types of effector cells mediate killing of targets

expressing gag and env proteins. *The Journal of Virology*, 63, (5) 2270-2277 available from: PM:2522999

Rogers, PR, Pilapil, S, Hayakawa, K, Romain, PL, & Parker, DC 1992. CD45 alternative exon expression in murine and human CD4+ T cell subsets. *J.Immunol.*, 148, (12) 4054-4065 available from: PM:1351092

Romeu, MA, Mestre, M, Gonzalez, L, Valls, A, Verdaguer, J, Corominas, M, Bas, J, Massip, E, & Buendia, E 1992. Lymphocyte immunophenotyping by flow cytometry in normal adults. Comparison of fresh whole blood lysis technique, Ficoll-Paque separation and cryopreservation. *J.Immunol.Methods*, 154, (1) 7-10 available from: PM:1401946

Rosenblatt, HM, Stanley, KE, Song, LY, Johnson, GM, Wiznia, AA, Nachman, SA, & Krogstad, PA 2005. Immunological response to highly active antiretroviral therapy in children with clinically stable HIV-1 infection. *J.Infect.Dis.*, 192, (3) 445-455 available from: PM:15995958

Rothenberg, EV 2009. Decision by committee: new light on the CD4/CD8-lineage choice. *Immunol.Cell Biol.*, 87, (2) 109-112 available from: PM:19079359

Rothenberg, EV, Moore, JE, & Yui, MA 2008. Launching the T-cell-lineage developmental programme. *Nat.Rev.Immunol.*, 8, (1) 9-21 available from: PM:18097446

Rothstein, DM, Yamada, A, Schlossman, SF, & Morimoto, C 1991. Cyclic regulation of CD45 isoform expression in a long term human CD4+CD45RA+ T cell line. *J.Immunol.*, 146, (4) 1175-1183 available from: PM:1671403

Ruiz, L, Martinez-Picado, J, Romeu, J, Paredes, R, Zayat, MK, Marfil, S, Negredo, E, Sirera, G, Tural, C, & Clotet, B 2000. Structured treatment interruption in chronically HIV-1 infected patients after long-term viral suppression. *AIDS*, 14, (4) 397-403 available from: PM:10770542

Saha, K, Yuen, PH, & Wong, PK 1994. Murine retrovirus-induced depletion of T cells is mediated through activation-induced death by apoptosis. *The Journal of Virology*, 68, (4) 2735-2740 available from: PM:8139049

Sallusto, F, Geginat, J, & Lanzavecchia, A 2004. Central memory and effector memory T cell subsets: function, generation, and maintenance. *Annu.Rev.Immunol.*, 22, 745-763 available from: PM:15032595

Sallusto, F, Langenkamp, A, Geginat, J, & Lanzavecchia, A 2000. Functional subsets of memory T cells identified by CCR7 expression. *Curr.Top.Microbiol.Immunol.*, 251, 167-171 available from: PM:11036772

Sallusto, F, Lenig, D, Forster, R, Lipp, M, & Lanzavecchia, A 1999. Two subsets of memory T lymphocytes with distinct homing potentials and effector functions. *Nature*, 401, (6754) 708-712 available from: PM:10537110

Sancho, D, Gomez, M, & Sanchez-Madrid, F 2005. CD69 is an immunoregulatory molecule induced following activation. *Trends Immunol.*, 26, (3) 136-140 available from: PM:15745855

Santagostino, A 1999. An Italian national multicenter study for the definition of reference ranges for normal values of peripheral blood lymphocyte subsets in healthy adults. *Haematologica*, 84, (6) 499-504 available from: http://metalib.ucl.ac.uk:9003/sfx_local?sid=google&auinit=A&aulast=Santagostino&atitle=An%20Italian%20national%20multicenter%20study%20for%20the%20definition%20of%20reference%20ranges%20for%20normal%20values%20of%20peripheral%20blood%20lymphocyte%20subsets%20in%20healthy%20adults&id=pmid%3A10366792

Savarino, A, Bottarel, F, Malavasi, F, & Dianzani, U 2000. Role of CD38 in HIV-1 infection: an epiphenomenon of T-cell activation or an active player in virus/host interactions? *AIDS*, 14, (9) 1079-1089 available from: PM:10894271

Savino, W 2006. The thymus is a common target organ in infectious diseases. *PLoS.Pathog.*, 2, (6) e62 available from: PM:16846255

Schander, C & Kenneth, HM 2003. DNA, PCR and formalinized animal tissue - a short review and protocols. *Organisms Diversity & Evolution*, 3, (3) 195-205 available from: http://www.sciencedirect.com/science/article/B7GJ9-4DPMC62-25/2/662b1231494039a9330abccd9facf536

Scharl, M & Rogler, G 2010. Microbial sensing by the intestinal epithelium in the pathogenesis of inflammatory bowel disease. *Int.J.Inflam.*, 2010, 671258 available from: PM:21188218

Schendel, DJ & Johnson, JP 1985. T cells specific for different antigens express different HLA-D region products. *Eur.J.Immunol.*, 15, (12) 1239-1243 available from: PM:3878791

Schmid-Schonbein, GW, Shih, YY, & Chien, S 1980. Morphometry of human leukocytes. *Blood*, 56, (5) 866-875 available from: PM:6775712

Scholzen, T & Gerdes, J 2000. The Ki-67 protein: from the known and the unknown. *J.Cell Physiol*, 182, (3) 311-322 available from: PM:10653597

Sedaghat, AR, Siliciano, JD, Brennan, TP, Wilke, CO, & Siliciano, RF 2007. Limits on Replenishment of the Resting CD4+ T Cell Reservoir for HIV in Patients on HAART. *PLoS Pathogens*, 3, (8) e122 available from: http://dx.doi.org/10.1371%2Fjournal.ppat.0030122

Sharp, PM, Bailes, E, Chaudhuri, RR, Rodenburg, CM, Santiago, MO, & Hahn, BH 2001. The origins of acquired immune deficiency syndrome viruses: where and when? *Philos.Trans.R.Soc.Lond B Biol.Sci.*, 356, (1410) 867-876 available from: PM:11405934

Shearer, WT, Quinn, TC, LaRussa, P, Lew, JF, Mofenson, L, Almy, S, Rich, K, Handelsman, E, Diaz, C, Pagano, M, Smeriglio, V, & Kalish, LA 1997. Viral load and disease progression in infants infected with human immunodeficiency virus type 1. Women and Infants Transmission Study Group. *N.Engl.J.Med*, 336, (19) 1337-1342 available from: PM:9134873

Shearer, WT, Rosenblatt, HM, Gelman, RS, Oyomopito, R, Plaeger, S, Stiehm, ER, Wara, DW, Douglas, SD, Luzuriaga, K, McFarland, EJ, Yogev, R, Rathore, MH, Levy, W, Graham, BL, & Spector, SA 2003. Lymphocyte subsets in healthy children from birth through 18 years of age: the Pediatric AIDS Clinical Trials Group P1009 study. *J.Allergy Clin.Immunol.*, 112, (5) 973-980 available from: PM:14610491

Sigal, LH 2005. Basic science for the clinician 35: CD1, invariant NKT (iNKT) Cells, and gammadelta T-cells. *J.Clin.Rheumatol.*, 11, (6) 336-339 available from: PM:16371809

Singer, A, Adoro, S, & Park, JH 2008. Lineage fate and intense debate: myths, models and mechanisms of CD4- versus CD8-lineage choice. *Nat Rev.Immunol.*, 8, (10) 788-801 available from: PM:18802443

Smith, JG, Joseph, HR, Green, T, Field, JA, Wooters, M, Kaufhold, RM, Antonello, J, & Caulfield, MJ 2007. Establishing acceptance criteria for cell-mediated-immunity assays using frozen peripheral blood mononuclear cells stored under optimal and suboptimal conditions. *Clin.Vaccine Immunol.*, 14, (5) 527-537 available from: PM:17376862

Sousa, AE, Carneiro, J, Meier-Schellersheim, M, Grossman, Z, & Victorino, RM 2002. CD4 T cell depletion is linked directly to immune activation in the pathogenesis of HIV-1 and HIV-2 but only indirectly to the viral load. *J.Immunol.*, 169, (6) 3400-3406 available from: PM:12218162

Spina, CA, Prince, HE, & Richman, DD 1997. Preferential replication of HIV-1 in the CD45RO memory cell subset of primary CD4 lymphocytes in vitro. *J.Clin.Invest*, 99, (7) 1774-1785 available from: PM:9120023

Sprecher, S, Soumenkoff, G, Puissant, F, & Degueldre, M 1986. Vertical Transmission of Hiv in 15-Week Fetus. *Lancet*, 2, (8501) 288-289 available from: ISI:A1986D428400043

Sprent, J & Surh, CD 2002. T cell memory. *Annu.Rev.Immunol.*, 20, 551-579 available from: PM:11861612

Starr, TK, Jameson, SC, & Hogquist, KA 2003. Positive and negative selection of T cells. *Annu.Rev.Immunol.*, 21, 139-176 available from: PM:12414722

Stephenson, J 1999. Hopes for HIV eradication dim as stopping HAART allows resurgence. *JAMA*, 282, (14) 1317-1318 available from: PM:10527163

Sterling, TR, Vlahov, D, Astemborski, J, Hoover, DR, Margolick, JB, & Quinn, TC 2001. Initial plasma HIV-1 RNA levels and progression to AIDS in women and men. *N.Engl.J.Med.*, 344, (10) 720-725 available from: PM:11236775

Stewart, SJ, Fujimoto, J, & Levy, R 1986. Human T lymphocytes and monocytes bear the same Leu-3(T4) antigen. *J.Immunol.*, 136, (10) 3773-3778 available from: PM:3084644

Strebel, K, Luban, J, & Jeang, KT 2009. Human cellular restriction factors that target HIV-1 replication. *BMC.Med.*, 7, 48 available from: PM:19758442

Streeck, H & Nixon, DF 2010. T cell immunity in acute HIV-1 infection. *J.Infect.Dis.*, 202 Suppl 2, S302-S308 available from: PM:20846037

Sugita, K, Hirose, T, Rothstein, DM, Donahue, C, Schlossman, SF, & Morimoto, C 1992. CD27, a member of the nerve growth factor receptor family, is preferentially expressed on CD45RA+ CD4 T cell clones and involved in distinct immunoregulatory functions. *J.Immunol.*, 149, (10) 3208-3216 available from: PM:1358967

Surh, CD & Sprent, J 2008. Homeostasis of naive and memory T cells. *Immunity.*, 29, (6) 848-862 available from: PM:19100699

Switzer, WM, Salemi, M, Shanmugam, V, Gao, F, Cong, ME, Kuiken, C, Bhullar, V, Beer, BE, Vallet, D, Gautier-Hion, A, Tooze, Z, Villinger, F, Holmes, EC, & Heneine, W 2005. Ancient co-speciation of simian foamy viruses and primates. *Nature*, 434, (7031) 376-380 available from: PM:15772660

Taghon, T & Rothenberg, EV 2008. Molecular mechanisms that control mouse and human TCR-alphabeta and TCR-gammadelta T cell development. *Semin.Immunopathol.*, 30, (4) 383-398 available from: PM:18925397

Takeda, S, Rodewald, HR, Arakawa, H, Bluethmann, H, & Shimizu, T 1996. MHC class II molecules are not required for survival of newly generated CD4+ T cells, but affect their long-term life span. *Immunity.*, 5, (3) 217-228 available from: PM:8808677

Tan, JT, Dudl, E, LeRoy, E, Murray, R, Sprent, J, Weinberg, KI, & Surh, CD 2001. IL-7 is critical for homeostatic proliferation and survival of naive T cells. *Proc.Natl.Acad.Sci.U.S.A*, 98, (15) 8732-8737 available from: PM:11447288

Tanchot, C, Lemonnier, FA, Perarnau, B, Freitas, AA, & Rocha, B 1997. Differential requirements for survival and proliferation of CD8 naive or memory T cells. *Science*, 276, (5321) 2057-2062 available from: PM:9197272

Taylor, BS, Sobieszczyk, ME, McCutchan, FE, & Hammer, SM 2008. The challenge of HIV-1 subtype diversity. *N.Engl.J.Med*, 358, (15) 1590-1602 available from: PM:18403767

Tchilian, EZ, Dawes, R, Ramaley, PA, Whitworth, JA, Yuldasheva, N, Wells, RS, Watera, C, French, N, Gilks, CF, Kunachiwa, W, Ruzibakiev, R, Leetrakool, N, Carrington, CV, Ramdath, DD, Gotch, F, Stephens, HA, Hill, AV, & Beverley, PC 2002. A CD45 polymorphism associated with abnormal splicing is absent in African populations. *Immunogenetics*, 53, (10-11) 980-983 available from: PM:11862398

Terry, LA, Brown, MH, & Beverley, PC 1988. The monoclonal antibody, UCHL1, recognizes a 180,000 MW component of the human leucocyte-common antigen, CD45. *Immunology*, 64, (2) 331-336 available from: PM:2455685

Tesselaar, K, Arens, R, van Schijndel, GM, Baars, PA, van, d, V, Borst, J, van Oers, MH, & van Lier, RA 2003. Lethal T cell immunodeficiency induced by chronic costimulation via CD27-CD70 interactions. *Nat.Immunol.*, 4, (1) 49-54 available from: PM:12469117

Tilton, JC & Doms, RW 2009. Entry inhibitors in the treatment of HIV-1 infection. *Antiviral Res.* available from: PM:19683546

Torimoto, Y, Rothstein, DM, Dang, NH, Schlossman, SF, & Morimoto, C 1992. CD31, a novel cell surface marker for CD4 cells of suppressor lineage, unaltered by state of activation. *J.Immunol.*, 148, (2) 388-396 available from: PM:1345920

Tough, DF, Sun, S, Zhang, X, & Sprent, J 1999. Stimulation of naive and memory T cells by cytokines. *Immunol.Rev.*, 170, 39-47 available from: PM:10566140

Turner, BG & Summers, MF 1999. Structural biology of HIV. *J.Mol.Biol.*, 285, (1) 1-32 available from: PM:9878383

UNAIDS 2002, *Paediatric HIV infection and AIDS.*

UNAIDS 2008, *Report on the Global AIDS Epidemic*, UNAIDS, Geneva.

van Rossum, AM, Scherpbier, HJ, van Lochem, EG, Pakker, NG, Slieker, WA, Wolthers, KC, Roos, MT, Kuijpers, JH, Hooijkaas, H, Hartwig, NG, Geelen, SP, Wolfs, TF, Lange, JM, Miedema, F, & de, GR 2001. Therapeutic immune reconstitution in HIV-1-infected children is independent of their age and pretreatment immune status. *AIDS*, 15, (17) 2267-2275 available from: PM:11698700

Veazey, RS, DeMaria, M, Chalifoux, LV, Shvetz, DE, Pauley, DR, Knight, HL, Rosenzweig, M, Johnson, RP, Desrosiers, RC, & Lackner, AA 1998. Gastrointestinal tract as a major site of CD4+ T cell depletion and viral replication in SIV infection. *Science*, 280, (5362) 427-431 available from: PM:9545219

Veazey, RS, Lifson, JD, Pandrea, I, Purcell, J, Piatak, M, Jr., & Lackner, AA 2003. Simian immunodeficiency virus infection in neonatal macaques. *The Journal of Virology*, 77, (16) 8783-8792 available from: PM:12885897

Vergis, EN & Mellors, JW 2000. Natural history of HIV-1 infection. *Infect.Dis.Clin.North Am.*, 14, (4) 809-8vi available from: PM:11144640

Viola, A, Schroeder, S, Sakakibara, Y, & Lanzavecchia, A 1999. T lymphocyte costimulation mediated by reorganization of membrane microdomains. *Science*, 283, (5402) 680-682 available from: PM:9924026

Violari, A, Cotton, MF, Gibb, DM, Babiker, AG, Steyn, J, Madhi, SA, Jean-Philippe, P, & McIntyre, JA 2008. Early antiretroviral therapy and mortality among HIV-infected infants. *N.Engl.J.Med.*, 359, (21) 2233-2244 available from: PM:19020325

von Andrian, UH & Mempel, TR 2003. Homing and cellular traffic in lymph nodes. *Nat Rev.Immunol.*, 3, (11) 867-878 available from: PM:14668803

Vrisekoop, N, van, GR, de Boer, AB, Otto, SA, Borleffs, JC, Steingrover, R, Prins, JM, Kuijpers, TW, Wolfs, TF, Geelen, SP, Vulto, I, Lansdorp, P, Tesselaar, K, Borghans, JA, & Miedema, F 2008. Restoration of the CD4 T cell compartment after long-term highly active antiretroviral therapy without phenotypical signs of accelerated immunological aging. *J.Immunol.*, 181, (2) 1573-1581 available from: PM:18606713

Wagner, D 2006. Re-shaping the T cell repertoire: TCR editing and TCR revision for good and for bad. *Clinical Immunology*, 123, (1) 1-6

Wainberg, MA 2003. HIV resistance to nevirapine and other non-nucleoside reverse transcriptase inhibitors. *J.Acquir.Immune.Defic.Syndr.*, 34 Suppl 1, S2-S7 available from: PM:14562852

Wallace, DL, Zhang, Y, Ghattas, H, Worth, A, Irvine, A, Bennett, AR, Griffin, GE, Beverley, PC, Tough, DF, & Macallan, DC 2004. Direct measurement of T cell subset kinetics in vivo in elderly men and women. *J.Immunol.*, 173, (3) 1787-1794 available from: PM:15265909

Wallace, M, Waterman, PM, Mitchen, JL, Djavani, M, Brown, C, Trivedi, P, Horejsh, D, Dykhuizen, M, Kitabwalla, M, & Pauza, CD 1999. Lymphocyte activation during acute simian/human immunodeficiency virus SHIV(89.6PD) infection in macaques. *The Journal of Virology*, 73, (12) 10236-10244 available from: PM:10559340

Wallis, RS, Kalayjian, R, Jacobson, JM, Fox, L, Purdue, L, Shikuma, CM, Arakaki, R, Snyder, S, Coombs, RW, Bosch, RJ, Spritzler, J, Chernoff, M, Aga, E, Myers, L, Schock, B, & Lederman, MM 2003. A study of the immunology, virology, and safety of prednisone in HIV-1-infected subjects with CD4 cell counts of 200 to 700 mm(-3). *J.Acquir.Immune.Defic.Syndr.*, 32, (3) 281-286 available from: PM:12626887

Wang, X, Rasmussen, T, Pahar, B, Poonia, B, Alvarez, X, Lackner, AA, & Veazey, RS 2007. Massive infection and loss of CD4+ T cells occurs in the intestinal tract of neonatal rhesus macaques in acute SIV infection. *Blood*, 109, (3) 1174-1181 available from: PM:17047153

Warren, HS & Skipsey, LJ 1991. Loss of activation-induced CD45RO with maintenance of CD45RA expression during prolonged culture of T cells and NK cells. *Immunology*, 74, (1) 78-85 available from: PM:1834549

Weichold, FF, Bryant, JL, Pati, S, Barabitskaya, O, Gallo, RC, & Reitz, MS, Jr. 1999. HIV-1 protease inhibitor ritonavir modulates susceptibility to apoptosis of uninfected T cells. *J.Hum.Virol.*, 2, (5) 261-269 available from: PM:10551732

Weiss, A. & Samelson, L. E. 2003, "T-Lymphocyte Function," *In Fundamental Immunology*, 5 ed. W. E. Paul, ed., pp. 321-364.

WHO. The top 10 causes of death. WHO media centre . 2009.
Ref Type: Online Source

Williams, SA & Greene, WC 2007. Regulation of HIV-1 latency by T-cell activation. *Cytokine*, 39, (1) 63-74 available from: http://www.sciencedirect.com/science/article/B6WDF-4P7FCWN-1/1/df87876b8ac6213c9840ed2c78652b77

Wu, Y & Marsh, JW 2003. Gene transcription in HIV infection. *Microbes.Infect.*, 5, (11) 1023-1027 available from: PM:12941394

Yamashita, M & Emerman, M 2006. Retroviral infection of non-dividing cells: old and new perspectives. *Virology*, 344, (1) 88-93 available from: PM:16364740

Yerly, S, Gunthard, HF, Fagard, C, Joos, B, Perneger, TV, Hirschel, B, & Perrin, L 2004. Proviral HIV-DNA predicts viral rebound and viral setpoint after structured treatment interruptions. *AIDS*, 18, (14) 1951-1953 available from: PM:15353981

Zanchetta, M, Walker, S, Burighel, N, Bellanova, D, Rampon, O, Giaquinto, C, & de, RA 2006. Long-term decay of the HIV-1 reservoir in HIV-1-infected children treated with highly active antiretroviral therapy. *J.Infect.Dis.*, 193, (12) 1718-1727 available from: PM:16703516

Zaunders, JJ, Kaufmann, GR, Cunningham, PH, Smith, D, Grey, P, Suzuki, K, Carr, A, Goh, LE, & Cooper, DA 2001. Increased turnover of CCR5+ and redistribution of. *J.Infect.Dis.*, 183, (5) 736-743 available from: PM:11181150

Zeitz, M, Ullrich, R, Schneider, T, Schieferdecker, HL, & Riecken, EO 1994. Cell differentiation and proliferation in the gastrointestinal tract with respect to the local immune system. *Ann.N.Y.Acad.Sci.*, 733, 75-86 available from: PM:7978905

Zhu, J, Yamane, H, & Paul, WE 2010. Differentiation of effector CD4 T cell populations (*). *Annu.Rev.Immunol.*, 28, 445-489 available from: PM:20192806

Ziegler, SF, Ramsdell, F, & Alderson, MR 1994. The activation antigen CD69. *Stem Cells*, 12, (5) 456-465 available from: PM:7804122